Influence of Non-Thermal Plasma Species on the Structure and Functionality of Isolated and Plant-based 1,4-Benzopyrone Derivatives and Phenolic Acids

vorgelegt von

Diplom-Chemikerin

Franziska Grzegorzewski

aus Berlin

Von der Fakultät III – Prozesswissenschaften
der Technischen Universität Berlin
zur Erlangung des akademischen Grades

Doktor der Naturwissenschaften
-Dr. rer. nat.-

genehmigte Dissertation

Promotionsausschuss:

Vorsitzender: Prof. Dr. rer. nat. habil. Helmut Schubert
Berichter: Prof. Dr. rer. nat. habil. Lothar W. Kroh
Berichter: Prof. Dr. rer. nat. Sascha Rohn
Berichter: Dr.-Ing. Oliver Schlüter

Tag der wissenschaftlichen Aussprache: 17.12.2010

Berlin 2011

D 83

This work was prepared at the Institute of Food Technology and Food Chemistry of the Technical University Berlin in the Department of Food Chemistry and Food Analysis from January 2008 till October 2010 under the supervision of Prof. Dr. Lothar W. Kroh.

Parts of this work are or will be published under the following title:

1. GRZEGORZEWSKI, F.; ROHN S.; QUADE, A.; SCHRÖDER, K.; EHLBECK, J.; SCHLÜTER, O.; KROH, L.W. Reaction chemistry of 1,4-benzopyrone derivates in non-equilibrium low-temperature plasmas. *Plasma Process. Polym.* **2010**, *7*(6), 466.

2. GRZEGORZEWSKI, F.; ROHN, KROH, L.W.; GEYER, M.; S. SCHLÜTER, O. Surface Morphology and Chemical Composition of lamb's lettuce (*Valerianella locusta*) after exposure to a low pressure oxygen plasma. *Food Chemistry* **2010**, *122*(4), 1145.

3. GRZEGORZEWSKI, F.; SCHLÜTER, O.; GEYER, M.; EHLBECK, J.; WELTMANN, K.-D.; KROH, L.W.; ROHN, S. Plasma-oxidative degradation of polyphenolics – Influence of non-thermal gas discharges with respect to fresh produce processing. *Czech J. Food Sci*. **2009**, *97*, S35.

4. GRZEGORZEWSKI, F.; ROHN, S.; EHLBECK, J.; KROH, L.W.; SCHLÜTER, O. Treating lamb's lettuce with a cold plasma- influence of atmospheric pressure Ar plasma immanent species on the phenolic profile of *Valerianella locusta*. (*submitted to LWT-Food Science and Technology*).

5. GRZEGORZEWSKI, F.; ZIETZ, M.; SCHLÜTER, O.; ROHN, S.; KROH, L.W. Influence of a low pressure oxygen plasma on the stability and antioxidant activity of flavonoid compounds in Kale (*Brassica oleracea* convar. *sabellica*) (*in prep.*).

Parts of this work have been presented as poster or talk at the following conferences:

1. GRZEGORZEWSKI, F.; SCHULZ, E.; SCHLÜTER, O.; EHLBECK, J.; KROH, L.W.; ROHN, S. Einfluss von Niedertemperaturplasmen auf polyphenolische Verbindungen in Feldsalat (Talk). *GDL-Kongress Lebensmitteltechnologie*, **2009**, *Oct. 22-24*, Lemgo.

2. GRZEGORZEWSKI, F.; SCHLÜTER, O.; EHLBECK, J.; KROH, L.W.; ROHN, S. Niedertemperaturplasmen– Schonendes Verfahren zur Sterilisation minimal prozessierter pflanzlicher Lebensmittel? (Talk). *38. Deutscher Lebensmittelchemiker-Tag*, **2009**, *Sept. 14-16*, Berlin.

3. GRZEGORZEWSKI, F.; SCHLÜTER, O.; EHLBECK, J.; KROH, L.W.; ROHN, S. Effect of atmospheric pressure plasma treatment on the stability of flavonoids (Talk). *CIGR – 5th International Postharvest Symposium,* **2009**, *Aug. 31 - Sept. 2*, Potsdam, Germany.

4. GRZEGORZEWSKI, F.; SCHLÜTER, O.; EHLBECK, J.; KROH, L.W.; ROHN, S. Influence of non thermal plasma-immanent reactive species on the stability and chemical behaviour of bioactive compounds (Talk). *EURO FOOD CHEM XV - FOOD FOR THE FUTURE,* **2009**, *July 5-8*, Copenhagen, Denmark.

5. GRZEGORZEWSKI, F.; SCHLÜTER, O.; EHLBECK, J.; KROH, L.W.; ROHN, S. Plasma-oxidative degradation of polyphenolics – Influence of non-thermal gas discharges with respect to fresh produce processing (Talk). *Chemical Reactions in Foods VI, EuCheMS*, **2009**, *May 13 – 15*, Prague, Czech Republic.

6. GRZEGORZEWSKI, F.; EHLBECK, J.; GEYER, M.; KROH, L.W.; ROHN, S.; SCHLÜTER, O. Einfluß von Niedertemperaturplasmen auf sekundäre Pflanzeninhaltsstoffe am Beispiel ausgewählter polyphenolischer Verbindungen (Talk). *45. Gartenbauwissenschaftliche Tagung,* **2009**, *Febr*. *25-28*, Berlin, Germany.

7. GRZEGORZEWSKI, F.; SCHLÜTER, O.; EHLBECK, J.; KROH, L.W.; ROHN, S. Effect of atmospheric pressure plasma treatment on the stability of flavonoids (Talk). *Postharvest unlimited,* **2008**, *Nov. 4–7*, Potsdam/Berlin, Germany.

8. SCHULZ, E.; GRZEGORZEWSKI, F.; SCHLÜTER, O.; EHLBECK, J.; KROH, L.W.; ROHN, S. Der Einfluss von Niedertemperaturplasmen auf die Flavonoide des Feldsalats (Poster). *38. Deutscher Lebensmittelchemiker-Tag,* **2009**, *Sept*. *14-16*, Berlin.

9. GRZEGORZEWSKI, F.; SCHLÜTER, O.; EHLBECK, J.; KROH, L.W.; ROHN, S. Plasma-chemical reactions at polyphenolic surfaces - Influence of non-thermal plasma with respect to fresh produce processing (Poster). *19th International Symposium on Plasma Chemistry,* **2009**, *July 26-31*, Bochum.

10. GRZEGORZEWSKI, F.; SCHLÜTER, O.; EHLBECK, J.; KROH, L.W.; ROHN, S. Low-Temperature Plasma - Mild preservation technology for minimal processed fresh food? (Poster). *SKLM-Symposium on "Risk Assessment of phytochemicals in food-novel approaches"*, **2009**, *March 30-April 1*, Kaiserslautern, Germany.

11. GRZEGORZEWSKI, F.; SCHLÜTER, O.; EHLBECK, J.; KROH, L.W.; ROHN, S. Study on plasma chemistry of oxygen radicals in cold atmospheric pressure plasma with respect to fresh produce processing (Poster). *Postharvest unlimited,* **2008**, *Nov. 4-7*, Potsdam/Berlin, Germany.

12. GRZEGORZEWSKI, F.; SCHLÜTER, O.; EHLBECK, J.; KROH, L.W.; ROHN, S. Einfluß von Niedertemperaturplasmen auf die Stabilität von Flavonoiden (Poster). *37. Deutscher Lebensmittelchemikertag,* **2008**, *Sept*. *8-10*, Kaiserslautern.

13. GRZEGORZEWSKI, F.; SCHLÜTER, O.; EHLBECK, J.; KROH, L.W.; ROHN, S. Untersuchungen zur Chemie von Sauerstoffradikalen (ROS) in Niedertemperatur-Plasmen (Poster). *37. Deutscher Lebensmittelchemikertag,* **2008**, *Sept. 8-10*, Kaiserslautern.

14. GRZEGORZEWSKI, F.; SCHLÜTER, O.; EHLBECK, J.; KROH, L.W.; ROHN, S. Effect of atmospheric pressure plasma treatment on the stability of selected phenolic acids (Poster). *Ferulate 08, International Conference on Hydroxycinnamates and Related Plant Phenolics,* **2008**, *Aug. 25-27*, Minnesota/Saint Paul, USA.

Was immer Du tun kannst oder erträumst tun zu können, beginne es.
Kühnheit besitzt Genie, Macht und Magische Kraft.
Beginne es jetzt.

Johann Wolfgang Goethe

Acknowledgement

Foremost, I want to express my special gratitude to Prof. Dr. Lothar W. Kroh for the supervision of this thesis. It has been a great fortune to have an advisor who gave me the freedom to explore on my own. The many fruitful discussions significantly influenced the focus of my work.

Thanks to Prof. Dr. Sascha Rohn for providing this interesting project and supervising the thesis as a second reviewer. He pushed me through daily lab work by helping at the bench and controversly discussing results. I deeply acknowledge my co-advisor from the Leibniz Institute ATB Potsdam, Dr. Oliver Schlüter, who was not only kicking off the project, but also gave valuable hints and stimulating suggestions at different stages of my research. Without them, the plasma story would never have started.

I am particularly grateful to Dr. Jörg Ehlbeck and Dr. Karsten Schröder from INP Greifswald for introducing me to the fascinating field of plasma chemistry and for their encouraging help with XPS and CA experiments, which lay the basis for my work. Many thanks as well to Dr. Oliver Görke from the Material Science Department of TU Berlin for his kind help with scanning electron microscopy and for providing spin coating and RFGD plasma facilities.

Many thanks to all the people of the Kroh lab for the warm reception and the nice atmosphere over the years, in particular to Paul Haase, Yvonne Pfeiffer, Daniel Wilker, the “AG PP”, Maria-Anna Bornik and Tamer Moussa Aoub for profound scientific exchange during lunch or coffee breaks. Working with you made even bad days bearable. Thanks as well to Eileen Schulz for her constructive and committed assistance in the lab and to ATB Potsdam, namely to Dr. Martin Geyer, for giving me the great privilege to work and complete this thesis at the TU.

Thanks to my fellow students and friends Dr. Ingo Dönch from MPIKG Golm for sparing his time to help with AFM (unfortunately without success!) and Achim Wiedekind from the FU Chemistry Department for inter-universitary “paper delivery”.

I am furthermore deeply grateful to Dr. Daniel de Graaf and Oliver Kreutzkamp for encouraging me in many difficult times to go ahead with my graduate studies, their perpetual support and cheers.

None of this though would have been possible without the love and care of my parents, Claudia and Bernd, to whom this dissertation is dedicated to. Their upbringing and education helped me to stand upright despite the many setbacks and to carry on with my plans and goals. Thank you for your support and your patience!

Table of Content

1 Abstract

Conventional thermal food preservation methods can significantly change the concentration, bioavailability and bioactivity of phytochemicals in food. These limitations have fostered the development of mild techniques that enhance the shelf-life of foods while maintaining the health-beneficial effects of bioactive compounds. In this context, non-thermal plasma (NTP) seems to be a promising alternative. Due to its efficient inactivation of microorganisms at low temperatures and ambient pressure up to 1 atm (= 1 bar, 1013 mbar) it is already commercially used for the sterilisation of medical devices. Yet, the interactions of plasma-immanent species with dietary bioactive compounds in foods are not clearly understood. This emphasizes the need to elucidate the influence of these highly reactive species on the stability and chemical behaviour of phytochemicals. To this end, specific phenolics and polyphenolics were exposed to various cold gas discharges. The selected substances are ideal target compounds due to their antioxidant activity protecting cells against the damaging effects of reactive oxygen species (ROS), such as singlet oxygen, superoxide, peroxyl radicals, hydroxyl radicals and peroxynitrite. Reactions were carried out at various plasma sources, using different feeding gases, and gas flow rates. The excited gaseous species on the plasma were analysed with optical emission spectroscopy (OES). Degradation was followed by high performance liquid chromatography/diode-array detection (HPLC-DAD). The samples are further characterized using contact angle (CA) measurements, X-ray photoelectron spectroscopy (XPS) and attenuated total reflectance-Fourier transform infrared spectroscopy (ATR-FTIR). Results show that under the influence of non-thermal plasmas, all chosen compounds are degraded in a time- and structure-dependent manner. The degradation is probably due the combined impact of ions, ROS and radicals present in the discharge volume. The formation of carbonyl and carboxyl functions and the decrease of C-C bonds point to an oxidative erosion of the upper monolayers. This is in agreement to results showing that during roasting and cooking processes oxidative species lead to the formation of characteristic low-molecular weight degradation products. Regarding plant systems, plasma treatments significantly raised the flavonoid content in leaf tissue Epicuticular waxes on the abaxial side were visibly degraded. Results are discussed in view of a plasma stimulated biosynthesis and improved extraction properties, respectively.

2 Zusammenfassung

Die Anwendung herkömmlicher thermischer Verfahren zur Lebensmittelsterilisation ist aufgrund der Empfindlichkeit der Nahrungsmittel starken Einschränkungen unterworfen. Unter der Einwirkung von Temperaturen über 100 °C (373 K) werden nicht nur unerwünschte Mikroorganismen, sondern auch wertvolle Nährstoffe verändert. Eine vielversprechende Alternative zu konventionellen Sterilisationsverfahren sind Niedertemperaturplasmen (NTP), für die eine effektive Inaktivierung von Mikroorganismen bei gleichzeitig moderaten Temperaturen nachgewiesen werden konnte. Elektroneninduzierte Ionisations-, Anregungs- und Dissoziationsreaktionen im Plasma führen jedoch zur Bildung von energiereichen und reaktiven Spezies (Ionen, Atome, Radikale, metastabile Zustände, ħω), die ihrerseits durch Wechselwirkung mit Luftmolekülen reaktive Sauerstoff- und Stickstoffspezies bilden können. Dadurch werden in einem Plasma Reaktionswege initiiert, die unter Standardbedingungen gehinderte Reaktionen ermöglichen bzw. zu neuen Zwischen- und Endprodukten führen können, deren Einfluß auf biologische Oberflächen sowie pflanzliche Sekundärmetaboliten bislang völlig unbekannt ist. Ziel dieser Studie war es daher, den Einfluß von Niedertemperaturplasmen auf die Stabilität wertgebender Pflanzeninhaltsstoffe zu charakterisieren. Zu diesem Zweck wurden verschiedene Flavonoide mit unterschiedlichen Plasmaquellen behandelt und anschließend mittels Hochdruckflüssigkeitschromatographie (HPLC-DAD) bzw. oberflächenanalytischen Methoden (Kontaktwinkelmessung, Röntgeninduzierte Photoelektronenspektroskopie, ATR-FTIR) analysiert. Für Polyphenole konnte ein strukturabhängiger Abbau bei bereits geringen Plasmaleistungen beobachtet werden. Die Bildung von Carbonyl- und Carboxylfunktionen und die gleichzeitige Abnahme von C-C-Bindungen weisen auf einen oxidativen Abbau der obersten Monolagen hin, welcher im Hinblick auf einen thermisch-induzierten Abbau diskutiert wird. Desorptionsprozesse durch photochemische oder thermolytische Spaltung wurden hingegen nicht beobachtet. Phenolsäuren zeigten gegenüber der Plasmabehandlung ein inertes Reaktionsverhalten, dessen Ursache bis dato unbekannt ist. Ebenso reagierten glykosidierte Flavonoide langsam und schwach im NTP - ein deutlicher Hinweis darauf, daß die Funktionalisierung bestimmter Positionen im Flavonoidgerüst die antioxidative Wirkung stark verändert. Untersuchungen mit pflanzlichen Systemen ergaben unabhängig von den verwendeten Plasmaquellen ein anderes Bild: So führte bei Feldsalat die Plasmabehandlung

zu einer Abnahme an phenolischen Säuren und einem deutlichen Anstieg des Flavonoidgehaltes. Plasmabehandelte Grünkohl-Proben wiederum zeigten einen verminderten Gesamtphenolgehalt und eine geringere antioxidative Aktivität im Vergleich zu den unbehandelten Kontrollproben. Durch oberflächenanalytische Untersuchungen (u.a. REM) konnte nachgewiesen werden, dass epikutikulare Wachse der Blattoberfläche durch Wechselwirkung mit dem Plasma stark abgebaut werden. Die in diesem Zusammenhang erhöhte Eindringtiefe der plasma-eigenen UV-Strahlung in das Blattinnere wird hinsichtlich einer UV-induzierten Flavonoidbiosynthese als Schutzmechanismus des der Strahlung ausgesetzen Gewebes diskutiert. Als weiterer Erklärungsansatz ist eine durch Zerstörung der Zellmembranen (Zellyse) verbesserte Extrahierbarkeit denkbar.

3 Introduction

The production and consumption of minimally processed or fresh-cut food (fruit vegetables, sprouts) have grown rapidly over the past decades (EU SCIENTIFIC COMMITTEE ON FOOD, 2002), promoted by recent governmental health publicity campaigns (USDHHS AND USDA, 2005) and fitness trends in the western world. The convenience of fresh-cut, pre-washed and packaged salads benefits consumers and provides the industry with considerable savings in transportation, storage, and refrigeration costs (DELAQUIS *et al*., 1999). Unfortunately, all food undergoes varying degrees of biological, chemical and physical deterioration after harvest and during food storage, coming along with losses in nutritional value, safety and aesthetic appeal like colour, texture, and flavour (Figure 1). Pre- prepared raw food is in particular prone to rapid decline in post-processing quality due to undesirable biochemical reactions associated with wound response and microbial decay (BRECHT, 1995) and promoted by increased handling and longer times between preparation and consumption (FAIN, 1996).

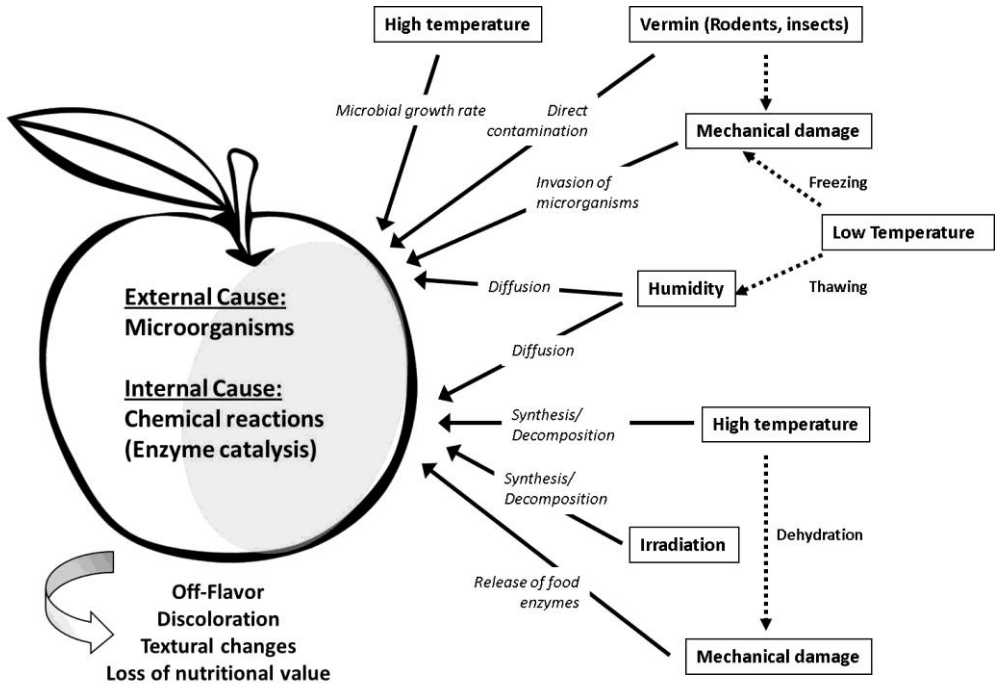

Figure 1. External and internal factors enhancing food deterioration.

Therefore, concomitant with the popularity of pre-processed food (and changed eating habits) an increased number of microbial infections associated with the consumption of fresh-cut fruit and vegetables have been documented (NAT. INST. INF. DIS., 1997; GUTIERREZ,

1997; CUMMINGS *et al*., 2001; DE ROEVER, 1998; FDA, 2006; PHLS, 2000; PEZZOLI *et al*., 2007). The consumption of *E.coli* O157:H7 (postharvest) contaminated lettuce was the cause for several recent foodborne outbreaks (MERMIN *et al*., 1996; ACKERS *et al*., 1996; HILBORN *et al*., 1999; BEUCHAT, 2002; HARRIS *et al*., 2003; DELAQUIS, BACH, AND DINU, 2007). Typical other human pathogens are *Salmonella*, *L. monocytogenes*, *Aeromonas hydrophila*, and *Candida* (ABADIAS *et al*., 2008; BEUCHAT, 1996; FRANCIS, THOMAS, AND O'BEIME, 1999; FEHD, 2002; JOHANNESSEN, LANCAREVIC, AND KRUSE, 2002; SAGOO *et al*., 2003) (Table 1).

Table 1. Typical microorganisms leading to spoilage of vegetable crops (TOURNAS, 2005).

Organism	Type of spoilage	Affected vegetables
Bacteria		
Erwinia carotovora	Bacterial soft rot	Leafy crucifers, lettuce, endives, parsley, celery, carrots, onions, garlic, tomatoes, beets, pepper, cucumbers
Pseudomonas chicoricii	Bacterial zonate spot	Cabbage and lettuce
P. marginalis group	Soft rod	Lettuce
Xanthomonas campestris	Black rot	Cabbage and cauliflower
Fungi		
Alternaria brassicola , *A. oleracea*	Alternaria rot	Leafy crucifers
Botrytis cinerea	Gray mould rot	Leafy crucifers, lettuce, onions, garlic, asparagus, pumpkin, squash, celery, carrots, sweet potatoes
Bremia lactucae	Downy mildew	Lettuce
Geotrichum candidum	Sour rot	Asparagus, crucifers, onions, garlic, beans, carrots, parsley, parsnips, lettuce, endives, tomatoes, globe artichokes

To stop or greatly slow down spoilage and to prevent food-borne diseases, different food preservation techniques such as thermal processing, γ- radiation, exposure to toxic chemicals (O_3, oxirane, H_2O_2) are known. The main objectives of these processes are (i) to guarantee a safe consumption of the processed food, achieved by deactivating, killing or removing harmful microorganisms or substances of biological origin that can be present on the surface of fresh or freshly-prepared food and (ii) to increase the food's shelf life by inhibiting the rate of undesirable chemical reactions (e.g. formation or degradation of food pigments, lipid peroxidation, denaturation of proteins, autolysis, acidification, degradation of bioactive compounds). However, all these methods have in common that they impose a severe stress on the objects to be decontaminated or that a low consumer acceptance or high regulatory hurdles hinder their industrial application (Table 2). There clearly exists a significant economical demand to improve the efficiency of preservation in order to increase

the microbiological stability of minimally processed food while maintaining as much as possible of the pre-harvest quality.

Table 2. Disadvantages of conventional preservation technologies.

Technology	Disadvantages
Heating	Varying susceptibility Nutritional deterioration, modified bioavailability/bioactivity of phytochemicals Colour, flavour, texture changes
Freezing	Varying susceptibility Oxidation (Rancidity and discolouration) Texture changes
Drying	Varying susceptibility (virus resistant) Nutritional deterioration, modified bioavailability/bioactivity of phytochemicals Oxidation (Rancidity and discolouration) Texture changes
Chemical treatment	No complete removal/inactivation for fresh produce[a] High-volume formation of hazardous materials (O_3, glutaraldehyde, Cl_2, H_2O_2, organic acids) Extensive rinsing required Long immersion time High costs, low consumer's acceptance
Irradiation (UV, γ-, β-, X-rays)	Varying susceptibility Formation of toxic compounds in lipid-rich food[b] Off-flavours High costs, low consumer's acceptance

[a] = KOSEKI AND ITOH, 2001; PARK *et al*., 2001; [b]= DELINCÉE AND POOL-ZOBEL, 1998

These limitations have fostered the development of mild food process techniques that assure the inactivation of bacteria and spores or complete elimination of protein contamination, enhance the shelf life of food while maintaining the organoleptic quality, the nutritional value and the health-beneficial effects of bioactive compounds. Mild preservation technologies usually operate at room temperature and thus have a minor impact on the quality and fresh appearance of food products. In this context, NTP operating at atmospheric pressure seem to be a promising alternative to conventional thermal treatments to enhance the shelf-life and prevent the consumer from food-borne diseases. NTP are already known to be very efficient in inactivating bacterial spores (MOISAN *et al*., 2001; LEROUGE, WERTHEIMER, AND YAHIA 2001; LAROUSSI, 2002; LAROUSSI, 2005) and pyrogenic compounds (ROSSI, KYLIÁN, AND HASIWA, 2006; KYLIAN *et al*., 2006; HASIWA *et al*., 2008) (Figure 2).

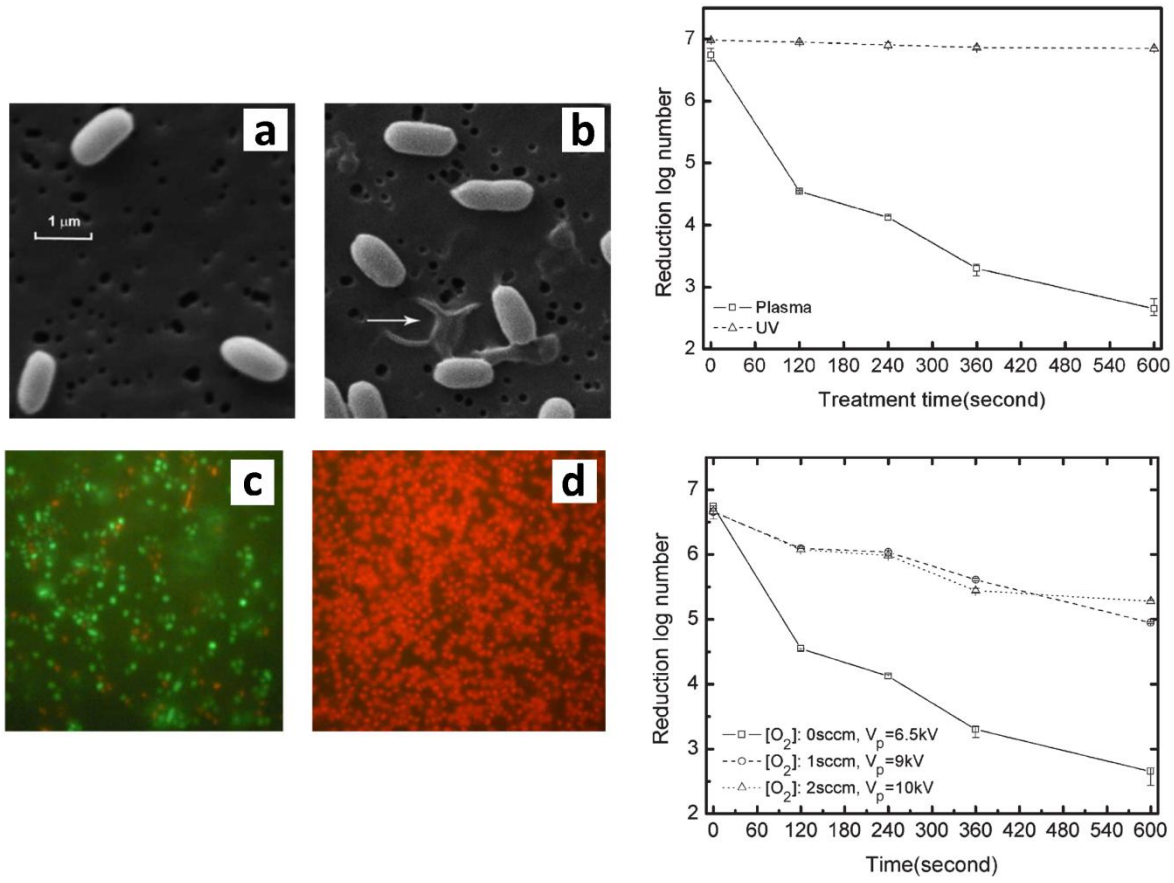

Figure 2. Helium-plasma treatment of *Bacillus subtilis* spores leads to leakage of the cytoplasma and membrane fragmentation as shown by SEM (top) and fluorescence images of propidium iodide of stained spores (below) (a, c) untreated spores, (b, d) after plasma treatment (ruptured spore pointed). Inactivation is clearly induced by plasmas particles than by UV photons of the plasma alone (top, right). Addition of oxygen shows a weaker effect (bottom, right) (DENG *et al.*, 2006).

The efficient inactivation of microorganisms comes along with a moderate heating of the treated surface at ambient pressure up to 1013 mbar (MOISAN *et al.*, 2001). Moreover, cold plasma processes are dry techniques so that no toxic chemicals are left on the objects after the treatment. By-products of sterilization are primarily volatile organic compounds as water or CO, CO_2 which makes plasma processes particularly environmentally friendly. However, in contrast to conventional sterilization where heat or toxic chemicals can rather easily reach even remote areas of complicated shaped objects, the plasma state can only be maintained on finite length scales, such that small geometries are difficult to sterilise (RABALLAND *et al.*, 2008). A long-time disadvantage of plasma techniques was that most of the plasma reactions operated under low pressure conditions (low-pressure plasma, LPP) which required special vacuum sealing and reactant feeding systems and limited the size of selected substrates for surface modification. This was one of the main reasons why applications of plasma were long-time limited to heat-and vacuum resistant materials and mainly used in the

semiconductor and microsystem industry. Today plasmas can operate in open air at ambient pressure (atmospheric pressure plasma, APP), keeping the processing temperature low, which has opened up new fields in plasma science and technology (Figure 3). Much work has already been done in the field of plasma medicine and related topics.

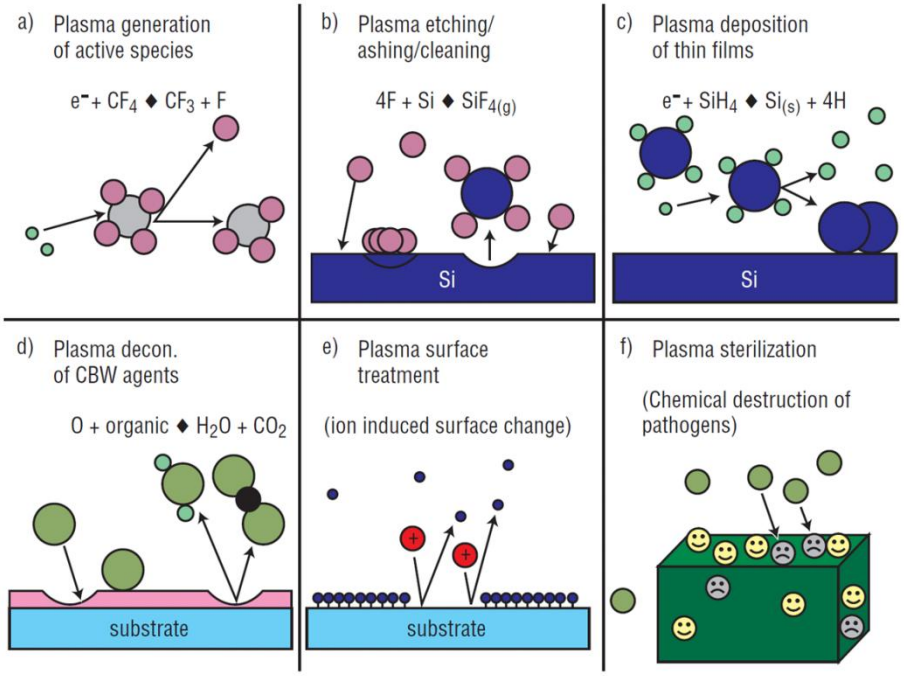

Figure 3. Fundamental processes used in plasma processing of materials (SELWYN *et al.*, 2001).

As a consequence, NTP are already commercially used for the sterilization of medical devices. It is generally believed, that the inactivation is caused by UV radiation which penetrates deep into the cell and cause DNA strand breaks. In contrast to conventional UV C preservation, where shadowing of the UV radiation by multilayered stacks of spores or by biofilms, in which the spores are embedded, can largely reduce the sterilization efficiency, the combined effect of incident UV photons, ions and chemical active species make plasma extremely efficient for decontamination purposes. At typical photon fluxes in low temperature plasma sterilisation times of the order of seconds for inactivating isolated spores are sufficient (PHILIP *et al.*, 2002; HALFMANN *et al.*, 2007). Therefore, in addition to an intense UV photon flux a significant plasma-induced chemical or physical etching of the target system is required, the latter being mild enough to not harm any delicate object being sterilised (RABALLAND *et al.*, 2008). This is especially true for biological systems as food and beverages if plasma-based sterilization once should become a potential option to conventional preservation procedures. Although much work has already been done in

investigating the effects of non-thermal plasma on microorganisms, information of plasma interaction with food or food components is rare. First steps towards an understanding of plasma chemical reactions with biological systems have already been taken and recent research increasingly concentrates on plasma treatment of living vegetative or mammalian cells and tissues (STOFFELS, SAKIYAMA, AND GRAVES, 2008; SHASHURIN *et al*., 2008). Using non-thermal atmospheric pressure plasma jets (APPJ), eradication of yeast grown on agar (KOLB *et al*., 2008), blood coagulation, tissue sterilization (FRIDMAN *et al*., 2006) and ablation of cultured liver cancer cells (ZHANG *et al*., 2008) has been shown. These studies mainly focus on possible medical applications of cold plasma. The idea of applying NTP to enhance the shelf-life of fresh or freshly-prepared food however is new, which is underlined by the fact that the total number of publications dealing with the effects of NTP on food is very limited (the actual number of relevant food related publications to our knowledge is below 20) and essentially date from only the past five years. The majority of the papers report about the inactivation of foodborne pathogens inoculated on fresh food surfaces; a few of them study the influence of plasma on seed germination rate or changes to agrochemicals or other food related organic compounds. All thus have in common that a direct analysis of the food's chemical composition is missing, and that food changes are only studied from an organoleptic, sensory point of view (Table 3). The interest mainly focuses on the inactivation efficiency of cold plasma with respect to contaminated pericarps of mangos, melons or bell pepper (PERNI *et al*., 2008; VLEUGELS *et al*., 2005), fresh cut fruit surfaces (PERNI, SHAMA, AND KONG, 2008; CRITZER *et al*., 2007), or almonds and nuts (DENG *et al*., 2007; BASARAN, BASARAN-AKGUL, AND OKSUZ, 2008). Possible inactivation mechanisms are likely to be associated to plasma-immanent reactive species such as atomic oxygen and OH radicals, since UV photons get easily absorbed in atmospheric air and charged particles cannot access the sample in its downstream position (VLEUGELS *et al*., 2005). The effect of cold low-pressure plasma on two pathogenic fungi (*Aspergillus* spp. and *Penicillum* spp.) inoculated on different seeds and the influence on seed germination has been investigated by Selcuk and co-workers (SELCUK, OKSUZ, AND BASARAN, 2008). While a significant reduction of surface fungal contamination was reported, no relationship was found between the plasma treatment conditions and changes in the food quality (e.g. moisture content, cooking quality, gluten index) of the studied wheat and legumes. For seed germination, effects strongly depended on the feed gas used in the discharge.

Table 3. Plasma Processing of food and food related compounds.

Studied Effect	Target System	Plasma System
Inactivation of bacteria	Apples, melons, lettuce	APP (Air)[a]
	Mangos, melons, bell peppers	APP (He/O_2)[b]
	Apple Juice	APP (Air)[c]
	Sliced cheese and ham	APP (He)[d]
	Almonds	APP (Air)[e]
Inactivation of fungi	Hazelnut, peanut, pistachio nut	LPP (Air, SF_6)[f]
Inactivation of fungi Seed germination Cooking quality	Seeds (tomato, wheat, bean, lentils, barley, oat, soybean, chick pea, rye, corn)	LPP (Air, SF_6)[g]
Seed germination	Seeds (Radish. Pea, soybean, bean, corn)	LPP (CF_4, other)[h]
	Safflower	LPP (Ar)[i]
Degradation of organic compounds/ macro molecules	Pesticides (in maize)	LPP (O_2)[j]
	Mycotoxins	APP (Ar)[k]
	Starch (aq.)	LPP (Ar)[l]
	Proteins (BSA)	APP (He, He/O_2)[m]

[a]= CRITZER *et al.*, 2007; NIEMIRA AND SITES, 2008, [b]= PERNI *et al.*, 2008; PERNI, SHAMA, AND KONG, 2008; VLEUGELS *et al.*, 2005, [c]= MONTENEGRO *et al.*, 2002, [d]= SONG *et al.*, 2009, [e]= DENG *et al.*,2007, [f]= BASARAN, BASARAN-AKGUL, AND OKSUZ, 2008, [g]= SELCUK, OKSUZ, AND BASARAN, 2008,[h]= VOLIN *et al.*, 2000, [i]= DHAYAL, LEE, AND PARK, 2006, [j]= BAI *et al.*, 2009, [k]= PARK *et al.*, 2007, [l]= ZOU, LIU, AND ELIASSON, 2004, [m]= DENG *et al.*, 2007.

The use of N_2 and O_2 resulted in seed surface discoloration, visible damages and a reduced germination (attributed to a degradation of surface polysaccharides; SELCUK *et al.*, 2008), while for plasmas operating with Ar, hydrazine or aniline an increased germination rate has been observed (DHAYAL, LEE, AND PARK, 2006; VOLIN *et al.*, 2000). In all of the aforementioned cases, however, treatment did not adversely affect the appearance of the food and a relation between plasma treatments and perceptual sensory character of the treated food could not be established (Figure 4).

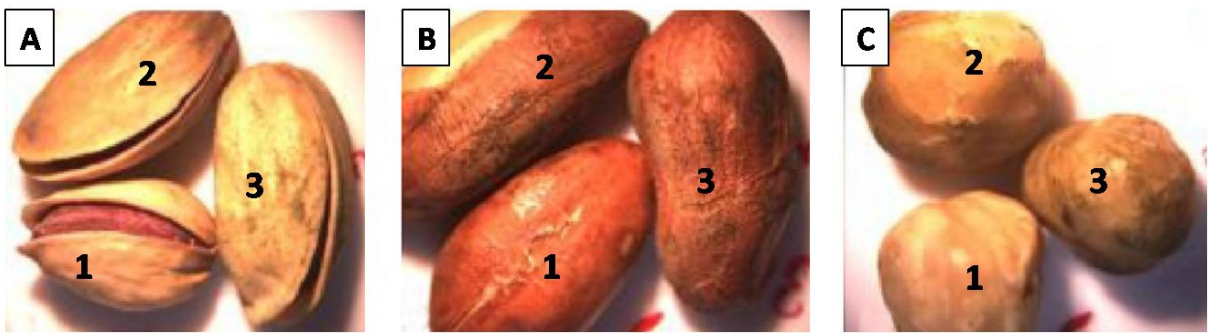

Figure 4. Plasma treated nut samples showed no visual changes after plasma treatment. (A) Pistachio nuts, (B) peanuts, and (C) unshelled hazelnuts (1: no treatment, 2: 10 min SF_6 plasma treatment, 3: 20 min SF_6 plasma treatment (BASARAN, BASARAN-AKGUL, AND OKSUZ, 2008).

Regarding the elimination of organic compounds such as microbial toxins or chemical residues, state-of-the-art literature is broader, covering the fields of pesticide decontamination, and biological as well as chemical warfare agent decontamination (HERRMANN *et al*., 1999; HERRMANN *et al*., 2002). Mycotoxin treatment in a microwave-induced atmospheric pressure argon plasma resulted in a significant time-dependent decrease in aflatoxin B1, deoxynivalenol and nivalenol coming along with a dose-dependent reduced cytotoxity (Park, 2007). A clear plasma parameter dependent reduction has as well been observed for organophosphorus pesticides deposited on solid surfaces (KIM *et al*., 2007), or more recently when fortified in maize (BAI *et al*., 2009). While volatile degradation products have been clearly identified by GC/MS, Bai and co-workers do not report whether and, if so, how plasma treatment affected maize or any of its compounds.

It is a general problem that currently little is known about the effect of plasma treatment on food model substances: The modification of starch in an argon glow discharge plasma was shown by Zou and co-workers. Changes are manifested in a loss of OH groups which is probably due to the cross-linking of α-D-glucose units (ZOU, LIU, AND ELIASSON, 2004). Surface proteins and proteinaceous matters are degraded due to the impact of atomic oxygen playing the dominant role in degradation reactions (DENG *et al*., 2007). A potential synergistic effect of nitric oxide contributing to the decomposition and minor roles for UV photons, OH radicals and O_2 metastable states have been identified (PERNI *et al*., 2007). The complexity of plasma chemistry though makes the explicit elucidation of the underlying reaction pathways a challenging and up to date not fully resolved task.

4 Motivation

It is known that non-thermal plasmas can destroy a wide spectrum of organic compounds as well as biological pathogens. However, the principal mechanisms leading to microorganism or protein elimination remain still unclear and there are many uncertainties with regard to the reaction chemistry of plasma-immanent reactive species (radicals, reactive oxygen and nitrogen species, energetic electrons and ions, VUV and UV photons) with phytochemical compounds. It is therefore of particular interest to elucidate and understand the basic interactions of plasma species with bioactive compounds in order to avoid nutritional degradation or any other undesired effects in future applications. Monitoring the nature and relative abundance of plasma species of the gas phase and identifying structural modifications of surfaces exposed to the discharge are imperative for understanding the mechanisms of plasma-induced chemical reactions and for predicting structural and functional changes of molecular or macroscopical target systems. Given that investigations on plasma-food interactions on a molecular level are still in their infancy, the main object of this study was to ascertain if and how non-thermal plasma is changing the morphological structure and chemical composition of highly perishable fruits and vegetables. To this end the influence of plasma immanent highly reactive species on the stability and chemical behaviour of dietary bioactive food compounds adsorbed on solid surfaces and embedded in a plant matrix is described. Reactions were followed by means of reversed-phase high-performance liquid chromatography (RP-HPLC). Samples were further characterized using CA measurements, X-ray photoelectron spectroscopy and attenuated total reflectance Fourier-transform infrared spectroscopy. Changes in the plant surface morphology were followed by scanning electron microscopy (SEM). The outcomes of this work represent a first step towards a molecular approach of plasma-food interactions and aim to open up novel insight into the reaction of flavonoids with reactive oxygen species at the solid-gas interface.

5 Theory

5.1 Introduction to Plasma Chemistry

In the following, the basic concepts of plasma physics and the consequences for plasma chemistry are described. Focus will be put on the description of non-thermal laboratory plasmas. For a more detailed derivation of plasma physics fundamentals, several excellent textbooks are recommended (PERRUCA, 2010; FRIDMAN, 2004, FRIDMAN AND KENNEDY, 2008).

5.1.1 Plasma as 4th State of Matter

Based on the idea that phase transitions occur by continuously supplying energy to a system, various states of matter are recognized. Besides the 'traditionally' known solid state, liquid and gas phase and the more recently found low-temperature states (BOSE-EINSTEIN condensate), high-temperature states, such as plasmas exist. Although the generation of a plasma from the gas phase (Figure 5) is strictly spoken not a real phase transition, plasma was recognized as the 4th state of matter due to its distinct properties, which substantially discriminates it from the gas phase.

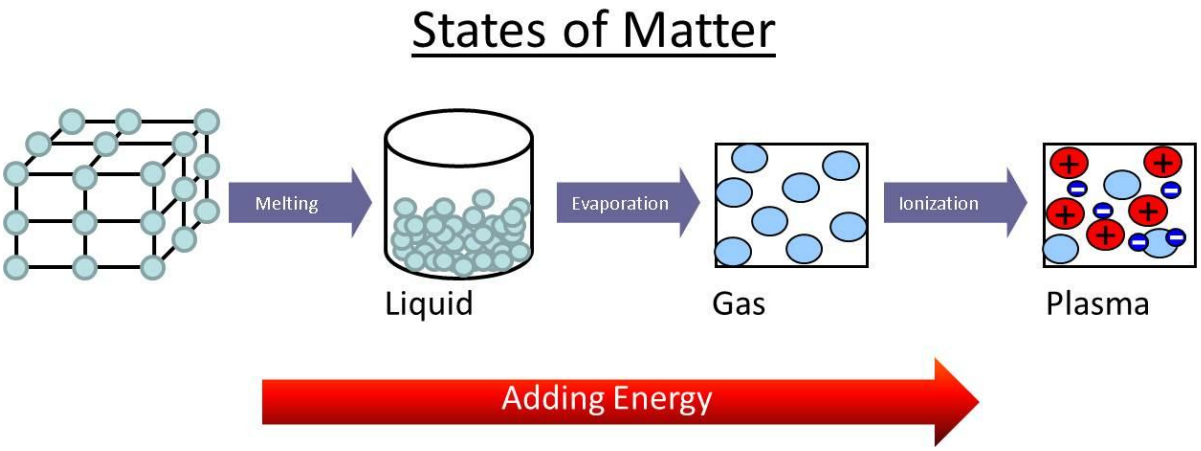

Figure 5. Four states of matter. Plasma is characterized by a collective behavior of its free charge carriers.

The term plasma was first used by Lewi Tonks and Irving Langmuir (LANGMUIR, 1928), defining a state of matter in which a significant and equal number of atoms and/or molecules are electrically charged or ionized. In contrast to ideal gases, ionized gases exhibit a dynamic, collective behavior due to long-range COULOMB interactions, originating from

electromagnetic coupling between the charged particles (COULOMB attraction and repulsion) and electric and magnetic collective perturbations (due to free charge carrier motions). Although this makes any theoretical description a challenge, biasing the collective behavior by applying suitable electromagnetic fields leads to a temporary spatial confinement of the plasma and thereby allows a certain controlling of the plasma dynamics.

5.1.2 Thermal and Non-Thermal Plasmas

Another fundamental characteristic of plasmas is the existence of multiple temperature regimes, related to different plasma particles and degrees of freedom. From kinetic theory of gases, the plasma species temperature T is related to the average kinetic energy <ε> of the particles in the system (eq. 1), derived from the velocity distribution function second order momentum (eq. 2).

$$< \varepsilon > = \frac{3}{2} k_B T \tag{1}$$

$$= \int_{-\infty}^{+\infty} \left(\frac{1}{2} m v^2 \right) \mathrm{f}(v) \mathrm{d}v \tag{2}$$

with k_B = BOLTZMANN constant,
T = temperature,
m = mass,
v = velocity

Unless quantum effects can be neglected, the velocity distribution function f(v) is given from MAXWELL-BOLTZMANN statistics (eq. 3).

$$\mathrm{f}(v)\,\mathrm{d}v = \frac{N(v)}{N}\,\mathrm{d}v = \frac{D(v)\; N_\varepsilon \mathrm{d}v}{\int_0^{+\infty} D(v)\; N_\varepsilon \mathrm{d}v} = \left(\frac{m}{2\pi\, k_B T} \right)^{3/2} 4\pi v^2 \exp\left(-\frac{m v^2}{k_B T} \right) \mathrm{d}v \tag{3}$$

with D(ε) = density of states with energy ε in interval [ε, ε + dε],
N = total number of particles in the system,
N(ε) = fraction of particles with energy ε in interval [ε, ε + dε]

Due to the large difference in mass, electron velocities are several orders of magnitude higher than nuclei velocities. Hence the electronic motion can be described as the motion of the electrons within the field of stationary nuclei (adiabatic system).

A common classification of plasmas is done in terms of their thermodynamic properties by which thermal plasmas (TP) and non-thermal plasmas, also regarded as plasmas in thermodynamic equilibrium and non-equilibrium plasmas, can be discriminated (Table 4).

Table 4. Subdivision of plasmas (RUTSCHER, 2008).

Thermal Low Temperature Plasma	$T_e \approx T_i \approx T \leq 2 \times 10^4$ K	e.g., arc plasma at normal pressure
Non-thermal Low Temperature Plasma	$T_i \approx T \approx 300$ K; $T_i << T_e \leq 10^5$ K	e.g., low-pressure glow discharge
High-temperature plasma	$T_e \approx T_i \geq 10^7$ K	e.g., fusion plasmas

Thermal plasmas are characterized by (nearly) total ionization of the system. In these plasmas the collision frequency is high with respect to the particles transit time on the plasma scale length, so that the efficient energy transfer in electron-ion collisions leads to thermalization of the different particle species to the thermodynamic equilibrium temperature with the energy content equally shared among vibration, rotation and translation energies (Equipartition theorem). Due to the extremely high energy content fragmentation reactions of all organic molecules present in the plasma to atomic levels are induced and the application of these so-called hot plasmas is often limited. Partially ionized plasmas in contrast are in a thermodynamic non-equilibrium state: While electrons are found to have temperatures of the order of 10^4 K heavy weight particles (neutrals and ions), representing the main plasma compounds, may be at almost ambient temperature. Due to the low electron heat capacity and density n_e, collisions of the electrons with the background gas and to the walls are inefficient in terms of energy exchange. The plasma temperature therefore is determined by the interactions of the neutrals or ions with walls and is generally close to room temperature. Although NTP are in a steady, non-local thermodynamical equilibrium, thermal equilibrium among identical particle species populations is maintained so that NTP as well can be described in MAXWELL-BOLTZMANN formalism. If the interactions among different species (e.g. electron-ion or electron-neutral collisions) increase either by increase of the pressure or the density of the electrons, the electron and gas temperatures tend to equilibrate and converge to similar values (Figure 6).

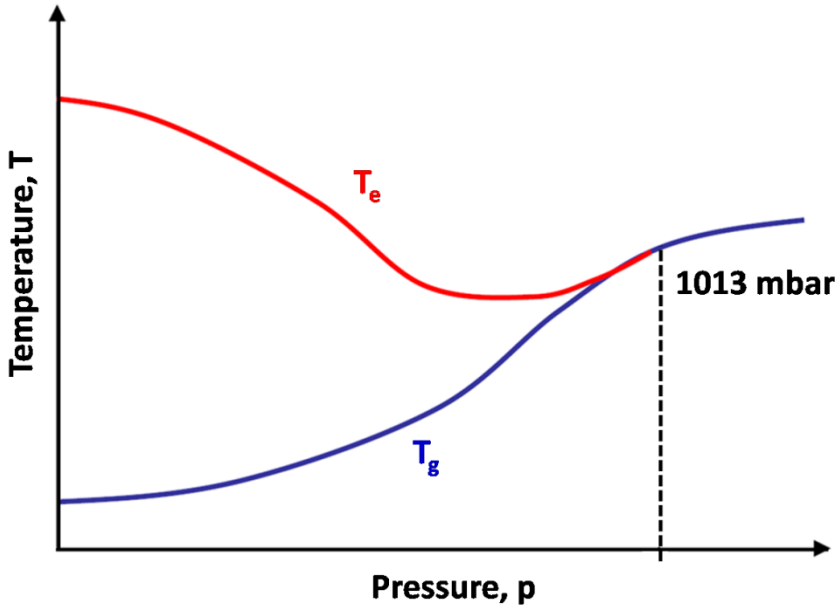

Figure 6. Electron and ion temperatures as a function of gas pressure. With rising pressure the individual temperatures converge as a result of increasing collisions between electrons and ions (adapted from VON KEUDELL, 2008).

5.1.3 Plasma Parameters

A key parameter of plasmas is the plasma density, n, which is the sum of the electron density n_e and the ion density, n_i. The importance of n derives from the fact that the efficiency and the reaction rates of almost all plasma processes are directly related to n. Plasma particles can be characterized by their mean free path λ (eq. 4).

$$\lambda = \left(\frac{k_B T}{\sqrt{2}\pi p r_g^2} \right) \tag{4}$$

with k_B = BOLTZMANN constant,
T = gas temperature,
p = gas pressure,
r_g= radius of the particle

λ represents the average distance, a single particle traverses in rectilinear motion within a cubic box with volume V and edge length l between successive scattering by other particles or collision to the wall. The degree of ionization, α, defines the fraction of ionized particles in the gas:

$$\alpha = \frac{n_i}{n} \tag{5}$$

with n = particle density,
n_i= ion density

Considering that only single-charged ions are present (which is generally fulfilled in case of non-thermal plasmas), the densities of electrons and positive ions are equal and the plasma is electrically neutral (quasi-neutrality). Local spatiotemporal deviations of the quasi-neutrality, responsible for the existence of COULOMB potentials in the plasma, are confined in time (frequency) and space by the plasma frequency and DEBYE length. The latter is a characteristic feature of charged liquids and plasmas, representing the characteristic distance over which the plasma enforces charge neutrality. Due to the larger mass of the nuclei, only the small and mobile electrons can respond immediately to perturbations and participate in restoring a charge imbalance. The DEBYE length (eq. 6) describes the attenuation of a COULOMB potential V_0 produced by a local charge in the plasma by electrical shielding of each charged particle with surrounding particles of opposite polarity (eq. 7).

$$\lambda_D = \left(\frac{\varepsilon_0 k_B T_e}{n_e q_e^2} \right)^{1/2} \tag{6}$$

$$V(d) = \frac{q_e}{4\pi\varepsilon_0 d} \exp\left(-\frac{d}{\lambda_D} \right) = V_0 \exp\left(-\frac{d}{\lambda_D} \right) \tag{7}$$

with ε_o the vacuum permittivity,
k_B the BOLTZMANN constant,
n_e, T_e, and q_e the electron density, temperature, and charge
d the distance

For a many particle system, the number of particles present in the volume defined by λ_D (DEBYE sphere) has to be small in order to fulfil the plasma approximation. Departure from this limit implies that pairwise interactions (i.e. collisions) become more relevant and dominate over collective electrostatic interactions. In this case the plasma may not be treated as an ideal gas. The response to the perturbation will be through rapid oscillations of the electron density (LANGMUIR waves). The rate of these oscillations can be determined by the electron plasma frequency (LANGMUIR frequency), $\omega_{p,e}$ (eq. 8).

$$\omega_{p,e} = \left(\frac{n_e q_e^2}{m_e \varepsilon_0} \right)^{1/2} = \frac{1}{\lambda_D} \left(\frac{k_B T_e}{m_e} \right)^{1/2} = \frac{1}{\lambda_D} \langle v_e \rangle \tag{8}$$

with ε_o the vacuum permittivity,
k_B the BOLTZMANN constant,
n_e, T_e, and q_e the electron density, temperature, and charge,
m_e = electron mass,
v_e = velocity of electrons

The electron plasma frequency is a measure of the electron density, influencing the transmission (or damping) of specified frequency external electromagnetic waves. As a consequence, if a perturbation of frequency $\omega < \omega_{p,e}$ occurs, electrons react quickly and neutrality of the plasma is maintained. In case of $\omega > \omega_{p,e}$ electrons are not able to shield out perturbations of the plasma.

Plasma quasi-neutrality is violated only in a close vicinity of surfaces bounding the plasma or immersed into the plasma. The region where the quasi-neutrality condition is not satisfied is called a plasma sheath. Across this sheath ions are accelerated from within the plasma to the surface. Due to the higher thermal velocity, electrons exhibit a higher flux towards surfaces than the heavier ions (by two orders of magnitude because of the disproportioned mass ratio $m_e/m_i << 1$). As a result they are rapidly lost to the walls. This lack of negatively charged particles leads to the formation of a positively charged layer of several DEBYE length thickness in the vicinity of the surface. An electric field directed from the plasma to the walls develops. The sheath potential of a planar surface (eq. 9) is rapidly decreasing within the plasma sheath space-domain and approaching zero close to the walls. Within the sheath electrons are reflected by the sheath potential whereas ions are accelerated towards the walls, causing ion bombardment of the surface.

$$V_S = \frac{k_B T_e}{2q_e} \ln\left(\frac{m_e}{2.3m_i}\right) \tag{9}$$

with k_B the BOLTZMANN constant,
m_e, T_e, and q_e the electron mass, temperature, and charge,
m_i = ion mass

The thermal DE BROGLIE wavelength λ_{dB} is the average DE BROGLIE length of a particle in an ideal gas:

$$\lambda_{dB} = \frac{h}{\sqrt{2\pi m k_B T}} \tag{10}$$

with: h, the PLANCK constant ,
T= thermodynamic particle temperature,
m = particle mass

To consider the plasma as a classical system that can be described by MAXWELL-BOLTZMANN statistics, λ_{dB} has to be on the order of or lower than the mean interparticle distance or the

nearest neighbor distance in COULOMB interactions. Otherwise degeneracy of states occurs and the gas has to be described by FERMI–DIRAC or BOSE–EINSTEIN quantum statistics depending on the nature of the gas particles.

5.1.4 Plasma Generation and Sources

Laboratory plasmas can be generated by supplying energy to a neutral gas. This can be done in principal regardless of the nature of the energy source employed. Plasma generation can be therefore of mechanical, radiant, chemical and thermal origin or occur under the influence of electric and electromagnetic fields with sufficient high field strength, E_0. As the lifetime of the individual plasma particles may be small due to collision with walls and radiant processes, the energy lost to the surroundings must be supplied continuously to the system to sustain the plasma state. Electrical energy has been shown to be the most suitable for balancing energy losses. Therefore electrical discharges are the most common for generating non-thermal plasmas. Plasmas can be operated continuously (CW) or pulsed, in closed (cavities) or open structures (e.g. surfatron, plasma jet). They show distinct differences in the physical shape but also in the temporal behaviour of the sustaining electric field. Depending on the nature of the initiating and sustaining electric and electromagnetic fields, many types of plasmas sources, including inductively and capacitively coupled installations can be recognized (direct current (DC) and alternating current (AC) plasmas, low- and high-frequency, microwave based discharges (e.g. electron cyclotron resonance plasmas, ECR). The various geometries of the reactors and the number and location of the electrodes employed (electrode systems involving two or multiple electrode configurations or electrodeless systems) make the number of plasma reaction chambers almost countless and technological applications of plasmas formed in these sources are numerous. Several features however make radio-frequency (RF) configurations the most popular laboratory plasmas.

5.1.5 Elementary Plasma Chemical Reactions

Plasma chemistry can be divided into two parts: A volume chemistry, which deals with the formation and loss reactions of species in the discharge volume and a surface chemistry, implying adsorption and desorption of molecules at the substrate surface or etching.

5.1.5.1 Volume Chemistry

Gas ionization is initiated if the applied voltage is greater than the ionization potential of the gas used. Free charge carriers, always present in small amounts in a neutral gas due to the influence of cosmic rays or radioactive radiation, are accelerated by the electric or electromagnetic fields during their mean free path, causing the gas to break down. By electron impact various reactions are initiated. Elastic collisions are characterized by kinetic and internal energy conservation of the colliding particles which results in geometrical scattering events and a redistribution of kinetic energy. The average fraction γ of kinetic energy transferred is determined by the mass ratio of the particles:

$$\gamma = \frac{2m_e M}{\left(m_e + M\right)^2} \qquad (11)$$

with M= mass of heavy particle,
m_e= mass of electron

For an elastic collision of an electron with a heavy target, such as an argon atom, $m_e << M$ and hence, $\gamma = 2m_e/M$, which means that the fraction of transferred energy is very small ($\gamma = 10^{-4}$). By contrast, a significant amount of energy is exchanged in a collision between electrons. All other collisions, like ionization are inelastic. Electrons can transfer almost all its energy to the heavy particle, creating energetic plasma species by which the plasma state is sustained. Inelastic collisions involve energy transfer in amounts that vary from less than 0.1 eV (for rotational excitation of molecules) to more than 10 eV (for ionization). Processes, in which the internal energy is transferred back into kinetic energy, are referred to as superelastic collisions.

The elementary processes by which plasma-immanent species are generated can be divided into primary and secondary processes. Primary processes start with the electrons accelerated by the external electric field. Energy is transmitted through inelastic collisions to the various plasma components and specific degrees of freedom of the system, which leads to excitation, ionization, dissociation, and further electron impact reactions, like dissociative ionization or dissociative attachment (Table 5).

Table 5. Gas phase reactions involving electrons.

Reactions	Description	
$AB + e^- \rightarrow AB + e^-$	Elastic Scattering	(R1)
$AB + e^- \rightarrow AB^* + e^-$	Excitation	(R2)
$AB^* + e^- \rightarrow AB + e^- + \hbar\omega$	De-excitation	(R3)
$AB + e^- \rightarrow AB^+ + 2e^-$	Ionization	(R4)
$AB + e^- \rightarrow A + B + e^-$	Dissociation	(R5)
$AB + e^- \rightarrow A + B + e^-$	Fragmentation	(R6)
$AB + e^- \rightarrow A + B^+ + e^-$	Dissociative Ionization	(R7)
$AB + e^- \rightarrow A + B^-$	Dissociative Attachment	(R8)
$A^+ + B + e^- \rightarrow A + B$	Volume Recombination	(R9)

Ionization follows various mechanisms (Figure 7): In non-thermal plasmas direct ionization of neutral, ground-state atoms, molecules, or radicals by electron impact is the most prominent ionization mechanism, when the electron energy does not greatly exceed the ionization potential (IP). In case of molecular targets, dissociation occurs for collisions having threshold energies higher than IP, followed by excitation (transition b) or further ionization (transition c). Electronic transitions are vertical following the FRANCK-CONDON principle.The dissociative ionization proceeds via electronic excitation into a repulsive state of AB^+ followed by its decay. In secondary reactions, these species and some of the neutral compounds (e.g. radicals) interact not only with the electric and electromagnetic fields but as well with each other, leading to recombination, neutralization, fragmentation and agglomeration (oligomerization). Processes such as resonant and non-resonant charge transfer and energy transfer reactions (Table 6) can occur. Other ionization processes taking place are due to collisions of heavy particles, provided that the total energy of the colliding particles exceeds the ionization potential.

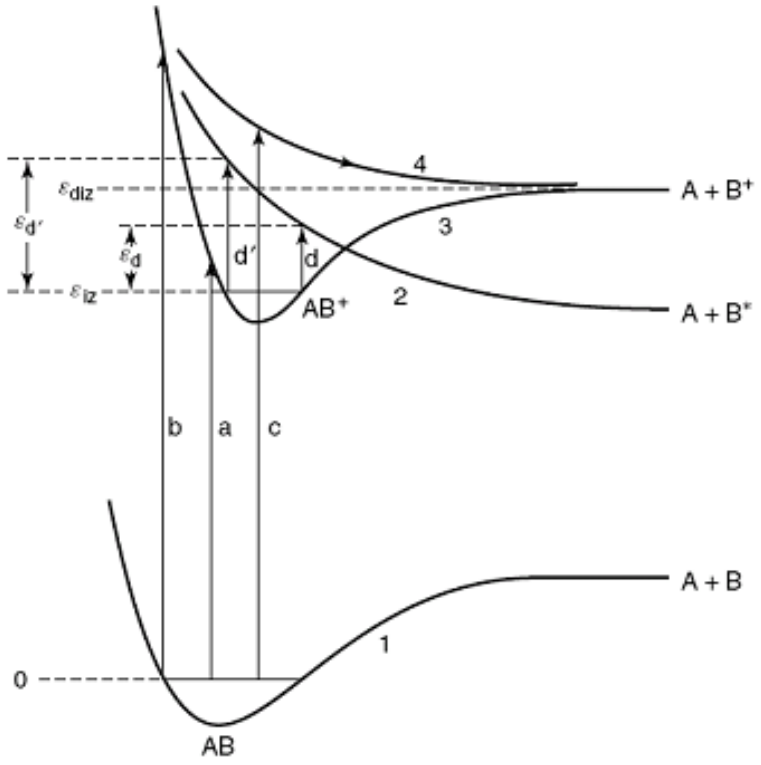

Figure 7. One-dimensional potential energy surfaces for collisional excitation and ionization of molecules AB and AB^+ by electron impact. Energy transfer results in different electronic states according to the FRANCK-CONDON principle. If the energy transferred from electron impact exceeds the ionization energy ε_{iz}, dissociation may occur (transitions b and c; PERRUCA, 2010).

However, they are often not very efficient in energy transfer to valence electrons inside an atom because the process is far from resonant. One example of heavy particle impact ionization is the so-called PENNING ionization (eq. R12) which usually proceeds by the intermediate formation of an unstable excited-state molecule in the state of auto-ionization. Ionization is even possible if the total energy of the colliding particles is not sufficient, supposed that crossing of the electronic energy term of the colliding particles with an electronic energy term of AB^+ exists This non-adiabatic process is called associative ionization (eq. R13) and is limited to only a few numbers of excited species (FRIDMAN, 2008).

Table 6. Gas phase reactions involving Ions and neutrals.

Reactions	Description	
$A^+ + B \rightarrow A + B^+$	Charge Transfer	(R10)
$X^* + AB \rightarrow AB^* + X$	Energy Transfer	(R11)
$X + AB \rightarrow AB^+ + e^- + X$	PENNING Ionization	(R12)
$A^* + B \rightarrow AB^+ + e^-$	Associative Ionization	(R13)
$\hbar\omega + A \rightarrow A^+ + e^-$, $\lambda < 12.400/IP(eV)$ Å	Photoionization	(R14)

Photoionization (eq. R14) as a result of the collision of neutrals with photons ħω usually does not play a significant role due to the low concentration of high-energy photons in most discharge systems. Cross-sections however are quite high (Table 7).

Table 7. Photoionization cross sections (FRIDMAN, 2008).

Atoms / molecules	Wavelength, λ [Å]	Cross sections [cm²]
Ar	787	3.5×10^{-17}
Ne	575	0.4×10^{-17}
He	504	0.7×10^{-17}
H	912	0.6×10^{-17}
O	910	0.3×10^{-17}
H_2	805	0.7×10^{-17}
N_2	798	2.6×10^{-17}
O_2	1020	0.1×10^{-17}

Just as the so-called stepwise ionization by electronically excited neutrals (FRIDMAN, 2008; FRIDMAN AND KENNEDY, 2004), these processes are limited to or mostly important in thermal plasmas. In non-thermal plasmas this process occurs mainly in some mechanisms of propagation. As can be seen, a wide variety of different species is formed and many more, two-body and three-body processes, including association, dissociation, recombination, attachment, detachment, and excitation transfer processes of increasing complexity may occur.

5.1.5.2 Plasma-Surface Interactions

Many fundamental processes take place at the plasma-substrate interface (Table 8). The surface undergoes bombardment by fast electrons, ions, and free radicals, combined with the continued electromagnetic radiation emission in the UV-vis spectrum enhancing chemical-physical reactions in order to obtain the desired functional and aspect geometries. The most prominent one is the secondary electron emission from solids, related to surface bombardment by various electrons, ions or metastable states, evidenced from the detection of Auger electrons. The minimum energy required to remove an electron from the highest filled level in the FERMI distribution of a solid into vacuum (to a point immediately outside the solid surface) is given by the work function eϕ, with ϕ being the electron emission

potential. The energy can be provided thermally (phonons, k_BT), photons ($\hbar\omega$) or from the internal potential energy or kinetic energy of atoms and ions or metastable excited states.

Table 8. Plasma-surface reactions (adapted from BRAITHWAITE, 2000).

Reactions	Description	
AB + C(solid) → A + BC(gas)	Etching	(R15)
AB(gas) + C(solid) → A(gas) + BC(solid)	Deposition	(R16)
$e^- + A^+ \rightarrow A$	Recombination	(R17)
$A^* \rightarrow A$	De-excitation	(R18)
$A^* \rightarrow A + e^-$ (from surface)	Secondary Emission	(R19)
A^* (fast) → $A + e^-$ (from surface)	Secondary Emission	(R20)

In the first case, thermionic emission can be estimated from RICHARDSON-DUSHMAN equation:

$$J = AT^2 e^{\left(-\frac{e\phi}{k_B T}\right)} \qquad (12)$$

with J is the emitted electron density,
***T* the absolute temperature,**
k_B the BOLTZMANN's constant
A the RICHARDSON's constant, $A = 4\pi m k_B^2 e/h^3$, having the theoretical value 120 amp cm^{-2} deg^{-2}

The thermionic current shows strong temperature dependence. Since *A* contains the reflection coefficient, which varies with temperature, experimentally found values for *A* are usually lower than predicted. According to EINSTEIN's equation for the photo effect, photoelectrons are emitted if the photon energy is greater than the work function Φ of a solid,

$$h\nu = \Phi + \frac{1}{2} m_e v^2 \qquad (13)$$

with h= PLANCK constant,
ν = frequency,
m_e = mass of photoelectron,
v= velocity of photoelectron

In case of molecules in the gas phase, the work function is replaced by the ionization energy. Photoelectron emission is characterized by the quantum yield φ which gives the ratio of emitted electrons per quantum $\hbar\omega$ of radiation. The photoelectric effect takes place with photons with energies from about a few electronvolts (1 eV-100 keV). Electron emission stemming from heavy particle impact is another important mechanism. In this case recombination of positive ions on a surface releases an amount of energy equivalent to the

binding energy. If the total ion energy exceeds twice the work function on the surface then in addition to neutralization a secondary electron may be released (BRAITHWAITE, 2000),

$$\frac{1}{2} m_i v_i^{\,2} + q_e V_i \geq 2\Phi \qquad (14)$$

with m_i = mass of ion,
v_i = ion velocity,
q_e = elementary charge,
V_i = electrostatic potential of the ion,
Φ= work function of the solid

5.1.6 Plasma Immanent Species

Plasma basically is an ensemble of charged, and neutral, ground-state and excited species like electrons and ions, atoms, molecules, radicals and their corresponding fragments or oligomers, and photons, covering a broad spectrum of radiation ranging from the infrared to the deep ultraviolet. Ions do not necessarily have to be positively charged. In gases of 'electronegative' gases, like O_2, Cl_2, SF_6 that are constituted of atoms of high electron affinity, negative ions can be as well effectively formed. Radicals in turn are often reactive oxygen species, if the plasma is generated with oxygen as feed gas or if mixing with ambient air is possible. Presence and concentration of plasma active species is strongly dictated by the operational parameters of the plasma discharge used. Since electrons initialize ionization, changes of the electron gas (density, temperature, electron energy distribution function, (EEDF)) strongly influence the formation, the concentration and chemical reaction rate of reactive species and the intensities of the different wavelength emissions. The electron gas parameters in turn depend on the operational parameters of the plasma (power, excitation frequency, gas flow and pressure) and can therefore all be controlled to some extent by controlling the plasma conditions (LEROUGE, WERTHEIMER, AND YAHIA, 2001; WROBEL, LAMONTAGNE, AND WERTHEIMER, 1988). For simplicity's sake we focus in this section on the most important species and their reactions in rare gas or oxygen plasmas. For nitrogen plasmas or air plasmas further information can be found in BECKER *et al*. (2004).

5.1.6.1 Electrons

Plasma electrons are not monoenergetic. This is important as the rates of plasma-chemical reactions depend on the number of electrons with energy equal or higher to the reaction-specific threshold. The probability density for an electron having a specific energy ε can be described by means of the EEDF which can be determined experimentally from the second

derivative of an electron current-voltage (IV)-curve as measured by a LANGMUIR-probe. The EEDF strongly depends on the electric field and the gas composition in a plasma and often is very far from being a real equilibrium distribution. Due to the various assumptions made in the quasi-equilibrium MAXWELL-BOLTZMANN approximation, the EEDF of non- local thermodynamic equilibrium (LTE) plasmas is often better approximated by the DRUYVESTEYN distribution function (eq. 15).

$$f(\varepsilon) = 1.04\langle\varepsilon\rangle^{-3/2}\,\varepsilon^{1/2}\exp\left(-\frac{0.55\varepsilon^2}{\langle\varepsilon^2\rangle}\right) \tag{15}$$

As can be seen in Figure 8, the DRUYVESTEYN distribution function is characterized by a shift toward higher electron energies.

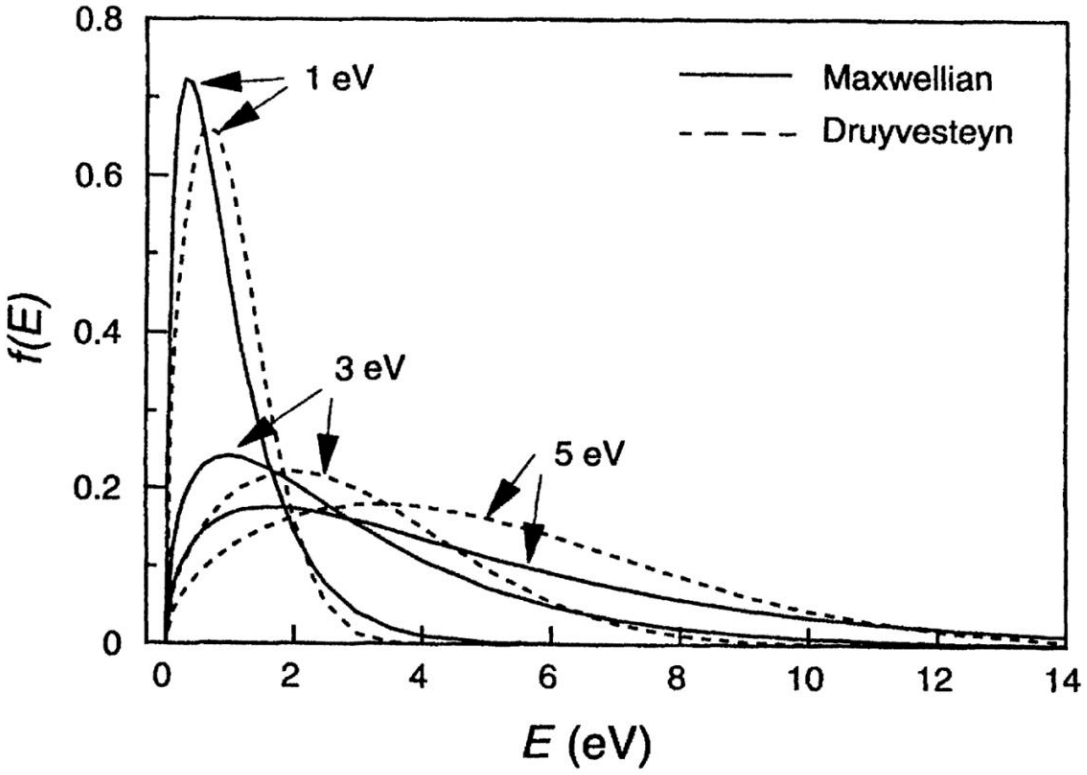

Figure 8. Electron energy distributions according to DRUYVESTEYN and MAWELL. The numbers indicate the average electron energy for each distribution (GRILL, 1994).

Both energy distributions however, regardless of the adopted approximation, show an important fact: While the majority of the electrons in non-LTE plasma have a low electron energy range (0.5-4 eV), there exist a very small but significant number of electrons characterized by a depleted high-energy tail region (8-15 eV). Though small in concentrations, these electrons significantly influence the overall reaction rates in a plasma,

contributing to reactions, requiring a specific energy threshold value. Most of the electrons in NTP have energies high enough to dissociate almost all chemical bonds involved in organic compounds (Table 9).

Table 9. Dissociation energies of organic compounds (MATHEW *et al*., 2008).

Bond type	Bond energy ($kJmol^{-1}$)	Bond energy (eV)
C-H	411	4.25
C-C	346	3.56
C-N	276	2.86
C-O	358	3.70
C-S	272	2.80
C=C	602	6.23
C=O	724	7.50
C≡C	835	8.65
N-H	385	3.99
O-H	456	4.73

5.1.6.2 Ions

The importance of ions in plasma chemistry has been the subject of debate for many years. As ionization rates are lower than those for molecular dissociation, radical species density can be orders of magnitude higher than that of ions. Therefore, plasma chemistry was inferred of being mainly governed by radical reactions, or by photochemical means. Nowadays, the role of ions is critically reviewed. Due to the often high kinetic energy they gain in the plasma sheath, ions are considered to substantially contribute to plasma-chemical kinetics (BECKER *et al*., 2004). Reactions with neutrals and electron-ion recombinations are strongly exothermic processes; dimer and cluster ions such as He_2^+, N_3^+ or N_4^+ have been confirmed recently by MS measurements (STOFFELS *et al*., 2006, STOFFELS *et al*., 2007). Ion formation reactions have been already discussed in chapter 5.1.5. The various loss channels of positive and negative ions are listed in Table 10.

Table 10. Loss reactions of positive and negative ions in plasma (FRIDMAN, 2008).

Reactions	Description	
$e^- + AB^+ \rightarrow (AB)^* \rightarrow A + B^*$	Dissociative Electron-Ion Recombination	(R21)
$e^- + A^+ \rightarrow A^* \rightarrow A + \hbar\omega$	Radiative Electron-Ion Recombination	(R22)
$2\ e^- + A^+ \rightarrow A^* + e^-$	Trimolecular Electron-Ion Recombination	(R23)
$A^- + B^+ \rightarrow A + B^*$	Bimolecular Ion-Ion Recombination	(R24)
$A^- + B^+ + M \rightarrow A + B + M$	Trimolecular Ion-Ion Recombination	(R25)
$e^- + M \rightarrow (M^-)^* \rightarrow M^- + \hbar\omega$	Radiative Electron Attachment	(R26)
$e^- + A + B \rightarrow A^- + B$	Trimolecular Electron Attachment	(R27)
$A^+ + B \rightarrow A + B^+$	Ion-Atom Charge Transfer	(R28)
$A^+ + 2\ A \rightarrow A_2^+ + A$	Ion Conversion	(R29)
$e^- + AB \rightarrow A^+ + B^- + e^-$	Polar Dissociation	(R30)
$e^- + A^- \rightarrow A + 2\ e^-$	EIectron Attachment	(R31)

When the pressure is elevated (p> 1013 mbar) and electron energies are too low for dissociative attachment, third- order kinetic processes such as three-body electron attachment are feasible (Table 11).

Table 11. Reaction rate coefficients of electron attachment to oxygen molecules at room temperature and different third-body partners (FRIDMAN, 2008).

Three-body attachment	k_{298} ($cm^6\ s^{-1}$)	Three-body attachment	k_{298} ($cm^6\ s^{-1}$)
$e^- + O_2 + Ar \rightarrow O_2^- + Ar$	3×10^{-32}	$e^- + O_2 + Ne \rightarrow O_2^- + Ne$	3×10^{-32}
$e^- + O_2 + N_2 \rightarrow O_2^- + N_2$	1.6×10^{-31}	$e^- + O_2 + H_2 \rightarrow O_2^- + H_2$	2×10^{-31}
$e^- + O_2 + O_2 \rightarrow O_2^- + O_2$	2.5×10^{-30}	$e^- + O_2 + CO_2 \rightarrow O_2^- + CO_2$	3×10^{-30}
$e^- + O_2 + H_2O \rightarrow O_2^- + H_2O$	1.4×10^{-29}	$e^- + O_2 + H_2S \rightarrow O_2^- + H_2S$	10^{-29}
$e^- + O_2 + NH_3 \rightarrow O_2^- + NH_3$	10^{-29}	$e^- + O_2 + CH_4 \rightarrow O_2^- + CH_4$	$>10^{-29}$

Ion chemistry of atmospheric plasmas is said to be rich. One example is the ion-induced formation of dangling bonds, acting as chemisorption sites for alkyl or any other free radicals (VON KEUDELL AND JACOB, 2004). Their formation from impinging energetic ions has been recently demonstrated by particle beam experiments (KYLIÁN *et al*., 2009; RABALLAND *et al*., 2008). The surface active sites can in a second step be attacked by oxygen species (atomic or molecular oxygen) which leads either to fast passivation of the surface defect structure giving rise to various oxygen functional groups (Figure 9) or gradual volatilization occurs, namely of H_2O, ·OH, CO and CO_2, which diffuse from the bulk to the surface and desorb (COBURN AND WINTERS, 1979).

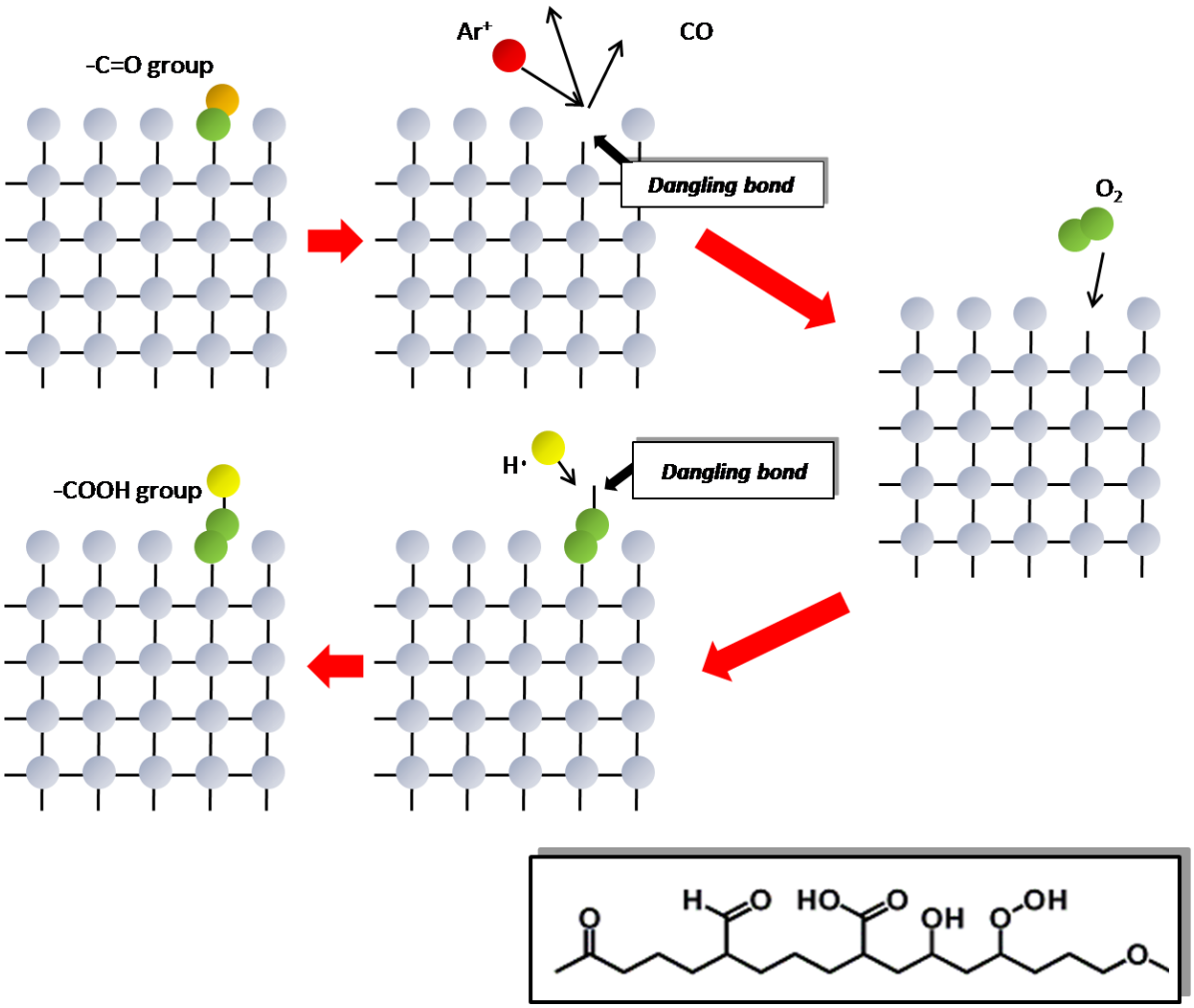

Figure 9. In plasma radicals can interact with compounds present in the gas discharge or with adjacent bulk solid surfaces. With regard to surface modification several positions at the substrate surface can be functionalized.

Although the generation of dangling bonds is a strongly endothermic process, the high ion kinetic energy is usually sufficient for homolytical cleaving bonds in typical organic compounds (Table 9). Depending on the method of plasma generation, ion energies between a few eV and several hundred eV are possible (Figure 10, SEEBÖCK, KÖHLER, AND RÖMHELD, 1992; BARTON *et al*., 1999; HOPF *et al*., 2008).

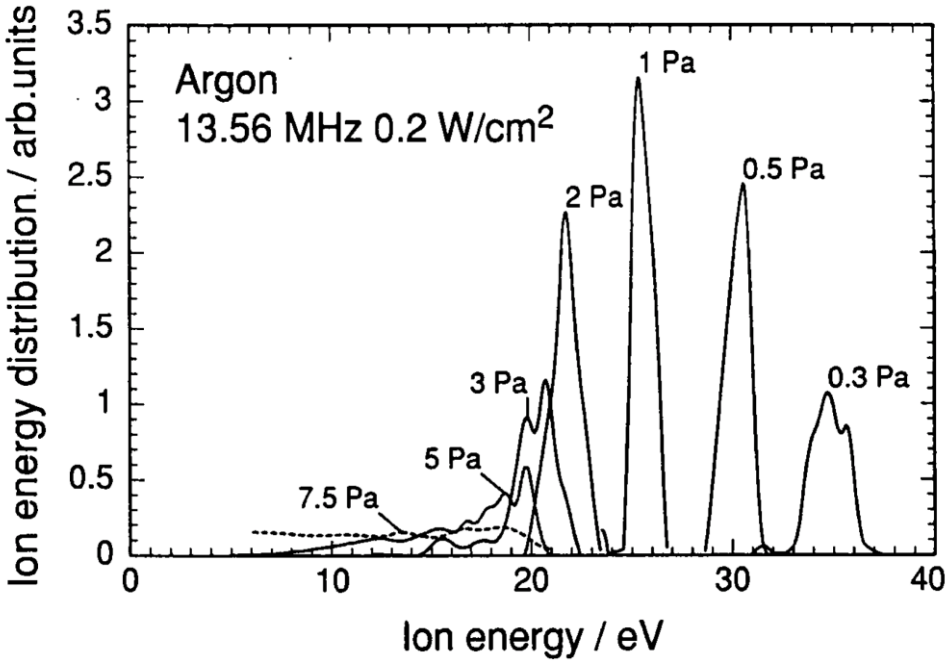

Figure 10. Differential ion energy spectra of Ar^+ for different discharge pressures of a RF plasma at 0.2 W/cm². The ion energy distribution functions show a pronounced peak for pressures below 3 Pa (= 0.03 mbar) which gradually decreases at higher pressure due to increasing charge-exchange and elastic collisions of the Ar ions in the plasma sheath (SEEBÖCK, KÖHLER, AND RÖMHELD, 1992).

5.1.6.3 Radicals and Reactive Oxygen Species

Due to their unpaired valence shell electron, radicals are highly reactive species. Although some persistent free radicals are known, most free radical reactions involve intermediates having fleeting lifetimes and being present at very low concentrations. Radicals are generated by homolytical bond cleavage. They take part in various addition and substitution reactions. Many free-radical reactions are chain reactions. Unless they are not undergoing self-annihilation (from recombination) radicals participate in manifold reactions, such as atom or group transfer reactions, addition reactions or fragmentations.

In biological systems reactive oxygen species are capable of oxidizing cellular proteins, nucleic acids, membranes and lipids thus giving rise to cellular aging, mutagenesis, or carcinogenesis. ROS contribution possibly proceeds through destabilization of membranes, DNA damage and oxidation of low-density lipoprotein (LDL, HEIM, TAGLIAFERRO, AND BOBYLA, 2002). Given their usually high reactivity, they can react with almost all cell components, leading to single-stranded DNA breaks, base and sugar modifications, and DNA-protein cross-links (RAGU *et al.*, 2007). They arise from incomplete reduction of O_2 in the electron transporting chain of from the catalytic cycle of redox enzymes involved in purine and lipid metabolism or antibacterial defence (Scheme 1; SIES, 1986).

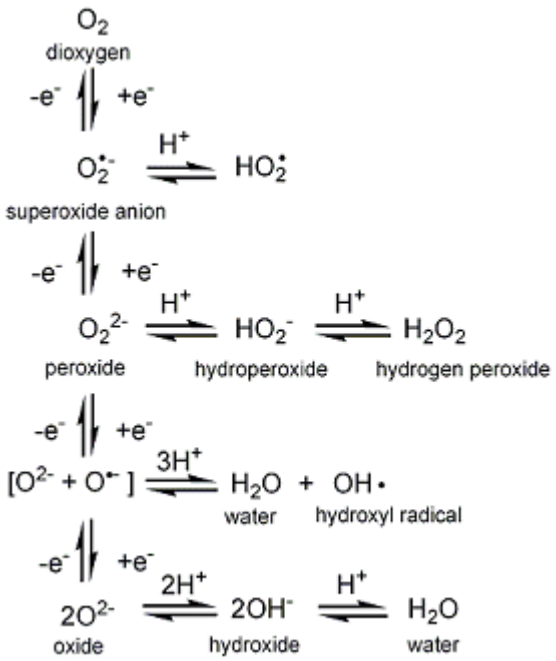

Scheme 1. ROS are generated in the oxygen metabolism but are also produced by ionizing radiation, metabolism of exogenous compounds, or pathological processes such as infection and inflammation (adapted from KAIM AND SCHWEDERSKI, 1995).

One of the prime radicals in plasma chemistry is atomic oxygen, present in the ground state O(^{3}P) and the low-lying excited states O(^{1}D) and O(^{1}S) (Figure 11).

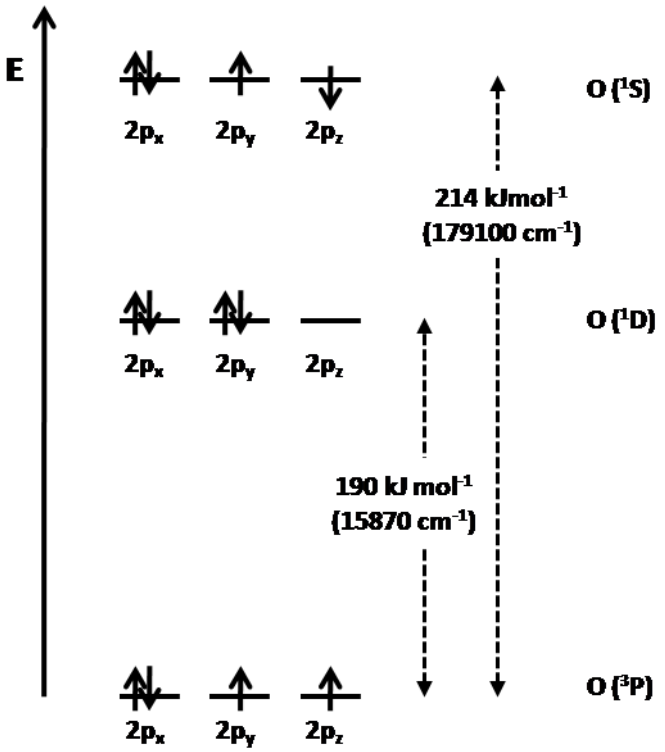

Figure 11. Electronic configuration of the partially filled 2p orbitals in lower energy states of atomic oxygen.

$O(^1D)$ is mainly generated by electron impact induced dissociation of triplet and singlet molecular oxygen or due to direct electronic excitation of ground state $O(^3P)$ (Table 12). For $O(^1S)$ the main formation processes are electron impact dissociation of molecular oxygen (eq. R35), dissociative recombination of O_2^+ (eq. R36) and electron impact excitation of ground state atomic oxygen (eq. R37). $O(^1D)$ atoms are mainly lost through quenching reactions (by $O_2(X^3\Sigma)$, O_3, O; eq. R38- R43) or due to diffusion to the walls (eq. R44). $O(^1S)$ in turn is lost through different collisional deactivation processes with ground state atomic oxygen, $O_2(X^3\Sigma)$ or $O_2(a^1\Delta)$ (VIALLE *et al.*, 1991).

Table 12. Formation and loss reactions of atomic oxygen.

Reactions	
$e^- + O_2(X^3\Sigma) \rightarrow O(^3P) + O(^1D) + e^-$	(R32)
$e^- + O_2(a^1\Delta) \rightarrow O(^3P) + O(^1D) + e^-$	(R33)
$e^- + O(^3P) \rightarrow O(^1D) + e^-$	(R34)
$e^- + O_2 \rightarrow O(^1S) + O + e^-$	(R35)
$O_2^+ + e^- \rightarrow O(^1S) + O$	(R36)
$e^- + O(^3P) \rightarrow O(^1S) + e^-$	(R37)
$O(^1D) + O_2(X^3\Sigma) \rightarrow O(^3P) + O_2(b^1\Sigma)$	(R38)
$O(^1D) + O_2(X^3\Sigma) \rightarrow O(^3P) + O_2(a^1\Delta)$	(R39)
$O(^1D) + O_3 \rightarrow 2\ O_2$	(R40)
$O(^1D) + O_3 \rightarrow O_2 + 2\ O$	(R41)
$O(^1D) + O_3 \rightarrow O_2(a^1\Delta) + O_2$	(R42)
$O(^1D) + O \rightarrow 2\ O$	(R43)
$O(^1D) \rightarrow O(^3P)$	(R44)

Despite of the many possible loss reactions, even small concentrations of metastable $O(^1D)$ and $O(^1S)$ are strongly influencing the kinetics of other species in an oxygen glow discharge such as $O_2(b^1\Sigma)$, $O_2(a^1\Delta)$ and O_3 (VIALLE *et al.*, 1991). Atomic oxygen is an extremely strong oxidizing agent and LEWIS acid. It reacts readily with hydrogen compounds, abstracting hydrogen and adds to LEWIS bases (Table 13).

Table 13. Atomic oxygen reactions.

Reactions	
$H_2 + O \rightarrow H + \cdot OH$	(R45)
$CH_4 + O \rightarrow \cdot CH_3 + \cdot OH$	(R46)
$H_2O + O \rightarrow 2\ \cdot OH$	(R47)
$O_2 + O \rightarrow O_3$	(R48)
$CO + O \rightarrow CO_2$	(R49)

Another common radical in plasma chemistry is the hydroxyl radical, mainly formed by water molecules present in the dilute gas of a discharge or due to mixing with the surrounding air. Generation occurs either by electronic dissociation (eq. R50) or due to collisions with long lived species (eq. 51; BRANDENBURG *et al.*, 2007).

$$e^- + H_2O \rightarrow \cdot OH + \cdot H + e^- \qquad (R50)$$

$$O(^1D) + H_2O \rightarrow 2 \cdot OH \qquad (R51)$$

Although the standard potential of the ·OH radical is very high (E^0 = 2.81 V, aq. solution) its comparatively short half-life ($\tau \sim 10^{-7}$ ms) makes it less important than for instance atomic oxygen (E^0 = 2.42 V, $\tau \sim$ 1.0 ms; Table 14).

Table 14. Standard potentials of oxygen compounds.

Reactions	$E^0_{pH<7}$ [V]
$O + 2\ H_3O^+ + 2e^- \rightleftharpoons 3\ H_2O$	+ 2.42
$O_2 + 4\ H_3O^+ + 4e^- \rightleftharpoons 6\ H_2O$	+ 1.23
$O_3 + 2\ H_3O^+ + 2e^- \rightleftharpoons 3\ H_2O + O_2$	+ 2.07
$\cdot OH + H_3O^+ + e^- \rightleftharpoons 2\ H_2O$	+ 2.81

Once ·OH and O are generated, a cascade of reactions will follow, leading to the appearance of other ROS such as ozone. Most commonly, O_3 is formed from the action of oxygen atoms on molecular oxygen. Dissociation (eq. R52, Table 15) can be achieved by providing electrical, photochemical or chemical energy while high temperatures favor almost exclusively the formation of atomic oxygen. Usually, third-order kinetic processes like reaction (R53) are only preferable in systems with elevated pressure (p> 100 mbar). Therefore their generation can be effectively inhibited using low operational pressures p ~ 10^{-4} mbar (FRIDMAN, 2008). Formation can as well proceed from interaction of ground state molecular oxygen with excited state O_2 (eq. R54). The oxidizing power of ozone is much greater than that of oxygen and nearly as great as that of atomic oxygen as can be seen by comparison of the standard potentials in aqueous solution (Table 14). However, while kinetically metastable, ozone is strongly endothermic and therefore easily decomposes to oxygen (eq. R55). The decomposition is accelerated by irradiation with near UV radiation (λ < 310 nm, eq. R56 and R57) or by heating. The loss of ozone by metastable quenching is a

reversible chemical reaction so that atomic oxygen decrease is balanced by ozone decrease (HERRMANN *et al*., 2002).

Table 15. Ozone formation reactions and decay into dioxygen.

Reactions		
½ O_2 → O	ΔH^{Θ}= +249 kJmol^{-1}	(R52)
O + O_2 + M → O_3 + M	ΔH^{Θ}= -106.5 kJmol^{-1}	(R53)
O_2* + O_2 → O_3 + O	ΔH^{Θ}= -285.6 kJmol^{-1}	(R54)
O_3 ⇌ 3/2 O_2		(R55)
O_3 + ħω → O_2 + O (^{1}D)		(R56)
O_3 + ħω → O_2 + O (^{3}P)		(R57)
O_3 + O → 2 O_2	ΔH^{Θ}= -392 kJmol^{-1}	(R58)
O_3 + O_2 ($a^1\Delta$) ⇌ 2 O_2 ($X^3\Sigma$) + O (^{1}D)		(R59)

Equally important for plasma-substrate chemistry is the presence of triplet and metastable singlet molecular oxygen. Although there is a widespread belief that atomic oxygen is the most important neutral species (even at room temperature), experiments have indicated that plasma-substrate reactions are mainly governed by O_2, synergistically contributing to surface bombardment from reactive ions (VIETZKE *et al*., 1987). Due its electronic structure $^3O_2$ mediated autooxidation reactions of certain organic compounds can already occur at ambient atmosphere but oxidation is usually slow. Spin-allowed energy transfer from the first excited triplet state (intersystem crossing, ISC) leads to the formation of the much more reactive singlet oxygen. The high energy form, O($^1\Sigma^+_g$), is very short-lived ($\tau < 10^{-9}$ s) whereas the comparatively long-lived low energy singlet oxygen ($\tau \sim 10^{-4}$ s) is chemically more effective (Figure 12).

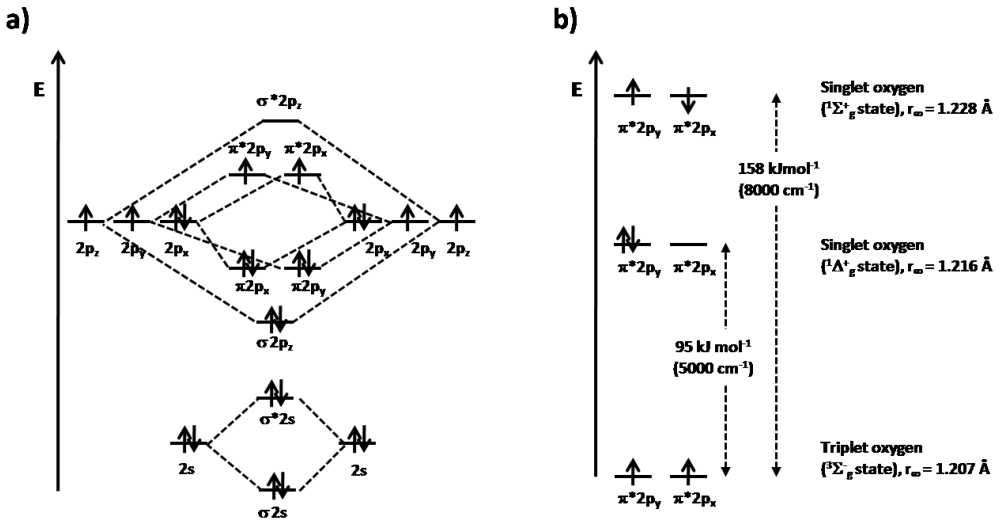

Figure 12. (a) Molecular orbital energy diagram for ground state molecular oxygen, (b) Different energy states of molecular oxygen.

Singlet oxygen is a very efficient oxidizing agent and adds to many π-electron-system, giving rise to pericyclic reactions, such as [2+2] or [4+2] cycloaddition or *ene*-like reactions (Scheme 2). The collisional de-excitation of $O_2(^1\Sigma_g^+)$ occurs rapidly within the first hundred microseconds after the discharge has been extinguished. $O_2(^1\Delta_g)$ persists about 10 ms before declining (Figure 13). Both species are quenched by second-order reactions with O_3. The reaction of metastable $O(^1S)$ with O_2 though contributes to the formation of O_3. With increasing distance from the lower electrode, the concentration of $O(^1S)$, O_2 $(^1\Sigma_g^+)$ and $O_2(^1\Delta_g)$ diminishes. By contrast, O_3 increases by a factor of 2, going from 0.2 to 10 mm, staying almost constant thereafter.

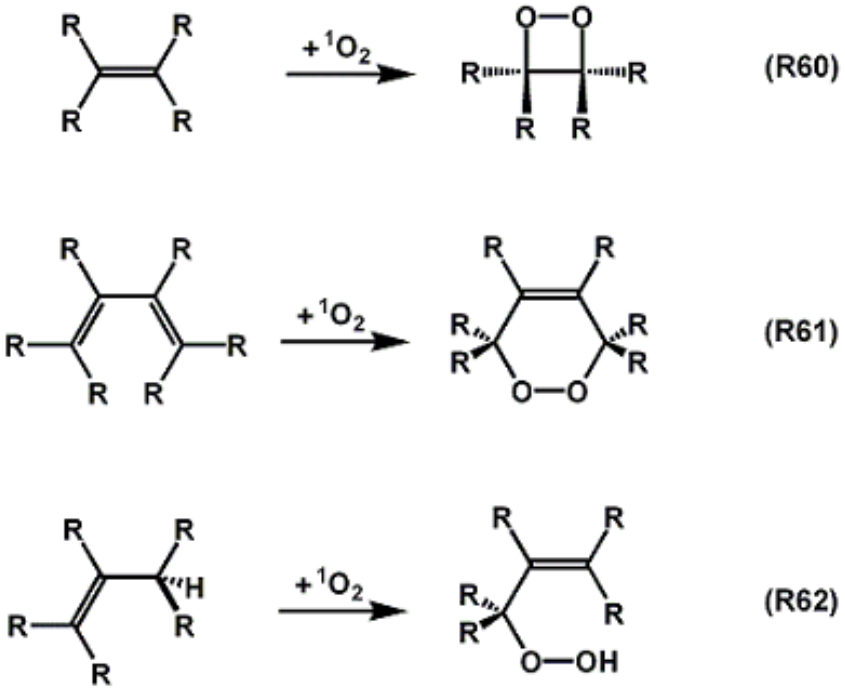

Scheme 2. Pericyclic reactions of olefins with singlet oxygen: (a) [2+2] cycloaddition of electron-rich compounds leads to the formation of 1,2 dioxetanes, (b) with conjugated dienes endoperoxides are generated, (c) olefins with allylic hydrogen react in a diastereoselective *ene*-like reaction to allylic hydroperoxides (SCHENK *ene*-reaction).

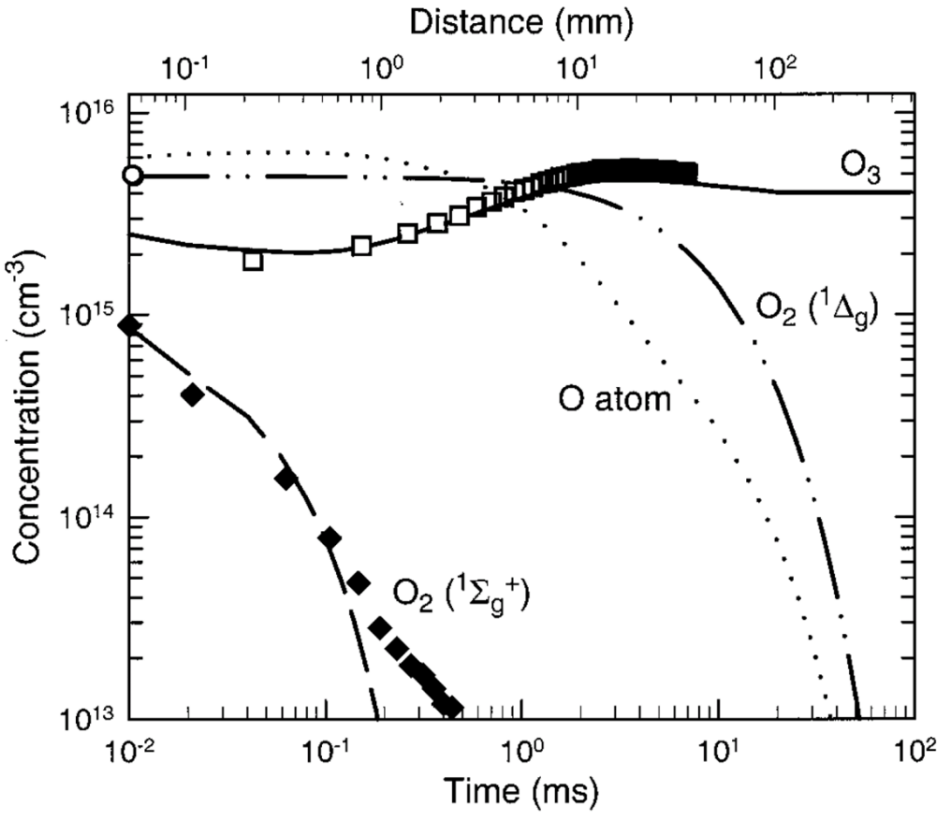

Figure 13. Dependence of atomic and metastable molecular oxygen, and ozone concentrations on time and distance in a capacitively coupled RF plasma (400 W, $p(O_2)$ = 8 mbar, T= 393 K; symbols = experimental data, curves = numerical model prediction). The densities have been determined in the afterglow region 10 µs after the plasma was shut down (JEONG *et al.*, 2000).

The reaction of oxygen radicals with hydrocarbons (RH) leads to hydrogen atom abstraction, thereby generating novel radicals (RANBY AND RABEK, 1975),

$$RH + O \rightarrow \cdot R + \cdot OH \qquad (R63)$$

$$RH + \cdot OH \rightarrow H_2O + \cdot R \qquad (R64)$$

The substrate radicals, unless not stabilized by resonance, have very short lifetimes. They dimerize (eq. R65) or disproportionate (eq. R66) at a diffusion-controlled rate (Scheme 3).

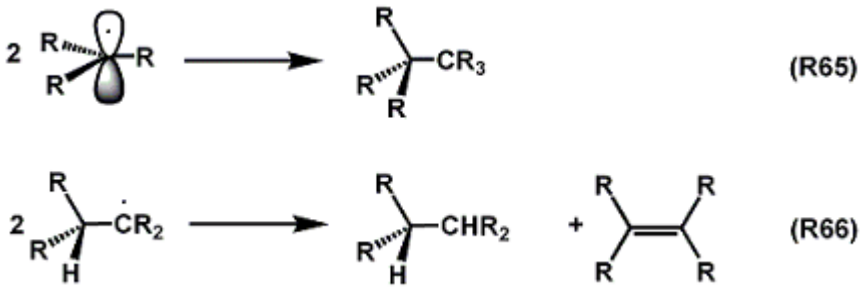

Scheme 3. Unless the electron is not delocalized alkyl radicals quickly recombine. The planar (or pyramidal) sp^2 hybridized radical can be attacked from either side. Reactions at stereogenic center give rise to racemization or diastereomer formation. Hydrogen abstraction leads to the formation of olefinic compounds.

Reaction of alkyl radicals with molecular oxygen leads to the formation of reactive peroxyl radicals of hydroperoxides (eq. R67, PETRUJ AND MARCHALL, 1980). As already mentioned, reactivity can be enhanced in combination with ion bombardment (VIETZKE *et al.*, 1987). These molecules are themselves potential radical chain initiators, interacting with each other (eq. R68) and/or rearranging to carbonyls under loss of OH (eq. R69) (Scheme 4, GUGUMUS, 1990).

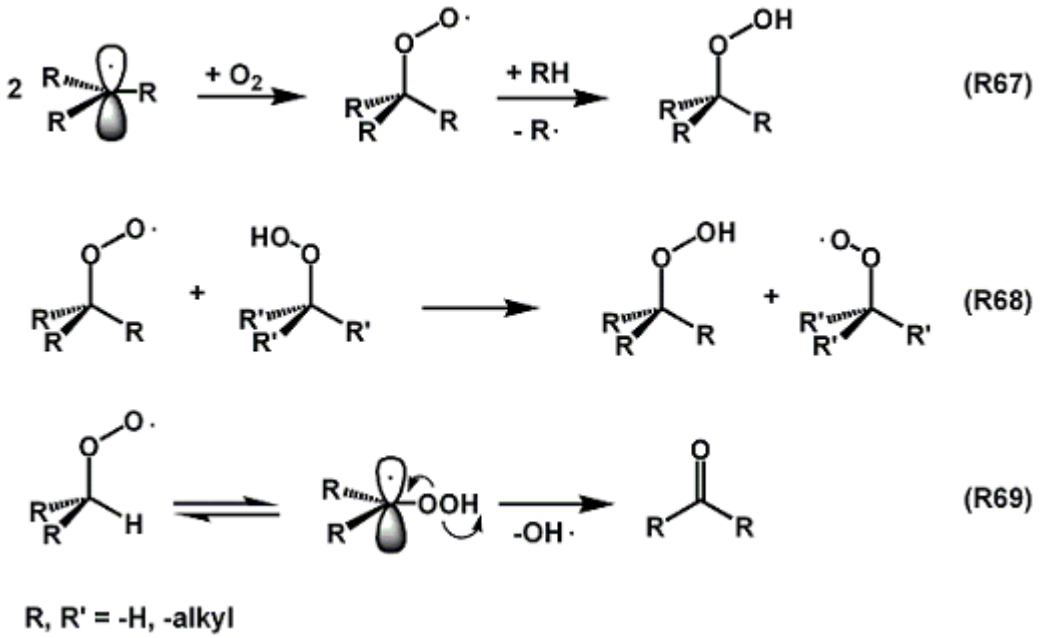

Scheme 4. Reactions of alkyl radicals with molecular oxygen lead to the formation of peroxyl radicals who can interact and propagate the radical chain or relocate forming carbonyls.

In addition to the formation of ROS, reactive nitrogen species (RNS) can appear if plasma is generated in air or if mixing of rare gas plasma with ambient air can occur. Although the dissociation of molecular nitrogen requires a higher minimum energy as the dissociation of O_2 (COSBY 1993 a,b; STEFANOVIC *et al.*, 2001), RNS participate in almost all of the plasma's complex chemical pathways. In a pure nitrogen plasma they lead to the formation of amines, imines, amide, nitrile and other onto polymer surfaces (PERTRAT *et al.*, 1994a,b ; LE, PIREAUX, AND VERBIST, 1994; GRÖNING *et al.*, 1996; COLLAUD-COEN *et al.*, 1996; NITSCHKE AND MEICHSNER, 1997; PAYNTER, 1998; PONCIN-EPAILLARD, CHEVET AND BROSSE, 1994). Table 16 exemplarily lists the various formation reactions of nitric oxide in air plasma. NO is not only an important biological molecule with varied indispensable physiological roles but also shows interesting chemical reactivity (CHACKO AND WENTHOLD, 2006). Due to the antibonding character of the LUMO, NO can act either as an electron donor or acceptor (Figure 14). In biological systems the reaction of nitric oxide with superoxide gives rise to peroxynitrite formation (SQUADRITO

AND PRYOR, 1998) which due to his high redox potential easily induces LDL oxidation (LEEUWENBURG *et al.*, 1997). In the presence of O_2 the otherwise metastable nitric oxide reacts to nitrogen dioxide which easily dimerizes to N_2O_4.

$$2 \cdot NO + O_2 \rightarrow 2\ NO_2 \quad , \Delta H^{\ominus} = -114\ kJ/mol \qquad (R70)$$

$$2\ NO_2 \rightarrow N_2O_4 \qquad (R71)$$

Table 16. Two-Body Reactions involving gound and excited states N and O species.

Reactions	k_{298} ($cm^3\ mol^{-1}\ s^{-1}$)
$O + NO_2 \rightarrow \cdot NO + O_2$	(9×10^{-12}) [a]
$N + O_2 \rightarrow \cdot NO + O$	(7.7×10^{-17}) [b]
$N + O_3 \rightarrow \cdot NO + O_2$	$(5.7 \times 10\text{-}13)$ [c], $(\leq 2 \times 10\text{-}16)$ [d]
$N + NO_3 \rightarrow \cdot NO + NO_2$	(3×10^{-12}) [a]
$O(^1D) + N_2O \rightarrow 2 \cdot NO$	(7.2×10^{-11}) [a]
$O(^1D) + NO_2 \rightarrow \cdot NO + O_2$	(1.4×10^{-10}) [a]
$N(^2D) + O_2 \rightarrow O(^3P, {}^1D) + \cdot NO$	(5×10^{-12}) [a]
$N(^2D) + O_3 \rightarrow O_2 + \cdot NO$	(1×10^{-10}) [a]
$N(^2D) + N_2O \rightarrow N_2 + \cdot NO$	(2.2×10^{-12}) [a]
$N(^2P) + O_2 \rightarrow O(^3P, {}^1D, {}^1S) + \cdot NO$	(2×10^{-12}) [a]
$N + O_2(^1\Delta_g) \rightarrow \cdot NO + O$	$(\leq 9\ 10^{-17})$ [a]
$N_2(A^3\Sigma^+_u) + NO_2 \rightarrow N_2 + \cdot NO + O$	(1.3×10^{-11}) [a]

[a] = HERRON AND GREEN, 2001; [b] = DORAI AND KUSHNER, 2003; [c] = STEFANOVIC et al., 2001; [d] = Herron, 2001

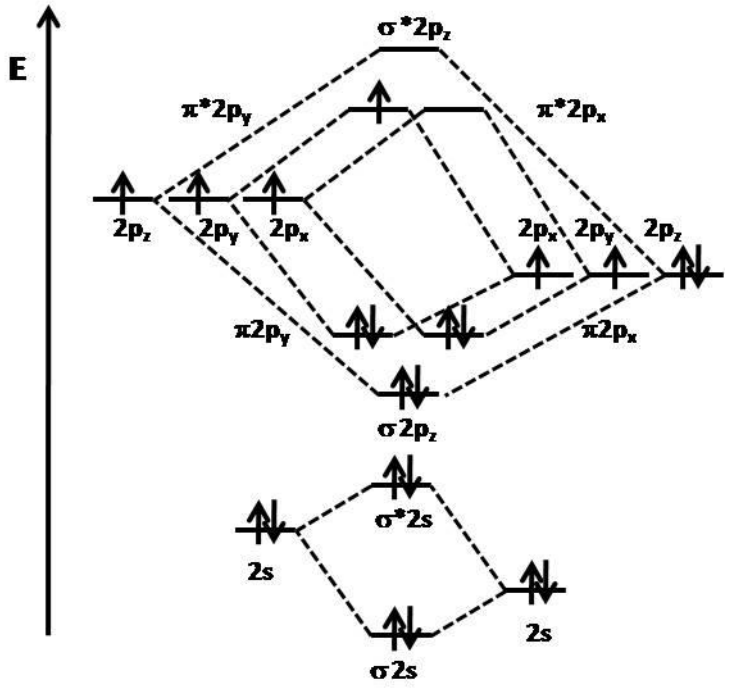

Figure 14. Electronic configuration, atomic orbitals, and molecular orbitals for nitric oxide.

In Figure 15 the primary chemical reactions up to the formation of N_2O_5 in air plasmas upon electron impact on N_2 and O_2 are shown. A more detailed description of air or nitrogen plasma chemistry can be found in BECKER *et al*. (2005).

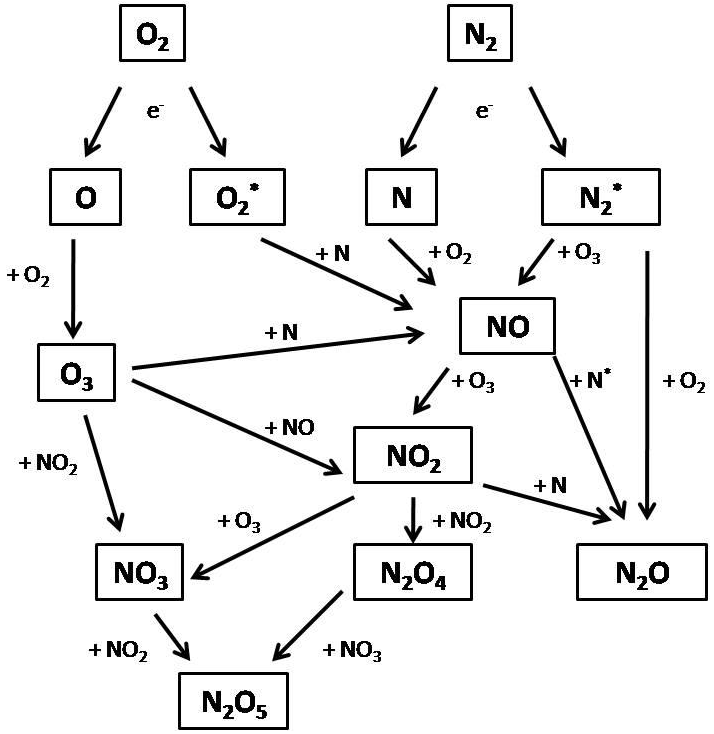

Figure 15. Schematic diagram of the primary chemical reactions in air plasmas. Only formation reactions up to N_2O_5 generation are shown (adapted from BECKER *et al.*, 2005).

5.1.6.4 Photons and Metastable States

Endothermic homolytical bond cleavage leading to the formation of radicals can as well be obtained by photochemical means. As a result of electron impact excitation line emission from the relaxation of discrete energy levels into the electronic ground state can be observed (spontaneous emission):

$$A_n \rightarrow A_m + \hbar\omega \qquad \text{(R72)}$$

The corresponding emission coefficient can be described by Equation (16).

$$\gamma_\nu(\nu,T) = \frac{E_n - E_m}{4\pi} \cdot A_{nm} \cdot n_n \cdot P_\nu(\nu) \qquad (16)$$

with A_{nm} the EINSTEIN coefficient of spontaneous emission[1]
, n_n the number density of atoms in the excited state n,
$P_\nu(\nu)$ the line profile of the transition

[1] may be calculated from first principles knowing the wavefunctions φ_1 and φ_2, and the first-order perturbation to the HAMILTONian $H^{(1)}$ caused by the atom's dipole moment

In addition continuous emission can be observed from thermal *Bremsstrahlung* due to deflection of a high-energy electron in the electric field of an atomic nucleus (free-free transition; eq. R73) or from radiative recombination as electrons pass from the vacuum levels into upper bound levels of ions before relaxing into the ground state occurs (eq. R74).

$$e^-(\varepsilon) + A^{Z+} \rightarrow e\text{-}(\varepsilon') + A^{Z+} \hbar\omega \qquad \text{(R73)}$$

$$e^-(\varepsilon) + A^{Z+} \rightarrow e\text{-}(\varepsilon') + A^{(Z-1)+} \hbar\omega \qquad \text{(R74)}$$

Alternatively, free electrons can be scavenged by atoms in highly excited RYDBERG states. In this case the excess energy of the recombination is taken up by a second bound electron which by itself is promoted into an excited state. This resonant process is called dielectronic recombination and can be considered as an inverse AUGER process. RF driven atmospheric pressure plasma jets in argon have shown to emit a significant amount of UV and VUV radiation (Figure 16, BRANDENBURG *et al*., 2007; FOEST *et al*., 2007).

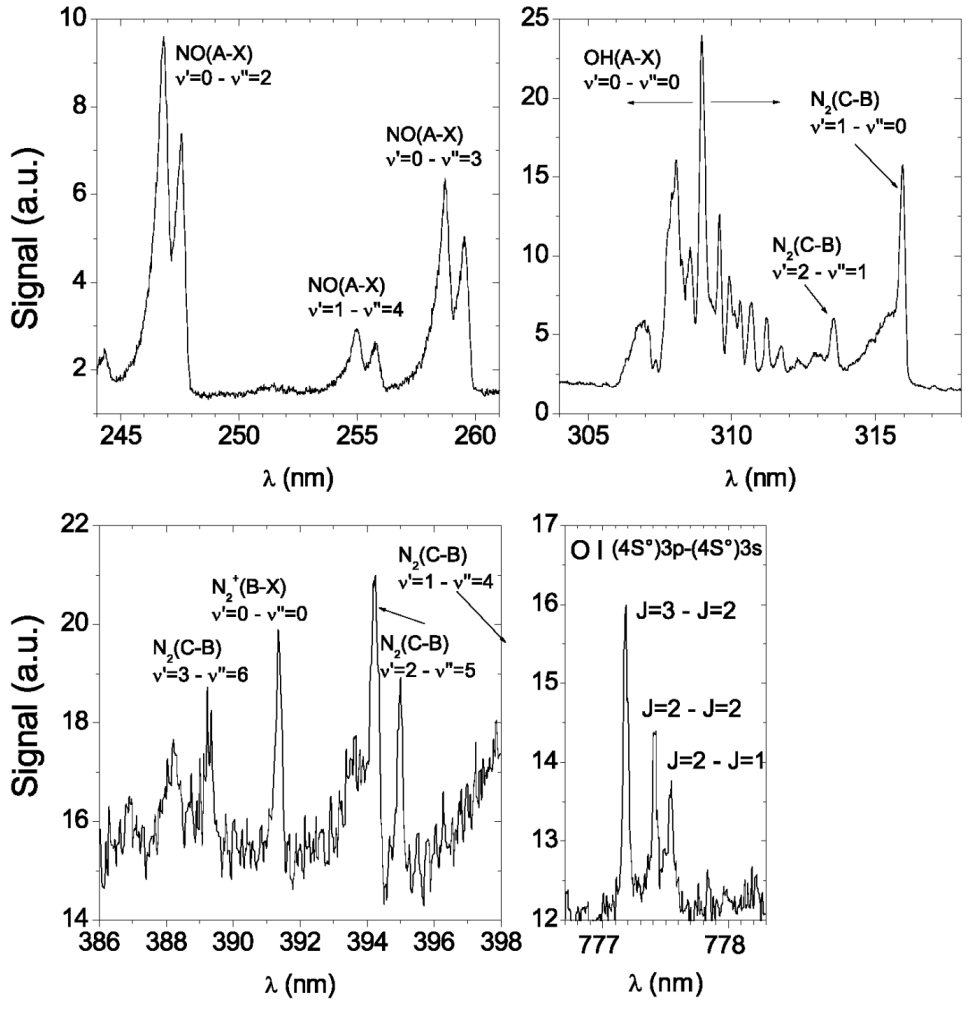

Figure 16. High-resolution optical emission spectra showing the typical spectral lines and molecular bands of an Ar APPJ in the vis and near UV spectral region (BRANDENBURG *et al*., 2007).

The energy of these photons (Table 17) is on the order of bond energies in organic molecules and thus photoreactions are frequently initiated. While damage due to ion bombardment is usually limited to the first few nanometers, (V)UV photons often penetrate 50-100 nm into the bulk depending on the surface dielectric properties inducing chain scission and cross-linking reactions in the bulk (BARTON *et al*., 1999).

Absorption occurs by virtue of the specific chromophores present in the molecule. Hydrocarbon polymers for instance display very strong absorption bands below 160 nm, originating of $\sigma \rightarrow \sigma^*$ transitions from electronic excitation of C-C and C-H bonds.

Table 17. Spectral regions according to DIN 5030-2 and DIN 51418-1 (DIN, 2001).

Spectral region	λ [nm]	E [eV]
Vis	780-380	1.6-3.3
UV-A	380-315	3.3-3.9
UV B	315-280	3.9-4.4
UV C	280-200	4.4-6.2
VUV	200-10	6.2-124
X-ray	10-0.01	$124\text{-}1.24 \times 10^5$

π-electron systems with or without conjugated auxochromic groups or compounds with atoms having at least one non-bonding electron such as oxygen or nitrogen efficiently absorb light with a wavelength shorter than 200 nm very strongly (Table 18).

Table 18. Absorption bands of selected isolated chromophores (shown are the Low-Energy Transitions). [a] = measured in diethyl ether or petroleum ether, [b] = *n*-hexane (HESSE, MEIER, AND ZEEH, 1991).

Chromophore	Transition	Example	λ [nm]	E [eV]	ϵ [l mol^{-1} cm^{-1}][a]
C-H	$\sigma \rightarrow \sigma^*$	CH_4	122	10.16	Intensive
C-C	$\sigma \rightarrow \sigma^*$	$H_3C\text{-}CH_3$	130	9.54	intensive
-O-	$n \rightarrow \sigma^*$	H_2O	167	7.43	1500
		CH_3OH	183	6.78	200
C=C	$\pi \rightarrow \pi^*$	$H_2C{=}CH_2$	165	7.52	16000
		$C_2H_5\text{-}CH{=}CH\text{-}C_2H_5$	185	6.70	7940
R-(CH=CH)$_n$-R	$\pi \rightarrow \pi^*$	$H_3C\text{-}CH{=}CH\text{-}CH_3$	174	7.13	24000
C≡C	$\pi \rightarrow \pi^*$	$HC{\equiv}CH$	173	7.17	6000
		$HC{\equiv}C\text{-}C_2H_5$	172	7.21	2500
C=O	$n \rightarrow \pi^*$	$H_3C\text{-}CH{=}O$	293	4.23	12
	$\pi \rightarrow \pi^*$	$H_3C\text{-}CO\text{-}CH_3$	187	6.63	950
	$n \rightarrow \pi^*$	$H_3C\text{-}CO\text{-}CH_3$	273	4.54	14
Aromatic hydrocarbons	$\pi \rightarrow \pi^*$	C_6H_6	189	6.56	257[b]
			208	5.96	7943[b]
			262	4.73	54954[b]

As a result of the latter, gases like oxygen or carbon dioxide dissociate and atoms in defined quantum states are generated in from the precursor molecules. Radicals therefore cannot only be generated from electron impact but as well from photodissociation.

Photochemical reactions may involve elimination, E-Z-isomerization or pericyclic reactions. Though bond breaking is the primary photochemical reaction, electronic and bond reorganization reactions via FRANCK-CONDON states are as well of substantial importance. Due to inter-and intramolecular energy transfer (ET) from ISC, triplet states can be generated, which clearly distinguishes photochemical reactions from thermally driven processes, where only singlet states can participate in the reaction. Changing the symmetry of the molecule's electronic configuration thus enables an otherwise inaccessible reaction path. The formation of novel intermediates may then lead to novel reaction products according to the WOODWARD-HOFFMANN selection rules.

For carbonyl compounds, chain scission reactions following photoexcitation are among the most thoroughly studied photoreactions. They are classified as α-cleavage (NORRISH I type) or β-cleavage (NORRISH II type) (Scheme 5). The generated alkoxyl radicals form final products by a variety of secondary reactions arising from recombination or propagation reactions. The product distribution differs from the thermal pyrolysis reaction according to the RICE-HERZFELD mechanism although the initiation by α-cleavage is the same.

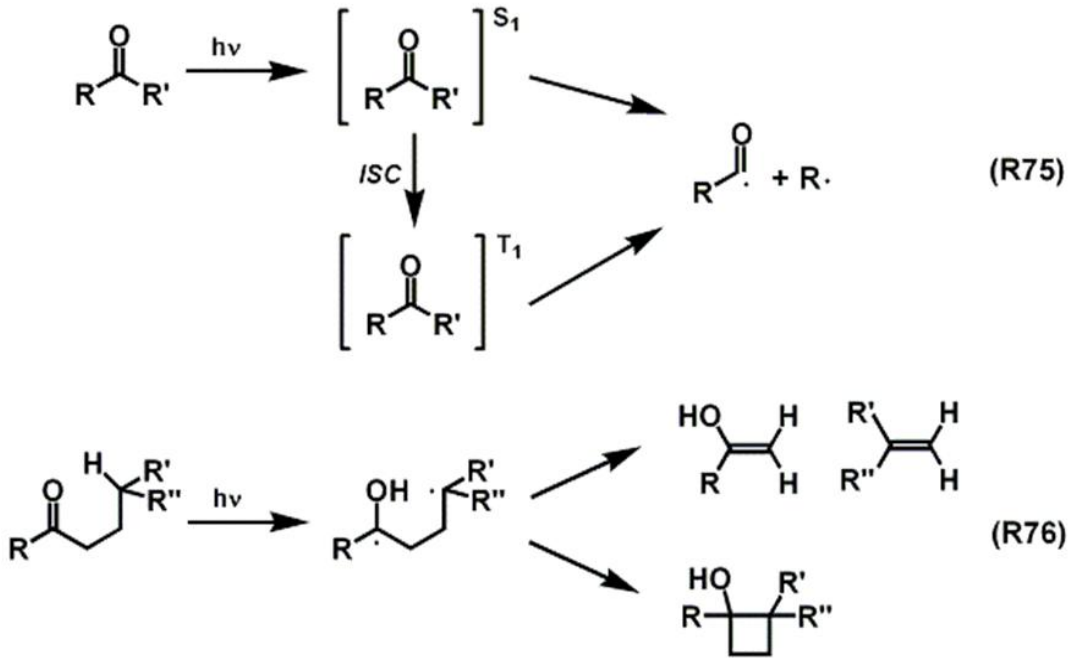

Scheme 5. Photoinduced NORRISH reactions of carbonyl compounds lead to the formation of intermediate acyl radicals (eq. R75) or 1,4-diradicals (eq. R76). Acyl radicals undergo radical coupling reactions, ß-elimination reactions or decarbonylation giving rise to various products. Diradicals can be stabilized if electrons are efficiently delocalized or sterically protected.

In the presence of molecular oxygen alkoxyl radicals give rise to peroxyl radicals which by intermediate formation of a peroxy acid react with another equivalent of aldehyde in a BAEYER-VILLIGER- like reaction (Scheme 6). Keto compounds rearrange to esters or in case of cyclic ketones give lactones.

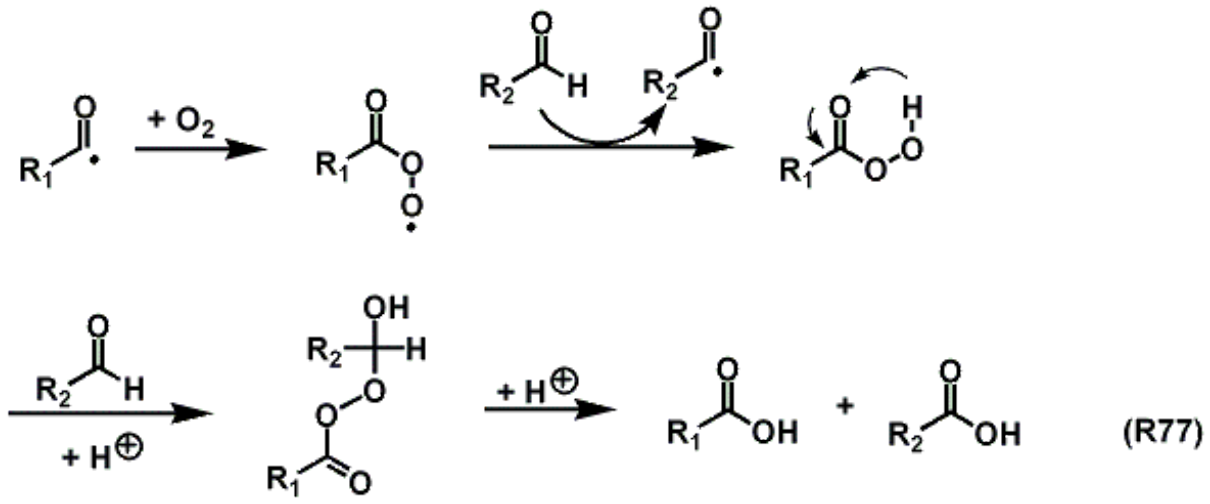

Scheme 6. Autooxidation of carbonyl radicals in the presence of O_2. The reaction mechanism proceeds through addition of a peroxy acid or ester to the carbonyl. The tetrahedral intermediate is called a CRIEGEE intermediate for its similarity with rearrangement of that name. In the final step a BAEYER-VILLIGER oxidation is taking place.

In cold plasma a complete degradation of macromolecules is reported (CLOUET AND SHI, 1992). The formation in this case is thought to proceed through intermediate formaldehyde formation which subsequently reacts with atomic oxygen to CO, CO_2, H_2 and other volatile compounds (HUIE AND HERRON, 1975). However, formaldehyde is known to basically undergo α-cleavage following excitation of the (n, π^*) state and major end products in the gas phase photolysis are H_2 and CO (HAAS, 2003).

Table 19. Ionization potential of organic compounds (HANDBOOK OF CHEMISTRY AND PHYSICS, 1994).

Compound	IP / eV	Compound	IP / eV
CH_4	12.5	CH_2Cl_2	11.32
HC≡CH	11.4	CH_2F_2	10.5
$H_2C=CH_2$	10.5	CH_2O_2	11.33
n-C_3H_6	9.73	CH_3-OH	10.85
n-C_3H_8	10.95	CH_3-COOH	10.66
n-C_8H_{16}	9.43	CH_3-CN	12.19
n-C_8H_{18}	9.82	C=O	14.01
n-$C_{10}H_{20}$	9.42	CO_2	13.77
n-$C_{10}H_{22}$	9.65	N≡C-C≡N	13.37

As most molecules have an ionization potential (Table 19) which is lower than the internal energies of metastable excited state rare gases (Table 20), ionization efficiently occurs provided that the reaction lifetimes of excited rare gas atoms are not affected by the occurrence of annihilation reactions.

Table 20. Excitation energies for rare gases.

Rare gas	Quantum state	Excitation energy [eV]
He	$^3S_1$	19.8
Ne	$^3P_0$	16.7
	$^3P_2$	16.6
Ar	$^3P_0$	11.72
	$^3P_2$	11.55
Kr	$^3P_0$	10.6
	$^3P_2$	9.9

For Ar metastable states, radiative lifetimes are usually high with $\tau(^3P_2)\sim$ 60 s and $\tau(^3P_0)\sim$ 50s (RADZIG AND SMIRNOV, 1985; SMALL-WARREN AND CHIU, 1975). With increasing number density of Ar* the rate of annihilation by chemi-ionization (eq. R78 and R79, Table 21) or superelastic collision (eq. R80) will concomitantly increase (HIRAOKA *et al*., 2004).

Table 21. Reactions of Ar metastables states

Reactions	
$X^* + X^* \rightarrow X^+ + X + e^-$	(R78)
$X^* + X^* \rightarrow X^+_2 + e^-$	(R79)
$X^* + e^-(\text{thermal}) \rightarrow X + e^-(\text{hot})$	(R80)
$Ar^*(^3P_{2,0}) + H_2O \rightarrow \cdot OH\ (A\ state) + \cdot H + Ar$	(R81)

Impurities as well may lead to annihilation of X*. In the presence of atmospheric water rare gas metastable excited states are rapidly quenched prior to ionization provided that the ionization potential of H_2O (IP = 12.6 eV) is higher than the internal energies of X*. This quenching involves homolytical cleavage of the neutral water molecule into atomic hydrogen and a hydroxyl radical ($\Delta H^{\ominus}$(HO-H) = 492 kJmol^{-1} = 5.10 eV; ATKINS, 1996). Considering the rate constant to be k= 8.1 $\times$ 10^{-10} cm^{3}s^{-1}, only a 40 ppb level of H_2O impurity in the atmospheric-pressure Ar reagent leads to the decay lifetime of Ar*(τ = ln2/k [H_2O]) being 1 ms (HIRAOKA *et al*, 2004). If pressures are low and intense short wavelength UV radiation exists, then however photoionization processes are taking place. For the He(2^3S)

electronic excited state having an internal energy of 19.8 eV, water clusters were recorded upon reaction with atmospheric water (Figure 17, CODY, LARAMÉE, AND DUPONT DURST, 2005):

$$He(2^3S) + n\ H_2O \rightarrow [(H_2O_{n-1})H]^+ + OH^- + He(1^1S) \qquad (R82)$$

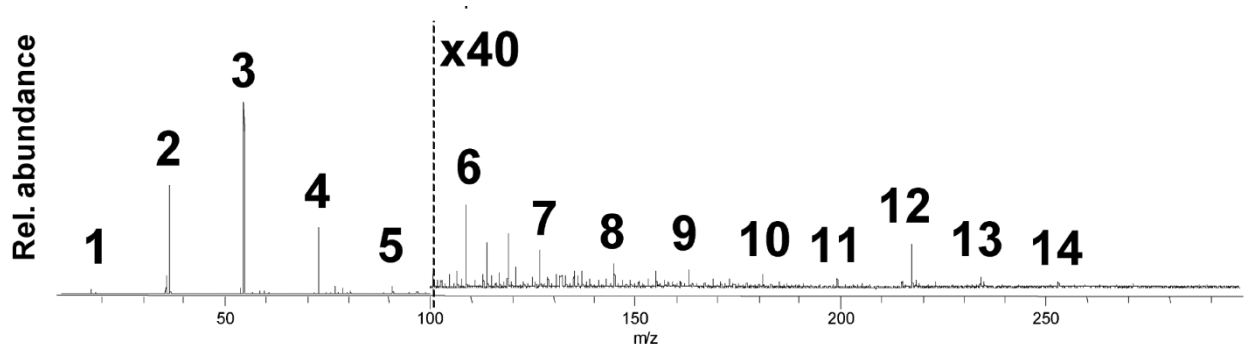

Figure 17. Ionized water clusters produced in room air by DART operated with helium carrier gas (CODY, LARAMÉE, AND DUPONT DURST, 2005).

At high pressures, single-collision conditions do not longer prevail. Beyond binary collisions, three-body interactions take place, leading to the formation of excimers. Rare gas excimer formation usually proceeds via electron-impact ionization (eq. R83) or directly by metastable rare gas atom excitation (eq. R84). In either case, the initial step is a three-body collision process in which two ground state atoms interact with an excited state atom (metastable state or resonance, Table 22). Efficient excimer formation requires both a sufficiently large number of electrons with energies above the threshold for the metastable formation (or ionization), and a pressure that is high enough to have a sufficiently high rate of three-body collisions (KURUNCZI *et al.*, 2001). In case of He, the minimum energy needed to form a metastable He atom by electron impact on ground-state He is ~20 eV (cf. Table 20) while ionization requires more than 24 eV (SOBELMAN, 1979).

Table 22. Rare gas excimer formation.

Reaction	Description	
$e^- + X \rightarrow X^+ + 2e^-$ $X^+ + 2\ X \rightarrow X_2^+ + X$ $X_2^+ + e^- \rightarrow X^* + X$ $X^* + 2\ X \rightarrow X_2^* + X$	Electron-impact ionization	(R83)
$e^- + X \rightarrow e^- + X^*$ $X^* + 2\ X \rightarrow X_2^* + X$	Electron-impact excitation	(R84)
$X_2^* \rightarrow 2\ X + \hbar\omega$	Radiative decay	(R85)

Emission spectra are dominated by the second continuum (for Ar_2*: λ = 126 nm) resulting from the transition of the lowest lying bound $^3\Sigma_u$ excimer state to the repulsive ground state (WALTER, SCHALLER, AND LANGHOFF, 1985; LORENTS, 1976). Radiative decay of vibrationally excited levels of $^1\Sigma_u$ excimer states (first excimer continua) are observed on the short-wavelength side of the second continua (BECKER, KURUNCZI, AND SCHOENBACH, 2002). Admixture of molecular gases leads to a decrease of the rare gas excimer emission together with the appearance of intense, monochromatic atomic emissions stemming from the added gas (BRANDENBURG *et al.*, 2009; KURUNCZI, SHAH, AND BECKER, 1999; Figure 18). As the most likely mechanism a near-resonant energy transfer reaction is suggested, involving the X_2*($^3\Sigma_u$) induced dissociation of the molecular gas, followed by atomic excitation and radiative decay (WIESER *et al.*, 1998).

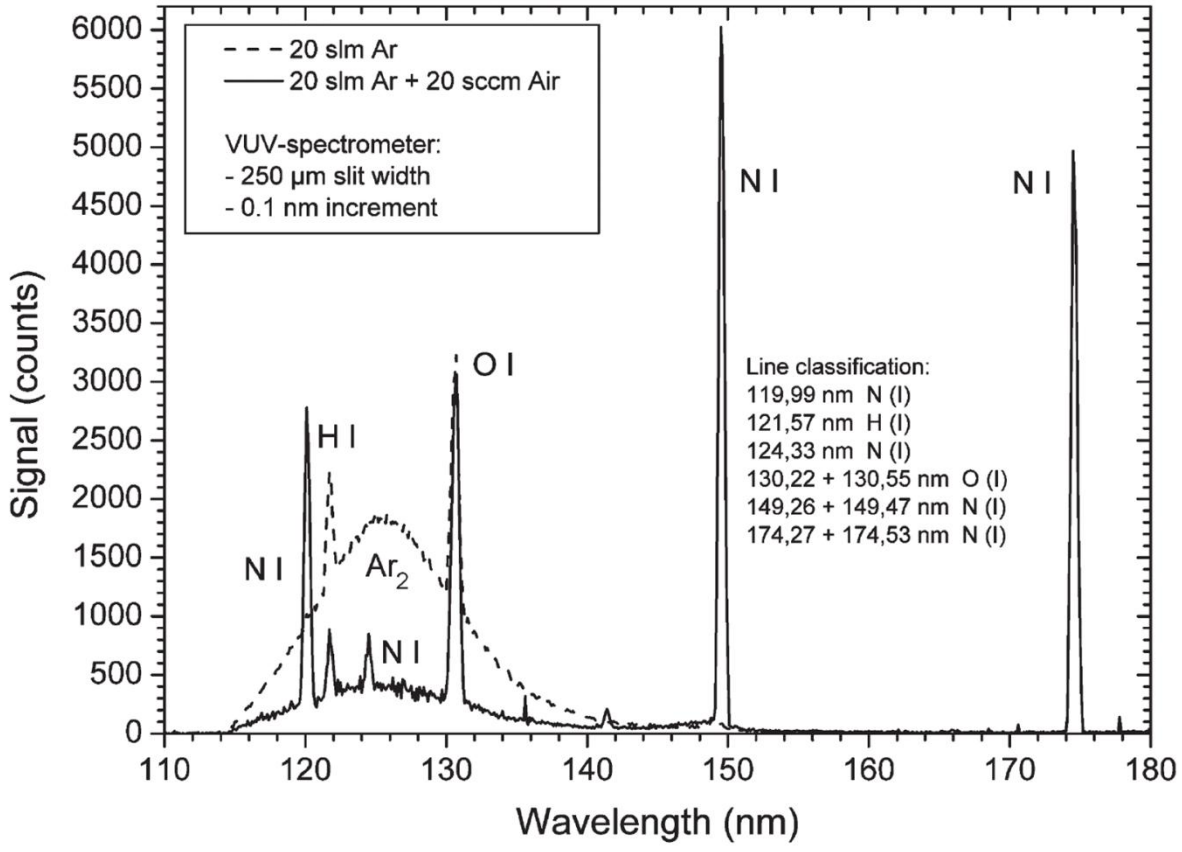

Figure 18. VUV spectrum of an Ar RF plasma jet with admixture of air to the carrier gas (BRANDENBURG *et al.*, 2009).

In this section only a small excerpt of the manifold chemical reactions taking place either in the volume of the discharge or at the substrate surface is shown. The various chemically reactive compounds, all contributing synergistically, make the underpinning plasma chemistry rather complex and a summary of all chemical reactions in different cold plasmas is almost impossible. It is due to this unique environment that non-LTE plasmas are not only

able to increase the efficiency of traditional chemical processes. They offer as well alternative approaches to in conventional chemical synthesis otherwise inaccessible reaction pathways, often by changing the symmetry of the molecule's electronic configuration. The initiation of novel reaction channels at moderate bulk temperatures might lead to new transient and secondary products, which is an often highly desired and already exploited result of plasma treatment. However, the generation of high chemically active species harbors as well the risk of not only uncontrollable but as well undesired plasma-chemical synthesis. A thorough knowledge of plasma reaction chemistry therefore is mandatory for any industrial application.

5.2 Flavonoids - Plant Secondary Metabolites of great Importance

From the many compounds that exist in plants, flavonoids have gained considerable interest within recent years because of their potential health beneficial effects (KRIS-ETHERTON *et al*., 2002). Epidemiological studies strongly suggest that the long-term consumption of diets rich in foods of plant origin is a major factor in preventing the etiology of many chronic diseases that involve free radical-mediated damage in pathologically generating processes, including allergies, cardiovascular and hepatic diseases, certain forms of cancer, and inflammation (COOK AND SAMMAN, 1996; HARBORNE AND WILLIAMS, 2000; LIPKIN et al., 1985; STEINMETZ AND POTTER, 1991; BLOCK, PATTERSON, AND SUBAR, 1992; HERTOG *et al*., 1996; WALLSTROM *et al*., 2000). In support of plant phenols are the seminal findings of Hertog and co-workers and the recognition of the so-called *French Paradox* (RENAUD AND DE LORGERIL, 1992) showing that coronary heart disease is inversely correlated with the intake of flavonoids (HERTOG *et al*., 1993; HERTOG, KROMHOUT, AND ARAVANIS, 1995). These studies are responsible for a growing interest in supplementing flavonoids in daily diet or as ingredients for food fortification. The health-promoting effects of flavonoids are attributed to a high antioxidant activity and metal-binding properties by which cells are protected against the damaging effects of ROS and RNS such as singlet oxygen, superoxide, peroxyl radicals, hydroxyl radicals and peroxynitrite (HAENEN *et al*., 1997; HU *et al*., 1995; Van ACKER *et al*., 1995). Since plasma might generate numerous of these reactive species, flavonoids are ideal target compounds to elucidate the interactions and effects of plasma-immanent reactive species on bioactive molecules.

5.2.1 Biosynthesis of Phenolic Compounds

Phenolic compounds form one of the major classes of secondary plant metabolites. Their composition is highly variable both qualitatively and quantitatively and large variations may even occur within a single species because of genetic factors and environmental conditions during plant ontogenesis. Although a large range of plant phenols exist, most of them are derived from deamination of the amino acids L-phenylalanine or L-tyrosine to cinnamic acids by the action of phenylalanine ammonia-lyase (PAL) in the phenyplpropanoid pathway (Scheme 7). The most common hydroxycinnamic acids (caffeic, ferulic and sinapic acid) produced from the shikimate pathway are usually conjugated to sugars, or esterified with cell wall carbohydrates or organic acids (e.g. chlorogenic acid). Lignin and suberin are prominent examples for highly cross-linked polymers formed from a complex mixture of simple specific phenylpropanoids. One of the most widespread and important class of plant metabolites are flavonoids, resulting from the chalcone synthase (CHS) catalyzed condensation of malonyl-CoA and coumaroyl-CoA (HARBORNE, 1994). They are widely distributed in fruits and vegetables at varying levels and thereby an integral part in human diet, some of them particularly concentrated in coffee, tea, cacao, and wine (CARANDO *et al*., 1999; BALENTINE, WISERMAN AND BOUWENS, 1997; ARTS, VAN DE PUTTE AND HOLLMAN, 2000). The initial product of CHS is a tetrahydroxychalcone which is further converted to flavones, flavanones, flavonols and other flavonoid classes. Flavonoids (2-phenyl-1,4-benzopyrones) consist of a benzene ring (A ring) condensed with a six-membered oxygen heterocycle (C ring) which is substituted at C2 by a phenyl group (B ring). The A ring can be *m*-trihydroxylated (phloroglucinol type) or *m*-dihydroxylated (resorcinol type). The B ring is monohydroxylated, *o*-dihydroxylated or vicinal-trihydroxylated. Flavonoids are divided into different subclasses according to the oxidation degree of the heterocyclic pyran ring, which commonly exists as a pyran, pyrilium or γ-pyrone (Figure 19).

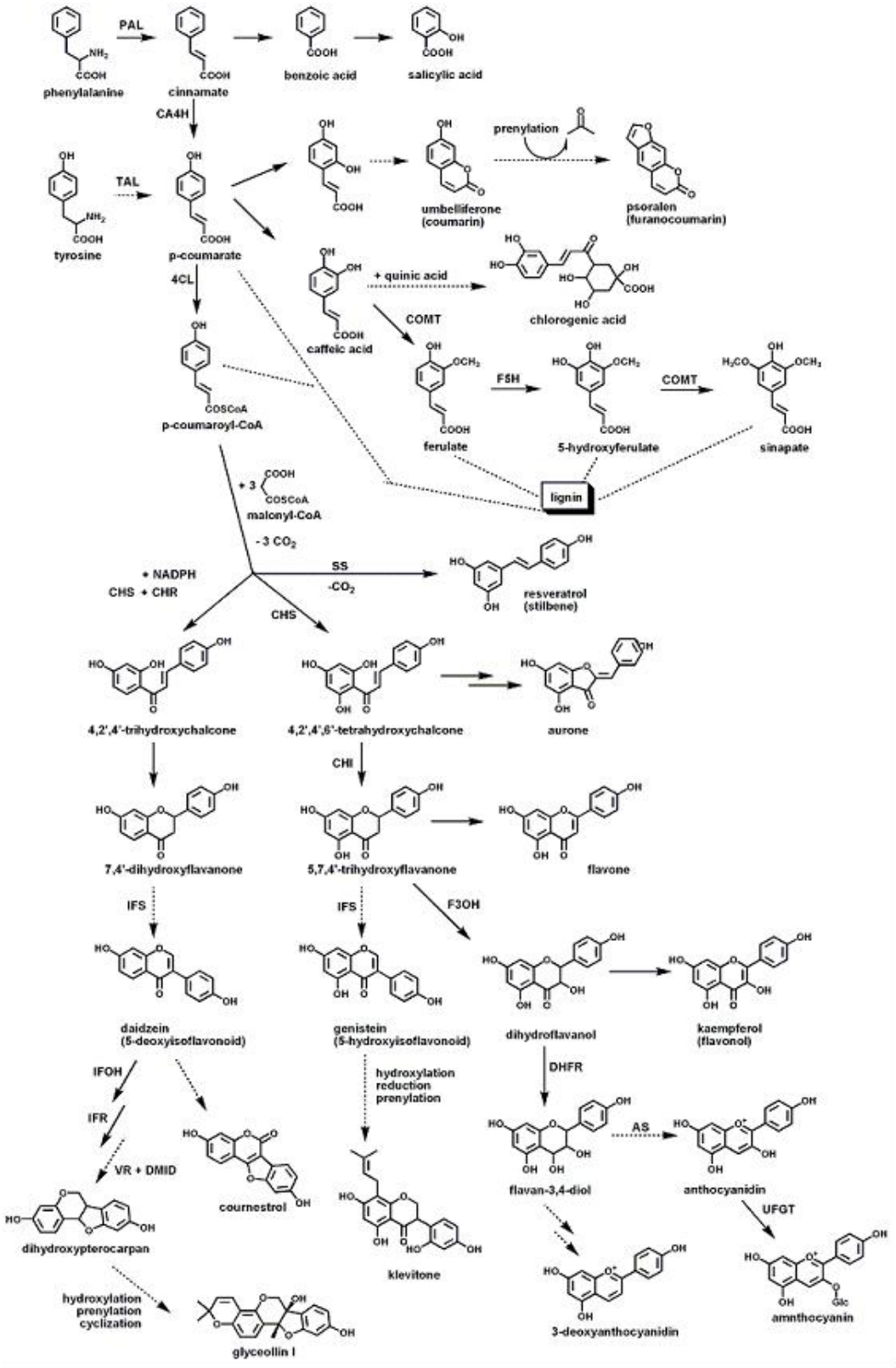

Scheme 7. Schematic of the major branch pathways of flavonoid biosynthesis. Starting with the general phenylpropanoid metabolism an enormous variety of plant-specific structures is formed (adapted from DIXON AND PAVIA, 1995. Solid lines = single enzyme catalyzed reactions, dashed lines = multiple enzyme reactions, less specific and less characzerized; CA4H = cinnamic acid 4-hydroxylase, CHI = chalcone isomerase, CHR = chalcone reductase, CHS = chalcone synthase, 4 CL = 4-coumarate coenzyme A ligase, COMT = caffeic acid =-methyltransferase, DHFR = dihydroflavonol reductase, DMID = 7,2'-dihydroxy-4'-methoxyisoflavanol dehydratase, F3OH = flavanone 3-hydroxylase, F5H = ferulic acid 5-hydroxylase, IFR = isoflavone reductase, IFS = isoflavone synthase, PAL = L-phenylalanine ammonia-lyase, SS = stilbene synthase, TAL = tyrosine ammonia-lyase, UFGT = UDP-glucose flavonol 3-O-glucosyl transferase, VR = vestitone reductase).

More than 6000 flavonoids have so far been identified in plants (HARBORNE AND BAXTER, 1999). The large variety of structures is brought about by regiospecific hydroxylation, *O*- and *C*-glycosylation, acylation, *C*-isoprenylation, *O*-sulfation, and methylation. A key step in the biosynthetic route is the addition of one or more hydroxyl groups into the phenyl ring (by the flavonoid 3'-hydroxylase, F3'H) or to the C3 atom of flavanone catalyzed by flavanone 3-β-hydroxylase (F3H). The most commonly occurring flavonones and flavonols are dihydroxylated in the C3' and C4' position of the B ring while monohydroxylated compounds are less prominent. Glycosylation is preferred at the C3 atom and to a lesser extent at the C7 position with glucose the most prevalent sugar residue. Other sugars include galactose, (gluco)rhamnose, arabinose, and xylose (COOK AND SAMMAN, 1996; HEIM, TAGLIAFERRO, AND BOBYLA, 2002). Besides 3-*O*-glycosides, flavonoids in food exist primarily as polymers such as condensed tannins (proanthocyanidins) consisting of up to 17 flavanol units (HEIM, TAGLIAFERRO, AND BOBYLA, 2002) or gallic acid esters (hydrolyzable tannins).

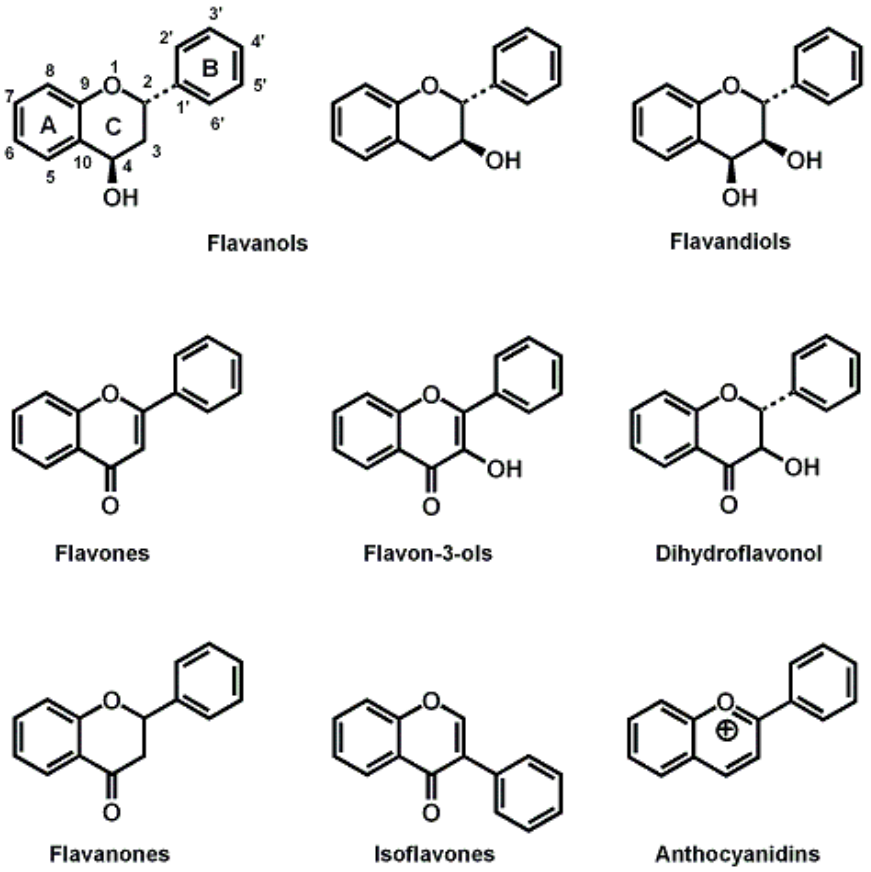

Figure 19. Basic structures of the main classes of flavonoid compounds.

5.2.2 Antioxidant and Prooxidant Properties of Flavonoids

Most of the pharmacological protective effects of flavonoids are ascribed to a number of properties, namely to their capacity to transfer electrons from free radicals, act as hydrogen donor or chelate low valent transition metal ions. By scavenging free radicals less reactive flavonoid phenoxyl radicals are formed and radical chain reactions are terminated. As a result of complexation, metal ions are sequestered which prevents the generation of hydroxyl radicals or alkoxyl radicals by decomposition of H_2O_2 or lipid hydroperoxides through superoxide-driven FENTON type redox reactions (HALLIWELL AND GUTTERIDGE, 1984; MINOTTI AND AUST, 1989),

$$M^{n+} + H_2O_2 \rightarrow M^{(n+1)+} + \cdot OH + OH^- \quad \text{(R86)}$$

$$M^{(n+1)+} + H_2O_2 \rightarrow M^{n+} + \cdot OOH + H^+ \quad \text{(R87)}$$

Likewise, enzymes carrying metal ions in their catalytic domain, such as various cytochrome P_{450} isoforms, lipoxygenases, cycloxygenases and xanthine oxidase (PARR AND BOLWELL, 2002; COS *et al.,* 1988), can be inhibited. Further protective effects are attributed to the ability of phenols to activate antioxidant enzymes (ELLIOTT *et al*., 1992) or regenerate the membrane bound antioxidant α-tocopherol by reducing its radicals (HIRANO *et al*., 2001). All these effects equally contribute to the concept of antioxidant activity. Besides antioxidant properties, pro-oxidative effects of phenolics are likewise reported and it seems that the same structural features that optimize antioxidant capacity may also exacerbate oxidative stress and damage to functional and structural cellular molecules. Autoxidation of quercetin in physiological conditions (pH 7.5, aqueous buffers) has shown to generate the superoxide anion radical which disproportionates to H_2O_2, the precursor of OH radicals in FENTON reactions (eq. R88; HODNICK *et al*., 1986)

$$O_2^{\cdot -} + 2\ H_2O \rightarrow O_2 + H_2O_2 + OH^- \quad \text{(R88)}$$

In the presence of transition metals quercetin and kaempferol have been shown to induce nuclear DNA damage and lipid peroxidation (SAHU AND GRAY, 1993; SAHU AND GRAY, 1994; RAHMAN *et al*., 1992; AHMAD *et al*., 1992). In addition flavonoids with pyrogallol structures, exhibiting three adjacent OH groups in the A and B rings (myricetin, baicelein) are considered to be particularly effective in promoting hydrogen peroxide production (HEIM, TAGLIAFERRO, AND BOBYLA, 2002 and references therein).

5.2.3 Structural Aspects of the Antioxidant Properties of Flavonoids

To efficiently scavenge free radicals, chelate metals or exert oxidant activity specific structural features are mandatory. The chelation of metal ions strongly depends on the arrangement of hydroxyl and carbonyl groups in the molecule, as will be seen later. To reduce free radicals hydrogen-/electron- donating substituents have to be present. Last but not least, the generated phenoxyl radicals have to be stable in order to prevent chain radical reactions. This requires that the unpaired electron has to be efficiently delocalized. For flavonoids three specific structural configurations have been identified. If present they facilitate the donation of hydrogen atoms and permit electron delocalization throughout the flavon skeleton. In descending order of efficacy these are: (i) the *o*-dihydroxycatechol structure in the B ring, (ii) the C2-C3 π-bond in conjugation with the pyran-4-one structure, responsible for π- electron delocalization between B and C ring, (iii) the 3- and 5-OH groups allowing hydrogen bonding to the keto group (Figure 20).

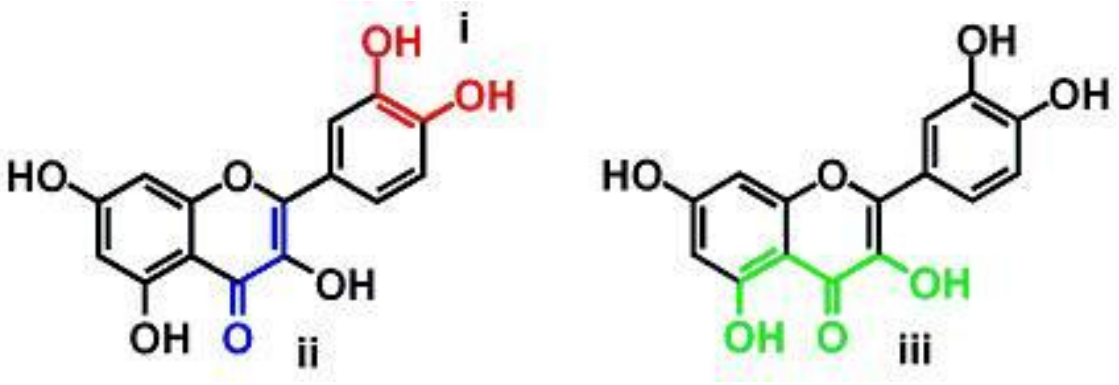

Figure 20. Three main structural components as requisites for antioxidant activity (adapted from HALBWITH, 2010).

The configuration and total number of hydroxyl groups substantially influences the antioxidative activity (Table 23). While A ring substitution correlates little with antioxidant activity, the B ring substitution pattern is the most significant determinant in ROS and RNS scavenging. The excellent antioxidant properties of flavonoids are first and foremost ascribed to the presence of the catechol function. *o*- Substitution of a second hydroxyl group or the introduction of one or two methoxy groups in *o*- position strongly enhances the antioxidant behaviour of monophenols (FUKUMOTO AND MAZZA, 2000; DEWICK, 2002).

Table 23. Classification of flavonoid compounds according to structure and Trolox equivalent antioxidant activities (TEAC). Higher TEAC values indicate greater antioxidant capability. Specific structural functionalities are responsible for superior activity to isoforms lacking these structures. ‡= HEIM, TAGLIAFERRO, AND BOBYLA, 2002 .

Class	General structure	Flavonoid	Substitution Pattern	TEAC (mM) ‡
Flavonol	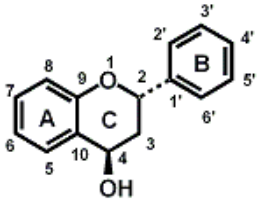	(+)-catechin	3,5,7,3‘,4‘-OH	2.4
		(-)-epicatechin	3,5,7,3‘,4‘-OH	2.5
		epigallocatechin gallate	3,5,7,3‘,4‘,5‘-OH, 3-gallate	4.75
Flavone	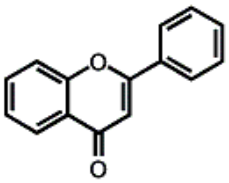	chrysin	5,7-OH	1.43
		apigenin	5,7,4‘-OH	1.45
		rutin	5,7,3‘,4‘-OH, 3-rutinose	2.4
		luteolin	5,7,3‘,4‘-OH	2.1
		luteolin glucosides	5,7,3‘-OH, 4‘-glucose	1.74
			5,4‘-OH, 4‘,7-glucose	0.79
Flavon-3-ol	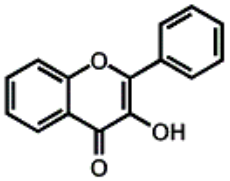	kaempferol	3,5,7,4‘-OH	1.34
		quercetin	3,5,7,3‘,4‘-OH	4.7
		myricetin	3,5,7,3‘,4‘,5‘-OH	3.1
Flavanone (dihydroflavone)	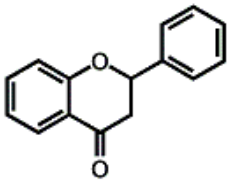	naringin	5,4‘-OH, 7-rhamnoglucose	0.24
		naringenin	5,7,4‘-OH	1.53
		taxifolin	3,5,7,3‘,4‘-OH	1.9
		eriodyctiol	5,7,3‘,4‘-OH	1.8
		hesperidin	3,5,3‘-OH, 4‘-OMe, 7-rutinose	1.08
Isoflavone	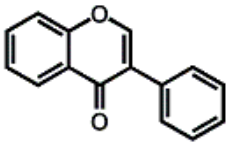	genistin	5,4‘-OH, 7-glucose	1.24
		genistein	5,7,4‘-OH	2.9
		daidzin	4‘-OH, 7-glucose	1.15
		daidzein	7,4‘-OH	1.25
Anthocyanidin	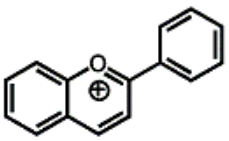	apigenin	5,7,4‘-OH	2.35
		cyanidin	3,5,7,4‘-OH, 3,5-OMe	4.42

From electronic calculations the 4’-OH group is reported to be the most acidic group for flavones and flavonols (MARTINS et al., 2004). The unpaired electron that is formed upon hydrogen abstraction can be stabilized by intramolecular hydrogen bonding (HB) from the adjacent hydroxyl group (Scheme 8).

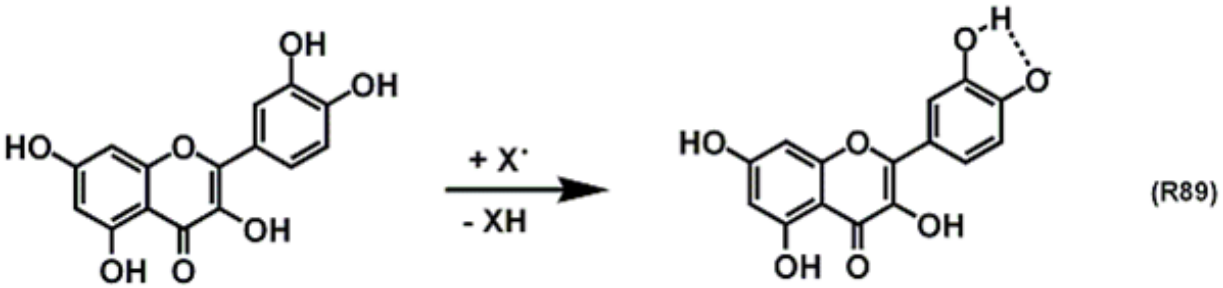

(R89)

Scheme 8. Hydrogen abstraction at C4' is thermodynamically favored due to radical stabilization from hydrogen bonding.

However, recent studies suggest that instead of being responsible for electron delocalization hydrogen bonding is more likely involved in increasing the electron density on the phenolic oxygen, thus lowering the ionization potential and facilitating subsequent electron transfer (HUVAERE, OLSEN, AND SKIBSTED, 2009). The presence of a 3-OH group increases the stability of the flavonoid phenoxyl radical. Due to hydrogen bonding with B ring hydroxyl groups flavonols and flavanols are planar, thus optimally permitting conjugation and π- electron dislocation (Table 24). Removal of 3-OH group or its methylation or *O*-glycosylation results in a minor twist of the B ring and thus abrogates coplanarity and conjugation (VAN ACKER *et al*., 1996; MARTINS *et al*., 2004; BORS *et al*., 1990).

Table 24. Torsion Angles (°) of the B Ring in both Parent Compound and Radical relative to O1. While Flavan-3-ols are planar the B Ring in Flavonones is slightly twisted (± 20°) relative to the Plane of A and C Rings (VAN ACKER *et al*., 1996).

Flavonoid	Molecule	Radical
quercetin	-0.29	-0.19
luteolin	16.29	0.04
(+)-catechin	35.64	39.19
apigenin	16.48	-0.05
diosmin	15.54	0.00
galangin	-0.27	0.07
kaempferol	-0.14	0.00
taxifolin	-27.64	-37.53
3-OMe-quercetin	-23.58	0.04
hesperitin	-42.28	-41.74
naringenin	-42.73	-41.34
rutin	27.17	nd

nd = not determined

Steric effects imparted by 4'-glycosylation exert a particularly suppressive influence through blocking the B ring catechol moiety (HEIM, TAGLIAFERRO, AND BOBYLA, 2002). Aside from occupying free OH groups necessary for hydrogen abstraction and radical scavenging, substitution of hydroxyl groups by methyl or glycosyl functions alters the solubility of flavonoids and consequently facilitates the uptake into membranes and the access to lipid

peroxyl and alkoxyl radicals. As for radical scavenging, metal complexation necessitates specific structural assignments. The biochemical activity of flavonoid complexes strongly depends on the relative position of OH groups on the rings (JOVANOVIC *et al.*, 1994) and the metal ion chelation sites (TORREGIANI *et al.*, 2005; CORNARD AND MERLIN, 2002; LEOPOLDINI, RUSSO, AND TOSCANO, 2006). However, statements about preferential metal binding sites and the binding mechanism are controversial remain unclear. This is mainly due to experimental difficulties in detecting the atomic structure of metal-flavonoid complexes with molecular resolution in solution (ZHOU *et al.*, 2001; DE SOUZA, SUSSUCHI, AND DE GIOVANI, 2003; CORNARD, DANGLETERRE AND LAPOUGE, 2005). Common flavon-3-ols are suggested to have three potential metal- binding sites, between (i) the *ortho*-catechol function in the B ring, (ii) the 3-OH and the 4-oxo group, and (iii) the 5-OH group and the 4-oxo function (Figure 21; MOREL, CILLARD, AND CILLARD, 1998).

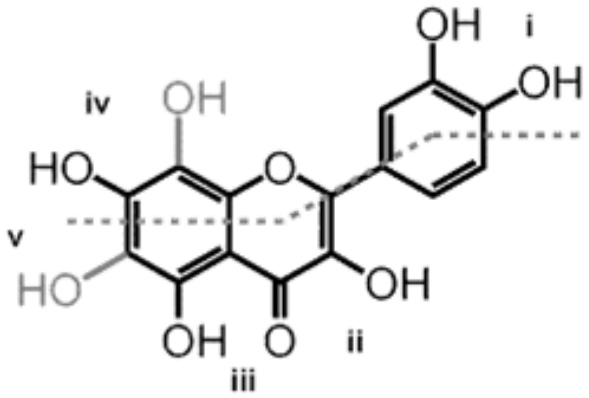

Figure 21. Possible metal binding sites of flavonoids (HALBWIRTH, 2010).

ESI-MS studies suggested that at pH 5.5 and pH 7.4 transition metal ions are preferably chelated between the 5-OH and 4-oxo groups (MIRA *et al.*, 2002). From first-principles calculations however Fe chelation at this position has shown to be thermodynamically and kinetically less favored. Position (ii) was clearly identified as the most probable chelation site for Fe^{n+} (REN *et al.*, 2008). The importance of position (ii) as the preferred site for iron complexation was confirmed by ^{1}H-NMR spectra, for which the 3-OH proton signal disappeared after formation of an M(III)-quercetin complex (DE SOUZA, SUSSUCHI, AND DE GIOVANI, 2003). Complexes at site IV, V or VI only occur if multiple hydroxyl groups are present in the A ring (HALBWIRTH, 2010). Depending on the pH and the concentration of both metal and ligand a number of stoichiometries for complexes can be formed ranging from 1:1

to 1:3 (FERNANDEZ *et al*., 2002). *O*-Methylated and *O*-glycosylated derivatives are not able to bind metal ions.

5.2.4 Flavonoid Oxidation obeys multiple Mechanisms

The molecular mechanism by which flavonoids exert their antioxidant potential has been widely and controversially discussed (RICE-EVANS AND MILLER, 1996; PARR AND BOLWELL, 2000; HEIM, TAGLIAFERRO, AND BOBYLA, 2002). Due to their low redox potentials (E_{pH7} < 0.75 V vs. NHE) flavonoids are able to easily reduce free radicals such as superoxide (≈ 0.9 V vs. NHE for $O_2^{-\cdot}$, H^+/H_2O_2 pair), alkoxyl (1.6 V vs. NHE for RO·, H^+/ROH), peroxyl (0.77-1.44 V vs. NHE for ROO·, H^+/ROOH), and hydroxyl radicals (2.3 V vs. NHE for ·OH, H^+/H_2O) (HALLIWELL AND GUTTERIDGE, 2007). Oxidation is mainly ascribed to two processes, either proceeding by hydrogen atom abstraction (HAT) of a free radical from a phenylic function,

$$R\cdot + ArOH \rightarrow RH + ArO\cdot \qquad (R90)$$

or by a proton coupled electron transfer (PCET) where single electron transfer (SET) is followed by proton migration from the resulting phenolic radical cation (HUSAIN, CILLARD, AND CILLARD, 1987; ROBAK AND GRYGLEWSKI, 1988; TOREL, CILLARD, AND CILLARD, 1986; CHEN *et al*., 1990),

$$R\cdot + ArOH \rightarrow R^- + ArOH^{+\cdot} \qquad (R91)$$

Electron transfer is determined by the ionization potential. By consequence SET is favoured in protic solvents due to solvation of the charged intermediate structures while in non-polar systems oxidation usually occurs via H-atom donation (JOVANOVIC *et al*., 1996). One-step HAT in contrast mainly depends on the O-H bond dissociation energy. As a result of hydrogen bonding between the antioxidant and the solvent, solvent effects have been shown to decrease the rate constants of hydrogen-atom transfer reactions (PEDRIELLI, PEDULLI, AND SKIBSTED, 2001). Experimental and theoretical studies of the gas-phase acidities of flavonoids have shown that the 4'-OH group is the most favored deprotonation site for flavones whereas for flavanones lacking the 3-OH and the C2-C3 double bond the most acidic hydroxyl group is located at C7 (Figure 22; MARTINS *et al*., 2004). The less acidic group in flavones is the 5-OH group due to loss of a stabilizing hydrogen bond with the 4-oxo function and a non-bonding electronic repulsion between the negative charge the negative charge of the deprotonated oxygen and the carbonyl oxygen lone pairs (LEOPOLDINI, RUSSO, AND TOSCANO, 2006). Oxidation mechanisms not only depend on the reaction conditions but are thought as

well to vary strongly with the oxidizing agent. However, different reaction conditions can lead to identical products as pathways proceed via common intermediates.

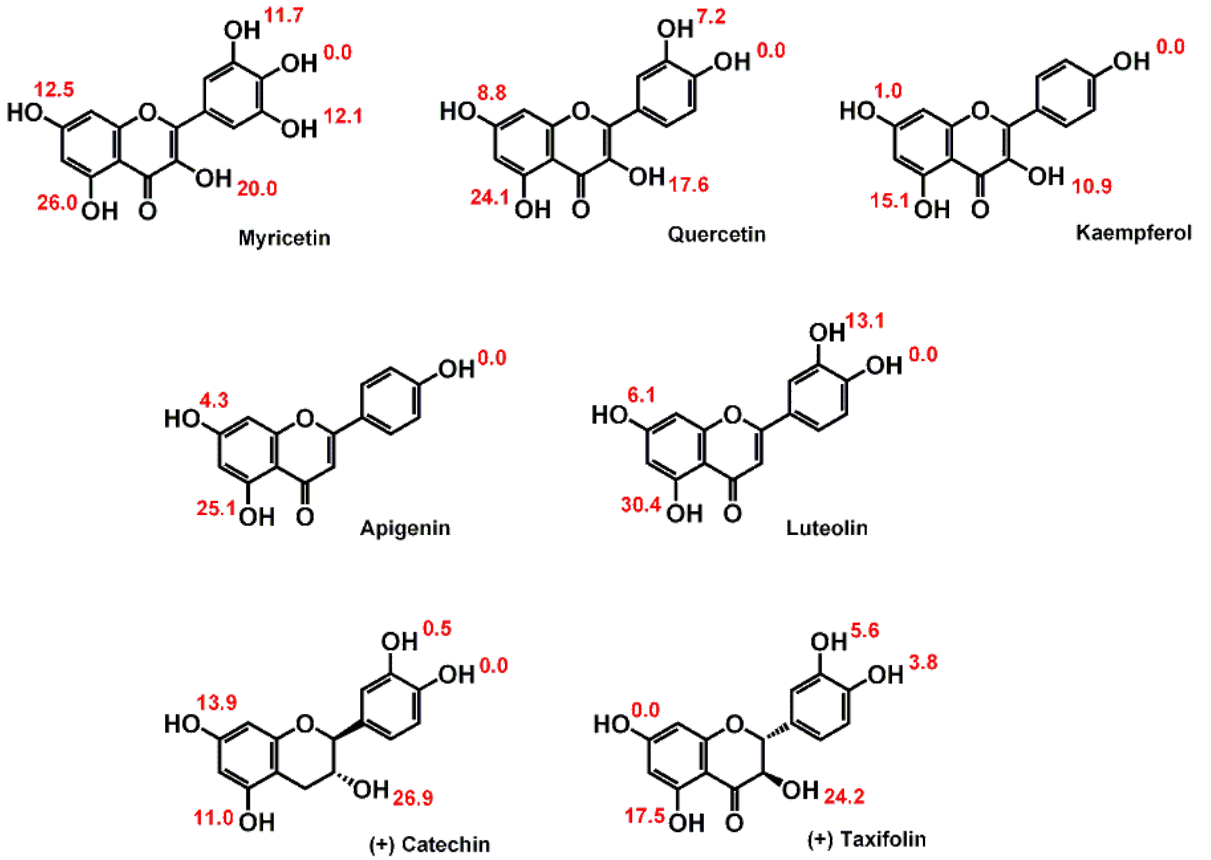

Figure 22. Gas phase relative acidities ($\Delta(\Delta_{AC}H)$) calculated for several flavonoids (DFT-B3LYP-6311+G(2d, 2p)-level, all values in kcal/mol; MARTINS *et al.*, 2004). Computed values support experimental trends. Differences to other DFT studies (LEOPOLDINI, RUSSO, AND TOSCANO, 2006) originate from the different electronic calculation levels and are negligible.

Several, in some cases unidentified reaction products have been reported. Photosensitized oxygenation of 3- hydroxyflavones by air was first described by Matsuura and co-workers (MATSUURA, MATSUSHIMA, AND SAKAMOTO, 1967; MATSUURA, MATSUSHIMA, AND NAKASHIMA, 1970), giving rise to the *O*-benzylsalicylic acid derivative 4,6-dihydroxy-2-(3,4-dihydroxybenzoyloxy)benzoic acid (**7**, Scheme 9). This depside was found as well under several other oxidizing conditions, including base-catalyzed oxygenolysis (NISHINAGA *et al.*, 1979), enzymatic catalysis with quercetin-2,3-dioxygenase (KRISHNAMURTHY AND SIMPSON, 1970; BROWN *et al.*, 1982; FUNABIKI, 1997), $O_2(^1\Delta_g)$ (TOURNAIRE, CROUX, AND MOURETTE, 1993) and upon reaction with the superoxide anion radical (Scheme 9; TOURNAIRE *et al.*, 1994). **7** is thought to be generated from a C2- centered carbanion **2b** followed in an electrophilic, rate-determining process by addition of *in situ* generated dioxygen to the deprotonated hydroperoxide species **3**. Alternatively a slow, rate-determining SET from **2b** to O_2 is

proposed, resulting in the generation of a C2- centered intermediate flavonoxyl radical and $O_2^{\cdot-}$, both reacting in a radical coupling reaction (BALOGH-HERGOVICH AND SPEIER, 2001).

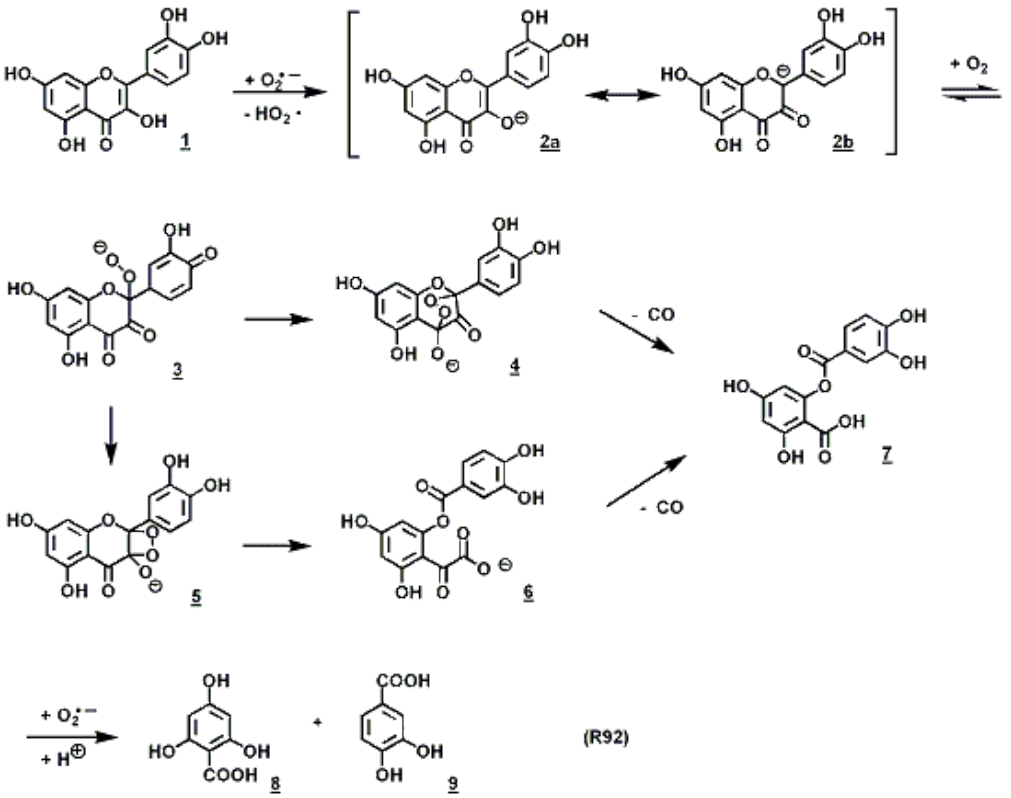

Scheme 9. Proposed mechanism for superoxide anion radical mediated oxidation of quercetin (KANO *et al.*, 1994; TOURNAIRE *et al.*, 1995).

The intramolecular nucleophilic attack of the peroxide function at C3 or C4 leads to the formation of either a 1,3-endoperoxide **4** or a 1,2-dioxetane **5**, which are both unstable and quickly decompose. **4** reacts under ring fission and decarbonylation directly to **7** while for **5** the formation of 2-(2-((3,4-dioxocyclohexa-1,5-dienyl)(hydroxyl)methoxy)-4,6-dihydroxyphenyl)-2-oxoacetic acid (**6**) has been reported (OSMAN, MAKRIS, AND KEFALAS, 2008). Hydrolysis of **7** leads to various benzoic acids derivatives, such as 2,4,6-trihydroxybenzoic acid (phloroglucinol carboxylic acid, **8**) or 3,4-dihydroxybenzoic acid (protocatechuic acid, **9**). Identical degradation products are found upon γ-irradiation (MARFAK *et al.*, 2002; MARFAK *et al.*, 2003) and heating of quercetin and its solutions in the presence of dioxygen (BUCHNER *et al.*, 2006; MAKRIS AND ROSSITER, 2000). Beyond depside formation, one-electron oxidation of quercetin with DPPH/CAN in protic and aprotic media has led to the formation of an intermediate methanol adduct **12** from solvent addition to the C2-C3 double bond. The reaction is proposed to proceed via dismutation of intermediate quercetin radicals **10**, reacting by second-order kinetics (2k in the range 10^6-10^7 dm^3 mol^{-1} s^{-1}) with the oxidant or

with themselves into quercetin (**1**) and an *o*-quinone **11a**, which subsequently isomerizes to the *p*-quinone methide type intermediate **11b**. In aqueous alkaline solution, solvent addition to **12** is followed by γ-pyrone ring opening (α-keto acid, **14**) and subsequent cleavage of the carbon chain, giving again the phenolic acids **8** and **9** (Scheme 10; DANGLES, FARGEIX, AND DUFOUR, 1999).

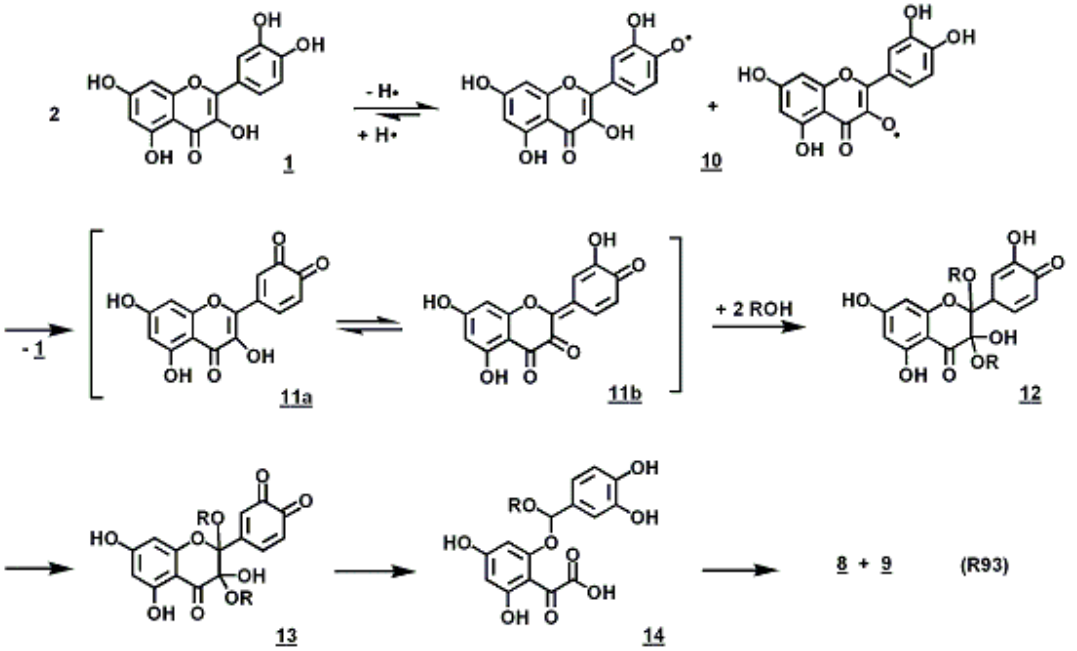

Scheme 10. Proposed mechanism for DPPH/CAN mediated oxidation of quercetin (DANGLES, FARGEIX, AND DUFOUR, 1999).

In addition, dimeric compounds such as **15** have been found (Scheme 11). The regiospecific formation of the RR and SS syn isomers points to a concerted [4+2] DIELS-ALDER type mechanism between the *o*-quinone moiety **11a** and the C2-C3 double bond of another mole quercetin **1** (KRISHNAMACHARI, LEVINE, AND PARÉ, 2002).

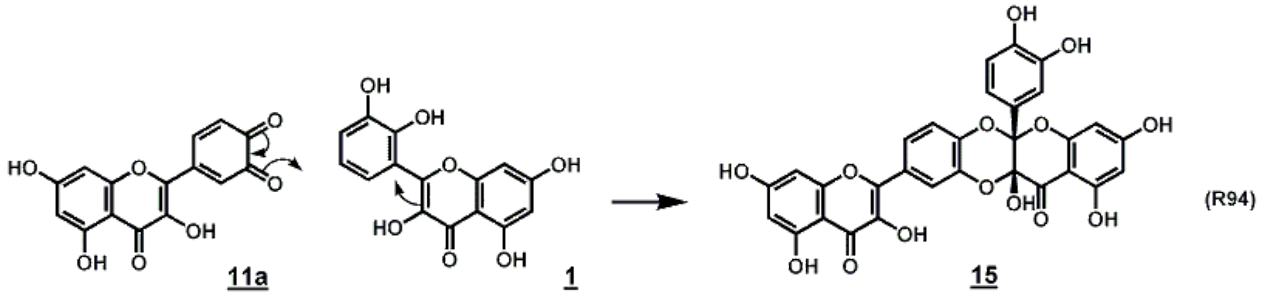

Scheme 11. [4+2] DIELS ALDER reaction between diene 11a and dienophile 1 leads to the formation of the 1,4-dioxane compound 15.

Like *o*-quinones, *p*- quinone methides are strong electrophiles. They are therefore capable as well of forming adducts through coupling reactions with themselves or various other macromolecules giving rise to manifold oligomeric compounds (AWAD *et al*., 2000; GUYOT,

VERCAUTEREN, AND CHEYNIER, 1996; ES-SAFI, GHIDOUCHE, AND DUCROT, 2007). Again luteolin which lacks the 3-OH group fails to generate dimeric products. Last but not least the electrochemical oxidation gives rise to 2-(3,4-dihydroxybenzoyl)-2,4,6-trihydroxy-3(2*H*)-benzofuranone (**19**) which is yet another new reaction product (Scheme 12, JØRGENSEN *et al.*, 1998). A two-electron oxidation is suggested with initial formation of a diradical, which after disproportionation to **11b** and intermediate formation of a strongly electrophilic flavylium ion **16** yields a 3,4-flavandione **17** with unchanged substitution pattern in the A and B ring. The keto compound **17** rearranges through the chalcan-trione tautomer **18** to the furanone derivative **19**. The presence of a 3-OH group seems to be crucial as no reaction products of luteolin could be isolated.

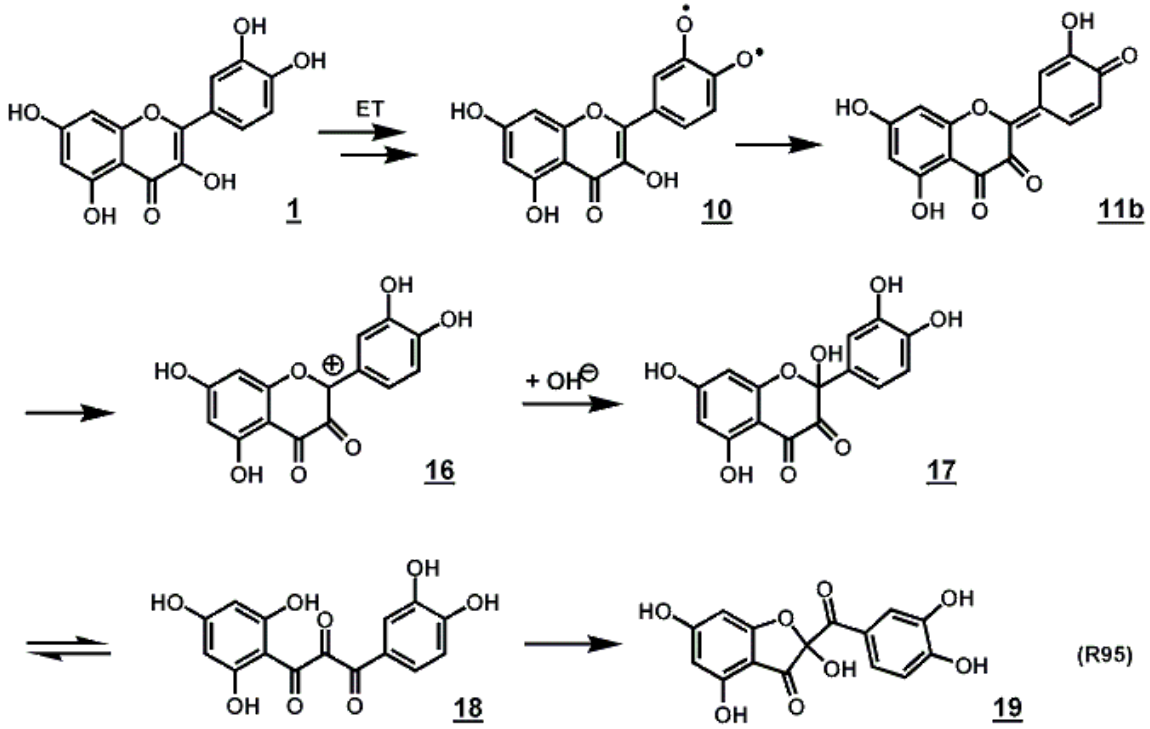

Scheme 12. The electrochemical oxidation of quercetin leads to the formation of a furanone derivative (JØRGENSEN *et al.*, 1998).

The furanone **19** was as well observed as end product of the oxidation of quercetin with mushroom tyrosinase (KUBO, NIHEI, AND SHIMIZU, 2004), from two electron transition metal ion mediated oxidation (JUNGBLUTH, RÜHLING, AND TERNES, 2000) and upon reaction with azodiisobutyronitrile (AIBN) in aprotic conditions (KRISHNAMACHARI, LEVINE, AND PARÉ, 2002).

5.2.5 Effects of Conventional Food Processing on Flavonoid Content

The importance of investigating the effects of plasma-based preservation technologies is underlined by the large number of plant-based food products. Phenolic compounds significantly contribute to the nutritional qualities of fruits and vegetables and are

responsible for major organoleptic characteristics such as color and taste of plant-based foods and beverages. The numerous enzymatic and non-enzymatic reactions phenolic compounds undergo during postharvest food storage, processing and preservation (Table 25) often have a significant impact on the aesthetic apparel and the nutritional value of food and beverages.

Table 25. Quality losses and degradation of polyphenolic compounds have been observed for various industrial processing technologies and domestic cooking procedures.

Procedures	Food
Solvent extraction	Juices (lemon, mandarin)[a]
SO_2 treatment	Raisins[b]
Pasteurization	Juices (blueberry, orange, grapes)[c]
Enzymatic Clarification	Juices and concentrates (peach, apple, black current)[d]
Canning	Beans, cherries cranberry juice[e]
Irradiation	Herbs , sesame, strawberries, grape pomace, lettuce[f]
Drying	Berries, corn, pear, prunes[g]
Fermentation	Grapes, berries, tea, beans[h]
Peeling, chopping	Peaches, apples, cherries, berries, grapes, onions, lettuce, amarant[i]
Cooking, boiling	Berries, onions, tomatoes, beans, peas, spinach, potatoes, broccoli[j]
Frying	Onions, tomatoes, beans, peas, olive oilk
Roasting	Buckwheat, coffee, Cocoa, Peanuts, Safflower[l]
Microwave cooking	Onions, Beans, peas[m]
Baking	Berries[n]

[a]= CALABRÒ *et al.*, 2004; MARIN *et al.*, 2002 ; NOGOTA *et al.*, 2003, [b]= KARADENIZ, DURST, AND WROLSTAD, 2000, [c]= SKREDE, WROLSTAD, AND DURST, 2000; GIL-IZQUIERDO,GIL, AND FERRERES, 2002; FULEKI AND RICARDO-DA SILVA, 2003, [d]= BENGOECHEA *et al.*, 1997; GÖKMEN *et al.*, 2001; LANDBO *et al.*, 2006, [e]= PRICE, *et al.*, 1998A; CHAOVANALIKIT AND WROLSTAD, 2004; CHEN, ZUO, AND DENG, 2001, [f]= KOSECKI *et al.*, 2002 ; LEE *et al.*, 2005 ; BREITFELLNER, SOLAR, AND SONTAG, 2002 ; AYED, YU, AND LACROIX, 1999; NUNES *et al.*, 2008, [g]= ASAMI *et al.*, 2003; FERREIRA *et al.*, 2002; DEL CARO *et al.*, 2004, [h]= PEREZ-MAGARINO AND GONZALES-SAN JOSE, 2004; MARTIN AND MATAR, 2005; SCHULZ, JOUBERT, AND SCHÜTZE, 2003; CHEN *et al.*, 2005, [i]= EWALD *et al.*, 1999 ; GENNARO *et al.*, 2002; ASAMI *et al.*, 2003 ; TSAO AND YANG, 2003; DUPONT *et al.*, 2000; ADEBOOYE, VIJAYALAKSHMI, AND SINGH, 2008, [j]= PRICE, BACON, AND RHODES, 1997 ; CROZIER *et al.*, 1997 ; EWALD *et al.*, 1999 ; GILL, FERRERES, AND TOMAS-BARBERAN, 1999 ; GU *et al.*, 2004, XU AND CHANG, 2009 ; LARRAURI, RUPEREZ, AND SAURA-CALIXTO, 1997 ; TUDELA *et al.*, 2002 ; HÄKKINEN *et al.*,, 2000 ; PRICE *et al.*, 1998b ; VALLEJO, TOMAS-BARBERAN, AND GARCIA-VIGUERA, 2003,[k]= PRICE, BACON, AND RHODES, 1997 ; CROZIER *et al.*, 1997; EWALD *et al.*, 1999 ; LEE *et al.*, 2008 ; GOMEZ-ALONSO *et al.*, 2003, [l]= DIETRYCH-SZOSTAK AND OLESZEK, 1999 ; DEL CASTILLO, AMES, AND GORDON, 2002 ; KOFINK, PAPAGIANNOPOULOS, AND GALENSA, 2007; CHUKWUMAH *et al.*, 2007; LEE, PARK, AND CHOI, 2005, [m]= CROZIER *et al.*, 1997; EWALD *et al.*, 1999, [n]= LYONS *et al.*, 2003

For example, storage of onions results in the loss of 25 to 33% of the quercetin during the first 12 days, but only small losses thereafter (PRICE, BACON, AND RHODES,, 1997). When cell integrity is affected, an increased risk of oxidative damage due to the activation of oxidative enzymes such as polyphenol oxidase has been reported (AMIOT *et al.*, 1995; LEE *et al.*, 1990). Heterogeneous polymers are formed from coupled oxidation reactions of quinones and browning of the tissue occurs, which usually is detrimental to quality (WALKER AND FERRAR, 1998; CHEYNIER, 2005). Unlike the original fresh product, industrially produced products (tea,

red wine, and fruit juice) are strongly different regarding their flavonoid levels and profiles and various procedures have been reported to affect procyanidin and catechin concentrations in fruit juice, quercetin glucosides, catechins, and procyanidins in grapes, procyanidin and flavonol levels in tomatoes and related sauces, and quercetin concentrations in berries (KYLE AND DUTHIE, 2006). Domestic preparation such as chopping or shredding affects the flavonoid content as well. Peeling and trimming accounted for 21 to 39% losses of flavonols in onions (PRICE, BACON, AND RHODES, 1997; EWALD *et al*., 1999), which is not surprising considering that 90 % of quercetin has been reported to be in the first and second layer of the onion (EWALD *et al*., 1999; BEESK *et al*., 2010). Similar effects have been observed for thermal processing of onions, tomatoes, and green beans with varying amounts of losses depending on the treatment (GENNARO *et al*., 2002; PRICE, BACON, AND RHODES, 1997; EWALD *et al*., 1999). For tomatoes and onions the quercetin content significantly decreased after microwave cooking an increased reduction, whereas losses from frying were less substantial (CROZIER *et al*., 1997). When cooked in water, foods having a high surface area or ruptured cell walls show a substantial reduction in the levels of flavonoids (PRICE *et al*., 1998; PRICE *et al*., 1998). Referring to studies by Mizuno and co-workers (MIZUNO *et al*., 1992), it was argued that thermal degradation of quercetin under the studied boiling conditions could be excluded and losses were mainly attributed to increased leaching of flavonoids from the cellular compartment of vegetables into the cooking water (a polar solvent) (EWALD *et al*., 1999; PRICE, BACON, AND RHODES, 1997). In contrast, quercetin conjugates are quite stable to high temperatures (373 K). Recent studies however could not confirm that flavonoids are as heat-stable as predicted, at least regarding isolated compounds and overall longer treatment times. Cooking flavonoids in aqueous solution at 373 K for more than 60 minutes resulted in a degradation of quercetin and rutin, with rutin being more stable due to the conjugated sugar moiety than the aglycone (BUCHNER *et al*., 2006). Several reaction products with often higher polarity than quercetin have been found, including protocatechuic acid and a furanone derivative (Figure 23). Under non-aqueous conditions (60 minutes roasting at 450 K), in turn, aglycones have shown to be inert whereas glycosidic compounds are rapidly (already within the first 5-15 minutes) and strongly degraded leading to glucosidase-mediated formation of monoglucosides and free quercetin (ROHN *et al*., 2007).

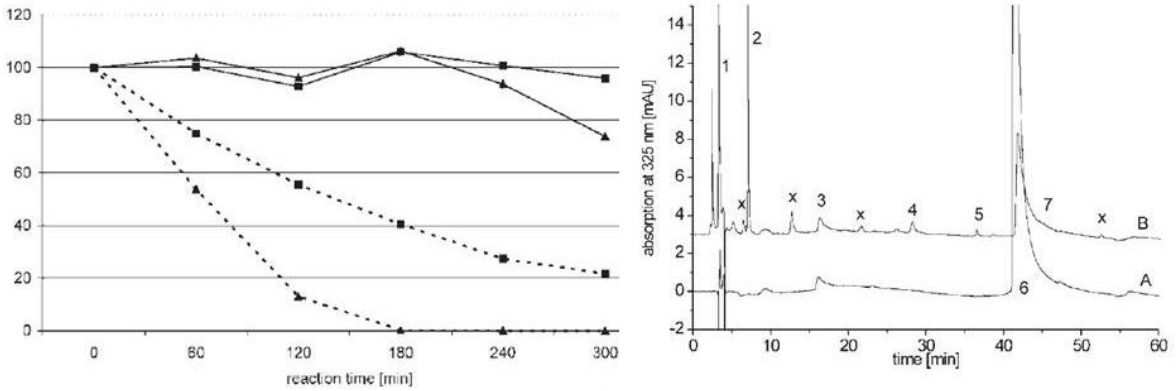

Figure 23. (Left) Degradation of quercetin (▲) and rutin (■) in aqueous solution (pH 8) at 100°C, comparison between air (dashed lines) and nitrogen perfusion (solid lines). (Right) HPLC-DAD chromatogram of quercetin degradation products with air perfusion (A) control, (B) after 60 minutes reaction time (1-7, identified compounds, including 6= quercetin, 2 = protocatechuic acid, 5 = furanone derivative; x = unidentified species; BUCHNER *et al.*, 2006).

Although plasma is considered to only generate pure surface effects and operating temperatures are far from causing thermal damage, the elucidation of plasma- flavonoids interactions is important to validate NTP as a new preservation method. In tradition of an outstanding expertise in the field of process-induced flavonoid modifications, questions in this work likewise tend to address on how such interactions could result in flavonoid degradation. Comparing reaction kinetics and characterizing major products is especially interesting with respect to often from a nutritional point of view disadvantageous conventional thermal processing technologies.

6 Materials and Methods

6.1 Materials

6.1.1 Reagents

Caffeic acid, chlorogenic acid, and protocatechuic acid (all HPLC grade) were purchased from Fluka Chemie GmbH (Buchs, Switzerland). Kaempferol, myricetin, luteolin, diosmetin (+) catechin, (-) epicatechin, and taxifolin (all reagent grade) were from Extrasynthese SA (Genay, France). Quercetin (dihydrate, 99%) was obtained from Sigma-Aldrich Chemie GmbH (Steinbach, Germany). Quercetin-4'-O-monoglucoside (spiraeoside, QMG) and quercetin-3,4'-O-diglucoside (QDG) were isolated from onions as described in the literature (Rohn et al., 2007). The onions were purchased from a local supermarket (Reichelt, Berlin, Germany). Rutin was obtained from Janssen Chimica (Beerse, Belgium). All solvents used were of HPLC grade quality (Carl Roth, Karlsruhe, Germany). Ethyl acetate (>99,8%, *p.a.*) was provided by Fisher Scientific GmbH (Schwerte, Germany). Hydrochloric acid (37%, *p.a*.) was purchased from Bernd Kraft GmbH Salze & Lösungen (Duisburg, Germany). Ultra- pure demineralized water (Milli-Q, Millipore, Schwalbach/Ts., Germany) was used for HPLC analysis.

6.1.2 Plant Material

Commercially grown lamb's lettuce of the genus *Valerianella* (*V. locusta*), savoy cabbage (*Brassica oleracea* convar. *capitata* var. *sabauda* L.) and red cabbage (*Brassica oleracea* convar. *capitata* var. *rubra* L.) was purchased from a local supermarket (Lidl, Berlin, Germany). Kale (*Brassica oleracea* var. *sabellica* L.) was obtained from the Leibniz-Institute of Vegetable and Ornamental Crops Grossbeeren and Erfurt e.V. (Grossbeeren, Germany). All vegetables were frozen at 233 K, lyophilized in a freeze-dryer (Christ Loc-1m, Alpha 2-4 unity, Martin Christ GmbH, Osterode, Germany) and stored at room temperature under anaerobic conditions until analysis. After plasma treatment leaves are immediately ground to a fine powder in a domestic blender and kept at 253 K until further analysis.

6.2 Plasma Sources

6.2.1 Atmospheric Pressure Plasma Jet (APPJ 1)

The atmospheric pressure plasma jet (APPJ 1) is a non-thermal, high-pressure, spatially uniform glow plasma discharge. It consists of a ceramic nozzle with a inner coaxial needle electrode mounted in the centre and an outer grounded ring electrode placed at the nozzle outlet (Figure 24). The discharge operates on a feedstock gas (Ar 5.0, Purity $\geq$ 99,999 %, Linde AG, Pullach, Germany) which flows between the two electrodes. An RF generator is coupled to the center electrode via a matching unit, necessary to match the impedance of the generator to that of the discharge in order to maximize the power transfer and minimize the reflected RF power (CONRADS AND SCHMIDT, 2000). By applying a 27.12 MHz electric field, a bulk plasma is generated between the electrodes, starting from the tip of the needle electrode and expanding outside the nozzle into the ambient air. High energetic electrons are present at the entire length of the jet (BRANDENBURG *et al.*, 2007). The Ar effluent is gradually mixed with the surrounding air before impinging on the substrate. Depending on the gas flow rate and the applied power, the plasma jet has a length of 10 mm. Due to the inner diameter of the nozzle outlet the plasma has a cross-section of around 7 mm, enabling the point-wise and simultaneous treatment of small spots.

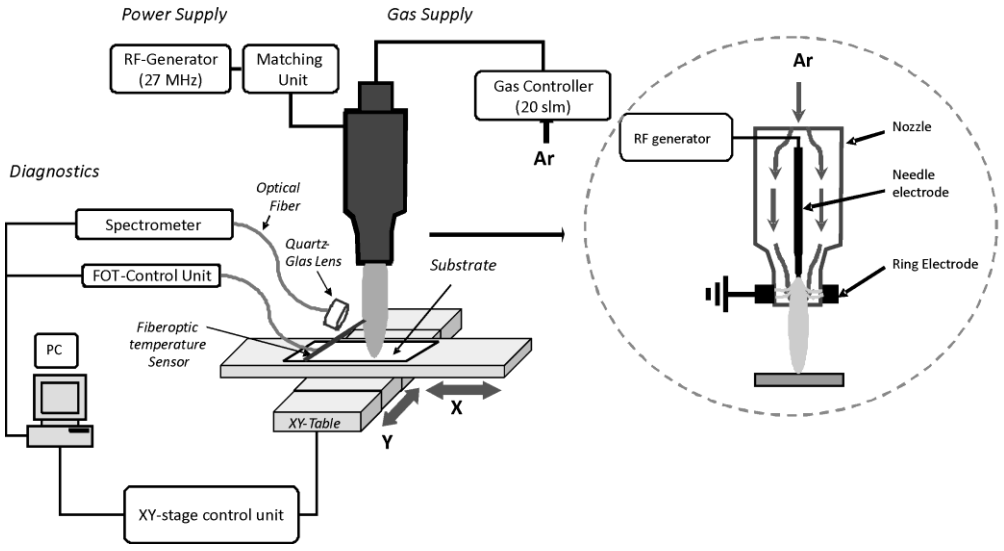

Figure 24. Experimental set-up of the APPJ 1 (BRANDENBURG *et al.*, 2007).

6.2.2 Radio-Frequency Glow Discharge (RFGD)

In addition to APPJ 1, a low-pressure RF driven glow discharge (RFGD, Emitech K1050 X Plasma Asher, Emitech Ltd, Kent, UK) was applied (Figure 25). The RF-generator is combined with a matching network. As feed gas, pure oxygen (Purity= 4.8; Air Liquide Deutschland GmbH, Düsseldorf, Germany) driven at 0.5 mbar was chosen. Treatment was carried out for up to 300 s at a power of 75 and 150 W. Before initiating the glow discharge, the reactor was evacuated, purged with the appropriate feed gas and re-evacuated again, finally achieving a pressure of $p < 10^{-2}$ mbar. When a stable pressure had been established, a capacitively coupled plasma was generated in the reactor. After treatment, the samples were exposed to the laboratory atmosphere while being transferred to surface analytical instruments or HPLC.

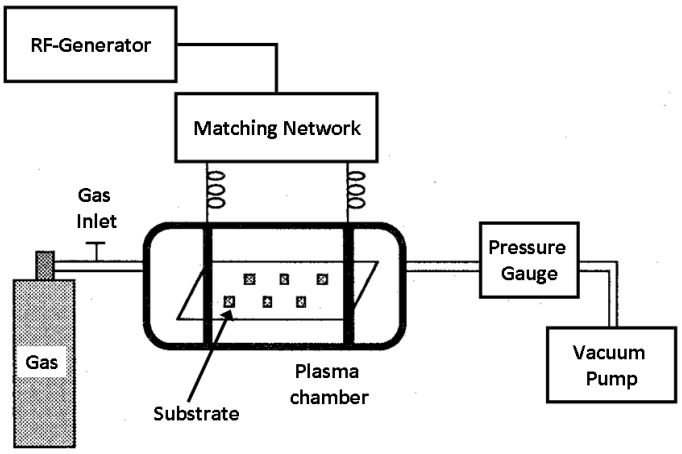

Figure 25. Experimental set-up of RFGD.

6.2.3 Various Plasma Sources for Surface Analytical Experiments

Changes in the physical properties and chemical composition of benzopyrone layers during APPJ 1 induced decomposition were investigated by different surface analytical measurements (see sections below) and compared to a series of different discharge configurations suitable for surface treatment at atmospheric pressure, including a non-thermal molecular ratio frequency jet plasma (APPJ 2). The operative parameters of the applied plasma sources are summarized in Table 26. A detailed description of the experimental setup of APPJ 2 can be found elsewhere (FOEST *et al.*, 2005). Optical emission

spectroscopy, mass spectroscopy and measurements of the axial and radial temperature profiles are used to characterize the discharge.

Table 26. Plasma Sources used in this work.

Parameters	Radio Frequency Plasma (Plasma Jets)				Microwave Plasma	
	APPJ 1	APPJ 2				
System Pressure (mbar)	1013.3	1013.3	1013.3		1	
Feeding gas	Ar	Ar	O_2	Ar	Ar	O_2
Gas flow [slm]	20	5	0.08	5	0.04	0.06
Power [W]	20	10	10		1200 (pulsed)	
Sample to electrode distance [mm]	4	5	5		110	
Treatment time [s]	60	60	60		100	

6.3 Sample preparation

6.3.1 Sample Preparation

Pure compounds were dissolved in 50% methanol (MeOH) to give a 0.5 mM stock solution. Samples were prepared by placing 100 µL of the solution into the mould (~15 mm diameter) of a microscope slide made of soda-lime glass (76 x 26 mm, 1.2-1.5 mm thickness; Carl Roth GmbH + Co. KG, Karlsruhe, Germany). The samples were then dried for at least 1h before being exposed to two plasma sources. Measurements were done in triplicate per parameter set, keeping the pressure and gas flow rate constant. After plasma treatment the adsorbates were rinsed off the slides with pure MeOH, and the collected solvent fractions evaporated to dryness under a constant flow of nitrogen. The dried samples were diluted again in 200 µL MeOH before being submitted to RP-HPLC.

6.3.2 Sample Preparation for Surface Analytical Experiments

For XPS, CA, and ATR-FTIR measurements quercetin samples were prepared as pellets from pure, well ground powder with a hydraulic laboratory press (LOT-Oriel GmbH & Co. KG, Darmstadt, Germany) using evacuable pellet dies (Graseby Specac Ltd., Kent, UK). The die assembly was evacuated for 1-2 minutes before a load of 10 tons was applied for another 10

minutes. After releasing the vacuum and load of the die, pellets had a thickness of about 700 µm with a diameter of about 13 mm.

6.4 Isolation and Characterization of Food Phenol Compounds

6.4.1 Extraction and Purification of Phenol Compounds

For *V. locusta:* Sample preparation was done according to Hohl and co-workers (HOHL *et al*., 2001), dissolving 2 g of dried lettuce 3 × 50 mL $CHCl_3$ under continuous stirring for 30 minutes each. After removing the solvent, samples were sonicated for 5 min and finally air-dried for about 2 hours. The colourless residue was then divided into two portions of 1 g, shaken in 2 × 35 mL aqueous methanol (70%, v/v) for 15 min at 323 K. The mixture was filtered by suction on a G4 glass filter covered with paper filter and the combined extracts evaporated *in vacuo* at 313 K. The aqueous residue was resolved in 10 mL 70 % methanol, purified by solid phase extraction (SPE, polyamide 500 mg). 20 µL of the solution were analysed by HPLC-DAD.

For *B. oleracea* var. *sabellica* L.: Leaves were frozen at 233 K, lyophilized and ground. 2 g of ground sample was dissolved in 25 mL of 62.5% aqueous methanol and stirred at 500 rpm for 1 h. The mixture was filtered, and aliquots were used for further analysis.

6.4.2 Hydrolysis and Isolation of Aglycones

For *V. locusta:* Hydrolysis was done without prior SPE. 5 mL of 2 N HCl were added to 5 mL of the extract and the solution hydrolyzed for 1.5 h at 363 K. As the reaction was stopped, the solution was cooled to room temperature, and the mixture extracted twice with 15 mL ethyl acetate for 15 min under continuous stirring. Flavonoid recovery was determined by spiking the methanolic extracts with *p*- coumaric acid before hydrolyzate extraction to measure eventual losses. The organic phases were concentrated to dryness under nitrogen. The residue was resolved in 5 mL methanol. A sample of 20 µL was analysed by HPLC-DAD.

6.5 Statistical Analysis

Concentration of flavonoids in foods can vary by many orders of magnitude due to the influence of numerous factors, such as species, variety, climate, degree of ripeness and

postharvest storage. The precision of replication for the different lettuce samples after extraction and hydrolysis therefore was investigated by comparing the concentration of selected compounds by HPLC-DAD. For phenolic acids a total deviation of 6.6% (chlorogenic acid), 11.6% (protocatechuic acid), and 13.6% (caffeic acid) has been found. For flavonoids the mean deviation ranges from 17.5% (diosmetin) to 24.6% (luteolin). Plasma and simulation experiments were repeated three (pure compounds) to four times (lettuce) and the standard deviation (SD) was calculated. The mean values along with the SD are reported in the respective figures.

6.6 Photochemical and Thermal Decomposition Studies

Plasma-induced decomposition was compared with photooxidative decomposition reactions and thermolysis. Samples were prepared on microscopic slides as described for plasma degradation experiments. In case of leaves no further preparation was needed. For the photodegradation a 254-nm UV lamp (Fisher-Bioblock Scientific, Illkirch, France) was used. The energy dose per mole was adjusted to the UV dose measured in the APPJ 1 driven with 20 slm Ar. Thermolysis was studied using a vacuum drying cabinet (Heraeus, Hanau, Germany). The temperature was 373 K.

6.7 Methods

6.7.1 Isocratic Reversed-Phase High-Performance Liquid Chromatography

Pure compounds were analyzed using an isocratic RP-HPLC. The HPLC system consisted of a HPLC pump (Model 64, Knauer, Berlin, Germany), an autosampler (Model 465, Kontron Instruments), and a variable UV-vis wavelength detector (Knauer, Berlin, Germany), operating at 280 and 365nm. The detector was connected to a C-R4AX chromatopac data processor (Shimadzu Co., Kyoto, Japan). The column was a 250 mm x 4.6 mm i.d., S-3 µm, YMC-Pack Pro C18 column (YMC Europe GmbH, Dinslaken, Germany) thermostatically controlled to maintain a temperature of 313 K. The mobile phase consisted of ACN/ H_2O/ CH_3COOH (30:65:5, v/v). Elution was performed at a flow rate of 0.4 ml min^{-1}.

6.7.2 Gradient-based Reversed-Phase High-Performance Liquid Chromatography

For *V. locusta:* Glycosidic compounds and the extracts of *V. locusta* were analyzed with a gradient-based RP-HPLC. The HPLC system (Shimadzu, Duisburg, Germany) consisted of a quaternary pump (LC-9A), a photodiode- array UV-vis detector (Shimadzu SPD-M6A) and an autosampler (AS-950, Jasco, Gross-Umstadt, Germany). A gradient elution was carried out on a 150 x 3.00 mm i.d., Prodigy 5u ODS3 100A column (phenomenex, Aschaffenburg, Germany). Separation was done using H_2O/ ACN/ CH_3COOH (94.5:5:0.5, v/v/v) (A) and ACN (B) as mobile phases. Gradient elution was performed as follows: 0% B (5 min); 0-4% B in 4 min; 4% B (6 min); 4-8% B in 15 min; 8-22% B in 15 min; 22-28% B in 5 min; 28% B (5 min); 28-45% B in 10 min; 45-0% B in 1 min at a flow rate of 0.7 mL/min and a column temperature of 300 K. Spectra were recorded from 200 to 500 nm. UV-spectra detection was performed simultaneously at 325, 365, and 280 nm. The intensity was calculated by integration of peak areas.

For *B. oleracea* var. *sabellica* L.: The extracts of kale were analyzed using a HPLC series 1100 from Agilent (Waldbronn, Germany) consisting of a degasser, binary pump, autosampler, thermostat and a photodiode array detector. Compounds were separated on a Prodigy (ODS 3, 150 x 3.0 mm, 5 µm, 100 A) column (phenomenex, Aschaffenburg, Germany) with a security guard C18 (ODS 3, 4 x 3.0 mm, 5 µm, 100 A) at a temperature of 298 K. Elution was done with H_2O/ CH_3COOH (99.5:0.5, v/v) (A) and ACN (100%, B) as mobile phases using a gradient method described by Schmidt et al. (SCHMIDT et al., 2010.) at a flow of 0.3 ml/min and a measured detection wavelength of 370 nm.

6.7.3 Total Phenolic Content

The total phenolic content of kale extracts was determined using the FOLIN-CIOCALTEU (FC) colorimetric method (SINGLETON, ORTHOFER, AND LAMUELA-RAVENTOS, 1999) modified by Zietz and co-workers (ZIETZ et al., 2010). The FC assay relies on the transfer of electrons in alkaline medium from phenol compounds to phosphomolybdic/phosphotungstic acid complexes, which are determined spectroscopically at 736 nm. Although the electron transfer reaction is not specific for phenol compounds, extraction procedures usually eliminate approximately 85% of ascorbic acid and other potentially interfering compounds (AINSWORTH AND GILLESPIE, 2007). To summarize, 400 µL of a 20-fold dilution of each extract was mixed with 2.5 mL of distilled water, 100 µL of FC reagent and neutralized with 1 mL of Na_2CO_3 (7.5 %, w/v). After

having incubated at 308 K for 15 min the absorbance of the solution was measured at room temperature (SPECORD 40, Analytik Jena AG, Jena, Germany). Results were expressed as millimoles of gallic acid equivalents per gram of dry matter (mmol GAE g^{-1} dm). All extracts were analyzed in duplicate.

6.7.4 Trolox Equivalent Antioxidant Capacity Assay (TEAC)

To assess the amount of radicals that can be scavenged by an antioxidant, the so-called antioxidant capacity, a modified TEAC assay (ROHN *et al*., 2004) was applied. 100 µL of a 25-fold dilution of methanolic kale extract was mixed with 500 µL of an 2,2'-azino-bis(3-ethylbenzthiazoline-6-sulphonic acid **(**ABTS) working solution (500 µM). The $ABTS^{+\bullet}$ radical was generated by chemical reaction with potassium persulfate ($K_2S_2O_8$, 10 mM, 200 µL). After a fixed time period (6 minutes), the remaining $ABTS^{+\bullet}$ concentration is quantified photometrically at a wavelength of λ= 734 nm (SPECORD 40, Analytik Jena, Jena, Germany), assuming a molar extinction coefficient of 1:5 $\times$ 10^4 M^{-1} (Re et al., 1999). The reduction in $ABTS^{+\bullet}$ concentration, induced by a certain concentration of antioxidant, is related to that of trolox and gives the TEAC value of that antioxidant, expressed as millimoles of trolox equivalents per gram of dry matter (mmol trolox g^{-1} dm). Each extract was investigated in duplicate.

6.7.5 Contact Angle Measurements

The surface wettability of the samples is evaluated by contact angle measurements at room temperature using the static sessile drop technique. In case of quercetin, measurements were performed using a DIGIDROP contact-angle meter (GBX Instrumentation Scientifique, Romans, France). A drop of ultra-pure water with a volume of 0.5 µl was placed on the flat horizontal sample surface with a microsyringe and was immediately (within 1 s) and automatically photographed with a black and white CCD camera (500 x 500). The contact-angle Θ was computationally determined from the captured images. The measurement error is ± 2°. In case of *V. locusta* leaves, measurements were performed on the adaxial surface of each leaf within 5-10 minutes after the plasma treatment. The camera was a Leica DFC 320 (Leica Microsystems GmbH, Wetzlar, Germany) connected to a computer based image capture system (stereomicroscope type 475052 from Carl Zeiss MicroImaging GmbH,

Göttingen, Germany). The reported contact angles are the average of at least five measurements (exception for 20 s exposure: 2), placed on different leaves and at different positions on the leaf itself. Contact angle determination was done using the open source software "Image J" (*http://rsb.info.nih.gov/ij/index.html*).

6.7.6 XPS Surface Chemical Analysis

The chemical composition of the surfaces was determined by XPS using an Axis Ultra spectrometer (Kratos, Manchester, UK). All wide-scan and high-resolution measurements were performed with monochromatic Al K_α line irradiation at 1486 eV and charge neutralization. The spot size was 250 µm in diameter. Small X-ray power of 150 W (15 kV anode voltage, 10 mA emission current) with a pass energy of 80 eV was applied for the estimation of the chemical element composition. Energetically highly resolved C 1s were recorded at a pass energy of 10 eV with an X-ray power of 225 W (15 kV and 15 mA). Data acquisition and processing were carried out using CasaXPS version 2.3.14dev29 (Casa Software Ltd., Teignmouth, UK). All values are given in atomic percent and ratios thereof. The peak fitting parameters were a GAUSS-LORENTZ (30% LORENTZ) distribution, linear baseline and a restricted FWHM between 1.0 and 1.2 eV.

6.7.7 Attenuated Total Reflexion FTIR Spectroscopy

Samples were analyzed ex-situ by a Bruker Equinox 55 FTIR spectrometer with a coherent 500 mW laser fitted with a Golden Gate diamond top-plate attenuated total reflection accessory (Specac Ltd., Orpington, Kent) (exception: quercetin; FTIR spectrometer: Spectrum One, Perkin Elmer, Rodgau-Jügesheim, Germany). Spectra were acquired over the range 4000 to 400 cm^{-1} as a mean of 32 scans and at a spectral resolution of 4 cm^{-1} using OPUS version 4.2 software (Bruker Optics Ltd.). Freeze-dried lettuce leaves were placed with their adaxial surface at different positions onto the centre of the diamond plate (Figure 26). Samples were prepared in triplicate for FTIR analysis.

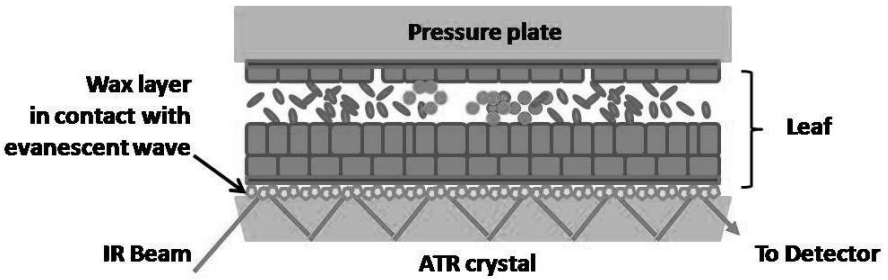

Figure 26. Scheme of a multiple reflection ATR system used for plant surface examination

6.7.8 Scanning Electron Microscopy

The morphology of lyophilized adaxial plant surfaces was analyzed by SEM using a Hitachi S-2700 scanning electron microscope (Nissei Sangyo GmbH, Ratingen, Germany; except native *V. locusta* and savoy cabbage leaves: SEM Type XL20, Philips, Germany; equipped with an energy dispersive X-ray microanalyzer (SEM-EDX). The accelerating voltage was 20 kV (native leaves: 10 kV). Surfaces were coated with carbon in a sputter coater before SEM examination. For these experiments APPJ 1 was driven at 20 W for 20 s and 60 s since higher voltages could induce combustion reactions of the lyophilized plant surface.

7 Results and Discussion

7.1 Plasma Treatment of Adsorbates

To elucidate the effect of plasma immanent species, various pure compounds were adsorbed on solid borosilicate slides and exposed to a low-pressure oxygen plasma (RFGD) and an atmospheric pressure Ar plasma (APPJ 1). The compounds represent four major chemical classes of compounds naturally present as secondary metabolites in plants: flavonoids, stilbenoids, phenolic acids and phenylpropanoids. Due to their structural differences these compounds vary significantly in their antioxidative properties. This behaviour should manifest itself as well in the interaction with reactive oxygen species from a non-thermal plasma. A strong correlation between the structure and the dynamics is anticipated. As plasma chemistry is characterized by a multitude of concomitant chemical reactions, pinpointing the origin of observed changes to one specific plasma species is a very challenging task and the principal mechanisms and possible synergisms between the different reactants are usually identified as a process of elimination. An elegant solution for is the use of calibrated sources of radiation, covering a wide spectral range or of particle beams of neutral and charged species (KYLIÁN *et al*., 2009 and references therein). In this study a similar approach is used simulating the influence of the plasma temperature and photon emission. Although experiments are for the time being only exemplarily, chemical kinetics should provide additional insight towards a possible catalytic effect from photolysis and thermolysis and corresponding desorption processes.

7.1.1 Plasma induces Degradation of Phenols and Polyphenols

Plasma exposed 1,4-benzopyrones deposited on solid surfaces showed a structure-dependent degradation at the surface. The degradation was characterized by fast kinetics at the initial stage (< 40s for APPJ, < 80s for RFGD) and a slow, asymptotic decay thereafter following a first order reaction rate. In the APPJ most compounds were completely removed after a plasma treatment of 120 s (Figure 27). The strongest decomposition has been observed for quercetin (reduction to 10%) and kaempferol, the latter being almost completely degraded (less than 2% amount). These compounds were already significantly

reduced by more than 60% after 20 s exposure while catechin and taxifolin, structures that lack the C2-C3 double bond of the C-ring, showed a weaker reduction of 23% and 26%, respectively. The slowest degradation occurs for the glycolized compounds QDG (93%), QMG (74%) and rutin (62%) for which a quasi-linear relationship with treatment time can be observed. Likewise phenolic acids showed a rather inert behaviour compared to flavonoids. Protocatechuic acid and caffeic acid are degraded by 35-45% after 120 s. Chlorogenic acid appears to be even more inert: 90% of the initial sample is still present after 120 s.

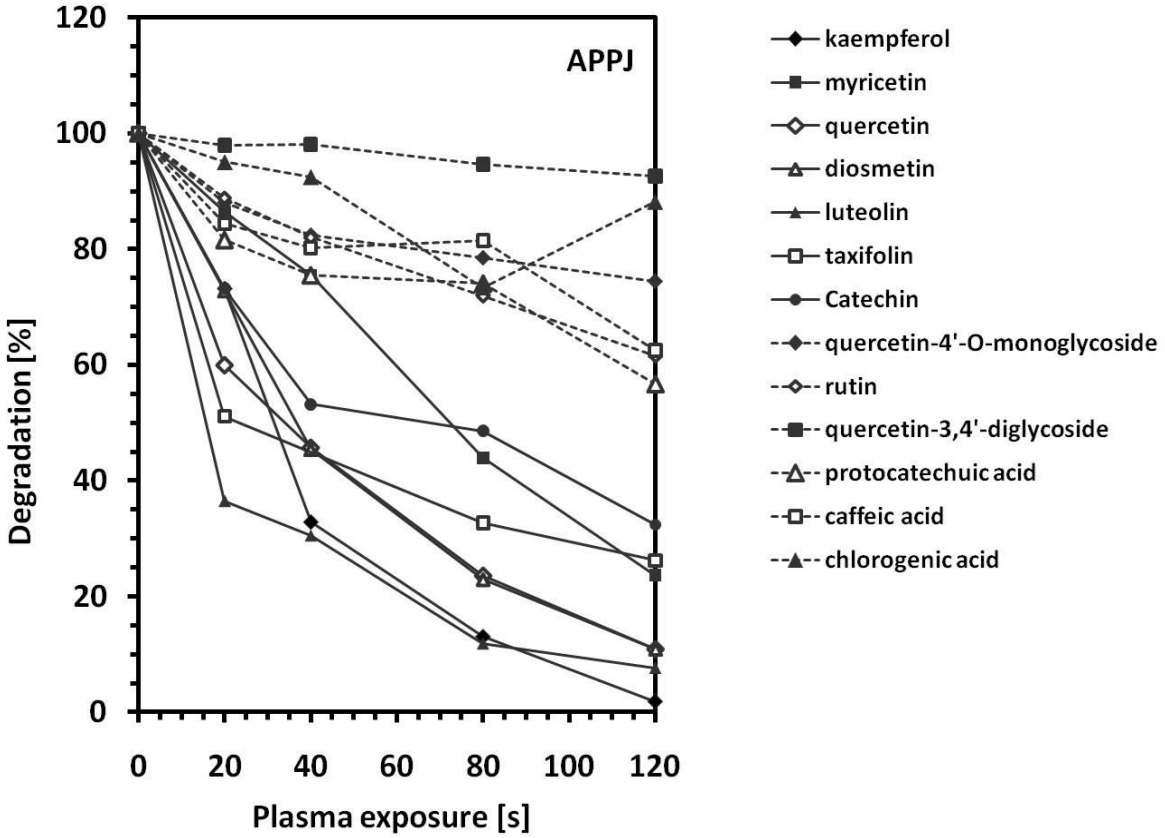

Figure 27. Degradation of poly- and monophenol compounds in APPJ 1 (Ar, 20 slm, 20 W).

While in the plasma jet a complete degradation of flavonoids already occurred after 2 min degradation in the low-pressure glow discharge was remarkably slower (Figure 28). However, the same trend could be observed. Despite of the substantial differences of the two plasma sources, flavonoids were again quickly and substantially degraded while within the same time range phenolic acids show a much slower decrease. As an example more than 98 % of kaempferol was removed after an exposure of 120 s, while still 75% of protocatechuic acid and 69% of chlorogenic acid can be determined. Due to the complex nature of plasma the mechanisms leading to degradation remain still unclear. In Figure 29

measurements simulating the gas flow of the discharge effluent are compared to measurements done under 'real' plasma conditions. Although a decrease of quercetin concentrations with increasing gas exposure can be observed, the overall effect of the heated gas flow on the quercetin substrates is moderate within the first 120 s.

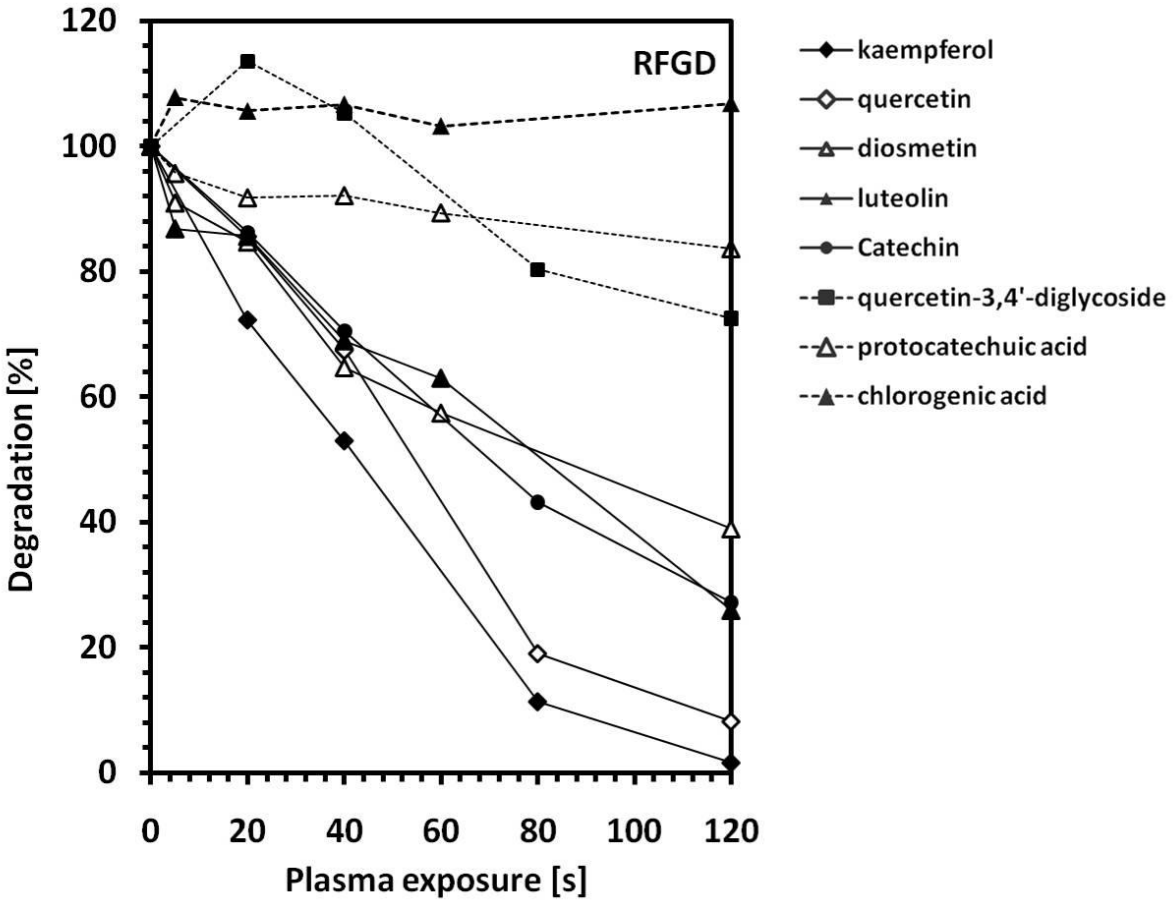

Figure 28. Degradation of poly- and monophenol compounds in RFGD (O_2, 0.5 mbar, 75 W).

Only from this point on degradation due to the gas flow can be determined. However, the influence is markedly lower relative to the plasma experiments. Thus, even though gas flow contributions cannot be neglected for longer exposure times, degradation mainly depends on plasma specific interactions with the substrate surface. Degradation is considered to proceed via incorporation of oxygen atoms onto the adsorbate surface due to random bond breaking reactions from interaction of ions and metastable excited states with surface molecules (HANSEN AND SCHONHORN, 1966). In a second step the remaining dangling bonds are attacked by reactive oxygen species (atomic or molecular oxygen), leading to a gradual fragmentation and desorption of volatile compounds, namely of H_2O, OH, CO and CO_2, which

diffuse from the bulk to the surface (CLOUET AND SHI, 1992; COBURN AND WINTERS, 1979). Independent of the concrete mechanism by which plasma-surface interaction is taking place, the above findings underline the importance of key structural elements for a high antioxidative potential (BORS *et al.*, 1990; RICE-EVANS *et al.*, 1995; COOK AND SAMMAN, 1996; RICE-EVANS AND MILLER, 1996; VAN ACKER *et al*, 1996). Whereas compounds with a C2-C3-π-bond and, more important, an acidic 4'-OH function (quercetin, kaempferol, and myricetin) are strongly degraded in both plasmas, their glycosidic derivatives seem to be almost inert.

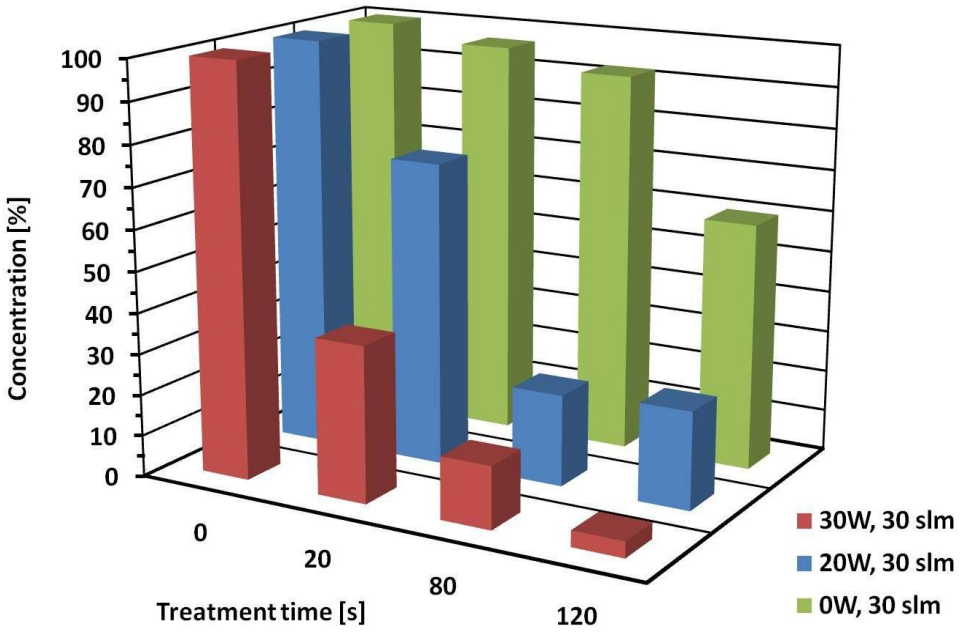

Figure 29. Measurements simulating the gas flow influence on the degradation of quercetin substrates are done at the same conditions as the plasma experiments but without plasma ignition.

The key step to degradation is the initial abstraction of hydrogen of the hydroxyl group at C4' due to interaction with atomic oxygen (^{3}P state) or OH radicals ($A^2\Sigma^+$) whose presence in the APPJ has already been proven (BRANDENBURG *et al.*, 2007). If the 4'-OH is substituted by ß-O D-glucose (QMG) or sterically hindered due to a sugar moiety in adjacent position (at C3' as in QDG), hydrogen abstraction is inhibited and a slower degradation of these compounds can be observed. It is interesting to note that the presence of a catechol structure (as in quercetin or myricetin), usually considered to stabilize the intermediate aryloxyl radical by hydrogen bonding of the adjacent OH group (LEOPOLDINI, RUSSO, AND TOSCANO, 2006) is not enhancing degradation. Yet, in case of kaempferol it is in fact its missing which favours a complete and rapid degradation. The absence of a C2-C3 double bond as in catechin and

taxifolin appears to have a minor impact on the degradation rate. For glycosidic flavonoids substitution of an OH-group on the B ring seems to be as well essential for decomposition. Of the three structures used in this study QMG and QDG, where the 3' or 4'-OH-group is substituted by a D- glucose group, are more stable towards degradation than rutin. This is noteworthy in view of the fact that usually a high stability of rutin against oxidation is reported, which is attributed to the presence of the rutinosyl group on O3 impeding *o*-quinone-*p*-quinonoid tautomerization (DANGLES, FARGEIX, AND DUFOUR, 1999). In the key step of the degradation reaction, the D-glucose moiety therefore acts as a protective group, either by substituting the OH-function itself or due to steric effects. In contrast substitution on C3 alone is not protecting the molecule against degradation (rutin). Only in combination with a D-glucose group in the B-ring (QDG) the inertness is increased. In the following, addition of metastable excited O_2 ($^1\Delta_g$ and $^1\Sigma_g^+$) or, due to its triplet character ground-state molecular oxygen ($X^3\Sigma_g^-$), to the flavoyl radical possibly gives rise to peroxy radicals who can rearrange to form aldehydes and ketones (CLOUET AND SHI, 1992). NORRISH type-1 -like photocleavage of carbonyls can be induced due to interaction with $O(^3P)$ (BAMFORD AND NORRISH, 1935; CALVERT AND PITTS, 1966; GILBERT, BAGGOTT, AND WAGNER, 1991) which is followed by formation of volatile CO, CO_2 and hydroxide and hydrogen radicals (HUIE AND HERRON, 1975).

7.1.2 Photolyis and Thermolysis Experiments

Due to the fact that no by-products have been identified, further information regarding the origin of the observed degradation had to be gained as a process of elimination. As aromatic rings of the uppermost layers can be easily destroyed by VUV resonance radiation, leading to random C-C single and double bond cracking, additional experiments were performed to ascertain whether simple photolysis or pyrolysis reactions are responsible for the observed decomposition. Plasma-induced degradation was compared with reactions of selected polyphenol compounds and caffeic acid after UV and temperature treatments. Table 27 and Table 28 show the degradation behaviour of the aglyconic compound diosmetin and quercetin, the quercetin glycoside QDG and caffeic acid upon irradiation at 254 nm and heating at 373 K. It has to be mentioned, that the temperature of 373 K is far beyond the temperatures that occur in the low-temperature plasmas that were used in this study; depending on the driving voltage and plasma source temperatures of 328-338 K have been measured. Yet, thermal degradation effects can be *a priori* excluded at these energetic

conditions. Although the temperature of 373 K was at least 40 K higher than the plasma temperature, no decomposition of caffeic acid or of the three flavonoid compounds has been determined. Only exception is the moderate thermolytic decomposition of 11% (after 2 minutes exposure) for quercetin.

Table 27. Influence of UV Radiation on the Degradation Behaviour of Quercetin, its Diglycosidic Derivative QDG, Diosmetin and Caffeic Acid as a Function of Exposure Time. Standard Deviations are given in Parentheses.

Time [s]	Concentration after UV irradiation [%± SD]			
	Quercetin	QDG	Diosmetin	Caffeic acid
0	100 (± 1.84)	100 (± 1.59)	100 (± 3.82)	100 (± 3.74)
20	95.84 (± 2.52)	99.25 (± 3.33)	103.29 (± 0.46)	103.24 (± 0.68)
40	95.93 (± 1.84)	95.85 (± 3.04)	101.77 (± 1.05)	101.52 (± 3.23)
80	99.76 (± 2.63)	102.66 (± 2.41)	104.68 (± 0.86)	104.07 (± 1.86)
120	99.56 (± 2.52)	101.69 (± 1.03)	105.65 (± 0.64)	106.44 (± 1.11)

Likewise the exposure to UV radiation (following the UV dose in the plasma jet) did not show significant changes. For both cases the decomposition is negligible and about 98-99% of the initial concentrations still remains on the substrate. It can be therefore concluded that at the operating plasma conditions the observed degradation of benzopyrones in non-equilibrium plasmas is not caused by photo- or thermodesorption processes but is a direct result of the plasma treatment. Degradation is first and foremost determined by plasma induced reactive species, leading to bond scissions, subsequent (photo-) oxidation and cleavage of the flavonoid skeleton (MAKRIS AND ROSSITER, 2001). As no products, by-products or reaction intermediates have been identified so far, an explicit formulation of the underlying mechanism, particularly in view of the monitored structure dependence of the degradation, however is still missing. Taking into consideration that plasma functionalization, which means the attachment of groups or molecules from the plasma gas onto the substrate surface only affects a few atomic layers, the analysis of plasma-surface modifications, reaching a few nanometres in the bulk, has to deal with groups present in a concentration of some nanomol per square centimetres. This is beyond the abilities of common

organochemical structural analysis like infrared spectroscopy or nuclear magnetic resonance spectroscopy. To characterize the surface chemical structures, surface sensitive methods were used in the following.

Table 28. Influence of Temperature on the Degradation Behaviour of Quercetin, its Diglycosidic Derivative QDG, Diosmetin and Caffeic Acid as a Function of Exposure Time. Standard Deviations are given in Parentheses.

Time [s]	Concentration after heating [%± SD]			
	Quercetin	QDG	Diosmetin	Caffeic acid
0	100 (± 6.19)	100 (± 3.06)	100 (± 0)	100 (± 1.48)
20	101.02 (± 3.62)	104.62 (± 0.92)	100.10 (± 0.10)	98.87 (± 3.25)
40	100.87 (± 8.36)	102.76 (± 1.31)	103.90 (± 3.90)	101.36 (± 0.25)
80	91.51 (± 1.43)	102.71 (± 1.53)	101. 69 (± 1.69)	95.41 (± 3.05)
120	89.09 (± 2.48)	101.07 (± 3.69)	103.24 (± 3.24)	98.23 (± 1.52)

7.1.3 Contact Angle Measurements of Quercetin

Surface functionalizations can be monitored on a macroscopic scale by measuring the contact-angle, correlating molecular properties to changes in the surface wettability. The technique consists in measuring the angle of a drop of liquid of known surface energy deposited on the solid surface (Figure 30).

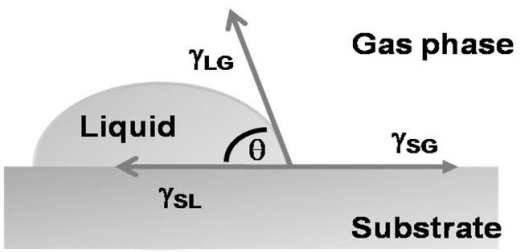

Figure 30. Contact angle of a liquid drop placed on a solid surface.

Given that the volume of the drop is sufficiently small to neglect effects of gravity relative to capillarity the shape of the drop assumes a spherical cap on the surface in equilibrium. The CA Θof the liquid, L, on the solid, S, can be described by the YOUNG equation (YOUNG, 1805)

$$\cos\theta = \frac{\gamma_{SG} - \gamma_{SL}}{\gamma_{LG}} \qquad (17)$$

with γ_{SV} the solid-vapor interfacial energy (surface free energy)
γ_{LV} = liquid-vapor energy (interfacial tension of the liquid),
γ_{SL} = solid-liquid interfacial free energy

The CA thus directly provides information on the interaction energy between the surface and the liquid. If the liquid is very strongly attracted to the solid surface the droplet will completely spread out on the solid surface and the angle will be close to 0°. Less strongly hydrophilic solids will have a CA up to 90° (Figure 31). The YOUNG equation assumes the ideal situation of perfectly flat and smooth solid surfaces. In the real case however, disordered and inhomogeneous surfaces (e.g. from impurities) significantly cause deviations in the experimental CA. Equation 17 therefore needs to be generalized to include spatial (x,y) dependent interfacial energy densities and CA (CHOW, 1998).

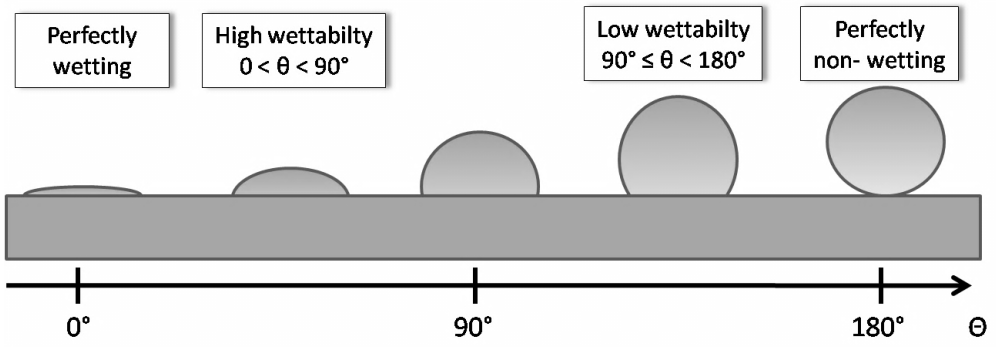

Figure 31. The wetting properties of a surface are best described by the contact angle between a liquid droplet and the solid substrate.

Despite of the fact that thermodynamics and kinetics of the spreading of water on a chemically and morphologically heterogeneous organic surface are not well understood, measurements of Θ provide a very useful method for the characterisation of surfaces. Contact angles are sensitive to the polarity of functional groups at the surface (cf. COULOMB interactions: hydrogen bonds, dipole-dipole interactions) and to local details of surface structure within a few Å of the liquid–solid interface (HOLMES-FARLEY AND WHITESIDES, 1987, BAIN *et al* 1989). The analyzed layer thickness amounts to 0.5 nm, which makes Θa simple

but efficient tool to study the adhesion properties of the upper monolayer. In Figure 32 the changes of the surface properties of quercetin induced by different discharges are compared (for details about plasma sources, see chapter 6.2.3). Two atmospheric pressure jets differing in the gas flow and plasma power and a microwave (MW) low-pressure discharge have been used. Results from static water contact angle evaluations of Ar and O_2 plasma treated quercetin samples allow to make the following observations: All Θof plasma treated substrates are significantly decreased regardless the nature of plasma gases or sources used. This indicates that the surface free energy is increased for all plasma treated surfaces compared to the untreated sample. The Ar driven APPJ 1, used already in the degradation experiments, shows a reduction from Θ= 35° for the pristine to Θ= 12° for the treated sample. A similar change was observed for microwave discharge -treated surfaces operated with Ar and O_2 as feed gases (0.06:0.04 [slm]). Θfor this treatment was measured to be 14°. The lowest values following plasma treatment can be observed for APPJ 2, driven either with 100% Ar or as a mixture with O_2 (5:0.08 [slm]). In both cases the water drop is almost spread out on the surface (Θ= 5°). For reaching this very low CA plasma treatment times as low as 0.5 minutes were sufficient.

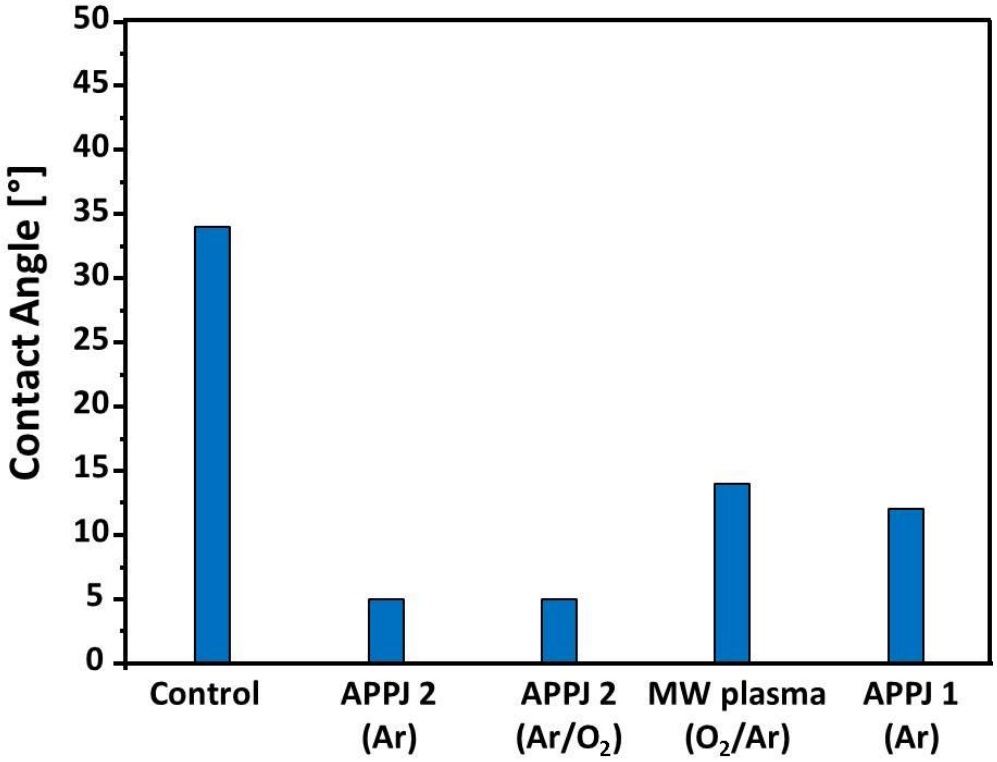

Figure 32. Exposure of quercetin to different discharges changes the substrates contact-angle. For all plasma treatments a clear reduction in the contact-angle can be observed. Addition of oxygen to the feed gas has not a significant effect on the surface properties of quercetin.

Although Friedrich et al. (FRIEDRICH *et al.,* 1999) found that adding oxygen as reactive gas to a rare gas plasma leads to an improved hydrophilicity, the admixture of oxygen to the Ar APPJ 2 did not significantly influence Θ This is probably due to the fact that the APPJ systems used in this study are not closed but open system. In these cases mixing with the surrounding air is possible right from the beginning making potential effects from the direct introduction of a relatively small quantity of oxygen negligible. The observed oxidation of the surfaces, initiated by free radical sites under the action of reactive Ar species, is therefore mainly of ex-situ origin.

Comparing Ar driven APPJ 1 and APPJ2 shows that higher power and gas flow have a negative effect on the contact angle. Although this effect has already been reported (DENES, YOUNG, AND SARMADI, 1997) it is quite surprising, as higher voltage and gas flow should in principle lead to an increased formation of rare gas ions which are considered to be the main reactive species causing etching of the surface (CHOI *et al.*, 2003). Kylián and co-workers however have shown that the simultaneous exposure of proteins to Ar^+ and O/O_2 beams resulted in markedly faster removal and a higher surface roughness compared to the sputtering process by energetic Ar^+ (100 eV) ions alone (KYLIÁN *et al.*, 2009). The addition of high rare gas concentrations is thought to enhance PENNING ionization of oxygen by charge transfer from elastic collisions of metastable, excited argon atoms and neutral oxygen species:

$$Ar\ (^5P) + O_2\ (X^3\Sigma_g^-) \rightarrow O_2^+ + e^- + Ar\ (^4S) \qquad (R96)$$

It seems thus reasonable that the higher gas flow of APPJ 1 is displacing the surrounding air to a comparably greater extent than does APPJ 2. Thus interaction of the sample with reactive oxygen species, namely atomic oxygen formed by electron impact dissociation from O_2, is hindered. Oxygen plasma treatments in a low-pressure microwave discharge led to similar results as Ar APPJ 1 treatment. MW plasmas are characterized by a higher directionality of the charged and neutral particles and a higher plasma density (DENES, YOUNG, AND SARMADI, 1997). The ion energy is generally low and can be controlled by additional DC fields or RF bias voltage (CONRADS AND SCHMIDT, 2000). This might be the reason, why ion bombardment of the substrate surface in the end is less effective than in case of the plasma jets, in addition to the overall lower concentration of oxygen species present in the bulk plasma. However comparing atmospheric and low pressure plasma surface treatments is

generally delicate as major dissimilarities might originate not only from huge differences between the electron and active species densities but as well from different discharge physics (SARRA-BOURNET *et al*., 2006).

Thus, the improved surface adhesion strength, namely the higher hydrophilicity of the plasma treated surfaces observed for all samples after plasma exposure indicates that a nm-sized oxidized layer has been generated independent of the plasma source used. The increased wettability is attributed to attributed to the incorporation of oxygen functional groups on the outermost surface layer (DE GEYTER *et al.,* 2007) initiated by adsorption of atomic oxygen from electron impact induced dissociation of molecular oxygen in the plasma.

7.1.4 Chemical Composition of Substrates – Atomic Ratio

The outcomes of the CA measurements indicating a strong surface oxidation after plasma treatment have been verified by analyzing the chemical composition of treated and untreated quercetin by wide-scan XPS. Figure 33 shows the survey spectra for typical untreated and plasma treated quercetin samples. The elemental composition in the surface region is plotted as atomic ratio against the different gas discharges used by integrating the surface area of the wide-scan XPS spectrum (Table 29). The analyzed layer thickness amounts to approximately 10 nm.

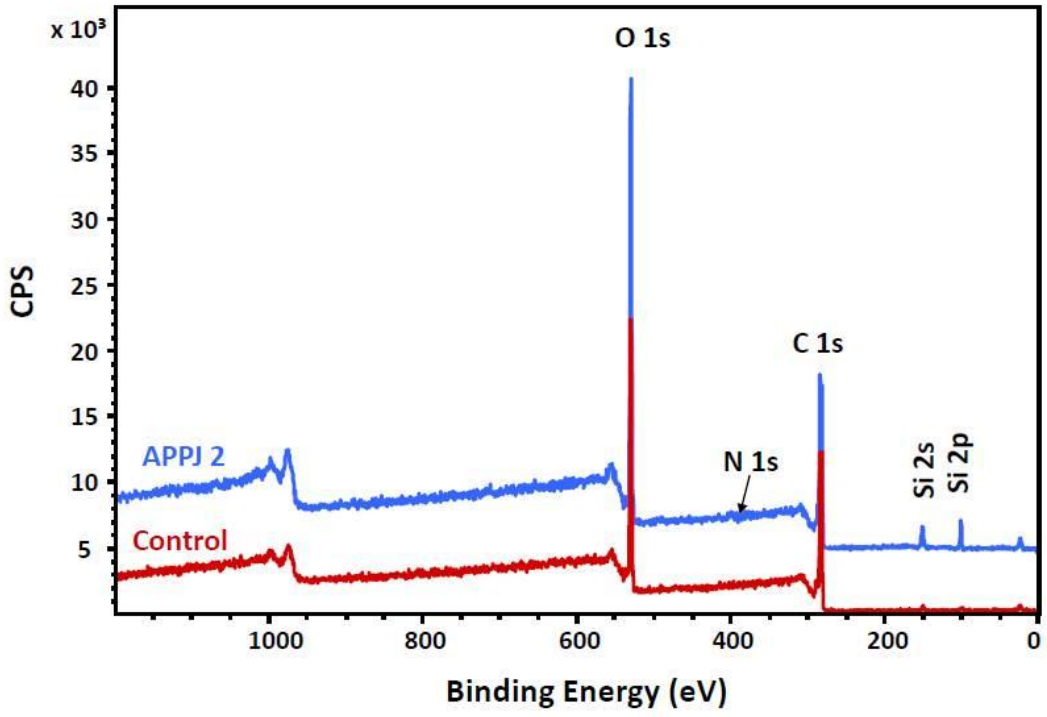

Figure 33. Wide scan XPS of quercetin samples showing distinct oxygen and carbon peaks, representing the major constituents of quercetin. Weak peaks of nitrogen and silicon were also observed.

Lowest N/C and O/C surface atomic ratios are related to the untreated sample and hence to the highest CA values: Virgin quercetin is characterized by an oxygen/carbon ratio of O/C = 0.4 which is in good agreement with the theoretical values derived from O/C stoichiometry of quercetin (deviation of theoretical value: 4.6 %). Major changes are evident for the APPJ treated samples, where a significant increase of oxygen at the sample surface occurs for both jets used. As expected, the admixture of oxygen in APPJ 2 leads to gradually higher O/C ratios whereas the N/C ratio is minor with respect to Ar driven APPJ 2. For MW-plasma treated quercetin which showed the smallest change in contact angle of all plasma treated samples, a less distinctive increase in O/C ratio can be observed.

Table 29. Atomic ratio of quercetin sample before and after plasma treatment.

Surface	Ratio ± SD		
	N/C	O/C	Si/C
untreated	0.36 ± 0.01	42.12 ± 0.48	1.72 ± 0.20
APPJ 2 (Ar)	1.77 ± 0.22	57.04 ± 2.02	5.92 ± 0.41
APPJ 2 (Ar/O_2)	0.76 ± 0.07	60.37 ± 5.45	5.37 ± 2.32
MW plasma (O_2/Ar)	0.97 ± 0.15	50.15 ± 0.36	1.96 ± 0.09

As any change in elemental ratio must be discussed in relation to the changes in the other elements a closer look to the surface elemental composition shows that in all cases plasma modification leads to a significant increase in oxygen content and decrease in carbon content. The amount of carbon lost by plasma treatment is bigger than the corresponding increase in oxygen (factor 1.3 for both APPJ), except in the case of MW plasma where loss and gain are almost equal (Figure 34). The presence of silicon (1-3 at.-%) and, to a minor extent, nitrogen (0.5-2 at.-%) for the treated and untreated samples suggests that the sample contains some contamination on the surface.

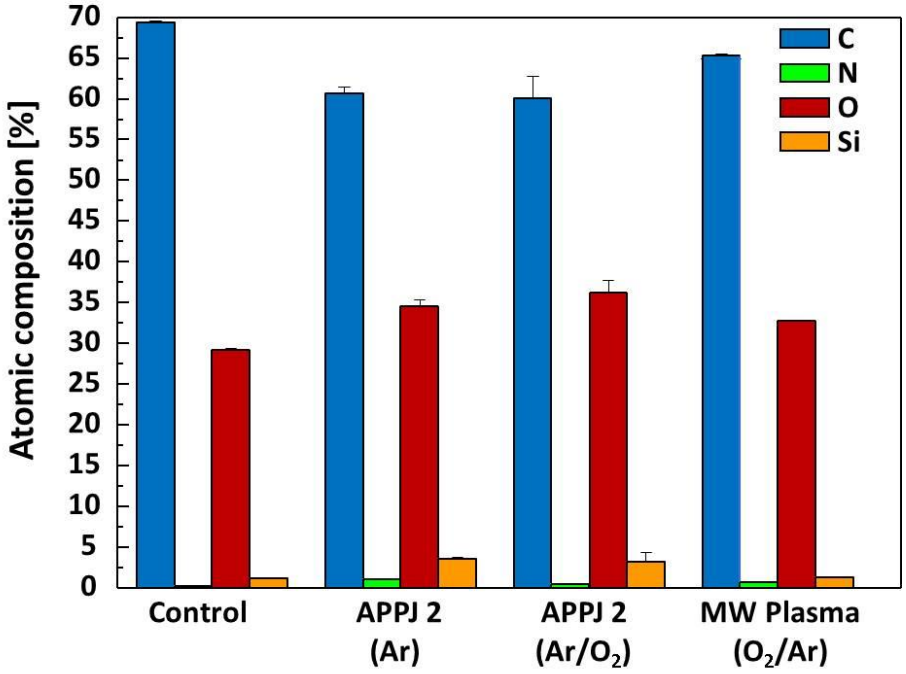

Figure 34. Atomic composition of quercetin surface after various plasma treatments.

The large decrease in water contact angle of all quercetin samples is therefore owing to the incorporation of oxygen-containing functionalities on the sample surface accompanied by a concomitant loss of C. Plasma parameters thus control the O/C and N/C surface atomic ratios.

7.1.5 XPS Surface Chemical Analysis

A deeper insight into the chemical structure of plasma-modified surface layers was gained by analysing in more detail the high-resolution (HR) spectra XP spectra of the C1s peak. Chemical assignments for deconvoluted peaks were based on binding energies (BE) as quoted in the literature (BRIGGS AND SEAH, 1992). Figure 35 exemplarily shows the highly resolved C1s spectra of the quercetin sample before and after 60 s treatment in the Ar/O_2 plasma jet (APPJ 2). The spectrum was deconvoluted into six individual component peaks. The peak with a BE of 284.5 eV has been attributed to the formation of -C=C-, -C-C- or -C-H_x- bonds from the aromatic backbone of quercetin. These groups cannot be resolved separately. The peak at 286.5 eV corresponds to -C-O bonds from either ether or phenol groups. Additionally, two peaks with BE of 288.0 and 289.0 eV can be observed. These high-BE contributions represent carbonyl and carboxyl groups, respectively (BRIGGS AND SEAH,

1992; MORENT *et al.*, 2008). They probably originate from low-level oxidation of oxygen functionalities on the quercetin surface (ageing effects). Shake-up satellites can be seen at higher BE shifted by around 5.5 and 8.5 eV from the (C-C_{arom}) C 1s main peak. These discrete structures result from 2-electron-processes accompanying core photoionization during relaxation when an electron from the valence band is promoted to an empty state above the Fermi level simultaneously to photoemission. The peaks at 291- 293 eV are the result of $\pi \rightarrow \pi^*$ transitions in the phenylic rings.

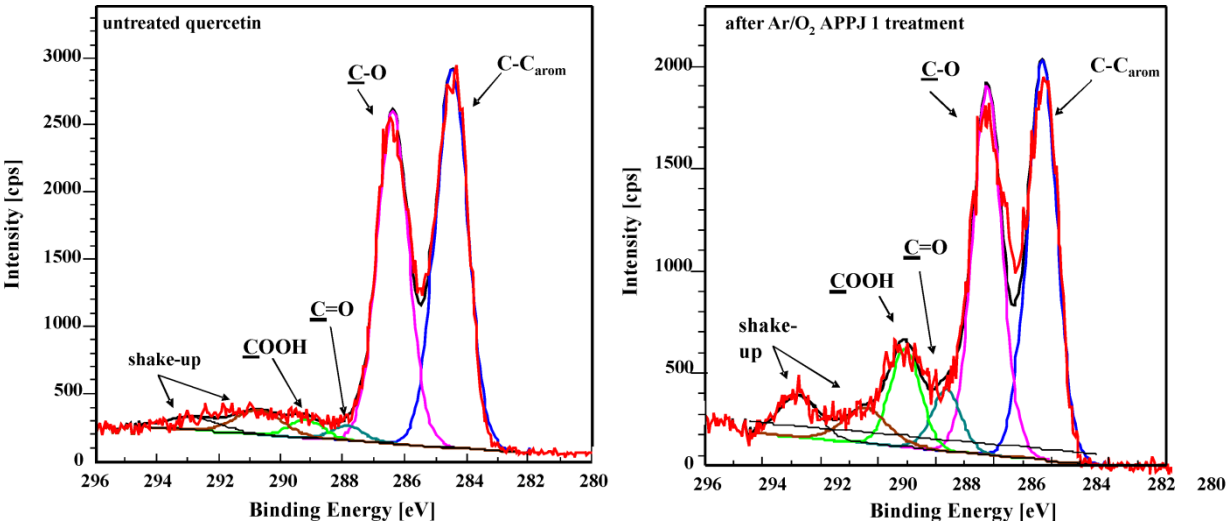

Figure 35. Comparison of the XPS high resolution spectra of untreated quercetin (left) and quercetin after Ar/O_2 plasma treatment with APPJ 2 (right). The density of carbonyl and carboxyl functions has increased. The presence of the COOH-peak in the untreated sample is still unclear.

Independent of the plasma sources used, the intensity of the –C=O and -O-C=O peaks increased strongly following plasma treatment, by factors of 2-3 for the carbonyl functions and by 3-4 for carboxylic function (Figure 36). These changes were accompanied by a simultaneous decrease of the low- BE carbon contributions in the 284-285 eV region which was more substantial for the C-C_{arom} fraction than for the C-OH groups. The amount of newly introduced carbonyl and carboxyl functions is highest for samples exposed to an admixture of Ar and oxygen gas indicating that the -C=O and -O-C=O bond ratio is clearly affected by the concentration of oxygen gas in the plasma (Figure 36). This is in clear contrast to the observed changes in CA measurements where the admixture of oxygen to an Ar plasma did not result in substantial changes of the CA.

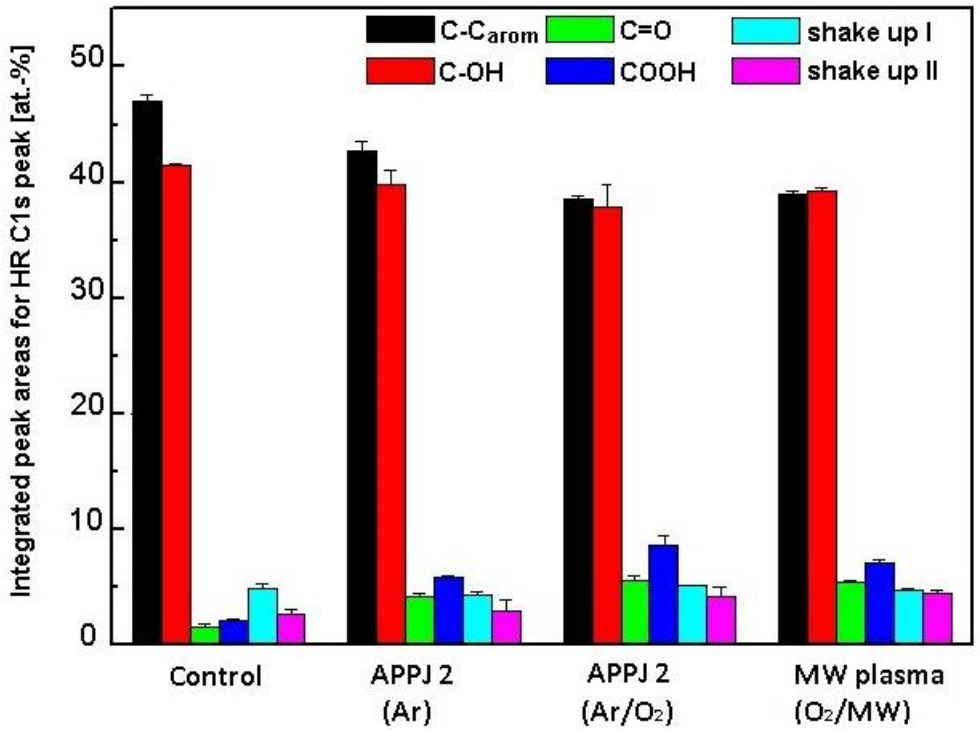

Figure 36. Integrated peak areas for deconvoluted HR C 1s spectra.

The findings are consistent with a chain scission mechanism by which low molecular weight fragments with new terminal end group functionalities are created (Scheme 13). The increase in carbonyl functions points to the intermediate formation of quinoidic compounds which subsequently rearrange with ring opening and the generation of phenolic acids.

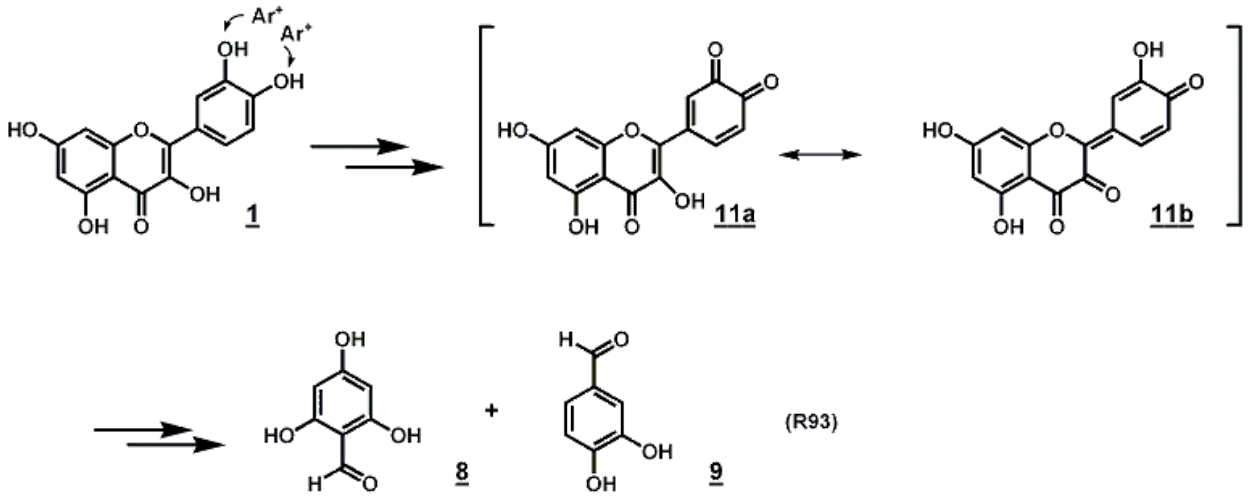

Scheme 13. Proposed mechanism for Ar ion induced oxidative fragmentation into phloroglucinol carboxylic acid 8 and protocatechuic acid 9.

The assumptions are supported by help of the bond ratios. As illustrated in Figure 37 the C=O/C$_{arom}$ ratio is increasing from 0.035 in the control samples to 0.09 in the Ar driven APPJ

2 and 0.14 in the Ar/O_2 APPJ 2 or the MW discharge, respectively. This means that in case of APPJ 2 for instance, the concentration of carbonyl functions tripled or quadrupled relative to the amount of alkyl carbon atoms upon plasma treatment. Significant changes can as well be seen for the $COOH/C_{arom}$ ratio. Here the content of carboxyl groups increases as follows: 0.05 (control) < 0.13 (Ar APPJ 2) < 0.23 (Ar/O_2 APPJ 2) < 0.18 (MW plasma).

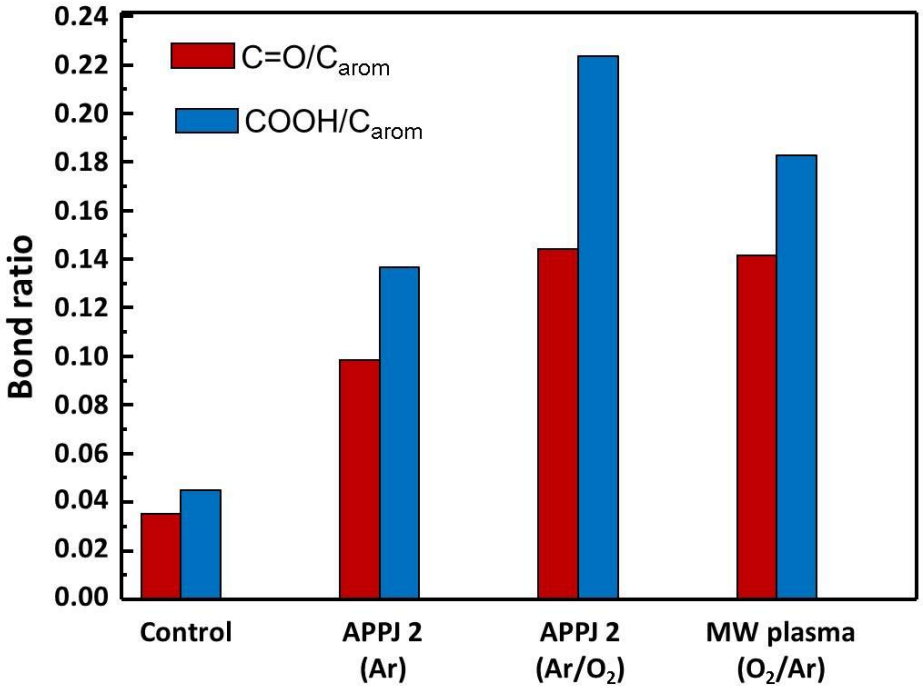

Figure 37. Comparison of $C=O/C_{arom}$ and $COOH/C_{arom}$ bond ratios for quercetin before and after treatment with different plasma sources.

While the amount of carbonyl groups with respect to alkyl carbon atoms was almost identical in the Ar/O_2 APPJ2 and MW plasma, the concentration of COOH functions in the MW plasma is significantly lower and the ratio C=O/COOH (= 1.30) resembles the situation in the untreated sample (= 1.29). It is therefore assumed that the oxidation of quinoid compounds in the MW plasma is slower than in the plasma jet.

7.1.6 ATR-FTIR Spectroscopy

Despite of the presence of carbonyl and carboxyl groups on the molecule surface, changes at 1720 cm^{-1} (-C=O stretching mode) and 1750 cm^{-1} (COOH- stretching mode) by means of ATR-FTIR have not been observed (Figure 38). This is because plasma treatment only changes the uppermost atomic layers of a material without modifying the bulk properties: The modification depth of the plasma treatment is only a few nanometres (MUKHOPADHYAY *et al.,*

2002; LARRIEU *et al.,* 2005). Thus, the missing changes in FTIR-spectra are due to the fact that in contrast to CA measurements or XPS, the analyzed layer thickness in ATR-FTIR amounts to several micrometers dependent on the wavelength. For food safety purposes this means that the bulk properties of any food system remain unaffected and that plasma is only changing the uppermost atomic layer.

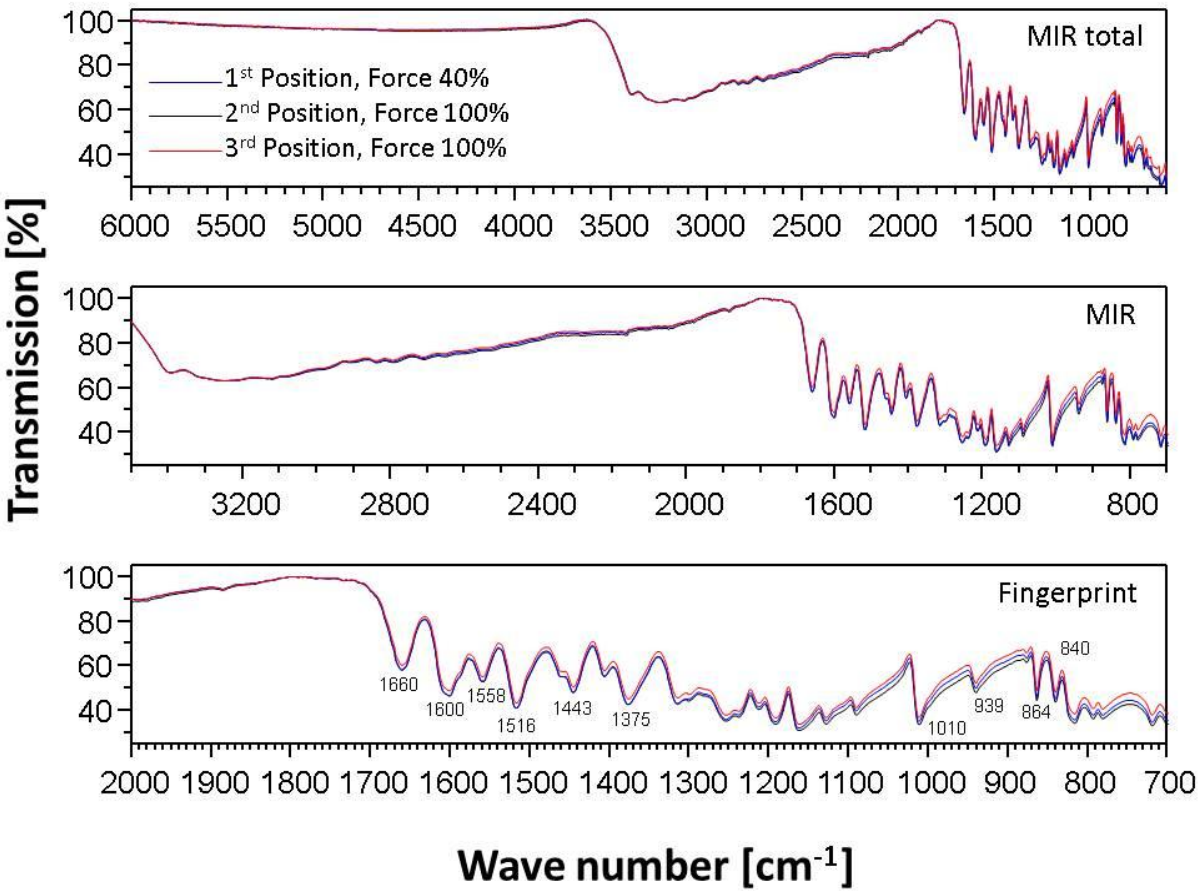

Figure 38. ATR-FTIR transmission spectra of quercetin adsorbate show no significant changes after plasma treatment (APPJ 1, 10 min, 20 W, 20 slm Ar). Different positions and forces exerted have been applied.

To enhance the surface to bulk ratio and thereby the quantity of modified sample in relation to the unmodified bulk material we tried to use of ultrathin films with a thickness on the order of 20-200 nm thickness (WEIDNER *et al.,* 1998). To this end, quercetin was solved in various molarities in MeOH or DMSO and spin-coated on a flat Si(100) wafer, varying spin speed, time, and repetition cycles (700-1500 rpm, t = 5- 15 s, repeated up to 5 times after drying at 298 K for 5 min). Spin coating is an ideal tool to prepare thin and ultrathin films especially for spectroscopic applications. By applying rotational speeds of several 1.000 rpm,

thin and ultrathin layers of extraordinary homogenity can be achieved which makes spin-coating to one of the most-applied coating techniques.

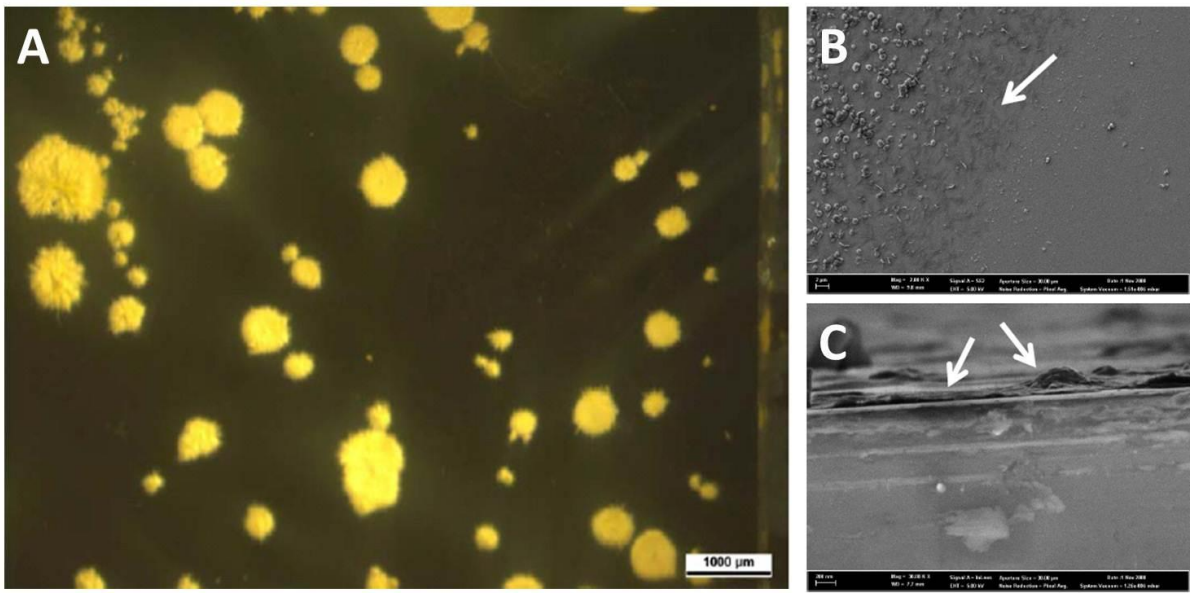

Figure 39. (A) Light electron micrograph showing the formation of small clusters of 10 mM Quercetin instead of a homogeneous coating after spin coating. Scanning electron micrograph of 1 mM quercetin solution on Si(100) wafer (B) top view (2000 ×magnification), (C) side-view (3×10^5 × magnification). Arrows point to quercetin colloids (C) and the colloid-wafer interface (B).

Disadvantages however of the approach are its limitation to higher viscosities (typically 0.01−10 mPa s). In case of quercetin light-electron micrographs and SEM (Figure 39) reveal that a uniform and homogeneous thin film cannot be produced. Independent of the spin coating cycles, the molar ratio, and the solvents viscosity used, isolated granular structures of 100-1000 µm average diameters are observed reaching heights of 200 and more nm. Spin coating therefore seems not to be the method of choice.

7.2 Plasma Treatment of Plant Systems

Despite the fact that cold plasma applications are working at moderate temperatures, all plasma enhanced surface functionalizations are accompanied by etching processes regardless of the nature of the substrates or plasma gases (demonstrated for polyphenolics in chapter 7.1). Therefore plasma processing of plant material for food may change the structure of the food matrix, which is of great importance for the bioavailability of phytochemicals ingested in the matrix (BUGIANESI *et al.*, 2004; CASTENMILLER *et al.*, 1999).

To evaluate possible protective effects of the plants tissue against plasma-induced degradation of secondary plant metabolites, leaves of different plant systems such as lamb's lettuce, savoy cabbage, and kale were exposed to two different plasma sources. Freeze-dried leaves were treated with the RFGD O_2 plasma at two different driving voltages (75 and 150 W, the latter being the maximum voltage of the device). Fresh leaves were exposed to an Ar APPJ for 40 s at the highest possible driving voltage (40 W). Although low-pressure plasmas are limited to solid, solvent-free materials, they represent as well a realistic application. While for fresh fruits and vegetables an open-environment at atmospheric pressure is highly desirable, permitting straightforward scale-up to larger dimensions and a continuous work flow, low-pressure plasma might be still the best option for the preservation of spices or other dried fruits and vegetables due to a number of distinct advantages (e.g. low breakdown voltages, uniform glow over a large gas volume) and an extensive characterization of the discharge itself and the reactions it is generating (SCHÜTZE *et al*., 1998). We therefore aimed to study the effects of both sources at various operating condition. Using the same biological system allows us to make decisive and conclusive statements regarding possible physiological changes.

7.2.1 Characterization of main Phenol Compounds of *V. locusta*

Lettuce varieties are an abundant source of flavonoids, primarily the flavanols quercetin and kaempferol (KYLE AND DUTHIE, 2006). In head lettuce quercetin and its glycosides are accumulated in the outer and apical leaves (HOHL *et al*, 2001; BYLIK AND SAPERS, 1985). Lamb's lettuce is particularly rich in luteolin glycosides, diosmetin and crysoeriol and contains as well various hydroxycinnamic acids and *p*-hydroxybenzoic acids (Table 30, KNACKSTEDT AND HERRMANN, 1981; GREGER AND ERNET, 1973; HERRMANN, 1956; SCHMIDTLEIN AND HERRMANN, 1975).

Table 30. Content of *p*-hydroxybenzoic acid and hydroxycinammic acid derivatives in lamb's lettuce leaves after hydrolysis [mg/kg fresh weight] (SCHMIDTLEIN AND HERRMANN, 1975).

Variety	Hydrolysis	Caffeic acid	Ferulic acid	Sinapic acid	*p*-Hydroxy-benzoic acid	Vanillic acid
Dark Green Full Heart	A	767	< 0.5	< 0.5	11	< 0.5
Dark Green Full Heart	B	874	< 0.5	< 0.5	22	< 0.5
Dutch Broad Leaved	A	1570	< 0.5	< 0.5	21	< 0.5
Dutch Broad Leaved	B	1440	10	4	40	< 0.5

A = enzymatic hydrolysis, B = alkaline/acidic hydrolysis

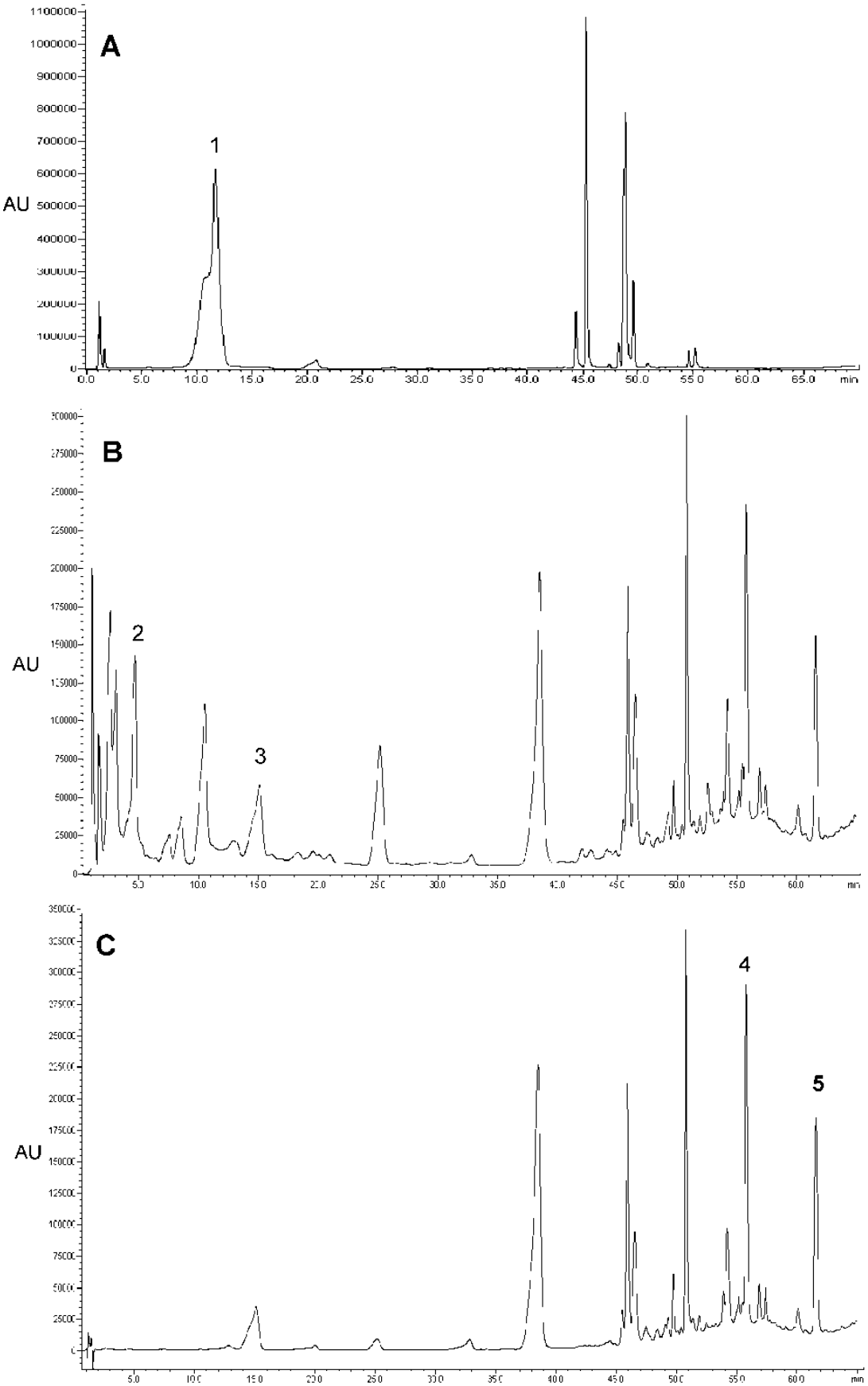

Figure 40. HPLC chromatograms of (A) MeOH extracts of *V. locusta* (untreated) at 280 nm, (B) samples after hydrolysis at 280 nm and (C) at 365 nm: 1, chlorogenic acid; 2, protocatechuic acid; 3 caffeic acid; 4, luteolin; 5, diosmetin. UV spectra of identified peaks are inserted.

Since a complete analysis of all compounds that exist in lamb's lettuce was outside the scope of this study a limited number of compounds were chosen to exemplarily study the influence of NTP exposure at various operating conditions and to elucidate possible secondary chemical effects from the plant matrix. Identifications were based on HPLC retention times and UV absorption spectra for unknowns and standards. Variability in HPLC retention times due to column aging and varying chromatographic conditions was small. The HPLC profile of the extract showed three major compounds of which chlorogenic acid had been clearly characterized at a retention time (R_t) of 11.6 min (Figure 40, A). Among the hydrolysis products protocatechuic acid, eluting at 4.5 min and caffeic acid (R_t= 15 min) had been detected (Figure 40, B). In all lettuce samples luteolin is one of the dominating compounds with a retention time of R_t= 55.5 min, while diosmetin (R_t= 61.5 min) appears to lesser amounts (Figure 40, C). Five substances appearing between 45 and 55minutes have not yet been identified. Their corresponding UV-vis spectra evidence that these compounds are presumably derivatives of flavonoids or their glycosides due to their typical absorption maxima at around 360 nm (Figure 41). Kaempferol, however, which is a common flavonoid in head lettuce species (HERTOG, HOLLMAN, AND KATAN, 1992; HEIMLER *et al.*, 2007) has not been found.

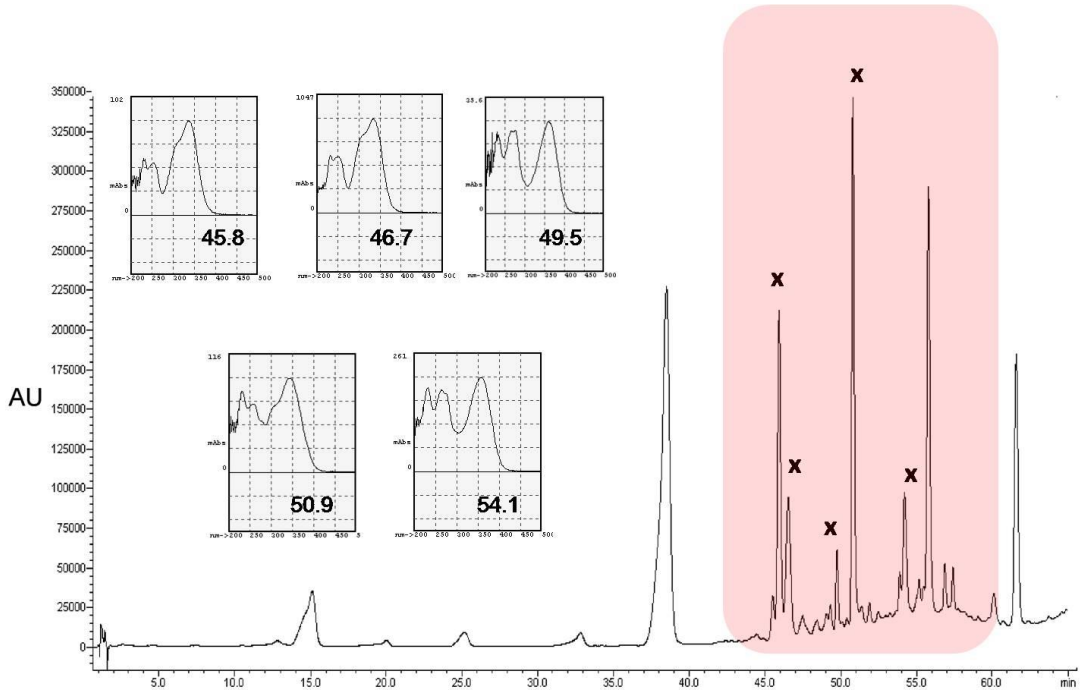

Figure 41. Recorded UV- spectra of five compounds eluting between 45-55 minutes. Absorption maxima correlate with π bonds and are therefore attributed to unsaturated systems.

The methods of extraction and analysis can markedly affect the determination of flavonoids in food. The depicted chromatograms however demonstrate that the sample preparation according to Hohl and co-workers (HOHL *et al.*, 2001) is appropriate for the elution of well resolved analytes.

7.2.2 Plasma Exposure of V. *locusta* Leaves

While the analysis of plasma chemical reactions is *a priori* difficult, it proves to be far more complicated in case of complex biological matrices and resolving the mechanisms of plasma interactions with living cells is still a challenge. In Figure 42 changes in the concentration upon exposure to the RFDG plasma are shown. Exposing the lettuce for 40 s to the plasma did not significantly alter the content of the selected substances. Although the concentration of all compounds changed upon short plasma exposure (except chlorogenic acid, whose concentration remained almost constant), the relatively large deviation of the samples obviates any firm conclusion regarding quantitative differences. Thus, the observed changes might as well represent simple fluctuations of the natural content. By contrast longer RFDG exposure strongly increased the content of protocatechuic acid, luteolin, and diosmetin, the relative proportions of the individual compounds being generally comparable for both plasma voltages used. The contents of protocatechuic acid and luteolin almost doubled upon plasma treatment, while the largest change is found for diosmetin (2.5 fold). It is interesting to note that for both voltages used a similar reaction pattern can be recognized. Since changes of the operational parameters of the plasma strongly influence the formation, concentration and rate of reactive species and the intensities of the different wavelength emissions, a different, yet indeterminate reaction behavior was expected.

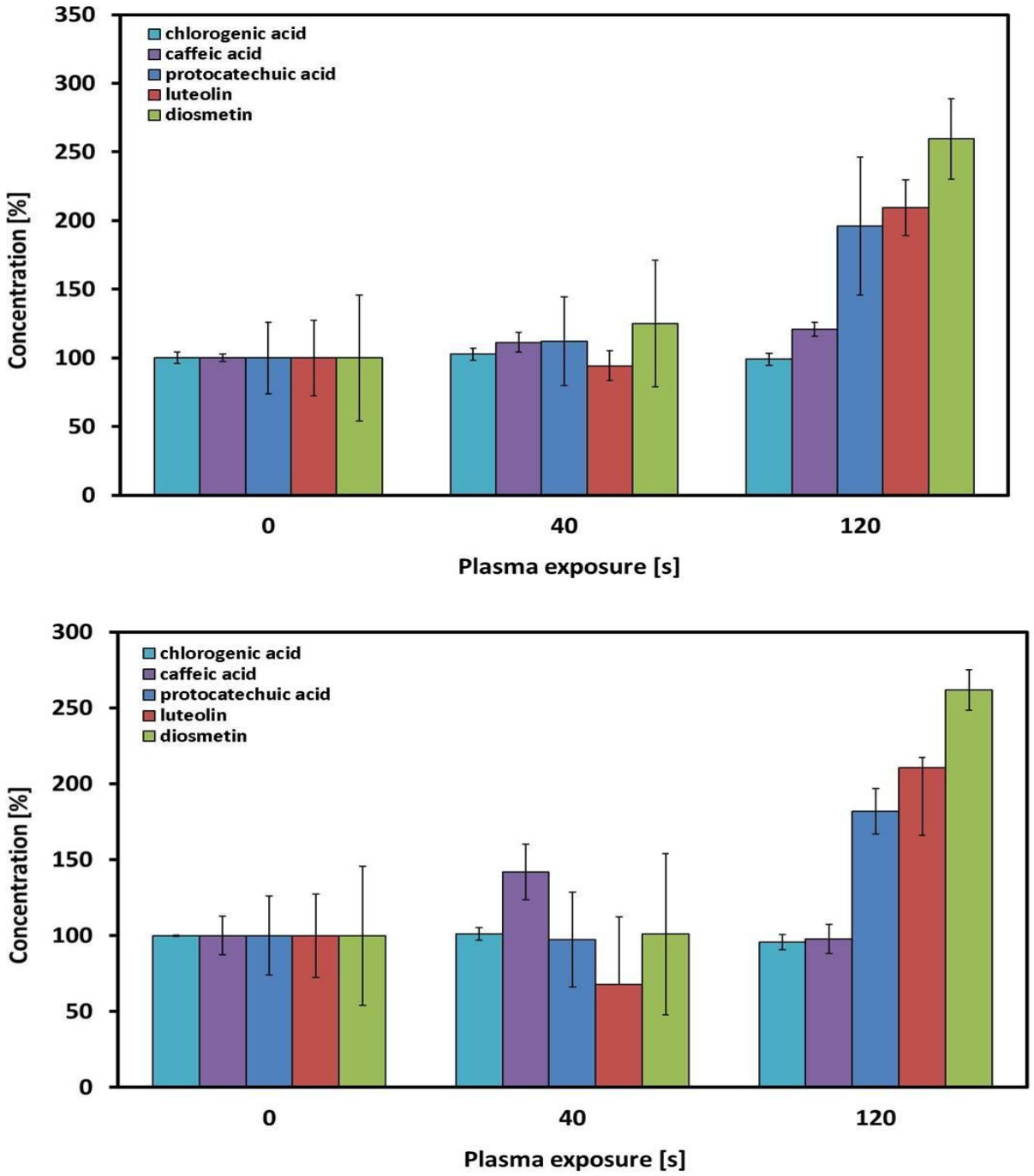

Figure 42. Contents of phenolic acids and flavonoids in freeze-dried lettuce leaves after exposure to the RFGD plasma ($p(O_2)$= 0.5 mbar) at 75 W (top), at 150 W (below).

To simulate realistic operating conditions fresh lettuce leaves were exposed to an atmospheric pressure plasma. Changes in the phenol content upon APPJ 1 treatment are shown in Figure 43. Leaves were treated at the maximum power (40 W) for 40 s. After the treatment they showed explicit signs of damage such as rough and dried leaf surfaces with sometimes brownish spots at the plasma-leaf interface. The plasma-treated extracts were distinctively darker than the control samples.

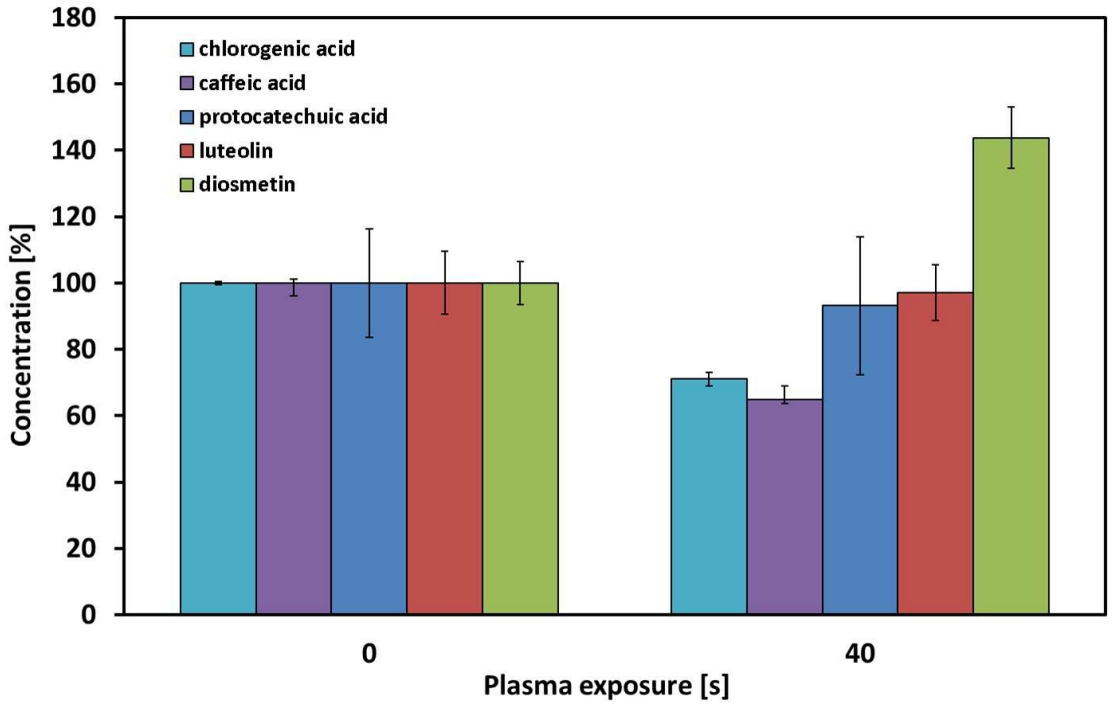

Figure 43. Treatment of fresh lettuce leaves with an atmospheric pressure plasma jet (APPJ 1, 40 W, 20 slm Ar) leads to an increase of diosmetin. Chlorogenic acid and caffeic acid content diminished.

Plasma treatment decreased the content of all phenolic acids ranging from 16% for protocatechuic acid to 29 % for chlorogenic acid. As a consequence, caffeic acid, which is generated from chlorogenic acid upon hydrolysis of the ester bond, is reduced as well (35%). Regarding the content of the flavonoid compounds, luteolin levels remained unchanged whereas a significant rise of diosmetin (44%) has been observed. As for RFGD experiments, considering the standard deviation the observed changes can as well be due to variations in the natural content among the different specimen. As already observed for pure compounds the time- and structure-dependent concentration changes look similar for both plasma sources even if in the end the 40-s exposure APPJ 1 leads to a stronger increase in diosmetin content than the RFGD - a trend that already has been observed for the pure compounds. This is quite surprising as plasma chemistry is strongly determined by the discharge source and the operating conditions.

Various studies have evidenced that plants subjected artificially to UV B radiation respond by changes in their flavonoid content namely in epidermal cells of the adaxial leaf surface, but occasionally as well in the leaf epicuticular waxes (KUBASEK *et al.*, 1992; GREGERSEN *et al.*, 1994; HARBORNE AND WILLIAMS, 2000; SCHNITZLER *et al.*, 1997). The up-regulation of several genes coding for key enzymes in the phenylpropanoid pathway is a common response to a

number of environmental stresses in plants, including UV B (DAUGHERTY *et al.*, 1994), resulting in a dramatic increase in the concentration of flavonoid compounds within leaves and flowers (REED, TERAMURA, AND KENWORTHY, 1992; SULLIVAN AND TERAMURA, 1990; SUDO *et al.*, 2009, and ref. therein). In wild-type *Petunia*, UV B induced an enhanced expression of PAL, cinnamate-4-hydroxylase (C4H), CHS, and chalcone flavone isomerase (CHI) (RYAN *et al.*, 2002). In addition to large increases in glycoflavone synthesis, increases in cell wall bound ferulic acid esters have been observed in both epidermal and mesophyll tissue of barley primary leaves (LIU, GITZ, AND MCCLURE, 1995). As *o*-dihydroxylated flavonoids are furthermore effective free radical scavengers than their monohydroxylated equivalents (MONTESINOS *et al.*, 1995) flavonoids with a higher level of B-ring hydroxylation are preferentially synthesised following UV B treatment (MARKHAM *et al.*, 1997; OLSSON *et al.*, 1998; RYAN *et al.*, 1998). The biosynthetic conversion of B-ring monohydroxylated flavonoids to their ortho-dihydroxylated equivalent is catalysed by the cytochrome P450 enzyme F3'H (GRAHAM, 1998) whose expression is markedly increased with UV B treatment, followed by flavonol synthase (FLS) and dihydroflavonol 4-reductase (DFR) (KIM *et al.*, 2008). A higher UV B tolerance of several plant species is thus correlated to an accumulation of flavonoid metabolites. For an APPJ, analogous to the one used in this study, molecular bands of the second positive system of N_2 (314, 316 nm) and emission of OH-radical (at 309 nm) have been determined in the UV B region along with a weak continuum from 200 nm to 600 nm (*Bremsstrahlung*, cf. Figure 16; BRANDENBURG *et al.*, 2007). As can be seen in Figure 44, the optical emission spectrum significantly differs according to the substrate's position from the nozzle. With increasing distance from the nozzle outlet (and in close vicinity to the sample) mixing of Ar with the surrounding air is gradually increasing, leading to the appearance of additional lines or bands in the UV. Therefore photo-induced transcription of flavonoid biosynthesis stimulated by UV B radiation might in principal be feasible and the observed increase of diosmetin content in lamb's lettuce upon both plasma treatments be the result in the plant cellular system. The fact that enzyme activities in freeze-dried leaves have been shown to be significantly higher than those in fresh tissue (LESTER *et al.*, 2004) evidences that in case of RFGD treated lettuce the solid state of matter of the leaves should not play a crucial role. It is evident that plant defense and the expression of plant defense must exhibit flexibility to allow appropriate defensive phenotypes to be displayed by plants all the time.

Flavonoid content quickly responds to ambient UV B conditions, even over a period of hours (VEIT *et al.*, 1996).

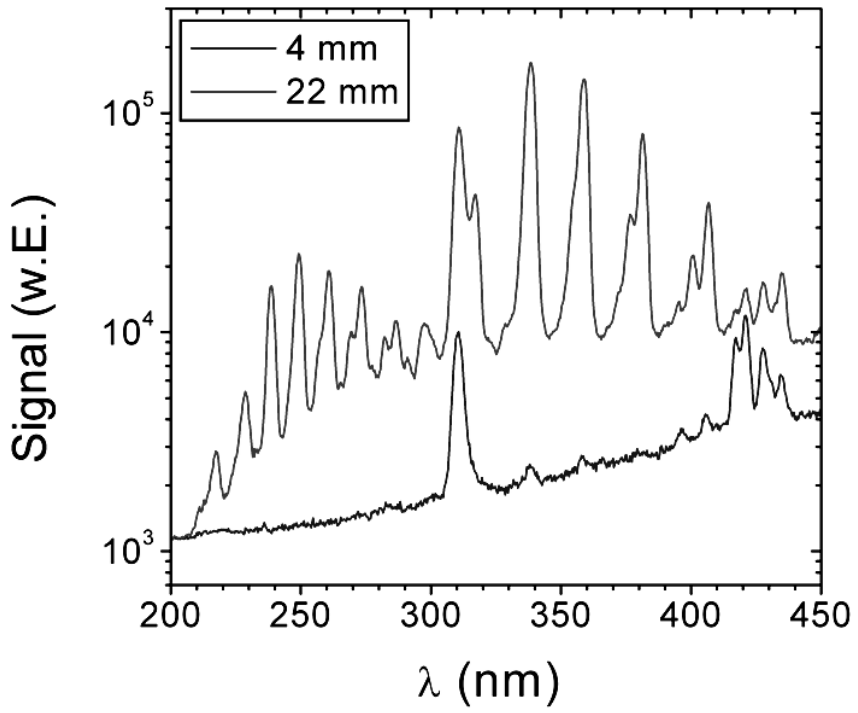

Figure 44. Typical optical emission spectrum measured as a function of the distance from the nozzle in an atmospheric pressure Ar plasma jet (BRANDENBURG *et al.*, 2007).

The transcription of PAL and CHS genes, both encoding key enzymes in the flavonoid biosynthetic pathway has been shown to be extremely rapid (LAWTON AND LAMB, 1987). It is however still questionable, whether the absorbed dose of the relatively short plasma exposure times used in this study is sufficient enough to induce the transcription of flavonoid biosynthetic genes. Furthermore, the quick absorption of UV radiation in the presence of O_3 (reactions R56 and R57) has shown to lower the UV radiance with increasing distance of the sample from the plasma nozzle. A concentration of 3 -5 ppm for an Ar plasma and Ar/Air plasma, respectively, has still been measured at a sample-to-nozzle distance of 200 mm (BRANDENBURG, 2009, *pers. comm.*).

7.2.3 Photolysis and Thermolysis Experiments of fresh Lettuce Leaves

Beside UV B enhanced biosynthesis, the accumulation of specific phenols in lamb's lettuce upon plasma exposure might have yet another origin. Many phenylpropanoid compounds

are induced in response to wounding or to feeding by herbivores (DIXON AND PAVIA, 1995; HAHLBROCK AND SCHEEL, 1989). In potato tubers, wounding greatly increased levels of chlorogenic acid (COTTLE AND KOLATTUKUDY, 1982), alkyl ferulate esters (BERNARDS AND LEWIS, 1992) and cell wall-bound phenolic esters, and amides (HAHLBROCK AND SCHEEL, 1989). The accumulation of kaempferol and its glycosides has been reported for wound-healing petunia stigmas (VOGT *et al.*, 1994). Significant morphological alterations in plant tissues can be as well observed after UV C radiation treatment (KOVÁCS AND KERESZTES, 2002; HOLLÓSY, 2002). Sugar beet leaves exposed to UV C showed collapse and near obliteration of epidermal and underlying palisade parenchyma cells (BORNMAN, EVERT, AND MIERZWA, 1983). Among the various cellular components chloroplasts appear to be most sensitive to UV C, expressed by a loss of integrity of the thylakoids. As already mentioned in chapter 5.1.6, UV C radiation is a common phenomenon in many low and atmospheric pressure plasmas. For an argon driven atmospheric pressure plasma jet analogous to APPJ 1, an intense UV radiation between 200 and 400 nm has been observed (FOEST *et al.*, 2007). Emission was caused mainly by the molecular bands of nitric oxide (γ-system of NO, λ = 236 nm) and OH radicals (A-X transition). In addition the jet is characterized by an intense VUV radiation, attributed to emission lines of atomic nitrogen (N I, λ_{max} = 120 nm), hydrogen (LYMAN-α, 122 nm), and oxygen (O I, λ = 130 nm), along with an Ar_2* excimer continuum (2nd continuum, λ_{max} = 126 nm). Under these circumstances structural alterations are certainly to be expected.

Last but not least, irreversible changes in cellular membranes can as well result from high temperature exposure. Heat injury leads to a loss of membrane integrity causing leakage of solutes and loss of other cell contents (INGRAM AND BUCHANAN, 1984; INGRAM, 1985; LEVIT, 1980). Furthermore high temperature stress has been shown to promote the production of various phenolic compounds (CHRISTIE, ALFENITO, AND WALBOT, 1994; DIXON AND PAVIA,. 1995; SIVACI AND SÖKMEN, 2004).

The enhanced levels of flavonoids and chlorogenic acid upon plasma exposure can therefore be as well the result of plasma- inherent UV C or heat - induced wounding of the plant. Since several studies have shown that, for instance, thylakoid and chloroplast envelope membranes persist intact to temperatures below 333 K (BAUER AND SENSER, 1979; BERRY AND BJORKMAN, 1980; KRAUSE AND SNATARIUS, 1975) irreversible thermal injuries of plant structures stemming from cold plasma exposure seem firstly to be negligible. However the temperature regime of a plasma strongly depends on specific experimental variables (e.g.

plasma source, feed gas, and driving voltage) so that under certain conditions a thermal effect cannot be completely excluded.

To elucidate the influence of UV C radiation and heat evolution in the plasma effluent on the degradation or modification of biological matrices simulation measurements were done. As both plasma sources used in this project were not or not fully characterized regarding either UV-vis emission spectra or irradiation dose, 254 nm was chosen as arbitrary wavelength. The energy dose per mol was adjusted to the UV dose measured in the APPJ 1 for 20 W and 20 slm Ar at a distance of 1 mm (BRANDENBURG, 2009, *pers. comm.*). Regarding heat simulation experiments, a temperature of 317 K has been measured for APPJ 1 when the jet was driven with pure argon at a power of 22 W. Thermal equilibrium was reached soon after plasma ignition and the temperature remained constant during the whole treatment time of 10 min. (Figure 45). At a maximum power of 45 W the temperature raised up to 335 K which already might be a critical value for denaturation of specific proteins, even though conformational changes at this stage might still be reversible. Experiments with Gelrite® gel (1 %) mimicking aqueous biosystems have shown that the temperature in these cases stays approximately constant within the first two minutes before increasing quickly to local temperatures of around 328 to 338 K (T_{max} at 3 min, 42 W). From this it can be concluded that in systems with high water content (high heat capacity) the heat is efficiently dissipated up to a critical time of 120 s. With a water content of more than 90 % (average dry matter content = 6.25 %), the influence of the plasma temperature on lamb's lettuce at a treatment time of 40 s should be negligible. Nevertheless, there is a general lack of reliable information so that despite of the fact that lamb's lettuce can be regarded as a high water content system, lettuce leaves were treated at 'plasma conditions' for 40 s and at a temperature of 323 K.

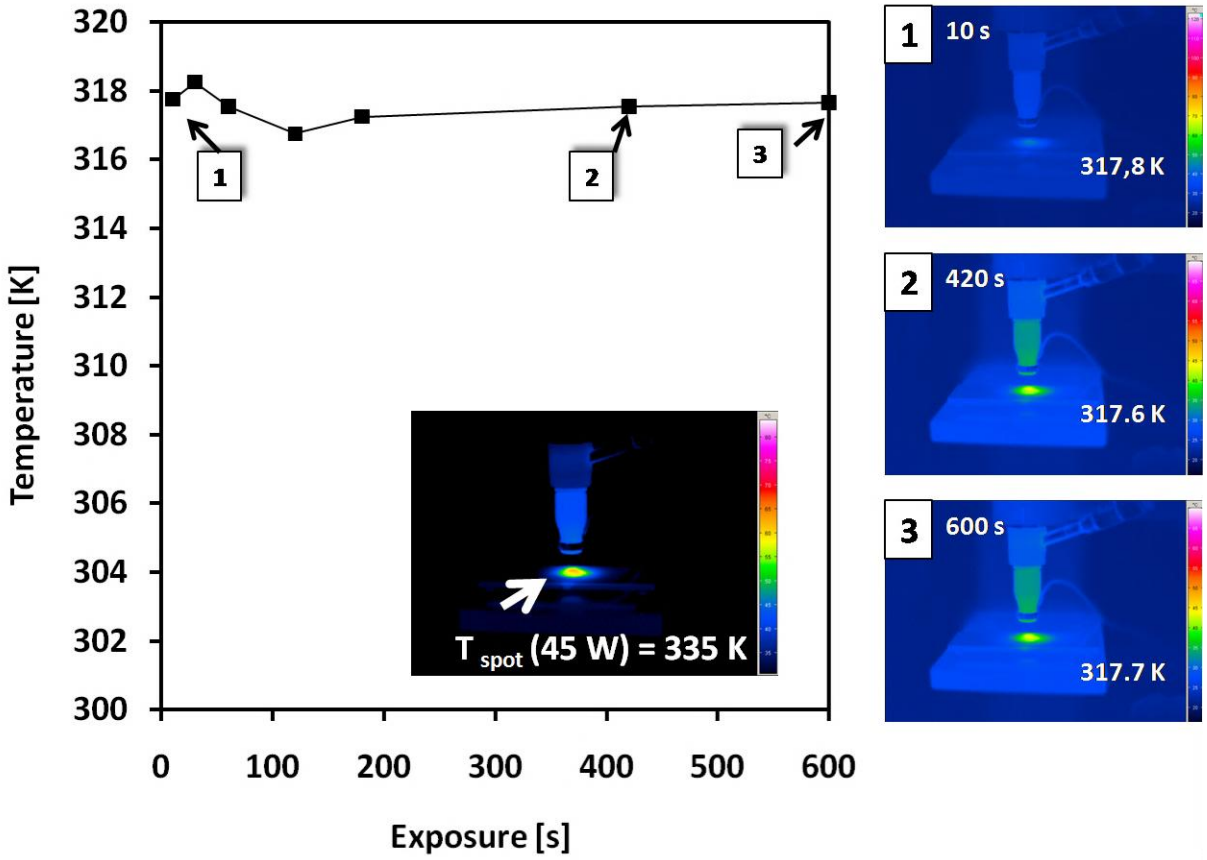

Figure 45. Thermal evolution on the surface of borosilicate slides during APPJ treatment under standard experimental conditions (22W, 20 slm Ar, d= 10 mm) measured by fiber-optical sensing. Thermal equilibrium is reached within the first ten seconds and is kept constant throughout the experiment. The inserted picture shows a snapshot of the substrate surface temperature at a plasma driving voltage of 45 W.

In Figure 46 the changes in concentration after UV C irradiation and heating are shown. For a better comparison the outcomes of the APPJ 1 exposure measurements are added. Although chlorogenic and caffeic acid levels showed a strong decrease after plasma exposure, changes upon UV C or heat exposure were in both cases negligible so that photochemical or heat-induced decomposition reactions do not occur under these conditions. By contrast the concentration of diosmetin increased significantly with heating (53%) and to an even greater extent with irradiation (101%) as compared to APPJ treatment. Likewise more protocatechuic acid (44% to 47% increase upon heating and UV C treatment) and luteolin (29% to 70% increase upon heating and UV C treatment) have been determined. It may be maintained, that unlike plasma exposure UV C and heat treatment of lettuce leaves did not result in decreasing contents of flavonoids and small phenolic acids but on the contrary led to a strong increase.

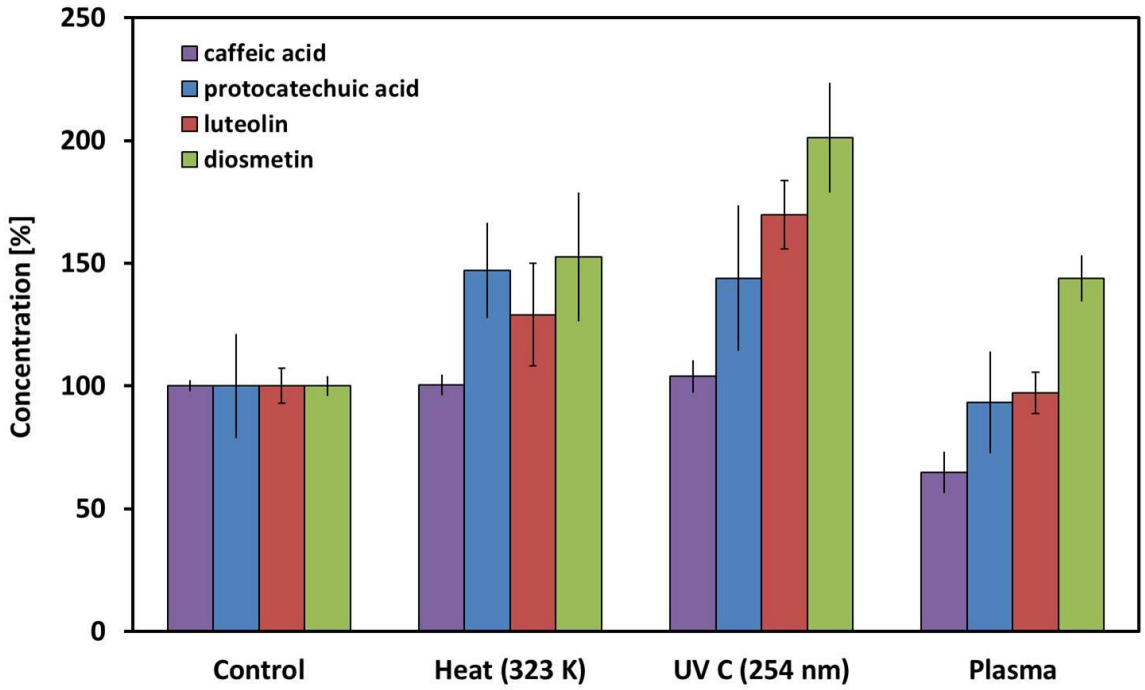

Figure 46. Effect of APPJ treatment (35 W, 20 slm Ar), heating (323 K), and UV (254 nm) on *V .locusta* chemical composition. Plasma-measurements (APPJ 1) have been added for a better comparison.

The observed changes can have different causes. It has been shown that both UV C radiation and high temperatures severely damage epidermal and mesophyll cells, like the underlying palisade parenchyma or other inner cell membranes (BORNMAN, EVERT, AND MIERZWA, 1983; ABASS AND RAJASHEKAR, 1991). As a result, leakage of solutes and loss of cellular components might occur. In the stems of red pigmented lettuce leaf wounding increased the content of phenolic acids two-fold (TOMÁS-BARBERÁN *et al.,* 1997). In processed midribs of lettuce leaves chlorogenic acid has been found to be the predominant phenolic acid accumulated (CANTOS, ESPIN, AND TOMAS-BARBERAN, 2001; FERRERES *et al.*, 1997). Most notably however a marked increase in the activity of PAL in wounded lettuce leaves has been observed (CANTOS, ESPIN, AND TOMAS-BARBERAN, 2001; TOMÁS-BARBERÁN *et al*., 1997). For the flavonoid biosynthesis to occur, enzymes have to be present in the same tissue and cell compartments as the substrates and co-factors. While some enzymes colocalize with flavonoids (POURCEL *et al.*, 2005) differential compartmentalization of enzyme and substrate is usually prevailing. Therefore oxidation reactions only occur after senescence or an environmental stress (pathogen attack, injury) has disorganized the cell or tissues and initiated decompartmentalization (WALKER AND FERRAR, 1998; YORUK AND MARSHALL, 2003, DEHON *et al.*, 2001). This in fact leads to the conclusion that the relative changes in protocatechuic acid

and flavonoid aglycones content might be either the result of a UV C or heat improved extractability by which flavonoids and other compounds accumulated in the vacuoles of leaf epidermal cells are released or that as in the latter case the accumulation is due to an enhanced biosynthesis from activated glucosidases or polphenol oxidases (PPO).

However, this is not explaining why in the end the polyphenol level after plasma treatment is lower. From the combined effects of heat and UV C radiation, additive effects would have been expected. The fact that within the same time an overall weaker augmentation is observed only for one of the compounds tested while all others are significantly degraded might indicate that erosion and cell abatement reactions due to plasma-immanent reactive species may follow almost immediately UV and heat induced accumulation. Just as in case of the pure compounds the direct interaction of energetic ions impinging on lamb's lettuce leaves might lead to erosion or rupture of the plant's upper epidermal layers, where flavonoids are generally concentrated (NIELSEN, NORBAEK, AND OLSEN, 1998). It is therefore anticipated that the impact and the simultaneous interaction of Ar ions and ROS, such as O_3, ·OH and most notably $O(^3P)$ and $O_2(^1\Delta_g$ and $^1\Sigma_g^+)$, lead to erosion of epidermal tissue layers and thus to a decrease of inherent phenolic compounds. This hypothesis is supported by the fact that leaves showed no visible external injuries upon heating and irradiation but were severely damaged upon plasma exposure. It would be as well in accordance to the sensory flavour perception after plasma treatment in both cases. Thus, the effect (wounding) is the same as for heat or UV treatment although the mechanisms behind these effects differ considerably.

7.2.4 Contact Angle Measurements of Plasma treated Lettuce Leaves

Cell ablation and waxy layer erosion should lead to altered surface properties. Therefore the surface wettability of the untreated and the plasma treated samples was determined using static CA measurements. Figure 47 shows the evaluation of the water CA of the lettuce leaves as a function of plasma exposure time. As expected the surface of the pristine leaves is hydrophobic, exhibiting a contact angle of 88°. After exposing the leaves to the RFDG oxygen plasma, the contact angle was gradually reduced until a value of 34° is reached (180 s treatment time). Just as the quercetin samples before (chapter 7.1.3, Figure 32), plant surfaces became more hydrophilic, a behaviour which not only has been already reported for several polymers (WILSON, WILLIAMS, AND POND, 2001; MORENT *et al.*, 2008) but as well for

cotton and wool surfaces (SUN AND STYLOS, 2006). The inserted pictures show that the water drop of the plasma oxidized lettuce leaf (on the right side) displays a considerably lower contact angle than the one of the untreated leaf (left picture), an expression of a higher surface energy and a higher hydrophilicity.

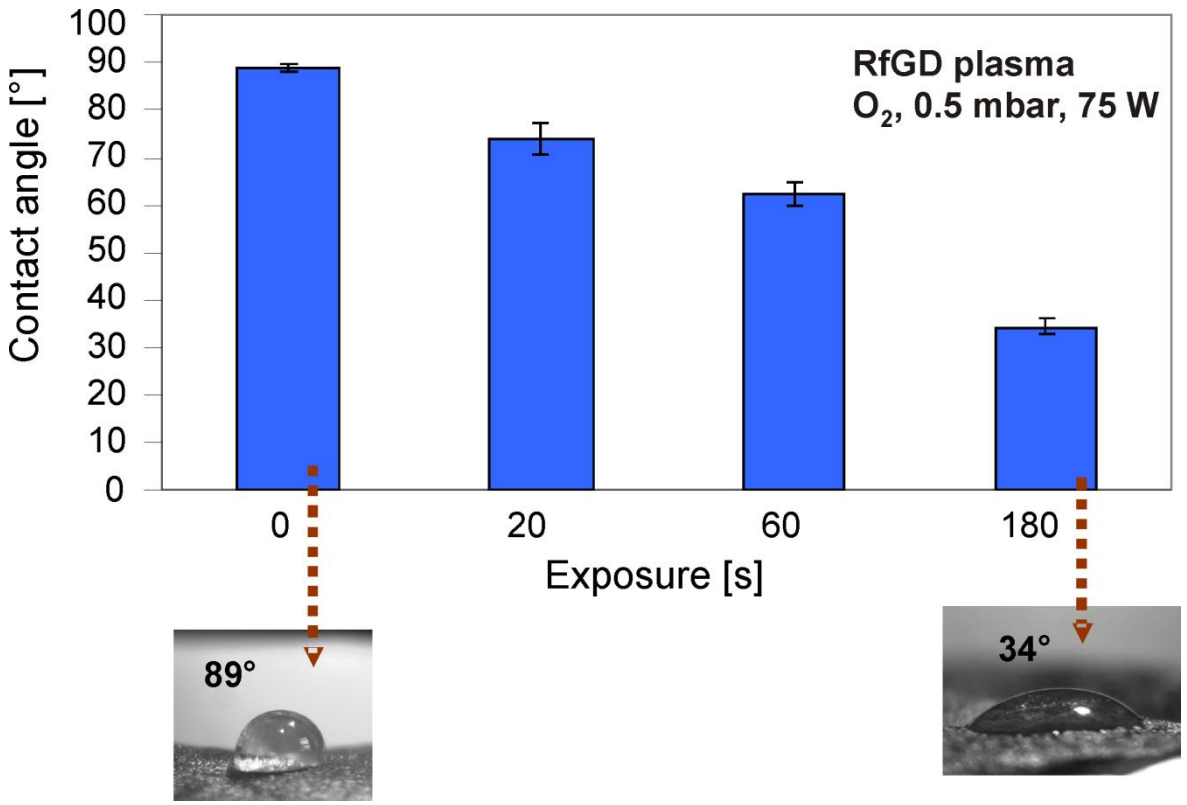

Figure 47. Changes in the contact angle of plasma treated lettuce leaves as a function of plasma-treatment time. The surfaces are getting more hydrophilic. After 180 s the water drop is almost spread out on the leaf surface.

In case of leaves the large reduction in contact angle upon plasma exposure cannot be unambiguously attributed to a plasma-induced formation of oxygen-containing functional groups on the sample surface (WILSON, WILLIAMS, AND POND, 2001; MORENT *et al.*, 2008). A degradation of the cuticle layer, which is composed of cutin and covered by miscellaneous hydrophobic cuticular and epicuticular waxes (RIEDERER AND SCHREIBER, 1995) is as well feasible. A thermal influence can be neglected as moderate warming of plant surfaces showed no significant effect on the CA (MOCKENHAUPT *et al.*, 2008). In addition to that, leaves reached ambient temperature before CA measurement was started, so that influences due to evaporating water from the heated leaf surface or dehydration effects of the lyophilised leaves from elevated plasma temperature can be excluded.

7.2.5 Scanning Electron Microscopy Analysis of Plasma treated Plant Leaf Surfaces

To verify whether the observed changes in the CA originate from a degradation of hydrophobic waxes on the leaves surfaces or are due to the formation of oxygen functional groups, attached or inserted to this layer, the leaf surface morphology was characterised by means of SEM. Although the existence and chemical composition of waxes has not yet been reported for *V. locusta*, a complex mixture of long chain aliphatic compounds (linear primary alcohols, and fatty acids) has been observed for head lettuce (*Lactuca sativa*) (BAKKER *et al.*, 1998). It was therefore anticipated that the outermost surfaces of lamb's lettuce are as well composed of epicuticular waxes. In Figure 48 the SEM micrographs of lamb's lettuce before and after exposing the leaves to the APPJ 1 are shown. As can be seen the leaf surface undergoes considerable morphological changes with increasing plasma exposure. While untreated lettuce leaves exhibit wide smooth areas with thick platelets and small-sized granular structures, the surface of plasma-treated leaves becomes rough and granular structures disappear. As exposure time is increasing the plant surface looks strongly desiccated and visibly stressed.

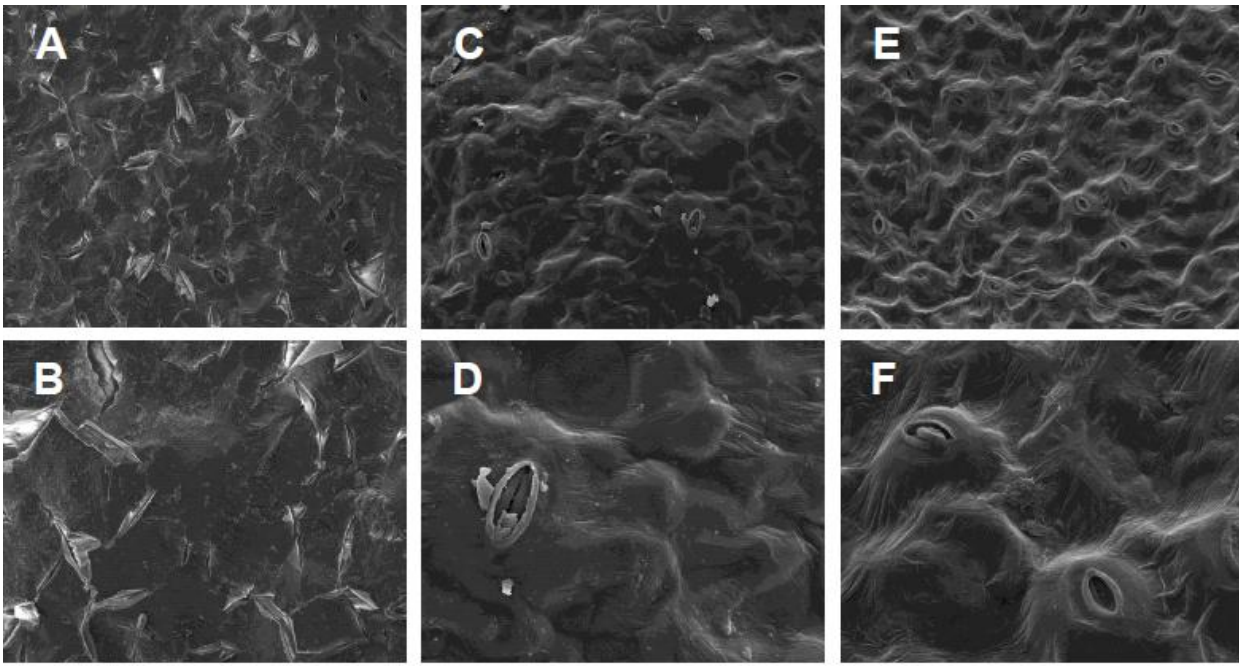

Figure 48. SEM micrographs of *V. locusta* adaxial surfaces after exposure to APPJ 1 (20 slm Ar, 20 W): Untreated leaf at 300x (A) and 1000x magnification (B), surfaces after 20 s at 300x (C) and 1000x magnification (D), surface after 60 s exposure at 300x (E) and 1000x magnification (F).

The same results are given after RFGD plasma treatment (Figure 49). Here as well surfaces get rough and bumpy. To ensure that the observed changes in the surface morphology are

real plasma-induced effects and do not originate from secondary factors like lyophilization for SEM sample preparation, further studies have been done with two different cabbages, known for their high coverage with epicuticular waxes. Adaxial leaf surfaces of kale have been found to exist in a number of distinct crystalline forms, such as tubes, deformed tubes and rods, generally lying perpendicular to the cuticle surface (SHEPHERD *et al.*, 1995).

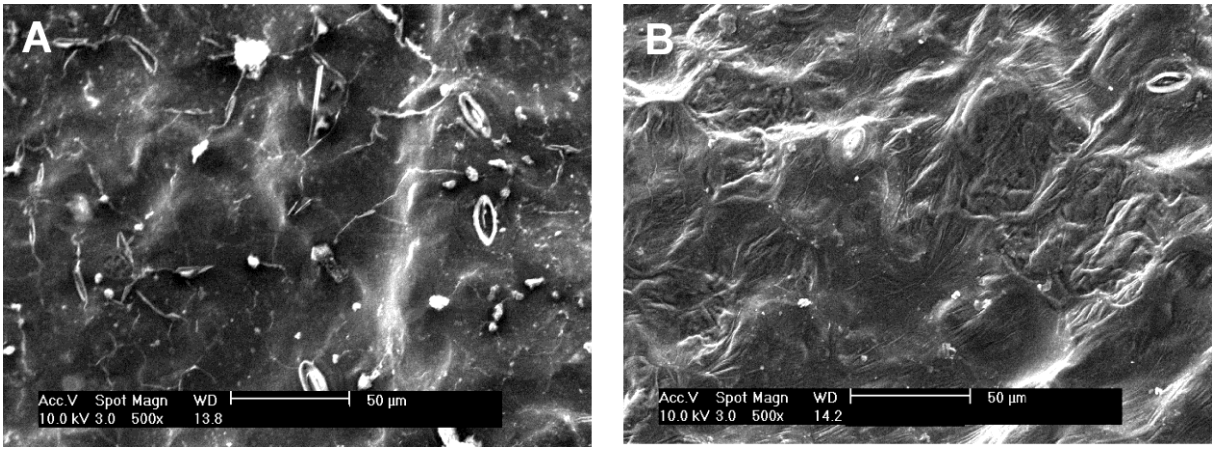

Figure 49. SEM micrographs of *V. locusta* leaf surfaces at 500x magnification: (A) untreated leaf, (B) leaf surface after RFGD exposure ($p(O_2)$= 0.5 mbar, 150 W, 60 s).

The chemical composition varies with environmental conditions but main compounds are *n*-acyl derived long chain alkanes and ketones with C_{29} being the major homologue, nonacosane primary and secondary alcohols and esters. For savoy cabbage no detailed studies on its chemical composition have been found. Our SEM studies show that waxes from savoy cabbage form long and branched three-dimensional structures, transversely oriented on the leaf. The longest rodlets have a length of around 5 µm (Figure 50). The only elements detected by SEM-EDX were carbon and oxygen and small traces of kalium. No trace of calcium and silicon commonly found in plant crystals was determined.

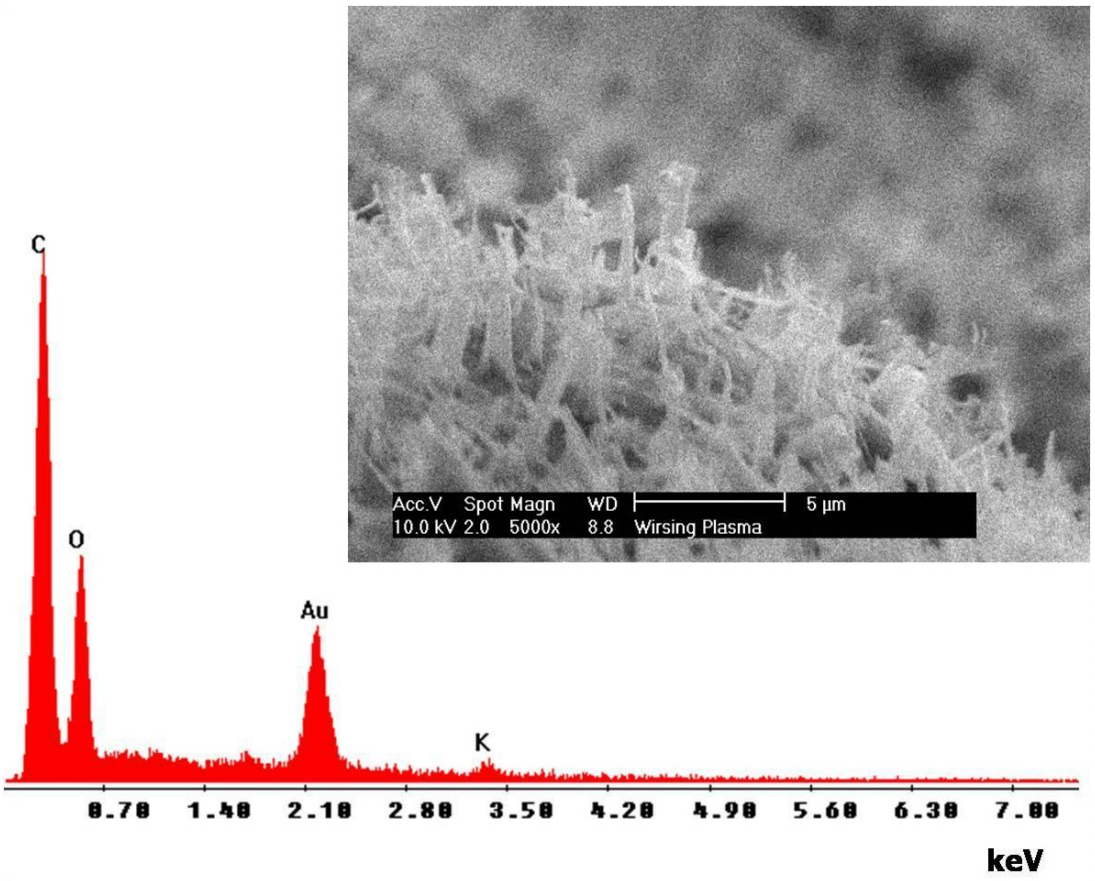

Figure 50. SEM- EDX analysis of epicuticular wax crystals found in savoy cabbage. The elemental composition shows the presence of carbon and oxygen. The Au peak was due to the gold coating of the sample.

Exposure to the oxygen RFGD plasma clearly destroys the waxy layer of adaxial plant epidermis already at comparatively mild conditions (Figure 51, B and E). With increasing treatment time more and more of the waxy layer is eroded and surfaces look either smooth and even or fairly frazzled (Figure 51, C and F). If the plasma power is raised to 150 W, savoy cabbage shows even more drastic morphological changes (Figure 52). While at 75 W epicuticular waxes have still been present after 60 s treatment time, they are already completely removed for 150 W. For kale the picture is not that clear, although increasing degradation is as well evident.

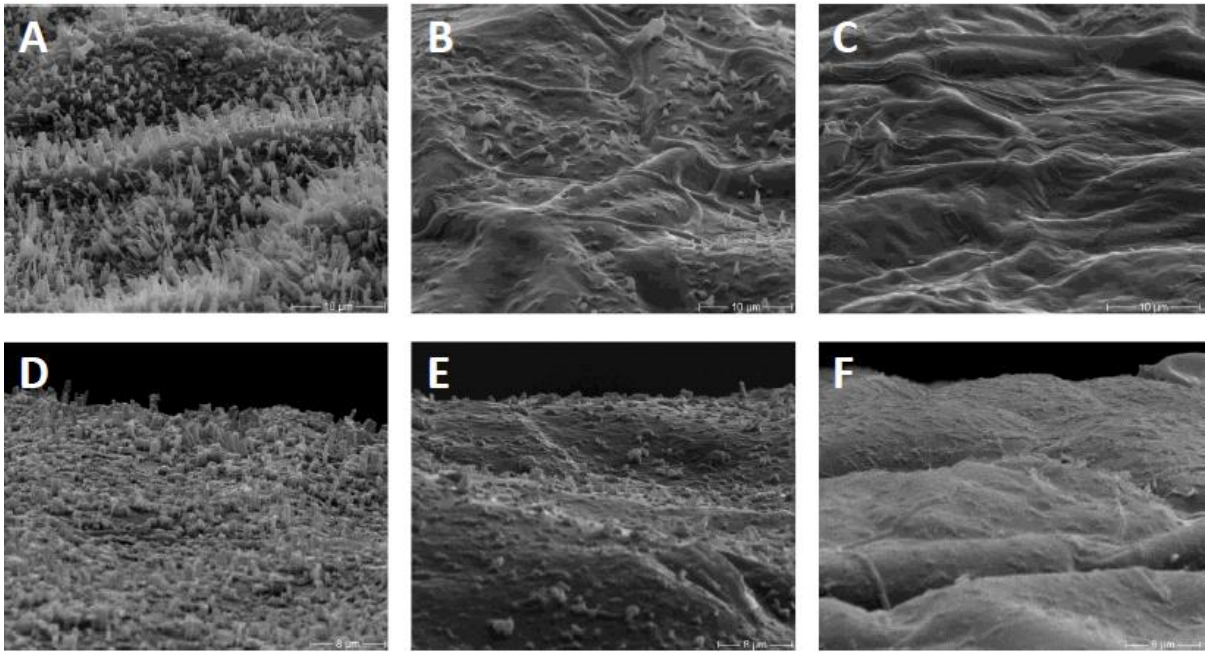

Figure 51. SEM micrographs of kale (A-C) and savoy cabbage (D-E) at 3000x magnification: (A+D) control sample, (B+E) leaves after 60s plasma exposure, (C+F) leaves after 120 s plasma exposure (RFDG, 0.5 mbar O_2, 75 W).

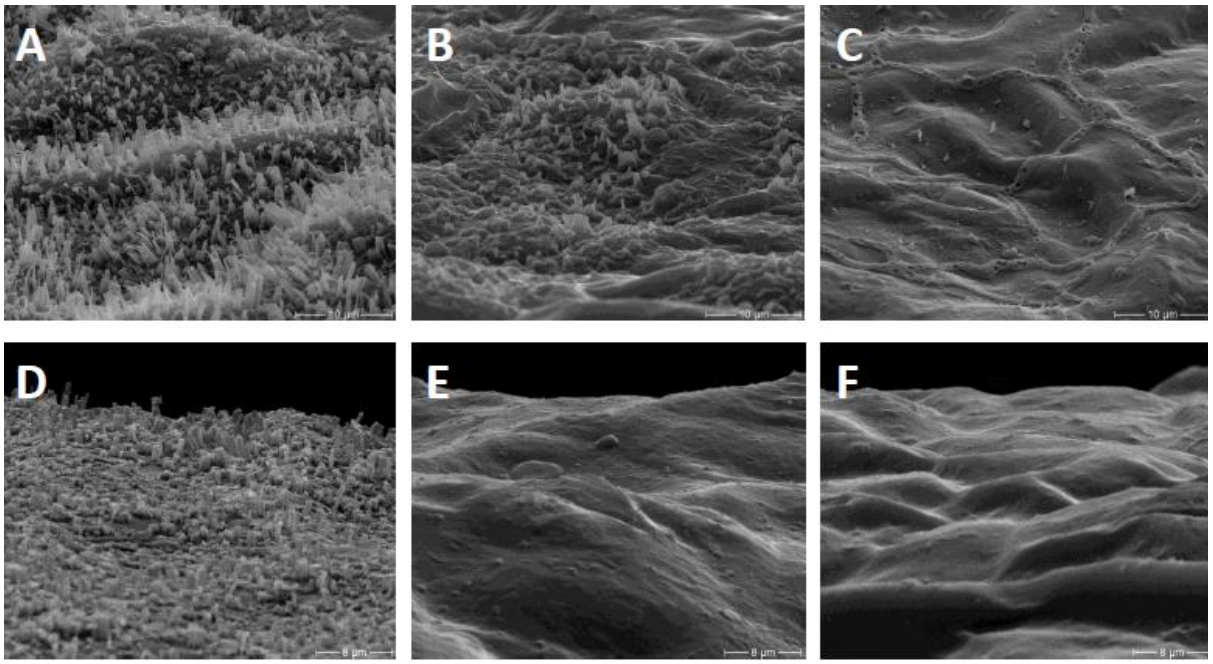

Figure 52. SEM micrographs of kale (A-C) and savoy cabbage (D-E) at 3000x magnification: (A+D) control sample, (B) leaf after 40s plasma exposure, (E) leaf after 60 s, (C+F) leaves after 120 s plasma exposure (RFDG, 0.5 mbar O_2, 150 W).

7.2.6 FTIR Analysis of Plant Leaf Surfaces

Since plasma treatment only changes the uppermost atomic layer of a material without modifying bulk properties, ATR-FTIR analysis of micrometer-thick leaves was initially not

supposed to be the ideal technique for studying changes on a nanometer scale. Indeed pristine and modified leaves feature the same profile in the fingerprint region from 1500 to 400 cm^{-1} even though in general a decrease of the absorption in case of plasma treated samples can be observed (Figure 53). However significant changes appear for the broad ν(O-H) mode between 3000 and 3500 cm^{-1}, stemming from H_2O (adsorbed or water of crystallization), whose intensity has decreased after plasma exposure, and, more drastically, for the strong and sharp (C-H) bands at 2914 cm^{-1} ($\nu_{as}(CH_2)$) and 2848 cm^{-1} ($\nu_s(CH_2)$) (SOCRATES, 2001), which account for most of the aliphatic absorption of the waxes. For all plasma treatments, the extinction is strongly reduced and a broad peak can be observed. The very weak modes at 2954 cm^{-1} ($\nu_{as}(CH_3)$) and 2871 cm^{-1} ($\nu_s(CH_3)$), clearly detectable in the second derivative spectra of the pristine samples, can no longer be discriminated after exposing the leaves to the plasma.

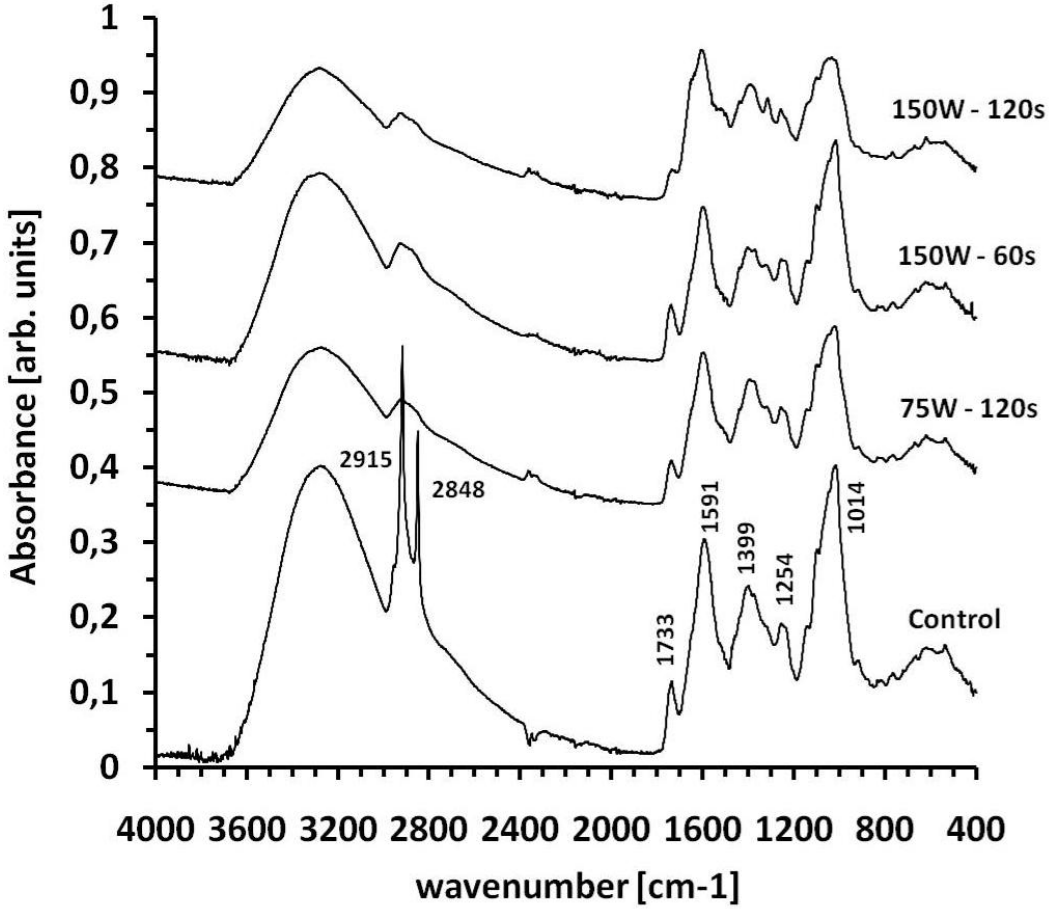

Figure 53. ATR–FTIR spectra of *V. locusta* leaf surfaces: Spectra shifted by 0.2 (75W - 120s), 0.5 (150W - 60s) and 0.6 (150W - 120s) in absorbance.

As contributions of epicuticular waxes to the intensity of (C-H) absorption bands are usually small (MARÉCHAL AND CHAMEL, 1996), plasma-induced degradation reactions, not only of waxes but as well of the underlying cutin layer, are suggested. Cutin represents the main structural component of the cuticular membrane (Figure 54). The polyester is composed of highly crosslinked long-chain hydroxy and epoxy fatty acids from C_{16} and C_{18} family (JEFFREE, 2006; STARK AND TIAN, 2006; HOLLOWAY, 1982). Small amounts of phenolic acids (*p*- coumaric acid and ferulic acid) are esterified to cutin. Regarding plasma treatment polyesters are very well known substrates and it has been demonstrated that the presence of only one ester function in a molecule is already clearly increasing the rates of weight loss, especially in an oxygen plasma (CLOUET AND SHI, 1992).

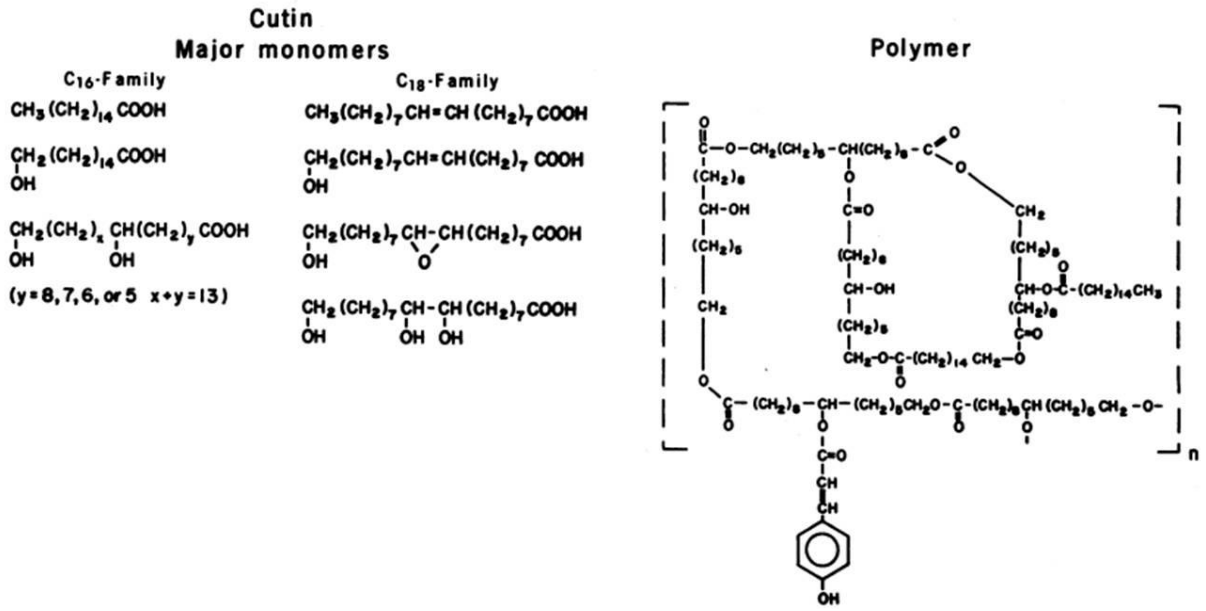

Figure 54. Structure of the major cutin monomers and proposed model of the polymer (KOLATTUKUDY, 1980). Despite intensive research very little is known about the intermolecular structure of the polymer.

More information is obtained for leaves rich in wax. In contrast to lettuce where wax layers are thin and more like a film, cabbage surfaces possess wax layers which are several times thicker. The comparison of the spectra of kale and lettuce leaves shows overall good correlation between them (Table 31). Differences were observed for the scissoring bands at 1472 and 1462 cm^{-1} and the rocking vibrations at 729 and 719 cm^{-1} which were absent in the lettuce spectra. All other bands occurred at nearly constant positions for both vegetables and have been found as well in other crop plants such as potato leaves or various ornamental plants (DUBIS, DUBIS, AND MORZYCKI, 1999). For spiderwort plants (*Tradescantia*)

the in plane bending modes at around 720 cm^{-1} have been as well observed although doubles seem to appear only in the spectra of solid samples (DUBIS, DUBIS, AND MORZYCKI, 1999). Bands at around 1600 cm^{-1} are attributed to the asymmetric stretching mode of the carboxylate function originating from unesterified polygalacturonic acids (pectin; SÉNÉ *et al.*, 1994).

Table 31. FTIR frequencies (cm^{-1}) of plant leaves and band assignments.

Lamb's lettuce	Kale	Potato*	Band assignments
3300	3300	3400	ν(OH)
2915	2915	2916	$\nu_s(CH_2)$
2848	2848	2848	$\nu_{as}(CH_2)$
1733	1737,1734	1732	ν(O-C=O)
	1717	1720	$\nu(R_2C=O)$
1591	1594		$\nu_{as}(COO^-)$
	1472, 1462	1463‡	$\delta_s(CH_2)$, scissoring
1254	1238		δ(C-O)
1141	1142	1154	$\nu(CH_2$-O-CO-)
1098	1097		ν(CO), ν(CC)
1014	1009		ν(CO), ν(CC), δ(OCH)
	729, 719		$\rho(CH_2)$, rocking

*=DUBIS, DUBIS, AND MORZYCKI, 1999, ‡= extract

After plasma exposure the intensity of the symmetric and asymmetric methylene stretching modes of kale at 2850 cm^{-1} and 2926 cm^{-1}, respectively, are likewise decreasing just as the deformation vibrations δ(CH) at 1462 cm^{-1} and 1472 cm^{-1} and the rocking vibrations at 929 and 917 cm^{-1} (Figure 55). In the carbonyl region (1450-1800 cm^{-1}) many peaks of varying intensities (all trace amounts!) appear which are not readily identifiable. In the C-O stretching region between 1100-1300 cm^{-1} the presence of ester bands can be seen. Bands are usually slightly broader and weaker than the corresponding C=O absorption bands. The incorporation of new oxygen-functional groups however could not be confirmed, neither in lettuce nor in kale leaves. The C=O stretching mode around 1730 cm^{-1} assigned to the ester function of the cutin polymer (MARÉCHAL,, 1996), remained nearly unaffected and formation of additional peaks from ν(C-O) modes in the 1000-1300 cm^{-1} region has not been observed. The reduced CA can therefore be attributed to the decomposition of the hydrophobic epicuticular waxes and the cutin layer, although concomitant effects of possible surface oxidation reactions cannot be excluded.

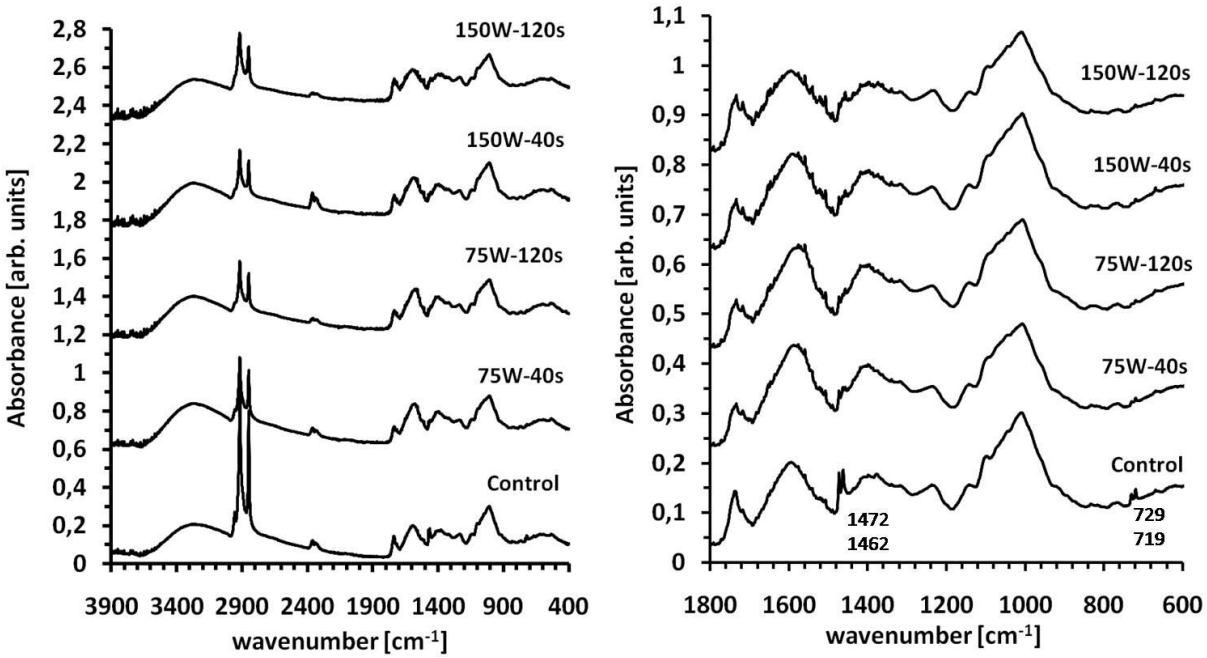

Figure 55. FTIR spectra of kale leaves after various plasma treatments. Left: Spectra from 400-4000 cm^{-1}. Right: Spectra from 1800-600 cm^{-1}. Detailed analysis in the range of 1300 to 1800 cm^{-1} have shown the presence of various carbonyl compounds in the cuticular layers. Spectra shifted by 0.6 (left) and by 0.15(right) in absorbance. CO_2 absorption peak from surrounding air appears at ~ 2350 cm^{-1}.

7.2.7 Influence of NTP on the Antioxidative Properties of Kale

The protective, health-beneficial effects of several plant based food products like fruits and vegetables or coffea and tea, are mainly associated to the presence of natural antioxidants. Extracts of several herbs and spices, e.g. rosemary, have been shown to retard oxidative degradation of lipids and thereby improve the quality and nutritional value of food (ERKAN, AYRANCI, AND AYRANCI, 2008). The intactness of plasma-treated plants regarding their antioxidant capacity is therefore an object of major concern. To this end, the influence of a low-pressure plasma (RFGD O_2 plasma) on the total phenolic content (TPC) and the antioxidant activity of kale was investigated. Samples were analyzed using the FC assay to determine the influence of a cold oxygen plasma on the total phenolic content (TPC) in relation to untreated control samples. The gallic acid equivalent concentration ranged between 0.054 and 0.071 mmol g^{-1} dry matter (dm). Compared to TPC data reported by other authors these values are significantly lower (ZIETZ *et al.*, 2010; HEIMLER, *et al.*, 2006; OLSEN, AABY, AND BORGE, 2009; ZHOU AND YU, 2006). However, it should be considerd that the phenolic content may vary considerably among leaf tissues and also with environmental stress and physiological aging of the plants (PASQUALINI *et al.*, 2003; VOGT AND GULZ, 1994).

As seen in Figure 56 plasma-treated samples are mainly characterized by low TPC values relative to the untreated control samples (0.069 mmol GAE g^{-1} dm). Sole exception is the plasma sample treated with the mildest plasma conditions (40s, 75 W) which is actually showing the highest GAE value (0.071 mmol GAE g^{-1} dm). The lowest TPC of all investigated samples is found after an exposure of 40s at a plasma power of 150 W. Here 0.054 mmol GAE g^{-1} dm have been found, which corresponds to a reduction of 80% relative to the control samples. Although the FC assay has commonly been used to assess the 'total phenolic content' it should be kept in mind that the FC assay is non-specific to phenolics. It rather reflects the reducing power of the whole sample and may include other reducing agents in plant extracts as well. These compounds can interfere in an inhibitory, additive, or enhancing matter depending on the number of phenolic groups they have (SINGLETON AND ROSSI, 1965; HUANG, OU, AND PRICE, 2005). The large deviations of the TPC among the different samples therefore suggest that during plasma exposure various, so far unknow reducing agents are both degraded and newly formed or released in the plant extract.

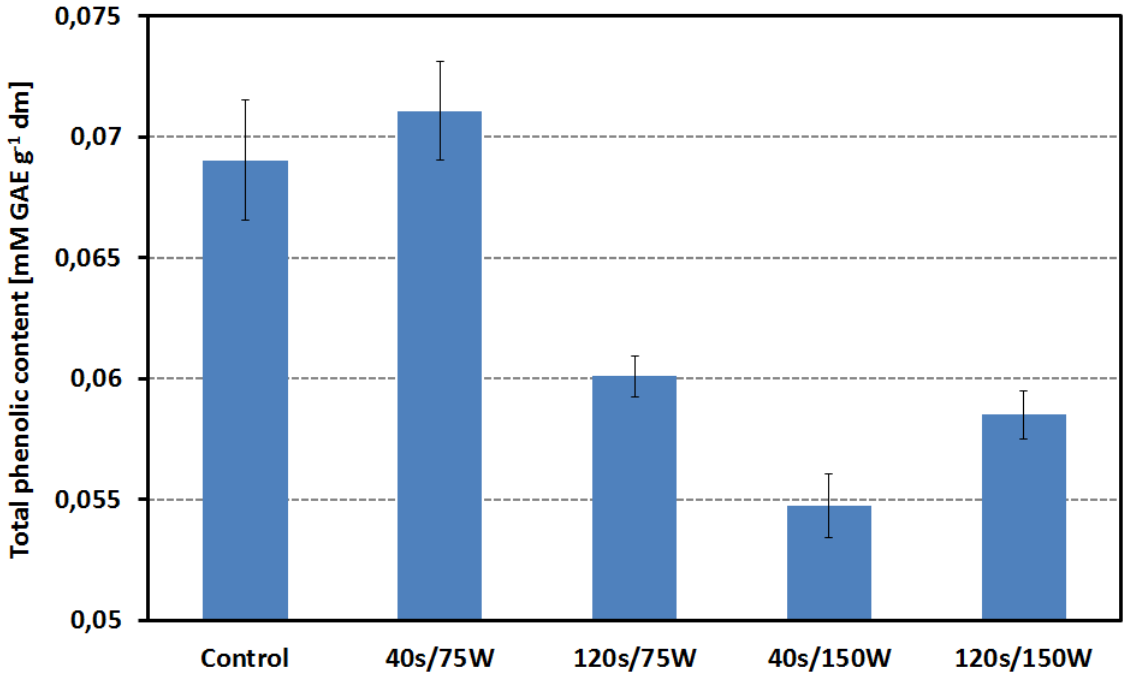

Figure 56. Non-thermal plasma influence (RFGD, $p(O_2)$= 0.5 mbar) on the total phenolic content of kale leaves. At relatively mild conditions (75 W) and short exposure times the TPC is not significantly changing with respect to the untreated control samples. Only with higher treatment times or plasma driving voltage the TPC drastically decreases. Results are expressed as millimoles of gallic acid equivalents per gram of dry matter.

To assess the total amount of radicals that can be scavenged by an antioxidant, i.e. the antioxidant capacity, and to determine potential changes originating from the plasma

treatment, the Trolox Equivalent Antioxidant Capacity (TEAC) assay was applied. As for the TPC the total antioxidant capacity is the sum of the antioxidant capacity of the parent compound and that of the oxidation product(s) of the parent compounds. Higher TEAC values demonstrate higher antioxidant activity. Our results show that in three of four cases, plasma-treated samples are less powerful antioxidants than the untreated samples (Figure 57).

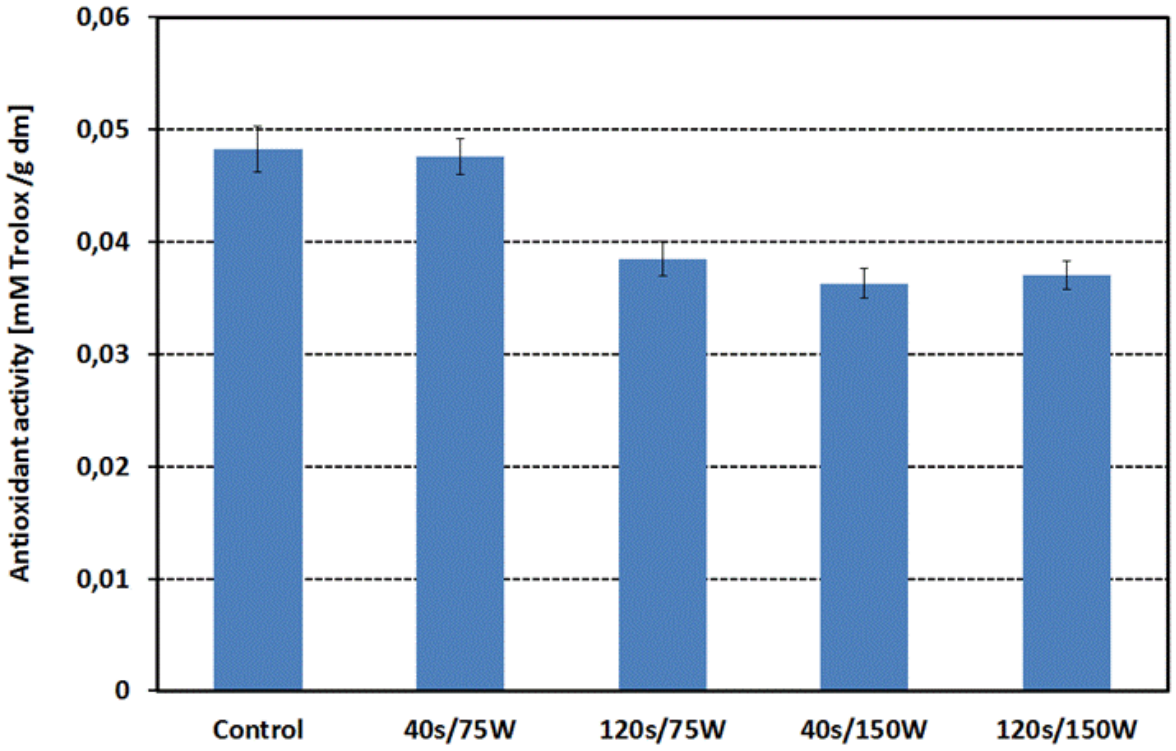

Figure 57. Influence of RFGD plasma ($p(O_2)$= 0.5 mbar) on the antioxidant activity (measured with TEAC) of kale samples . Results are expressed as millimoles of trolox equivalents per gram of dry matter. With increasing plasma exposure and power the antioxidant activity is decreasing.

As for the TPC content, only the mildest plasma treatment (40s, 75 W) was not resulting in any detrimental changes of the antioxidant capacity (0.047 mM trolox g^{-1} dm vs. 0.048 mM trolox g^{-1} dm in the untreated samples). This is in agreement with the results of the FC assay. With increasing plasma exposure and driving voltage the antioxidant activity is decreasing and TEAC values of 0.0363 mM trolox g^{-1} dm to 0.0385 mM TROLOX g^{-1} dm were recorded. In comparison to the FC results, this can be explained on the basis of the higher phenolic content in untreated kale samples, even if changes were less significant than expected (an average reduction of around 22%). Although it should be emphasized that any correlation between total phenolic content and the antioxidant activity of plant species is equivocal due to the insensitive of the FC assay, this leads us to the conclusion that TPC has a positive

correlation with the antioxidant activity. This has already been shown by ZIETZ *et al*. (2010) and ZHOU *et al*. (2006).

The interpretation of the results is difficult. From SEM and FTIR results (Figure 52 and Figure 55) it can be anticipated that epicuticular waxes, still present at the leaf surface after 40s exposure to a RFGD O_2 plasma driven at 75W, are responsible for the unchanged antioxidant properties of kale at these relatively mild plasma conditions. This would correspond as well to the outcomes for RFGD plasma-treated lamb's lettuce (Figure 42) which showed that a plasma treatment of 40 s and 75 W is not significantly changing the concentration of phenolic compounds in plants. Nonetheless it is difficult to draw any firm conclusion about the additive or synergistic contributions of individual antioxidants to the overall antioxidant activity of kale since not all antioxidant compounds have been identified up to date. As a preliminary statement, though, independent of all potential hypotheses, it can be concluded that the RFGD plasma treatment has not a significant, detrimental influence on the antioxidant capacity of kale.

8 Summary

In this study we have attempted to elucidate the influence of non-thermal plasma on the structure and reactivity of polyphenolic pure compounds and on the morphology and phenolic content of *V. locusta*. 1,4-benzopyrones were plasma-modified using an O_2-RFGD at low-pressure and a plasma jet driven with Ar at atmospheric pressure. A continuous, time and dose-dependent degradation has been observed for flavonoids known for their high antioxidant activity protecting cells against the damaging effects of ROS and radicals. The degradation was not caused from photodesorption or thermodesorption processes at the adsorbate surface but clearly stemmed from the combined interaction of the various plasma reactive species in the plasma effluent. Whereas phenolic acids showed a slow decrease, flavonoids were quickly degraded. Plasma reactive species were able to completely decompose thick layers of quercetin and kaempferol in a very short exposure time. The degradation rate strongly depended on the polyphenols substitution pattern. 1,4-benzopyrones that lack specific key structural features underwent a comparatively weaker decomposition. While aglycosidic flavonoids were quickly depleted, glycosidic derivatives showed a rather inert behavior throughout plasma treatment. This was explained by the glucose moiety position acting at the C3 and C4', respectively, as a kind of protective group to retain the flavonoid backbone structure. By blocking the 4'-OH and 3-OH functions, the formation of a quinone intermediates is inhibited, resulting in a slow oxidation of the molecule. Survey and HR XPS spectra collected from Ar and O_2 plasma treated flavonoid compounds indicated that the atomic composition of the treated samples significantly changed upon both plasma treatments in comparison to the virgin substrates. An increase of the oxygen content and the existence of a multitude of carbon and oxygen- based functionalities in the surface layers of the substrates have been observed. Ar plasma treated substrates exposed to open laboratory conditions exhibited identical surface functionalities relative to substrates treated with O_2 plasmas. However, the relative ratios of the plasma created functionalities were significantly different. These groups have been identified as carbonyl- and carboxyl-functions. The concerted decrease of the -C-C- and -C-H bonds strongly suggested that plasma immanent species led to -C-C- and/or -C-H bond breaking reactions giving rise to the formation of -C=O and -O-C=O groups. This is in agreement to results showing that during roasting and cooking processes oxidative species led to the

formation of characteristic low molecular weight degradation products such as phenolic acids.

In contrast to pure compounds freeze-dried leaves of *V. locusta* exhibited an enhanced accumulation of flavonoids though the concentration of chlorogenic and caffeic acids remained unchanged. As for pure compounds short treatment times did not lead to significant changes neither in the polyphenolic nor phenolic content upon exposure. Compared to pure compounds experiments the plant matrix thus seems at first glance to act as a protective shield against oxidation and fragmentation reactions from interaction with ROS or radicals of the plasma. Though a strong increase of diosmetin has been found in fresh leaves, the phenolic acid levels were reduced. It is still an open question whether the observed increase in flavonoid content is caused by UV B stimulated flavonoid biosynthesis or due to an improved extractability from protoplastic or apoplastic compartments of the leaf or its epidermal layers. Although leaves showed no visible damages, contact angle measurements revealed that the leaf surface became more hydrophilic as a function of plasma exposure time. SEM analysis of different cabbage and lettuce species yet illustrated that under certain conditions leaf surfaces are significantly affected by plasma treatment, leading to erosion phenomena of the upper epidermis. From FTIR-ATR experiments we suggest that this is mainly due to a plasma induced degradation of plant surface hydrophobic wax layers, namely epicuticular waxes and the cutin matrix, which would in fact lead to a deeper penetration of UV B radiation but could as well favor further degradation reactions from plasma-induced reactive species.

9 Conclusions and Outlook

Cold plasma chemistry opens up new pathways for the synthesis of fundamentally new macromolecular surface structures through surface functionalization mechanisms. This might offer many advantages with respect to conventional chemical synthesis but can harbour as well unforeseen disadvantages. Our experiments have shown that under the action of active plasma species dehydrogenation and macromolecular backbone scission reactions of 1,4-benzopyrones are induced. This leads to oxidation and cleavage of the flavonoid skeleton. The decomposition clearly depends on the chemical structure of the investigated molecules. The origin of the observed reactions has to be clarified in more detail. We propose that the decomposition reaction probably starts with the generation of active substrate species (free radical sites, unsaturated bonds) and is followed by various inter-and intramolecular reaction processes of the substrates. As a result, mono- and polyphenolics are oxidized into volatile compounds which diffuse from the bulk to the surface and desorb. In addition, we suggest that during plasma treatment CO, CO_2, H_2, H_2O, and other volatile low molecular weight compounds are formed from slow combustion. These compounds and the non-volatile reaction products present on the remaining substrate surfaces unfortunately have not yet been identified. In case of the latter, chromatographical methods as used in conventional food chemical analysis have shown to be too insensitive to detect changes on the nanometer scale. The isolation and characterization of the volatile products so far failed due to rapid and extensive mixing with the surrounding air. The successful application of this novel reaction chemistry as a standard procedure not only in food industry though strongly depends on the basic understanding of plasma-surface reaction mechanisms and on the control of plasma species formation. To elucidate underlying reaction pathways, a identification and quantification of the different gaseous plasma species and the isolation and characterization of the volatile and non-volatile reaction products emanating from plasma-induced surface processes is mandatory. While low-pressure plasmas are already well characterized with the current interest aiming towards a higher spatial and temporal spectroscopic resolution, the development of *in-situ* spatiotemporal diagnostic techniques for atmospheric pressure plasmas is still in its infancy. This is particularly true for atmospheric pressure plasma jets, considered to be the ideal candidates for food industrial purposes. To this end,major focus should be put on the design

and development of spectroscopic and spectrometric tools (OES, LANGMUIR probes, etc.) for systems operating in an open environment. One very promising method to separate and identify trace chemicals in gaseous media, such as air, is ion mobility spectrometry, especially if combined with GC, LC, and/or MS. Even more powerful for the detection of volatile organic compounds (VOC) at ultra low concentrations is PTR-MS (Proton Transfer Reaction-Mass Spectrometry) reaching detection limits in the single-digit ppt_v-range. If turbulences are aggravating the spectroscopic detection, a modification of the experimental set-up is thinkable. By the use of a closed reaction chamber coupled with a supply and extract volume flow system, a constant and well-defined reaction atmosphere can be generated. In this case reaction products emanating from plasma-induced desorption processes could possibly as well be isolated and determined by less sensitive Headspace- or Thermal Desorption-GC/MS. Changes in the set-up are furthermore useful if ions, reactive oxygen species and photons can be separated to study their effect on the sample independently. The use of particle beams simulating the influence of electron, ion and neutrals bombardment will give deeper insight into the individual contributions of plasma-inherent species on the ablation or modification of surfaces. Under conditions where an experimental approach is limited, the use of first principles calculations may be helpful in addition to or as an alternative to experiment Molecular simulations of plasma elementary reactions may be gained from a combined density functional theory calculation coupled with transition state theory and *ab initio* kinetic Monte Carlo. The fact that most effects of the energetic impacting species are completed within picoseconds makes molecular dynamics particularly useful for studying plasma-surface interactions and rationalizing energy and angular distributions of sputtered particles. From a food technological point of view, effects of plasma induced changes on the plant postharvest physiology need to be studied. As demonstrated in this study, the impact of a cold plasma on plant based compounds and food ingredients is strongly influenced by matrix effects. An improved extractibility due to the disintegration of cellular membranes from rare gas ion sputtering or ROS induced oxidation is just as plausible to explain increased levels of specific molecules as the activation of specific biosynthetic enzymes as a plant response to wounding or harmful UV radiation. Beyond sterilization, plasma treatment could thus enhance the bioavailability of a given flavonoid provided that the newly formed molecules are not lost along the food processing chain. Yet, most of the problems that probably arise when plant based food is treated with

plasma do not occur because the surface is oxidized in and polar and reactive functional groups are generated. The real danger seems to be an overtreatment: In a prolonged plasma exposure, epicuticular waxes are degraded and as already observed for several polymers form low molecular weight substances which can deteriorate the surface properties or can be washed off. This is particularly critical as the plant's surface barrier usually hinders most microorganisms to penetrate and spoil the inner tissues. In addition, tissue respiration rates usually increase with the extent of tissue disruption (KADER, 1992). This is of great importance in harvested and stored plant products, as respiration reduces product quality and weight (catabolizm of e.g. carbohydrates, lipids, proteins to CO_2) and increases storage costs (raising temperatures require ventilation or cooling systems) (KLOTZ, FINGER, AND ANDERSON, 2008). It is however as well conceivable that the ablation of the waxy layer offers distinctive advantages for further preservation steps. Attachment to the hydrophobic plant surface is usually believed to limit contact between chlorinated water and microbial contaminants (ADAMS, HARTLEY, AND COX, 1989). Changing the plants surface properties can thus impede microbial attachment and spoilage or improve conventional sterilisation procedures. Disintegration of cellular membranes from increased exposure to UV C radiation or rare gas ion sputtering should likewise be minimized, to avoid detrimental browning of tissues from PPO mediated polymerization reactions. In this context the investigation of enzyme activity and correlated genes by cell and molecular biology methods (Northern and/or Western Blotting, RT-PCR etc.) before and after plasma exposure of the plant matrix is another object of concern. Secondary metabolites produced and deposited by plant cells undergoing hypersensitive cell death can be visualized by UV stimulated autofluorescence. Economic limitations include the use of rare gases as discharge working gases. These gases are very cost-intensive and future studies should aim at substituting rare gases by "cheaper" molecular gases like O_2 or N_2 or gas mixtures like air. It is due to technological reasons that the APPJ we used in this study was almost exclusively limited to the use of rare gases and could not be applied to molecular gases. To this end, improvements in plasma source development have to be undertaken. We anticipate that these advances will help shed light on the complexities of low temperature plasmas altering bio-surfaces, aiming for a simple but controlled surface functionalization or food preservation. Whether the observed modifications are relevant to human health has to be elaborated by toxicological studies.

10 References

ABADIAS, M.; USALL, J.; ANGUERA, M.; SOLSONA, C.; VINAS, I. Microbiological quality of fresh, minimally-processed fruit and vegetables, and sprouts from retail establishments. *Int. J. Food Microbiol.* **2008**, *123*, 121.

ABASS, M.; RAJASHEKAR, C.B. Characterisation of Heat Injury in Grapes Using ^{1}H Nuclear Magnetic Resonance Methods-Changes in Transverse Relaxation Times. *Plant Physiol*. **1991**, *96*, 957.

ACKERS, M.; MAHON, B.; LEAHY, E.; DAMROW, T.; HUTWAGNER, L.; BARRETT, T.; BIBB, W.; HAYES, P.; GRIFFIN, P.; SLUTSKER, L. An outbreak of *Escherichia coli* O157:H7 infections associated with leaf lettuce consumption, Western Montana. *36th Interscience Conference on Antimicrobial Agents and Chemotherapy*, Abstract No. K43; Washington, D.C., Sept. 15-18, **1996**, p. 258.

ADAMS, M.R.; HARTLEY, A.D.; COX, L.J. Factors affecting the efficacy of washing procedures used in the production of prepared salads. *Food Microbiol.* **1989**, *6*, 69.

ADEBOOYE, O.C.; VIJAYALAKSHMI, R.; SINGH, V. Peroxidase activity, chlorophylls and antioxidant profile of two leaf vegetables (*Solanum nigrum* L. and *Amaranthus cruentus* L.) under six pretreatment methods before cooking. *Int. J.Food Sci. Technol.* **2008**, *43*(1), 173.

AGATI, G.; MATTEINI, P.; GOTI, A.; TATTINI, M. Chloroplast-located flavonoids can scavenge singlet oxygen. *New Phytol*. **2007**, *174*, 77.

AHMAD, M.S.; FAZAL, F.; RAHMAN, A.; HADI, S.M.; PARISH, J.H. Activities of flavonoids for the cleavage of DNA in the presence of Cu(II): Correlation with generation of active oxygen species. *Carcinogenesis* **1992**, *13*, 605.

AINSWORTH, E.A.; GILLESPIE, K.M. Estimation of total phenolic content and other oxidation substrates in plant tissues using Folin–Ciocalteu reagent. *Nature Protocols* **2007**, *2*, 875.

AMIOT, M.J.; TACCHINI, M.; AUBERT, S.Y.; OLESZEK, W. Influence of cultivar, maturity, stage and storage conditions on phenolic composition and enzymatic browning of pear fruits. *J. Agric. Food Chem.* **1995**, *43*, 1132.

ARTS, I. C. W.; VAN DE PUTTE, B.; HOLLMAN, P. C. H. Catechin contents of foods commonly consumed in the Netherlands. 1. Fruits, vegetables, staple foods, and processed foods. *J. Agric. Food Chem.* **2000**, *48*, 1746.

ASAMI, D. K.; HONG, Y. J.; BARRETT, D. M.; MITCHELL, A. E. Processing-induced changes in total phenolics and procyanidins in clingstone peaches. *J. Sci. Food Agric*. **2003**, *83*, 56.

ASAMI, D.K.; HONG, Y-J.; BARRETT, D.M.; MITCHELL, A.E. Comparison of the total phenolic and ascorbic acid content of freeze-dried and air-dried marionberry, strawberry, and corn grown using conventional, organic, and sustainable agricultural practices. *J. Agric. Food Chem.* **2003**, *51*, 1237.

ATKINS, P.W. Physikalische Chemie; 2. Aufl.; VCH Verlagsgesellschaft: Weinheim, **1996**.

AWAD, H.M.; BOERSMA, M.G.; VERVOORT, J.; RIETJENS, M.C.M. Peroxidase-catalyzed formation of quercetin quinone methide-gluthione addutcs. *Arch. Biochem. Biophys*. **2000**, *378*, 224.

AYED, N.; YU, H.-L.; LACROIX, M. Improvement of anthocyanin yield and shelf-life extension of grape pomace by gamma irradiation. *Food Res. Int.* **1999**, *32*(8), 539.

BABIOR, B.M. Superoxide: a two-edged sword. *Brazilian J. Med. Biol. Res.* **1997**, *30*, 141.

BAI, Y.; CHEN, J.; MU, H.; ZHANG, C.; LI, B. Reduction of Dichlorvos and Omeathe Residues by O_2 Plasma Treatment. *J. Agric. Food Chem*. **2009**, *57*, 6238.

BAIN, C.D.; TROUGHTON, E.B.;TAO, Y.-T.; EVALL, J.; WHITESIDES, G.M.; NUZZO, R.G. Formation of monolayer films by the spontaneous assembly of organic thiols from solution onto gold. *J. Am. Chem. Soc*. **1989**, *111*, 321.

BAKKER, M. I.; BAAS, W. J.; SIJM, D. T. H. M.; KOLLÖFFEL, C. Leaf wax of *Lactuca sativa* and *Plantago major*. *Phytochemistry* **1989**, *47*, 1489.

BALENTINE, D.; WISERMAN, S. A.; BOUWENS, L. C. M. The chemistry of tea flavonoids. *Crit. Rev. Food Sci. Nutr.* **1997**, *37*, 693.

BALOGH-HERGOVICH, E.; SPEIER, G. Oxidation of 3-hydroxyflavones in the presence of copper(I) and copper(II) chlorides. *J. Mol. Catal*. **1992**, *71*, 1.

BAMFORD, C. H.; NORRISH, R. G. W. Primary photochemical reactions. Part VII. Photochemical decomposition of isovaleraldehyde and di-*n*-propyl ketone. *J. Chem. Soc*. **1935**, 1504.

BARTON, D.; BRADLEY, J. W.; STEELE, D. A..; SHORT, R. D. Investigating Radio Frequency Plasmas Used for the Modification of Polymer Surfaces. *J. Phys. Chem. B* **1999**, *103*, 4423.

BASARAN, P.; BASARAN-AKGUL, N.; OKSUZ, L. Elimination of *Aspergillus parasiticus* from nut surface with low pressure cold plasma (LPCP) treatment. *Food Microbiol.* **2008**, *25*(4), 626.

BAUER, H.; SENSER, M. Photosynthesis of ivy leaves (*Hedera helix* L.) after heat stress. II. Activity of ribulose biphosphate carboxylase, hill reaction, and chloroplast ultrastructure. *Z. Pflanzenphysiol*. **1979**, *91*, 359.

BECKER, K.H.; KOGELSCHATZ, U.; SCHOENBACH, K. H.; BARKER, R.J. Non-equilibrium air plasmas at atmospheric pressure; Series in Plasma Physics, Taylor & Francis: New York, **2004**.

BECKER, K.H.; KURUNCZI, P.F.; SCHOENBACH, K.H. Collisional and radiative processes in high-pressure discharge plasmas. *Physics of Plasmas* **2002**, *9*(5), 2399.

BEESK, N.; PERNER, H.; SCHWARZ, D.; GEORGE, E.; KROH, L.W.; ROHN, S. Distribution of quercetin-3,4'-diglucoside, quercetin-4'-O-monoglucoside, and quercetin in different parts of the onion bulb (*Allium cepa* L.) influenced by genotype. *Food Chem.* **2010**, doi: 10.1016/jfoodchem.2010.03.011.

BENGOECHEA, M.L.; SANCHO, A.I.; BARTOLOMÉ, B.; ESTRELLA, I.; GÓMEZ-CORDOVÉS, C.; HERNÁNDEZ, M.T. Phenolic Composition of Industially Manufactured Purées and Concentrates from peach and Apple Fruits. *J. Agric. Food Chem*. **1997**, *45*, 4071.

BERNARDS, M.A.; LEWIS, N.G. Alkyl ferulates in wound-healing potato tubers. *Phytochemistry* **1992**, *31*, 3409.

BERRY, J.; BJORKMAN, O. Photosynthetic response and adaption to temperatures in higher plants. *Annu. Rev. Plant Physiol*. **1980**, *31*, 491.

BEUCHAT, L.R. Pathogenic microorganisms associated with fresh produce. *J. Food Prot.* **1996**, *59*, 204.

BEUCHAT, L.R. Ecological factors influencing survival and growth of human pathogens on raw fruits and vegetables. *Microbes and Infection* **2002**, *4*(4), 413.

BLOCK, G.; PATTERSON, B.; SUBAR, A. Fruit, vegetables and cancer prevention: a review of the epidemiological evidence. *Nutr. Cancer* **1992**, *18*, 1.

BORNMAN, J.F.; EVERT, R.F.; MIERZWA, R.J. The Effect of UV-B and UV-C Radiation on Sugar Beet Leaves. *Protoplasma* **1983**, *117*, 7.

BORS, W.; HELLER, W.; MICHEL, C.; SARAN, M. Flavonoids as antioxidants: determination of radical-scavenging efficiencies. *Methods Enzymol*. **1990**, *186*, 343.

BRAITHWAITE, N. ST. J. Introduction to gas discharges. *Plasma Sources Sci. Technol*. **2000**, *9*, 517.

BRANDENBURG, R., EHLBECK, J., STIEBER, M., VON WOEDTKE, T., ZEYMER, J., SCHLÜTER, O., & WELTMANN, K.-D. Antimicrobial Treatment of Heat Sensitive Materials by Means of Atmospheric Pressure Rf-driven Plasma Jet. *Contrib.Plasma Physics* **2007**, *47*(1-2), 72.

BRANDENBURG, R.; LANGE, H.; VON WOEDTKE, T.; STIEBER, M.; KINDEL, E.; EHLBECK, J.; WELTMANN, K.-D. Antimicrobial Effects of UV and VUV Radiation of Nonthermal Plasma Jets. *IEEE Trans. Plasma Sci.* **2009**, *37* (1), 877.

BRECHT, J.K. Physiology of lightly processed fruits and vegetables. *Hort. Sci.* **1995**, *301*, 8.

BREITFELLNER, F.; SOLAR, S.; SONTAG, G. Effecct of gamma irradiation on flavonoids on strawberries. *Eur. Food Res. Technol.* **2002**, *215*, 28.

BRIGGS, D.; SEAH, M.P. Practical Surface Analysis; John Wiley: Chichester, **1992**.

BROWN, S.B.; RAJANDA, V.; HOLROYD, J.A.; EVANS, E.G.V. A study of the mechanism of quercetin oxygenation by ^{18}O labelling. *Biochem. J*. **1982**, *205*, 239.

BUCHNER, N.; KRUMBEIN, A.; ROHN, S.; KROH, L. W. Effect of thermal processing on the flavonols rutin and quercetin. *Rapid Commun. Mass Spectrom*., **2006**, *20*, 3229.

BUGIANESI, R.; SALUCCI, M., LEONARDI, C., FERRACANE, R.; CATASTA, G.; AZZINI, E.; MAIANI, G. Effect of domestic cooking on human bioavailability of narigenin, chlorogenic acid, lycopene, and b-carotene in cherry tomatoes. *Eur. J. Nutr*. **2004**, *43*(6), 360.

BYLIK, A.; SAPERS, G.M. Distribution of Quercetin and Kaempferol in Lettuce, Kale, Chive, Garlic Chive, Leek, Horseraddish, Red Radish, and Red Cabbage Tissue. *J. Agric. Food Chem*. **1985**, *33*, 226.

CALABRÒ, M.L.; GALTIERI, V.; CUTRONEO, P.; TOMMASINI, S.; FICARRA, P.; FICARRA, R. Study of extraction procedure by experimental design and validation of a LC method for determination of flavonoids in *Citrus bergamia* juice. *J. Pharm. Biomed. Anal*. **2004**, *35*, 349.

CALVERT, J. G.; PITTS, J.N. Photochemistry; John Wiley and Sons: New York, **1966**.

CANTOS, E.; ESPIN, J.C.; TOMAS-BARBERAN, F.A. Effect of Wounding on Phenolic Enzymes in Six Minimally Processed Lettuce Cultivars upon Storage. *J. Agric. Food Chem*.**2001**, *49*(1), 322.

CARANDO, S.; TESSEIDRE, P. L.; PASCUAL-MARTINEZ, L.; CABANIS, J.C. Levels of flavan-3-ols in French wines. *J. Agric. Food Chem*. **1999**, *44*, 4161.

CASTENMILLER, J.J.M.; WEST, C.E.; LINSSEN, J.P.H.; VAN HET HOF, K.H.; VORAGEN, A.G.J. The food matrix of spinach is a limitig factor in detremining the bioavailability of β-carotene and to a lesser extent of lutein in humans. *J. Nutr.* **1999**, *129*, 349.

CHACKO, S.A.; WENTHOLD, P.G. The negative Ion Chemistry of Nitric Oxide in the Gas Phase. *Mass Spectrom. Rev.* **2006**, *25* (1), 112.

CHAOVANALIKIT, A.; WROLSTAD, R.E. Anthocyanin and Polyphenolic Composition of Fresh and Processed Cherries. *J. Food Sci.* **2004**, *69*, 73.

CHEN, Y.-C.; SUGIYAMA, Y.; ABE, N.; KURUTO-NIWA, R.; NOZAWA, R.; HIROTA, A. DPPH radical-scavenging compounds from Dou-Chi, a soy-bean fermented food. *Biosci. Biotechnol. Biochem*. **2005**, *69*, 999.

CHEN, Y.; ZHENG, R.; JIA, Z.; JU, Y. Flavonoids as superoxide scavengers and antioxidants. *Free Radic. Biol. Med.* **1990**, *9*, 19.

CHEN, H.; ZUO, Y.; DENG, Y. Separation and determination of flavonoids and other phenolic compounds in cranberry juice by high-performance liquid chromatography. *J. Chromatogr. A* **2001**, *913*, 387.

CHEVALIER, T.; DE RIGAL, D.; MBÉGUIÉ-A-MBÉGUIÉ, D.; GAUILLARD, F.; RICHARD-FORGET, F.; FILS-LYCAON, B.R. Molecular cloning and characterization of apricot fruit polyphenol oxidase. *Plant Physiol*. **1999**, *119*, 1261.

CHEYNIER, V. Polyphenols in Foods are more complex than often thought. *Am. J. Clin. Nutr*. **2005**, *81*(1), 223S.

CHOI, J.H.; LEE, E.S.; BAIK, H.K.; LEE, S.-J.; SONG, K.M.; HWANG, M.K.; HUH, C.S. Surface modification of natural leather using low-pressure parallel plate plasma. *Surf*. *Coat*. *Technol*. **2002**, *171*(1-3), 257.

CHOW, T.S. Wetting of rough surfaces. *J. Phys.: Condens. Matter* **1998**, *10*, L445.

CHRISTIE, P.J.; ALFENITO, M.R.; WALBOT, V. Impact of low-temperature stress on general phenylpropanoid and anthocyanin pathways, enhancement of transcript abundance and anthocyanin pigmentation in maize seedlings. *Planta* **1994**, *194*, 541.

CHUKWUMAH, Y.; WALKER, L.; VOGLER, B.; VERGHESE, M. Changes in the Phytochemical Composition and Profile of Raw, Boiled, and Roasted Peanuts. *J. Agric. Food Chem.* **2007**, *55*(22), 9266.

CLOUET, F.; SHI, M.K. Interactions of Polymer Model Surfaces with Cold Plasmas: Hexatriacontane as a Model Molecule of High-Density Polyethylene and Octadecyl Octadecanoate as a Model of Polyester. I. Degradation rate versus Time and Power. *J. Appl. Polymer Sci*. **1992**, *46*, 1955.

COBURN, J.W.; WINTERS, H.F. Ion- and electron- assisted gas-surface chemistry- An important efect in plasma etching. *J. Appl. Phys*. **1979**, *50*(5), 3189.

CODY, R.B.; LARAMÉE, J.A.; DUPONT DURST, H. Versatile New Ion Source for the Analysis of Materials in Open Air under Ambient Conditions. *Anal. Chem*. **2005**, *77*, 2297.

COLLAUD-COEN, M.; DIETLER, G.; KASAS, S.; GRÖNING, P. AFM measurements of the topography and the roughness of ECR plasma treated polypropylene. *Appl. Surf. Sci*. **1996**, *103*, 27.

CONRADS, H.; SCHMIDT, M. Plasma generation and plasma sources. *Plasma Sources Sci. Technol*. **2000**, *9*, 441.

COOK, N.C.; SAMMAN, S. Flavonoids: Chemistry, metabolism, cardioprotective effects, and dietary sources. *J. Nutr. Biochem*. **1996**, *7*, 66.

CORNARD, J.P.; DANGLETERRE, L.; LAPOUGE, C. Computational and spectroscopic characterization of the molecular and electronic structure of the Pb(II)-quercetin complex. *J. Phys. Chem. A* **2005**, *109*(44), 10044.

CORNARD, J.P.; MERLIN, J.C. Spectroscopic and structural study of complexes of quercetin with Al(III). *J. Inorg. Biochem*. **2002**, *92*(1), 19.

COS, P.; YING, L.; CALOMME, M.; HU, J.P.; CIMANGA, K.; POEL, B.V.; PIETERS, L.; VLIETINCK, A.J.; BERGHE, D.V. Structure-activity relationship and classification of flavonoids as inhibitors of xanthine oxidase and superoxide scavengers. *J. Nat. Prod*. **1988**, *61*, 71.

COSBY, P.C. Electron impact dissociation of nitrogen. *J. Chem. Phys.* **1993**, *98*(12), 9544.

COSBY, P.C. Electron impact dissociation of oxygen. *J. Chem. Phys.* **1993**, *98*(12), 9560.

COTTLE, W.; KOLATTUKUDY, P.E. Biosynthesis, deposition, and partial characterization of potato suberin phenolics. *Plant Physiol*. **1982**, *69*, 393.

CRITZER, F.J.; KELLY-WINTENBERG, K.; SOUTH, S.; ROTH, J.R.; GOLDEN, D.A.. Atmospheric plasma inactivation of foodborne pathogens on fresh produce surfaces. *J. Food Prot*. **2007**, *70*, 2290.

CROZIER, A.; LEAN, M.E.J.; MCDONALD, M.S.; BLACK, C. Quantitative analysis of the flavonoid content of commercial tomatoes, onions, lettuce, and celery, *J. Agric. Food Chem*. **1997**, *45* 590.

CUMMINGS, K.; BARRETT, E.; MOHLE-BOETANI, J.C.; BROOKS, J.T.; FARRAR, J.; HUNT, T.; FIORE, A.; KOMATSU, K.; WERNER, S.B.; SLUTSKER, L. A multistate outbreak of *Salmonella enterica Srotype Baildon* associated with domestic raw tomatoes. *Emerging Infectious Disease* **2001**, *7*, 1046.

DANGLES, O.; FARGEIX, G.; DUFOUR, C. One-electron oxidation of quercetin and quercetin derivatives in protic and non protic media. *J. Chem. Soc., Perkin Trans*. **1999**, *2*, 1387.

DAUGHERTY, C.J.; ROONEY, M.F.; PAUL, A.; DE VETTEN, N.; VEGA-PALAS, M.A.; LU, G.; GURLEY, W.B.; FERL, R.J. Environmental stress and gene regulation; In: Arabidopsis; Meyerowitz, E.M.; Somerville, C.R., Eds.; Cold Spring Harbor Laboratory Press: Cold Spring Harbour, N.Y., **1994**; pp. 769-806.

DE GEYTER, N.; MORENT, R.; LEYS, C.; GENGEMBRE, L.; PAYEN, E. Treatment of polymer films with a dielectric barrier discharge in air, helium and argon at medium pressure. *Surf. Coat. Technol*. **2007**, *201*, 7066.

DE ROEVER, C. Microbiological safety evaluations and recommandations on fresh produce. *Food Control* **1998**, *9*, 321-347.

DE SOUZA, R.F.V.; SUSSUCHI, E.M.; DE GIOVANI, W.F. Synthesis, Electrochemical, Spectral, and Antioxidant Properties of Complexes of Flavonoids with Metal Ions. *Synth. React. Inorg. Met.-Org. Chem*. **2003**, *33*, 1125.

DEHON, L.; MONDOLOT, L.; DURAND, M.; CHALIES, C.; ANDARY, C.; MACHEIX, J.-J. Differential compartmentation of o-diphenols and peroxidase activity in the inner sapwood of the *Juglans nigra* tree. *Plant Physiol. Biochem*. **2001**, *39*(6), 473.

DEL CARO, A.; PIGA, A; PINNA, I.; FENU, P.M.; AGABBIO, M. Effect of drying conditions and storage period on polyphenolic content, antioxidant capacity, and ascorbic acid of prunes. *J. Agric. Food Chem*. **2004**, *52*, 4780.

DEL CASTILLO, M.D.; AMES, J.M.; GORDON, M.H. Effect of roasting on the antioxidant activity of coffee brews. *J. Agric. Food Chem*. **2002**, 50, 3698.

DELAQUIS, P.J.; BACH, S.; DINU, L.D. Behavior of *Escherichia coli* O157:H7 in leafy vegetables. *J. Food Prot.* **2007**, *70*(8), 1966.

DELAQUIS, P.J.; STEWART, S.; TOIVONEN, P.M.A.; MOYLS, A.L. Effect of warm, chlorinated water on the microbial flora of shredded iceberg lettuce. *Food Res. Int*. **1999**, *32*, 7.

DELINCÉE, H.; POOL-ZOBEL, B.I. Genotoxic properties of 2-dodecylcyclobutanone, a compound formed on irradiation of food containing fat. *Radiat. Phys .Chem.* **1998**, *52*, 39.

DENES, F.; YOUNG, R.A.; SARMADI, M. Surface Functionalization of Polymers under cold plasma conditions –a mechanistic approach. *J. Photopolym. Sci. Technol*. **1997**, *10*(1), 91.

DENG, S.; RUAN, R.; MOK, C.K.; HUANG, G.; LIN, X.; CHEN, P. Inactivation of Escherichia coli on Almonds Using Nonthermal Plasma. *J. Food Sci.* **2007**, *72*(2), M63.

DEWICK, P.M. Medicinal natural products: a biosynthetic approach. John Wiley & Sons: New York, **2002**.

DHAYAL, M.; LEE, S.-Y.; PARK, S.-U. Using low-pressure plasma for *Carthamus tinctorium* L. seed surface modification. *Vacuum* **2006**, *80*, 499.

DIETRYCH-SZOSTAK, D.; OLESZEK, W. Effect of processing on the flavonoid content in buckwhaet (*Fagopyrum esculentum* Moench) grain. *J. Agric. Food Chem*. **1999**, *47* (10), 4384.

DIN. DIN Taschenbuch 340: Grundlagen der instrumentellen Analytik. Normen und Norm-Entwürfe DIN EN ISO 4257; DIN Deutsches Institut für Normung e.V.; Beuth Verlag: Berlin, **2002-03**.

DIXON, R.A.; PAVIA, N.L. Stress-induced phenylpropanoid metabolism. *Plant Cell*. **1995**, *7*, 1085.

DUBIS, E.N.; DUBIS, A.T.; MORZYCKI, J.W. Comparative analysis of plant cuticular waxes using HATR- FT- IR reflection technique. *J. Mol. Structure* **1999**, *511-512*, 173.

DUPONT, M.S.; MONDIN, Z.; WILLIAMSON, G.; PRICE, K.R. Effect of variety, processing, and storage on the flavonoid glycoside content and composition of lettuce and endive. *J. Agric. Food Chem*. **2000**, *48*, 3957.

EGLEY, G.H.; PAUL JR., R.N.; VAUGHN, K.C.; DUKE, S.O. Role of peroxidase in the development of water- impermeable seed coats in Sida spinosa L. *Planta* **1983**, *157*(3), 224.

ELIASSON, B.; KOGELSCHATZ, U. Nonequilibrium Volume Plasma Chemical Processing. *IEEE Trans. Plasma Sci.* **1991**, *19*(6), 1063.

ELLIOTT, A.J.; SCHEIBER, S.A.; THOMAS, C.; PARDINI, R.S. Inhibition of glutathion reductase by flavonoids. *Biochem. Pharmacol*. **1992**, *44*, 1603.

ENSIKAT, H.J.; BOESE, M.; MADER, W.; BARTHLOTT, W.; KOCH, K. Crystallinity of plant epicuticular waxes: Electron and X-ray diffraction studies. *Chem. Phys. Lipids* **2006**, *144*, 45.

ERKAN, N.; AYRANCI, G.; AYRANCI,E. Antioxidant activities of rosemary (*Rosmarinus Officinalis* L.) extract, blackseed (*Nigella sativa* L.) essential oil, carnosic acid, rosmarinic acid and sesamol. *Food Chem* **2008***, 110*(1),76.

ES-SAFI, N.-E.; GHIDOUCHE, S.; DUCROT, P.H. Flavonoids: Hemisynthesis, Reactivity, Characterization and Free Radical Scavenging Activity. *Molecules* **2007**, *12*, 2228.

EU SCIENTIFIC COMMITTEE ON FOOD (**2002**). Risk profile on the microbiological contamination of fruits and vegetables eaten raw. URL: http://ec.europa.eu/food/fs/sc/scf/out125_en.pdf.

EWALD, C.; FJELKNER-MODIG, S.; JOHANSSON, K.; AKESSON, B. Effect of processing on major flavonoids in processed onions, green beans, and peas. *Food Chem*. **1999**, *64*, 231.

FAIN, A.R. A review on the microbiological safety of fresh salads. *Dairy, Food Environ. San*. **1996**, 16, 146.

FDA (FOOD AND DRUG ADMINISTRATION, USA) (**2006**). Spinach and *E.coli* outbreak. URL: http://www.fda.gov/oc/poacom/hottopics/spinach.html.

FEHD (FOOD AND ENVIRONMENTAL HYGIENE DEPARTMENT, HKSAR) (**2002**). Microbiological risk assessment on salads in Hong Kong. Risk Assessment Studies. Report no.9, URL: http://fehd.gov.hk/safefood/report/salad/report.pdf

FELTON, G.W.; DONATO, K.K.; BROADWAY, R.M.; DUFFEY, S.S. Impact of oxidized plant phenolics on the nutritional quality of dietary protein to a noctuid herbivore, *Spodoptera exigua*. *J. Insect Physiol*. **1992**, *38*, 277.

FERNANDEZ, M. T.; MIRA, L.; FLORÊNCIO, M. H.; JENNINGS, K. R. Iron and copper chelation by flavonoids: an electrospray mass spectrometry study. *J. Inorg. Biochem.* **2002**, *92*, 105.

FERREIRA, D.; GYUYOT, S.; MARNET, N.; DELGADILLO, I.; RENARD, C.M.; COIMBRA, M.A. Composition of phenolic compounds in a Portuguese pear (*Pyrus communis* L. var. S. Bartolomeu) and changes after sun-drying. *J. Agric. Food Chem*. **2002**, *50*, 4537.

FERRERES, F.; GIL, M.I.; CASTANER, M.; TOMAS-BARBERAN, F.A. Phenolic metabolites in red pigmented lettuce (Lactuca sativa). Changes with minimal processing and cold storage. *J. Agric. Food Chem*. **1997**, *45*, 4249.

FOEST, R.; KINDEL, E.; OHL, A.; STIEBER, M.; WELTMANN, K.-D. Non-thermal atmospheric pressure discharges for surface modification. *Plasma Phys. Control. Fusion* **2005**, *47*, B525.

FRANCIS, G.A.; THOMAS, C.; O'BEIME, D. The microbiological safety of minimally processed vegetables. *Int. J. Food Sci. Technol*. **1999**, *34*, 1.

FRIDMAN, A. Plasma Chemistry; Cambridge University Press: New York, **2008**.

FRIDMAN, A.; KENNEDY, L.A. Plasma physics and engineering; Taylor and Francis: New York, **2004**.

FRIDMAN, G.; BROOKS, G.; BALASUBRAMANIAN, A.D.; FRIDMAN, A.; GUTSOL, A.; VASILETS, V.N.; AYAN, H.; FRIEDMAN, G. Comparison of direct and indirect effects of non-thermal atmospheric-pressure plasma on bacteria. *Plasma Process. Polym*. **2007**, *4*(4), 370.

FRIDMAN, G.; SHERESHEVSKY, A.; PEDDINGHAUS, M.; GUTSOL, A.; VASILETS, V.; BROOKS, A.; BALASUBRAMANIAN, M.; FRIEDMAN, G.; FRIDMAN, A. Paper No. AIAA-2006; *37th AIAA Plasma dynamics and Lasers Conference*; San Francisco, June 5-8, **2006**.

FRIEDRICH, J.F.; KÜHN, G.; GÄHDE, J. Untersuchungen zum Plasmaätzen von Polymeren. *Acta Polym*. **1979**, *30*, 470.

FRIEDRICH, J.F.; UNGER, W.E.S.; LIPPITZ, A.; KOPRINAROV, I.; KÜHN, G.; WEIDNER, S.; VOGEL, L. Chemical reactions at polymer surfaces interacting with a gas plasma or with metal atoms - their relevance to adhesion. *Surf. Coat. Technol*. **1999**, *116-119*, 772.

FUKUMOTO, L.R.; MAZZA, G. Assessing antioxidant and prooxidant activities of phenolic compounds. *J. Agric. Food Chem*. **2000**, *48*, 3597.

FUNABIKI, T. Oxygenases and Model Systems; In: Catalysis by Metal Complexes; Funabiki, T., Ed.; Kluwer Academic Press: Dordrecht, **1997**, vol. 19.

FULEKI, T.; RICARDO-DA SILVA, J.M. Effects of cultivar and processing method on the contents of catechins and procyanidins in grape juice. *J. Agric. Food Chem*. **2003**, *51*, 640.

GANDIA-HERRERO, F.; JIMÉNEZ-ATIÉNZAR, M.; CABANES, J.; GARCIA-CARMONA, F.; ESCRIBANO, J. Differential activation of a latent polyphenol oxidase mediated by sodium dodecyl sulfate. *J. Agric. Food Chem*. **2005**, *53*, 6825.

GENNARO, L.; LEONARDI, C.; ESPOSITO, F.; SALUCCI, M.; MAIANI, G.; QUAGLIA, G.; FOGLIANO, V. Flavonoid and carbohydrate contents in tropea red onions: Effects of homelike peeling and storage, *J. Agric. Food Chem*. **2002**, *50*, 1904.

GILBERT, A.; BAGGOTT, J.; WAGNER, P.J. Essentials of Molecular Photochemistry; CRC Press: Boca Raton, **1991**.

GIL-IZQUIERDO, A.; GIL, M.I. FERRERES, F. Effect of processing techniques at industrial scale on orange juice antioxidant and beneficial helath compounds. *J. Agric. Food Chem*. **2002**, *50*, 5107.

GILL, M. I.; FERRERES, G.; TOMAS-BARBERAN, F.A. Effects of postharvest storage and processing on the antioxidant constituents (flavonoids and vitamin C) on fresh-cut spinach. *J. Agric. Food Chem*. **1999**, *47*, 2213.

GÖKMEN, V.; ARTIK, N.; ACAR, J.; KAHRAMAN, N.; POYRAZOGLU, E. Effects of various clarification treatments on patulin, phenolic compound and organic acid compositions of apple juice. *Euro. Food Res. Technol.* **2001**, *213*(3), 194.

GOMÉZ-ALONSO, S.; FREGAPANE, G.; SALVADOR, M.D.; GORODN, M.H. Changes in phenolic composition and antioxidant activity of virgin olive oil during frying. *J. Agric. Food Chem*. **2003**, *51*, 667.

GOULD, K.S.; MCKELVIE, J.; MARKHAM, K.R. Do anthocyanins function as antioxidant in leaves? Imaging of H_2O in erd and green leaves after mechanical injury. *Plant, Cell & Environ.* **2002**, *25*, 1261.

GRACE, S.C.; B.A. LOGAN, ADAMS, W.W. Seasonal differences in foliar content of chlorogenic acid, a phenylpropanoid antioxidant, in Mahonia repens. *Plant Cell Environ*. **1998**, *21*, 513.

GRAHAM, T.L. Flavonoid and flavanol glycoside mtabolism in Arabidopsis. *Plant Physiol. Biochem*. **1998**, *36*, 135.

GREGER, H.; ERNET, D. Flavonoid Muster, Systematik und Evolution bei Valerianella. *Phytochemistry* **1973**, *12*, 1693.

GREGERSEN, L.; CHRISTENSEN, A. B.; SOMMER-KNUDSEN, J.; COLLINGE, D. B. A putative O-methyltransferase from barley is induced by fungal pathogens and UV light. *Plant Mol. Biol*. **1994**, *26*, 1797.

GRILL, A. Cold Plasma Materials Fabrication: From Fundamentals to Applications; Wiley-IEEE Press: New York, **1994**.

GRÖNING, P.; COLLAUD-COEN, M.; KUTTEL, O.M.; SCHLAPBACH, L. Influence of gas pressure on the plasma reaction on polyethersulfone. *Appl. Surf. Sci*. **1996**, *103*, 79.

GU, L.; KELM, M.A.; HAMMERSTONE, J.F.; BEECHER, G.; HOLDEN, J.; HAYTOWITZ, D.; GEBHARDT, S; PRIOR, R.I. Concentrations of Proanthocyanidins in Common Foods and Estimations of Normal Consumption. *J. Nutr*. **2004**, *134*: 613.

GUGUMUS, F. Photooxidation of polyethylene films. *Angew. Makromol. Chemie* **1990**, *182*, 111.

GUTIERREZ, E. Japan prepares as O157 strikes again. *Lancet* **1997**, *349*, 1156.

GUYOT, S.; VERCAUTEREN, J.; CHEYNIER.V. Structural determination of colourless and yellow dimers resulting from (+)-catechin coupling catalyzed by grape polyphenol oxidase. *Phytochemistry* **1996**, *42*, 1279.

HAAS, Y. Photochemical a- cleavage of ketones: revisiting acetone. *Photochem. Photobiol. Sci*. **2004**, 3. 6.

HAENEN, G. R.; PAQUAY, J. B.; KORTHOUWER, R. E.; BAST, A. Peroxynitrite scavenging by flavonoids. *Biochem. Biophys. Res. Commun.* **1997**, *236*, 591.

HÄKKINEN, S.; KÄRENLAMPI, S.O.; MYKKÄNEN, H.M.; TÖRRÖNEN, A.R. Influence of Domestic Processing and Storage on Flavonol Contents in Berries. *J. Agric. Food Chem*. **2000**, *48*, 2960.

HAHLBROCK, K.; SCHEEL, D. Physiology and molecular biology of phenylpropanoid metabolism. *Annu. Rev. Plant Physiol. Plant Mol. Biol.* **1989**, *40*, 347.

HALFMANN, H.; DENIS, B.; BIBINOV, N.; WUNDERLICH, J.; AWAKOWICZ, P. Identification of the most effcient VUV/UV radiation for plasma based inactivation of Bacillus atrophaeus sores. *J. Phys. D: Appl. Phys*. **2007**, *40*, 5907.

HALLIWELL, B.; GUTTERIDGE, J.M.C. Free Radicals in Biology and Medicine; Oxford University Press: New York, **2007**.

HALLIWELL, B.A.; GUTTERIDGE, M.C. Oxygen toxicity, oxygen radicals, transition metals and disease. *Biochem. J.* **1984**, *219*, 1.

HALLOIN, J.M. Localization and changes in catechin and tannins during development and ripening of cotton seed. *New Phytol.* **1982**, *90*, 651.

HANDBOOK OF CHEMISTRY AND PHYSICS; 75th Edn.; Lide, D.R., Ed.; CRC Press: Boca Raton, **1994**.

HANSEN, R.H.;SCHONHORN, H. Technique for preparing low surface energy polymers for adhesive bonding. *J. Polym. Sci. Polym. Lett.* **1966**, *4*, 203.

HARBORNE, J.B.; WILLIAMS, C.A. Advances in flavonoid research since 1992. *Phytochemistry*, **2000**, *55*, 481.

HARBORNE, J. B. The Flavonoids: Advances in Research since 1986. Chapman & Hall/CRC: London, **1994**.

HARBORNE, J.B.; BAXTER, H. A. Handbook of the Natural Flavonoids. John Wiley & Sons: Chichester, **1999**.

HARRIS, L.J.; FARBER, J.N.; BEUCHAT, L.R.; PARISH, M.E.; SUSLOW, T.V.; GARRETT, E.H.; BUSTA, F.F. Outbeaks associated with fresh produce: incidence, growth, and survival of pathogens in fresh and fresh-cut produce. Comprehensive Reviews. *Food Sci. Food Safety* **2003**, *2*, 78 (Supplement).

HASIWA, M.; KYLIÁN, O.; HARTUNG, T.; ROSSI, F. Removal of immune-stimulatory components from surfaces by plasma discharges. *Innate Immunity* **2008**, *14*, 89.

HEIM, K.E.; TAGLIAFERRO, A.R.; BOBYLA, D.J. Flavonoid antioxidants: chemistry, metabolism and srtucture-activity relationships. *J. Nutr. Biochem*. **2002**, *13*, 572.

HEIMLER, D.; ISOLANI, L.; VIGNOLINI, P.; TOMBELLI, S.; ROMANI, A. Polyphenol Content and Antioxidant Activity in Some Species of Freshly Consumed Salads. *J. Agric. Food Chem*. **2007**, *45*, 1724.

HEIMLER, D.; VIGNOLINI, P.; DINI, M.G.; VINCIERI, F.F.; ROMANI, A. Antiradical activity and polyphenol composition of local *Brassicaceae* edible varieties. *Food Chem*. **2006**, *99*, 464.

HERRMANN, H.W.; HENINS, I.; PARK, J.; SELWYN, G.S. Decontamination of chemical and biological warfare (CBW) agents using an atmospheric pressure plasma jet (APPJ). *Physics of Plasmas* **1999**, *6*(5), 2284.

HERRMANN, H.W.; SELWYN, G.S.; HENINS, I.; PARK, J.; JEFFERY, M.; WILLIAMS, J. M. Chemical Warfare Agent Decontamination Studies in the Plasma Decon Chamber. *IEEE Trans. Plasma Sci*., **2002**, *30*(4), 1460.

HERRMANN, K. Über das Vorkommen von Kaffeesäure und Chlorogensäure im Obst und Gemüse. *Z. Lebensm. Unters. Forsch.* **1956**, *43*, 109.

HERRON, J.T. Modeling Studies of the Formation and Destruction of NO in Pulsed Barrier Discharges in Nitrogen and Air*. Plasma Chemistry and Plasma Processing* **2001**, *21*(4), 581.

HERTOG, M. G. H. L.; HOLLMAN, P. C.; KATAN, M. B. Content of Potentially Anticarcinogenic Flavonoids of 28 Vegetables and Fruits Commonly Consumed in the Netherlands. *J. Agric. Food Chem*. **1992**, *40*, 2379.

HERTOG, M.G.; BUENO-DE-MESQUITA, H.B.; FEHILY, A.M.; SWEETNMA, P.M.; ELWOOD, P.C.; KROMHOUT, D. Fruit and vegetable consumption and cancer mortality in the Caerphilly Study. *Cancer Epidemiol. Biomarkers Prev*. **1996**, *5*, 673.

HERTOG, M.G.; KROMHOUT, D.; ARAVANIS, C. Flavonoid intake and long term risk of coronary heart disease and cancer in seven countries study. *Arch. Intern. Med*. **1995**, *155*, 381.

HERTOG, M.G.I.; FESKENS, E.J.M.; HOLLMAN, P.C.H.; KATAN, M.B.; KROMHOUT, D. Dietary antioxidant flavonoids and risk of coronary heart disease: A Zutphen Study. *Lancet* **1993**, *342*, 1007.

HERTOG, M.G.I.; HOLLMAN, P.C.H.; KATAN, M.B. Content of potentially anticancerogenic flavonoids of 28 vegetables and 9 fruits consumed in The Netherlands. *J. Agric. Food Chem.* **1991**, *40*, 2379.

HESSE, M.; MEIER, H.; ZEEH, B. Spektroskopische Methoden in der organischen Chemie; 4. Aufl.; Georg Thieme Verlag: Stuttgart, **1991**.

HILBORN, E.D.; MERMIN, J.H.; MSHAR, P.A.; HADLER, J.L.; VOETSCH, A.; WOJTKUNSKI, C.; SWARTZ, M.; MSHAR, R.; LAMBERT-FAIR, M.A.; FARRAR, J.A.; GLYNN, M.K.; SLUTSKER, L. A multistate outbreak of Escherichia coli O157:H7 infections associated with consumption of mesclun lettuce. *Arch. Intern. Med.* **1999**, *159*(15), 1758.

HIRANO, R.; SASAMOTO, W.; MATSUMOTO, A.; ITAKURA, H.; IGARASHI, O.; KONDO, K. Antioxidant ability of various flavonoids against DPPH radicals and LDL oxidation. *J. Nutr. Sci. Vitaminol*. **2002**, *47*, 357.

HIRAOKA,K.; FUJIMAKI, S.; KAMBARA, S.; FURUYA, H.; OKAZAKI, S. Atmospheric-pressure Penning ionization mass spectrometry. *Rapid Comm. in Mass Spectrom.* **2004**, *18*(19), 2323.

HODNICK, W.F.; KUNG, F.S.; ROETTGER, W.J.; BOHMONT, C.W.; PARDINI, R.S. Inhibition of mitochondrial respiration and production of toxic oxygen radicals by flavonoids. A structure-activity study. *Biochem. Pharmacol.* **1986**, *35*, 2345.

HOHL, U.; NEUBERT, B.; PFORTE, H.; SCHONHOF, I.; BÖHM, H. Flavonoid concentrations in the inner leaves of head lettuce genotypes. *Eur. Food Res. Technol*. **2001**, *213*, 205.

HOLLEMANN, A.F; WIBERG, E.; WIBERG, N. Lehrbuch der anorganischen Chemie; 101. Aufl.; De Gruyter: Berlin, New York, **1995**.

HOLLÓSY, F. Effects of ultraviolet radiation on plant cells. *Micron* **2002**, *33*, 179.

HOLLOWAY, P.J. The chemical constitution of plant cutins; In: The Plant Cuticle; Cutler, D.F.; Alvin, K.L.;Price, C.E., Eds.; Academic Press: London, New York, **1982**; pp. 45-85.

HOLMES-FARLEY, S.R.; WHITESIDES, G.M. Reactivity of carboxylic acid and ester groups in the functionalized interfacial region of "polyethylene carboxylic acid" (PE-CO_2H) its derivatives: differentiation of the functional groups into shallow and deep subsets based on a comparison of contact angle and ATR-IR measurements. *Langmuir* **1987**, ***3***(1), 62.

HOPF, C.; SCHLÜTER, M.; JACOB, W. Chemical sputtering of carbon films by argon ions and molecular oxygen at cryogenic temperatures. *Appl. Phys. Lett.* **2007**, *90*, 224106.

HOPF, C.; SCHLÜTER, M.; SCHWARZ-SELINGER, T.; VON TOUSSAINT, U.; JACOB, W. Chemical sputtering of carbon films by simultaneous irradiation with argon ions and molecular oxygen. *New J. Phys.* **2008**, *10*, 093022.

HU, J. P.; CALOMME, M.; LASURE, A.; DE BRUYNE, T.; PIETERS, A.; VLIETINCK, A.; VANDEN BERGHE, D. A. Structure-activity relationship of flavonoids with superoxide scavenging activity. *Biol. Trace Elem. Res.* ***1995***, *47*, 327.

HUANG, D.; OU, B.; PRIOR, R.L. The chemistry behind antioxidant capacity assays. *J. Agric. Food Chem*. **2005**, *53*, 1841.

HUIE, R.E.; HERRON, J.T. Reaction of atomic oxygen (O ^{3}P) with organic compounds; In: Progress in Reaction Kinetics, vol. *8*(1); Jennings, K.R., Cundall, R.B., Eds.; Pergamon Press: Oxford, 1978; pp. 1-80.

HUSAIN, S. R.; CILLARD, J.; CILLARD, P. Hydroxyl radical scavenging activity of flavonoids. *Phytochemistry* **1987**, *26*, 2489.

HUTZLER, P.; FISCHBACH, R.; HELLER, W.; JUNGBLUTH, T.P.; REUBER, S.; SCHMITZ, R.; VEIT, M.; WEISSENBÖCK, G.; & SCHNITZLER, J.-P. Tissue localization of phenolic compounds in plants by confocal laser scanning microscopy. *J. Exp. Bot*. **1998**, *49*(323), 953.

HUVAERE, K.; OLSEN, K.; SKIBSTED, L.H. Quenching of triplet-excited flavins by flavonoids. Structural assessment of antioxidative activity. *J. Org. Chem*. **2009** ,*74*(19),7283.

INGRAM, D.L. Modeling high temperature and exposure time interactions on Pittosporum tobira root cell membrane thermostability. J*. Am. Soc. Hort. Sci.* **1985**, *110*, 470.

INGRAM, D.L.; BUCHANAN, D.W. Lethal high temperatures for roots of three citrus rootstocks. *J. Am. Soc. Hort. Sci.* **1984**, *109*, 189.

JEFFREE, C. E. The fine structure of the plant cuticle; In: Biology of the plant cuticle; Riederer, M., Müller, C., Eds.;Blackwell: Oxford, **2006**; pp. 11-125.

JEONG, J.Y.; PARK, J. HENINS; I., BABAYAN; S.E., TU, V. J.; SELWYN, G.S.; DING, G.; HICKS, R.F. Reaction Chemistry in the Afterglow of an Oxygen-Helium Atmospheric-Pressure Plasma. *J. Phys. Chem. A* **2000**, *104*, 8027.

JOHANNESSEN, G.S.; LANCAREVIC, S.; KRUSE, H. Bacteriological analysis of fresh produce in Norway. *Int. J. Food Microbiol.* **2002**, *77*, 199.

JØRGENSEN, L.V.; CORNETT, C.; JUSTESEN, U.; SKIBSTEDT, L.H.; DRAGSTED, L.O. Two-electron electrochemical oxidation of quercetin and kaempferol changes only th flavonoid C-ring. *Free Radical Res.* **1998**, *29*(4), 339.

JOVANOVIC, S.V.; STEENKEN, S.; HARA, Y.; SIMIC, M.G. Reduction potentials of flavonoid and model phenoxyl radicals. *J. Chem. Soc., Perkin Trans*. **1996**, *2*, 2497.

JUNGBLUTH, G; RÜHLING, I.; TERNES, W. Oxidation of flavonols with Cu(II), Fe(II) and Fe(III) in aqueous media. *J. Chem. Soc., Perkin Trans*. **2000**, *2*, 1946.

KADER, A.A. Postharvest technology of horticultural crops. Univ. of Calif.: Oakland; **1992**; Pub. No. 3311.

KAIM, W.; SCHWEDERSKI, B. Bioanorganische Chemie; 2. Aufl.;.B.G. Teubner: Stuttgart, **1995**.

KANO, K.; MABUCHI, T.; UNO, B.; ESAKA, Y.; TANAKA, T.; IINUMA, M. Superoxide anion radical-induced dioxygenolysis of quercetin as a mimic of quercetinase. *J. Chem. Soc., Chem. Commum*. **1994**, 593.

KARADENIZ, F.; DURST, R.W.; WROLSTAD, R.E. Polyphenolic Composition of Raisins. *J. Agric. Food Chem*. **2000**, *48*, 5343.

KIM, B.G.; KIM, J.H.; KIM, J.; LEE, C.; AHN, J.-H. Accumulation of Flavonols in Response to Ultraviolet-B Irradiation in Soybean is Related to Induction of Flavanone 3- β- Hydroxylase and Flavanol Synthase, *Mol. Cells* **2008**, *25*(2), 247.

KLOTZ, K.L.; FINGER, F.L.; ANDERSON, M.D. Respiration in postharvest sugarbeet roots is not limited by repiratory capacity or adenylates. *J. Plant Physiol*. **2008**, *165*, 1500.

KNACKSTEDT, J. ;HERRMANN, K. Flavon(ol)glykoside der Puffbohnenblätter (*Vicia faba* L.) und des Feldsalates [*Valerianella locusta* (L.) Betcke]. *Z. Lebensm. Unters. Forsch* **1981**, *173*, 285.

KOFINK, M.; PAPAGIANNOPOULOS, M.; GALENSA, R. (-) Catechin in Cocoa and Chocolate: Occurence and Analysis of an atypical Flavan-3-ol Enantiomer. *Molecules* **2007**, *12*, 1274.

KOLB, J.F.; MOHAMED, A.A.H.; PRICE, R. O.; SWANSON, R. J.; BOWMAN, A.; CHIAVARINI, R.L.; STACEY, M.; SCHOENBACH, K. H. Cold atmospheric pressure air plasma jet for medical applications. *Appl. Phys. Lett*. **2008**, *92*(24), 241501.

KOSECKI, P.M.; VILLAVICIENCIO, A.L.C.H.; BRITO, M.S.; NAHME, L.C.; SEBASTIAO, K.I.; RELA, P.R.; ALMEIDA-MURADIAN, L.B.; MANCINI-FILHO, J.; FREITAS, P.C.D. Effects of irradiation in medicinal and eatable herbs. *Radiat. Phys. Chem*. **2002**, *63*, 681.

KOSEKI, S.; ITOH, K. Prediction of microbial growth in fresh-cut vegetables treated with acidic electrolyzed water during storage under various temperature conditions. *J. Food Prot*. **2001**, *64*, 1935.

KOVÁCS, E.; KERESZTES, A. Effect of gamma and UV-B/C radiation on plant cells. *Micron* **2002**, *33*, 199.

KRAUSE, G.H.; SNATARIUS, K.A. Relative thermostability of the chloroplast envelope. *Planta* **1975**, *127*, 285.

KRIS-ETHERTON, P. M.; HECKER, K. D.; BONANOME, A.; COVAL, S. M.; BINKOSKI, A. E.; HILPERT, K. F.; GRIEL, A. E.; ETHERTON, T. D. Bioactive Compounds in Foods: Their role in the prevention of Cardiovascular Diseases and Cancer. *Am. J. Med*. **2002**, *113*(9B), 71S.

KRISHNAMACHARI, LEVINE, AND PARÉ, Flavonoid Oxidation by the Radical Generator AIBN: A Unified Mechanism for Quercetin Radical Scavenging. *J. Agric. Food Chem*. **2002**, *50*, 4357.

KRISHNAMURTY, H.G.; SIMPSON, F.J. Degradation of rutin by *Aspergillus flavus*. Studies with oxygen 18 on the action of a dioxygenase on quercetin. *J. Biol. Chem*. **1970**, *245*, 1467.

KUBASEK, W. L.; SHIRLEY, B. W.; MCKILLOP, A.; GOODMAN, H. M.; BRIGGS, W.; AUSUBEL, F. M. Regulation of Flavonoid Biosynthetic Genes in Germinating Arabidopsis Seedlings. *The Plant Cell* **1992**, *4*, 1229.

KUBO, I.; NIHEI,K.-I.; SHIMIZU, K. Oxidation products of quercetin catalyzed by mushroom tyrosinase. Bioorganic & Medicinal Chemistry **2004**, 12(20), 5343.

KÜHN, G.; WEIDNER, S.; DECKER, R.; GHODE, A.; FRIEDRICH, J. Selective surface functionalization of polyolefins by plasma treatment followed by chemical reduction. *Surf. Coat. Technol*. **1999**, *116-119*, 796.

KURUNCZI, P.; LOPEZ, J.; SHAH, H.; BECKER, K. Excimer formation in high-pressure microhollow cathode discharge plasmas in helium initiated by low-energy electron collisions. *Int. J. Mass Spec.* **2001**, *205*(1-3), 277.

KURUNCZI, P.; SHAH, H.; BECKER, K. Hydrogen Lyman-α and Lyman-β emissions from high-pressure microhollow cathode discharges in Ne-H_2 mixtures. *J. Phys. B* **1999**, *32*, L651.

KYLE, J.A.M.; DUTHIE, G.G. Flavonoids in Foods; In: Flavonoids: Chemistry, Biochemistry, and Applications; Andersen, Ø. M., Markham, K.R. Eds.; CRC Press: Boca Raton, FL, **2006;** p. 225.

KYLIÁN, O.; BENEDIKT, J.; SIRGHI, L.; REUTER, R.; RAUSCHER, H.; VON KEUDELL, A.; ROSSI, F. Removal of Model Proteins Using Beams of Argon Ions, Oxygen Atoms and Molecules: Mimicking the Action of Low-Pressure Ar/O2 ICP Discharges. *Plasma Process. Polym.* **2009**, *6*, 255.

KYLIÁN, O.; HASIWA, M.; ROSSI, F. Plasma-based de-pyrogenization. *Plasma Proc. Polym.* **2006**, *3*(3), 272.

LANDBO, A.-K.R.; PINELO, M.; VIKJBERG, A.F.; LET, M.B.; MEYER, A.S. Protease-assisted clarification of black currant juice: synergy with other clarifying agents and effect on the phenol content. *J. Agric. Food Chem.* **2006**, *48*, 2960.

LANDREY, L.G.; CHAPPLE, C.C.S.; LAST, R.L. Arabidopsis mutants lacking phenolic sunscreens exhibit enhanced ultraviolet-B injury and oxidative damage. *Plant Physiol*. **1995**, *109*, 1159.

LANGMUIR, I. Oscillations in Ionized Gases. *PNAS* **1928**, *14*, 627.

LANGMUIR, I. The Interaction of Electron and Positive Ion Space Charges in Cathode Sheaths. *Phys. Rev*. **1929**, *33*, 954.

LAROUSSI, M. Nonthermal decontamination of biological media by atmospheric-pressure plasmas: review, analysis, and prospects. *IEEE Trans. Plasma Sci*. **2002**, *30*, 1409.

LAROUSSI, M. Low Temperature Plasma-Based Sterilization: Overview and State-of-the-Art. *Plasma Proc. Polym.* **2005**, *2*, 391.

LAROUSSI, M.; MENDIS, D.A.; ROSENBERG, M. Plasma interaction with microbes. *New. J. Phys*. **2003**, *5*(1), 41.1.

LARRAURI, J. A.; RUPEREZ, P.; SAURA-CALIXTO, F. Effect of drying temperature on the stability of polyphenols and antioxidant activity of red grape pomace peels. *J. Agric. Food Chem*. **1997**, *45*, 1390.

LARRIEU J; HELD, B; MARTINEZ H; TISON, Y. Ageing of atactic and isotactic polystyrene thin films treated by oxygen DC pulsed plasma. *Surf. Coat. Technol*. **2005**, *200*(7) 2310.

LAVOLA, A; JULKUNEN-TIITO, R; APHALO, P; DE LA ROSA, T; LEHTO, T. The effect of UV-B radiation on u.v.-absorbing secondary metabolites in birch seedlings grown under simulated forest soil conditions. *New Phytol*. **1997**, *137*, 617.

LAWTON, M.A.; LAMB, C.J. Transcriptional activation of plant defense genes by fungal elicitor, wounding and infection. *Mol. Cell. Biol*. **1987**, *7*, 335.

LE, Q.T.; PIREAUX, J.J.; VERBIST, J.J. Surface modification of PET films with RF plasma and adhesion of in situ evaporated Al on PET. *Surf. Interf. Anal*. **1994**, *22*, 224.

LEE, C.Y.; KAGAN, V.; JAWORSKY, A.W.; BROWN, S.K. Enzymatic browning in relation to phenolic compounds and polyphenoloxidase activity among various peach cultivars. *J. Agric. Food Chem.* **1990**, *38*, 99.

LEE, J.-Y.; PARK, K.-S.; CHOI, S.-W. Changes in flavonoid contents of Safflower leaf during growth and processing. *J. Food Sci. Nutr.* **2005**, *10*(1), 1.

LEE, S.-C.; JEONG, S.-M.; KIM, S.-Y.; NAM, K.C.; AHN, D.U. Effect of far-infrared irradiation on the antioxidant activity of defatted sesame meal extracts. *J. Agric. Food Chem.* **2005**, *53*, 1495.

LEE, S.U.; LEE, J.H; CHOI, S.H.; LEE, J.S.; OHNISI-KAMEYAMA, M.; KOZUKUE, N.; LEVIN, C.E.; FRIEDMAN, M. Flavonoid Content in Fresh, Home- Processed, and Light-Exposed Onions and in Dehydrated Commercial Onion Products. *J. Agric. Food Chem.* **2008**, *56*(18), 8541.

LEEUWENBURGH, C.; HARDY, M.M.; HAZEN, S.L.; WAGNER, P.; OH-ISHI, S.; STEINBRECHER, U.P.; HEINECKE, J.W. Reactive nitrogen intermediates promote low density lipoprotein oxidation in human atheriosclerotic intima. *J. Biol. Chem.* **1997**, *272*, 1433.

LEOPOLDINI, M.; RUSSO, N.; TOSCANO, M. Gas and liquid phase acidity of natural antioxidants. *J. Agric. Food Chem*. **2006**, *54*, 3078.

LEROUGE, S.; WERTHEIMER, M.R.; YAHIA,L'H. Plasma Sterilization: A Review of Parameters, Mechanisms, and Limitations. *Plasmas and Polymers **2001***, *6*(3), 175.

LESTER, G. E.; HODGES, D. M.; MEYER, R. D.; MUNRO, K. D. Pre-extraction Preparation (Fresh, Frozen, Freeze-dried, or Acetone Powdered) and Long-Term Storage of Fruit and Vegetable Tissues: Effects on Antioxidant Enzyme Activity. *J. Agric. Food Chem*. **2004**, *52*, 2167.

LEVIT, J. Response of Plants to Environmental Stresses. Vol. 1: Chilling, Freezing, and High Temperature Stresses. Academic Press: New York, N.Y., **1980**.

LIPKIN, M.; UEHARA, K.; WINAWER, S; SAANCHEZ, A.; BAUER, C.; PHILIPPS, R.; LYNCH, H.T.; BLATTNER, W.A.; FRAUMENI, J.F. Seventh-Day Adventist vegetarians have a quiescent proliferative activity in colona mucosa. *Cancer Lett*. **1985**, *26*, 139.

LIU, L.; GITZ, D.C.; MCCLURE, J.W. Effects of UV-B on flavonoids, ferulic acid, growth and photosynthesis in barley primary leaves. *Physiol. Plant.* **1995**, *93*, 725.

LORENTS, D.C. The physics of electron beam excited rare gases at high densities. *Physica* B+C **1976**, *82*, 19.

LYONS, M. M.; YU, C.; TOMA, R. B.; CHO, S. Y.; REIBOLDT, W.; LEE, J.; VAN BREMEN, R. B. Resveratrol in raw and baked blueberries and bilberries. *J. Agric*. *Food Chem*. **2003**, *51*, 5867.

MAKRIS, D.P.; ROSSITER, J.T. Quercetin and Rutin (Quercetin 3-O-Rhamnosylglucoside) Thermal Degradation in Aqueous Media under Alkaline Conditions. Special Publ.- *Roy. Soc. Chem*. **2000**, *248*, 216.

MAKRIS, D. P.; ROSSITER, J.T. Hydroxyl free radical-mediated oxidative degradation of quercetin and morin: A preliminary investigation. *J. Food Compos. Anal.* **2001**, *15*, 103.

MARÉCHAL, Y.; CHAMEL, A. Water in a Biomembrane by Infrared Spectrometry. *J. Phys. Chem*. **1996**, *100*, 8551.

MARÉCHAL, Y. Configurations adopted by H_2O molecules: results from IR spectroscopy. *Faraday Discuss*. **1996**, *103*, 349.

MARFAK, A.; TROUILLAS, P.; ALLAIS, D.P.; CALLISTE, C.A.; DUROUX, J.L. Redox Reactions Obtained by γ-Irradiation of Quercetin Methanol Solution are similar to in vivo Metabolism. *Radiat. Res*. **2003**, *159*, 218.

MARFAK, A.; TROUILLAS, P.; ALLAIS, D.P.; CHAMPAVIER, Y.; CALLISTE, C.A.; DUROUX, J.L. Radiolysis of Quercetin in Methanol Solution: Observation of Depside Formation. *J. Agr. Food Chem*. **2002**, *50*, 4827.

MARIN, F.R.; MARTINEZ, M.; URIBESALGO, S.; CASTILO, M.J.; FRUTOS, M.J. Changes in nutraceutical composition of lemon juices according to different industrial extraction systems. *Food Chem*. **2002**, *78*, 319.

MARKHAM, K.R.; GOULD, K.S.; RYAN, K.G. Cytoplasmic accumulation of flavonoids in flower petals and ist relevance to yellow flower coloration. *Phytochemistry* **2001**, *58*, 403.

MARKHAM, K.R.; RYAN, K.G.; BLOOR, S.J.; MITCHELL, K.A. A change in the luteolin:apigenin ratio in Marchantia polymorpha on UV-B enhancement. *Phytochemistry* **1997**, *48*, 791.

MARQUES, L.; FLEURIET, A.; CLEYET-MAREL, J.-C.; MACHEIX, J.-J. Purification of an apple polyphenoloxidase isoform resistant to SDS-proteinase K digestion. *Phytochemistry* **1994**, *36*, 1117.

MARTIN, L.J.; MATAR, C. Increase of antioxidant capacity of the lowbush blueberry (*Vaccinum Angustifolium*) during fermentation by a novel bacterium from the fruit microflora. *J. Sci. Food Agric*. **2005**, *85*, 1477.

MARTINS, H.F.P.; LEAL, J.P.; FERNANDEZ, M.T.; LOPES, V.H.C.; CORDEIRO, N.D.S. Toward the Prediction of the Activity of Antioxidants: Experimental and Theoretical Study of the Gas-Phase Acidities of Flavonoids. *J. Am. Soc. Mass Spectrom*. **2004**, *15*, 848.

MATHEW, T.; DATTA, R.N.; DIERKES, W.K.; NOORDERMEER, J.W.M.; VAN OOIJ, W.J. Mechanistic Investigations of Surface Modification of Carbon Black and Silica by Plasma Polymerisation. *Plasma Chem. Plasma Proc.* **2008**, *28*, 273.

MATSUURA, T.; MATSUSHIMA, H.; SAKAMOTO, H.Photosensitized oxygenation of 3-hydroxyflavones. A possible model for biological oxygenation. *J. Am. Chem. Soc*. **1967**, *89*(24), 6370.

MATSUURA, T.; MATSUSHIMA, H.; NAKASHIMA, R. Photoinduced reactions －XXXVI. Photosensitized oxygenation of 3-hydroxyflavones as a nonenzymatic model for quercetinase. *Tetrahedron* **1970**, *26*, 435.

MERMIN, J.; MEAD, P.; GENSHEIMER, K.; GRIFFIN, P. Outbreak of *E.coli* O157:H7 infections among Boy Scouts in Maine. Abstract No. K44; *36th Interscience Conference in Antimicrobial Agents and Chemotherapy*; Washington, D.C., Sept. 15-18, **1996,** p. 258.

MINOTTI, G.; AUST, S.D. The role of iron in oxygen radical mediated lipid peroxidation. *Chem. Biol. Interact.* **1989**, *71*, 1.

MIRA, L.; FERNANDEZ, M.T.; SANTOS, M.; ROCHA, R.; FLORÊNCIO, M.H.; JENNING, K.R. Interactions of Flavonoids with Iron and Copper Ions: A Mechanism for their Antioxidant Activity. *Free Radic. Res*. **2002**, *36*(11), 1199.

MIZUNO, M.; TSUCHIDA, H.; KOZUKUE, N.; MIZUNO, S. Rapid quantitative analysis and distribution of free quercetin in vegetables and fruits. *Nippon Shokuhin Kogyo Gakkaishi* 1992, *39*, 88.

MOCKENHAUPT, B.; ENSIKAT, H.-J.; SPAETH, M.; BARTHLOTT, W. Superhydrophobicity of Biological and Technical Surfaces under Moisture Condensation: Stability in Relation to Surface Structure. *Langmuir* **2008**, *24*, 13591.

MOISAN, M.; BARBEAU, J.; MOREAU, S.; PELLETIER, J.; TABRIZIAN, M.; YAHIA, L'H. Low-temperature sterilization using gas plasmas: a review of the experiments and an analysis of the inactivation mechanisms. *Int. J. Pharm*. **2001**, *226*(1/2), 1.

MONTENEGRO, J.; RUAN, R.; MA, H.; CHEN, P. Inactivation of *Escherichia coli* O157:H7 Using a Pulsed Non-thermal Plasma System. *J.Food Sci*. **2002**, *67*(2), 646.

MONTESINOS, M.C.; UBEDA, A.; TERENICIO, M.C.; PAYA, M.; ALCARAZ, M.J. Antioxidant profile of mono- and dihydroxylated flavone derivatives in free radical generating systems. *Z. Naturforsch*. **1995**, *50c*, 552.

MOREL, I.; CILLARD, P.; CILLARD, J. Flavonoid-metal interactions in biological systems; In: Flavonoids in health and disease; Rice-Evans, C., Packer, L., Eds.; Marcel Dekker: New York, **1998**; pp. 163.

MORENT, R.; DE GEYTER, N.; LEYS, C.; GENGEMBRE, L.; PAYEN, E. Comparison between XPS- and FTIR-analysis of plasma-treated polypropylene film surfaces. *Surf. Interface Anal*. **2008**, *40*, 597.

MUKHOPADHYAY, S.M.; JOSHI, P.; DATTA, S.; MACDANIEL, J. Plasma assisted surface coating of porous solids. *J. Appl. Surf. Sci*. **2002**, *201*(1-4) 219.

NAT. INST. INF. DIS. (NATIONAL INSTITUTE OF INFECTIOUS DISEASES AND INFECTIOUS DISEASES CONTROL DIVISION, MINISTRY OF HEALTH AND WELFARE OF JAPAN).(**1997**). Verocytotoxin-producing Escherichia coli (enterohemorrhagic E.coli) infection, Japan, 1996-1997. *Infectious Agents Surveillance Reports*, 18, 53.

NEILL, S.O.; GOULD, K.S. Anthocyanins in leaves: light attenuators or antioxidants? *Functional Plant Biology* **2003**, *30*, 865.

NIELSEN, J.K.; NORBAEK, R.; OLSEN, C.E. Kaempferol tetraglucosides from cabbage leaves. *Phytochemistry* **1998**, *49*(7), 2171.

NIEMIRA, B.A.; SITES, J. Cold plasma Inactivates *Salmonella* Stanley and *Escherichia coli* O157:H7 Inoculated on Golden Delicious Apples. *J. Food Prot*. **2008**, *71*(7), 1357.

NISHINAGA, A.; TOJO, T.; TOMITA, H.; MATSUURA, T. Base-catalysed oxygenolysis of 3-hydroxyflavones. *J. Chem. Soc., Perkin Trans*. **1979**,*1*, 2511.

NITSCHKE, M.; MEICHSNER, J. Low-pressure plasma polymer modification from the FTIR point of view. *J. Appl. Polym. Sci.* **1997**, *65*(2), 381.

NOGOTA, Y.; OHTA, H.; SUMIDA, T.; SEKIYA, K. Effect of extraction method on the concentrations of selected bioactive compounds in mandarin juice. *J. Agric. Food Chem.* **2003**, *51*, 7346.

NUNES, T.P.; MARTINS, C.G.; BEHRENS, J.H.; SOUZA, K.L.O.; GENOVESE, M.I.; DESTRO, M.T.; LANDGRAF, M. Radioresistance of *Salmonella* Species and *Listeria monocytogenes* on Minimally Processed Arugula (*Eruca sativa* Mill.): Effect of Irradiation on Flavonoid Content and Acceptability of Irradiated Produce. *J. Agric. Food Chem.* **2008**, *56*(4), 1264.

OLSEN, H.; AABY, K.; BORGE, G.I.A. Characterization and quantification of flavonoids and hydroxycinnamic acids in curly kale (*Brassica oleracea* L. convar. *acephala* Var. *sabellica*) by HPLC-DAD-ESI-MS^n. *J. Agric. Food Chem*. **2009**, *57*, 2816.

OLSSON, L.C.; VEIT, M.; WEISSENBÖCK, G.; BORNMAN, J.F. Differential flavonoid response to enhanced UV-B radiation in *Brassica napus*. *Phytochemistry* ***1998***, *49*, 1021.

OSMAN, A.; MAKRIS, D.P.; KEFALAS, P. Investigation on biocatalytic properties of a peroxidase-active homogentae from onion solid wastes: An insight into quercetin oxidation mechanism. *Process Biochem.* **2008**, *43*(8), 861.

PALIYATH, G.; PINHERO, R.G.; RAO, M.V.; MURR, D.P.; FLETCHER, R.A. Changes in activities of antioxidant enzymes and their relationship to genetic and paclobutrazol-induced chilling tolerance in maize seedlings. *Plant Physiol*. **1997**, *114*, 695.

PARK, B. J.; TAKATORI, K.; SUGITA-KONISHI, Y.; KIM, I.-H.; LEE, M.H.; HAN, D.W.; CHUNG, K.H.; HYUN, S.O.; PARK, J.C. Degradation of mycotoxins using microwave-induced argon plasma at atmospheric pressure. *Surf. Coat. Technol.* **2007**, *201*, 5733.

PARK, C.-M.; HUNG, Y.-C.; DOYLE, M.P.; EZEIKE, G.O.I.; KIM, C. Pathogen reduction and quality of lettuce treated with electrolyzed oxidizing and acidified chlorinated water. *J. Food Sci*. **2001**, *66*, 1368.

PARR, A.J.; BOLWELL, J.P. Phenols in the plant and in man. The potential for possible nutritional enhancement of the diet by modifiying the phenols content or profile. *J. Sci. Food Agric*. **2002**, *80*, 985.

PASQUALINI, S.; PICCIONI, C.; REALE, L.; EDERLI, L.; DELLA TORRE, G.; FRANCESCO FERRANTI, F. Ozone-induced cell death in tobacco cultivar Bel W3 plants. The role of programmed cell death in lesion formation. *Plant Physiol*. **2003**, *133*, 1122.

PAYNTER, R.W. XPS studies of the modification of polystyrene and polyethyleneterephthalate surfaces by oxygen and nitrogen plasmas. *Surf. Interface Anal*. **1998**, *26*, 674.

PEDRIELLI, P.; PEDULLI, G.F.; SKIBSTED, L.H. Antioxidant Mechanism of Flavonoids. Solvent Effect on Rate Constant for Chain-Breaking Reaction of Quercetin and Epicatechin in Autoxidation of Methyl Linoleate. *J. Agric. Food Chem*. **2001**, *49*, 3043.

PEREZ-MAGARINO, S.; GONZALES-SAN JOSE, M.L. Evolution of flavonols, anthocyans, and their derivatives during the aging of red wines, elaborated from grapes harvested at different stages of ripening. *J. Agric. Food Chem*. **2004**, *52*, 1181.

PERNI, S.; LIU, D.W.; SHAMA, G.; KONG, M.G. Cold Atmospheric Plasma Decontamination of the Pericarps of Fruit. *J. Food Prot.* **2008**, *71*(2), 302.

PERNI, S.; SHAMA, G.; KONG, M.G. Cold Atmospheric Plasma Disinfection of Cut Fruit Surfaces Contaminated with Migrating Microorganisms. *J. Food Prot.* **2008**, *71*(8), 1619.

PERNI, S.;SHAMA, G.; HOBMAN, J.L.; LUND, P.A.; KERSHAW, C.J.; HIDALGO-ARROYO, G.A.; PENN, C.W.; DENG, X.T.; WALSH, J.L.; KONG, M.G. Probing bactericidal mechanisms induced by cold atmospheric plasmas with *Escherichia coli* mutants. *Appl. Phys. Lett*. **2007**, *90*, 073902-1.

PERRUCA, M. Introduction to Plasma and Plasma Technology; In: Plasma technology for Hyperfunctional Surfaces. Food, Biomedical and Textile Applications; Rauscher, H., Perruca, M., Buyle, G., Eds.;, WILEY-VCH: Weinheim, **2010.**

PERTRAT, F.M.; WOLANY, D.; SCHWEDE, B.C.; WIEDMAN, L.; BENNINGHOVEN, A. Comparative in situ ToF-SIMS/XPS study of polystyrene modified by argon, oxygen and nitrogen plasmas. *Surf. Interface Anal*. **1994**, *21*, 402.

PERTRAT, F.M.; WOLANY, D.; SCHWEDE, B.C.; WIEDMAN, L.; BENNINGHOVEN, A. In situ ToF-SIMS/XPS Investigations of Nitrogen Plasma-Modified Polystyrene Surfaces. *Surf. Interface Anal*. **1994**, *21*, 274.

PETRUJ, J.; MARCHALL, J. Mechanism of ketone formation in the thermooxidation and radiolytic oxidation of low density polyethylene. *J. Radiat. Phys. Chem*. **1980**, *16*, 27.

PEZZOLI, L.; ELSON, R.; LITTLE, C.; FISHER, I.; YIP, H.; PETERS, T.; HAMPTON, M.; DE PINNA, E.; COIA, J.E.; MATHER, H.A.; BROWN, D.J.; MOLLER NIELSEN, E.; ETHERLBERG, S.; HECK, M.; DE JAGER, C.; THRELFALL, J. (**2007**). International outbreak of Salmonella Senftenberg in 2007. URL: http:// www.eurosurveillance.org/ew/2007/070614.asp.

PHILIP, N.; SAOUDI, B.; CREVIER, M.C.; MOISAN, M.; BARBEAU, J.; PELLETIER, J. The respective roles of UV photons and oxygen atoms in plasma sterilization at reduced gas pressure : the case of N_2-O_2 mixtures. *IEEE Trans. Plasma Sci*. **2002**, *30*, 1429.

PHLS (PUBLIC HEALTH LABORATORY SERVICE) (**2000**). Guidelines for the microbiological quality of some ready-to-eat foods sampled at the point of sale. *Communicable Disease and Public Health* (CDPH), *3*, 163.

PONCIN-EPAILLARD, F.; CHEVET, B.; BROSSE, J.C. Reactivity of a polypropylene surface modified in a nitrogen plasma. *J. Adhes. Sci. Technol*. **1994,** *8*(4), 455.

POURCEL, L.; ROUTABOUL, J.-M.; KERHOAS, L.; CABOCHE, M.; LEPINIEC, L.; DEBEAUJON, I. TRANSPARENT TESTA10 encodes a laccase-like enzyme involved in oxidative polymerization of flavonoids in Arabidopsis seed coat. *Plant Cell* **2005**, *17*, 2966.

POURCEL, L.; ROUTABOUL, J-M; CHEYNIER, V.; LEPINIEC, L.; DEBEAUJON, I. Flavonoid oxidation in plants: from biochemical properties to physiological functions, *TRENDS in Plant Science* **2006**, *12*(1), 29.

PRICE, K.R.; BACON, J.R.; RHODES, M.J.C. Effect of Storage and Domestic Processing on the Content and Composition of Falvonol Glucosides in Onion (*Allium cepa*). *J. Agric. Food Chem*. **1997**, *45*, 938.

PRICE K.R.; CASUSCELLI F.; COLQUHOUN I.J.; RHODES M.J.C. Composition and content of flavonol glycosides in broccoli florets and their fate during cooking. *J Sci. Food Agric.* **1998**, *77*, 468.

PRICE, K.R.; COLQUHOUN, I.J.; BARNES, K.A.; RHODES, M.J.C. Composition and Content of Flavonol Glycosides in Green Beans and Their Fate during Processing. *J. Agric. Food Chem*. **1998**, *46*, 4898.

RABALLAND, V.; BENEDIKT, J.; WUNDERLICH, J.; VON KEUDELL, A. Inactivation of *Bacillus atrophaeus* and of *Aspergillus niger* using beams of argon ions, of oxygen molecules and of oxygen atoms. *J. Phys. D: Appl. Phys*. **2008**, *41*, 115207.

RADZIG, A.A.; SMIRNOV, B.M. Reference Data on Atoms, Molecules, and Ions. Springer Verlag: Berlin, **1985**.

RAGU, S.; FAYE, G.; IRAQUI, I.; MASUREL-HENEMAN, A.; KOLODNER, R.D.; HUANG, M.-E. Oxygen metabolism and reactive oxygen species cause chromosomal rearrangements and cell death. *PNAS* **2007**, *104* (23), 9747.

RAHMAN, A.; FAZAL., F; GREENSILL, J., AINLEY, K., PARISH, J.H.; HADI, S.M. Strand scission in DNA induced by dietary flavonoids: Role of Cu(I) and oxygen free radicals and biological consequence of scission. *Mol. Cell. Biochem.* **1992**, *111*, 3.

RAIZER, Y.P. Gas Discharge Physics; Springer Verlag: Berlin, **1991**.

RANBY, B.; RABEK, J. F. Photodegradation, Photooxydation and Photostabilization of Polymers; Wiley: New York, **1975**.

RE, R.; PELLEGRINI, N.; PROTEGGENTE, A.; PANNALA, A.; YANG, M.; RICE-EVANS, C. Antioxidant activity applying an improved ABTS radical cation decolorization assay. *Free Radical Biol. Med.* **1999**, *26*, 1231.

REED, H.E.; TERAMURA, A.H.; KENWORTHY, W.J. Ancestral U.S. soybean cultivars characterized for tolerance to ultraviolet-B radiation. *Crop. Sci*. **1992**, *32*, 1214.

REN, J.; MENG, S.; LEKKA, C.E.; KAXIRAS, E. Complexation of Flavonoids with Iron: Structure and Optical Signatures. *J. Phys. Chem. B* **2008**, *112*, 1845.

RENAUD, S.; DE LORGERIL, M. Wine, alcohol, platelets and the French paradox for coronary heart disease. *Lancet* **1992**, *339*, 1523.

REUBER, S.; BORNMAN, J.F.; WEISSENBÖCK, G.A. Flavonoid mutant of barley (*Hordeum vulgare* L.) exhibits increased sensitivity to UV-B radiation in the primary leaf. *Plant Cell Environ*. **1996**, *19*, 593.

RICE-EVANS, C.; MILLER, N.J. Antioxidant activities of flavonoids as bioactive components of food. *Biochem. Soc. Trans.* **1996**, *24*, 790.

RICE-EVANS, C.; MILLER, N.J.; BOLWELL, P.G.; BRAMLEY, P.M.; PRIDHAM, J.B. The relative activities of plant-derived polyphenolic flavonoid. *Free Radical Res.* **1995**, *22*, 375.

RIEDERER, M. & SCHREIBER, L. Waxes – the transport barriers of plant cuticles; In: Waxes: chemistry, molecular biology and functions; Hamilton, R.J., Ed.; The Oily Press: Dundee, **1995**; pp. 131-156.

ROBAK, J.; GRYGLEWSKI, R.J. Flavonoids are scavengers of superoxide anions. *Biochem. Pharmacol*. **1988**, *37*, 837.

ROHN, S.; BUCHNER, N.; DRIEMEL, G.; RAUSER, M.; KROH, L.W. Thermal Degradation of Onion Quercetin Glucosides under Roasting Conditions. *J. Agric. Food Chem*. **2007**, *55*, 1568.

ROHN, S.; RAWEL, H.M.; KROLL, J. Antioxidant activity of protein bound quercetin. *J. Agric. Food Chem*. **2004**, *52*, 4725.

ROSSI F.; KYLIÁN O.; HASIWA M. Decontamination of surfaces by low pressure plasma discharges. *Plasma Processes Polym.* **2006**, *3*, 431.

RUTSCHER, A. Chararcteristics of Low-Temperature Plasmas under Nonthermal Conditions- A Short Summary; In: Low Temperature Plasma. Fundamentals, Technoogies, and Techniques, vol. 1, 2nd. Edn.; Hippler, R., Kersten, H., Schmidt, M., Schoenbach, K.H., Eds.; Wiley-VCH: Weinheim, **2008**.

RYAN, K.G.; MARKHAM, K.R.; BLOOR, S.J.; BRADLEY, J.M.; MITCHELL, K.A.; JORDAN, B.R. UVB radiation induced increase in quercetin: kaempferol ratio in normal and transgenic lines of Petunia. *Photochem. Photobiol.* **1998**, *68*(3), 323.

RYAN, K.G.; SWINNY, E.E.; MARKHAM, K.R.; WINEFIELD, C. Flavonoid gene expression and UV photoprotection in transgenic and mutant Petunia leaves. *Phytochemistry* **2002**, *59*, 23.

HUSAIN, S.R.; CILLARD, J.; CILLARD, P. Hydroxyl radical scavenging activity of flavonoids. *Phytochemistry* **1987**, *26,* 2489.

SAGOO, S.K.; LITTLE, C.L.; WARD, L.; GILLESPIE, I.A.; MITCHELL, R.T. Microbiological study of ready-to-eat salad vegetables from retail establishments uncovers a National outbreak of Salmonellosis. *J. Food Prot.* **2003**, *66*, 403.

SAHU, S.C.; GRAY, G.C. Interactions of flavonoids, trace metals and oxygen: Nuclear DNA damage and lipid peroxidation by myricetin. *Cancer Lett*. **1993**, *70*, 73.

SAHU, S.C.; GRAY, G.C. Kaempferol-induced nuclear DNA damage and lipid peroxidation. *Cancer Lett*., **1994**, *85*, 159.

SARANTOPOULOU, E.;KOVA, J.; KOLLIA, Z.; RAPTIS, I.; KOBE, S.; CEFALAS, A.C. Surface modification of polymeric thin films with vacuum ultraviolet light. *Surf. Interface Anal.* **2008**, *40*(3-4), 400.

SARRA-BOURNET, C.; TURGEON, S.; MANTOVANI, D.; LAROCHE, G. Comparison of Atmospheric-Pressure Plasma versus Low-Pressure RF Plasma for Surface Functionalization of PTFE for Biomedical Applications. *Plasma Process. Polym*. **2006**, *3*, 506.

SCHMIDT, S.; ZIETZ, M.; SCHREINER, M.; ROHN, S.; KROH, L. W.; KRUMBEIN, A. Genotypic and climatic influences on the concentration and composition of flavonoids in kale (*Brassica oleracea* var. *sabellica*) *Food Chem*. **2010**, *119*, 1293.

SCHMIDTLEIN, H.; HERRMANN, K. Über die Phenolsäuren des Gemüses. *Zeitschrift für Lebensmitteluntersuchung und – Forschung* **1975**, *159* (5), 255.

SCHNITZLER, J.-P.; JUNGBLUT, T. P.; FEICHT, C.; KÖFFERLEIN, M.; LANGEBARTLES, C.; HELLER, W. ; SANDERMANN JR., H. UV-B induction of flavonoid biosynthesis in Scots Pine (*Pinus sylvestris* L.) seedling. *Trees* **1997**, *11*, 162.

SCHULZ, H.; JOUBERT, E.; SCHÜTZE, W. Quantification of quality parameters for reliable evolution of green rooibos (*Aspalathus linearis*). *Eur. Food Res. Technol*. **2003**, *216*, 539.

SCHÜTZE, A.; JEONG, J.Y.; BABAYAN, S.E.; PARK, J.; SELWYN, G.S.; HICKS, R.F. The Atmospheric-Pressure Plasma Jet: A Review and Comparison to Other Plasma Sources. *IEEE Trans. Plasma Sci.*, **1998**, *26*(6), 1685.

SEEBÖCK, R.J.; KÖHLER, W.E.; RÖMHELD, M. Pressure Dependence of the Mean Electron Energy in the Bulk Plasma of an RF Discharge in Argon. *Contrib. Plasma Phys*. **1992**, *32*(6), 613.

SELZUK, M.; OKSUZ, L.; BASARAN, P. Decontamination of grains and legumes infected with *Aspergillus* spp. and *Penicillum* spp. by cold plasma treatment. *Bioresource Technology* **2008***, 99*(11),5104.

SELWYN, G.S.; HERRMANN, H.W.; PARK, J.; HENINS, I. Materials Processing Using an Atmospheric Pressure, RF-Generated Plasma Source. *Contrib. Plasma Phys*. **2001**, *6*, 610.

SENSION, R.J.; REPINEC, S.T.; SZARKA, A.Z.; HOCHSTRASSER, R.M. Femtosecond laser studies of the cis-stilbene photoisomerization reactions. *J. Chem. Phys*. **1993**, *98*, 6291.

SÉNÉ, C.F.B.; MCCANN, M.C.; WILSON, R.H.; GRINTER, R. Fourier-Transform Raman and Fourier-Transform Infrared Spectroscopy - An investigation of Five Higher Plant Cell Walls and Their Components*. Plant Physiol*. **1994**, *106*, 1623.

SHASHURIN, A.; KEIDAR, M.; BRONNIKOV, S.; JURJUS, R.A.; STEPP, M.A. Living tissue under treatment of cold plasma atmospheric jet. *Appl. Phys. Lett*., **2008**, *93*, 181501.

SHEPHERD, T.; ROBERTSON, G.W.; GRIFFITHS, D.W.; BIRCH, A.N.E.; DUNCAN, G. Effects of Environment on the Composition of Epicuticular Wax from Kale and Swede. *Phytochemistry* **1995**, *40*(2), 407.

SHEVEREV, V.A.; STEPANIUK, V.P.; LISTER, G.G. Chemi-ionization in neon plasma. *J. Appl. Phys*. **2002**, *92*, 3454.

SHIBATA, M.; NAKANO, N.; MAKABE, T. Effect of $O_2(a^1\Delta_g)$ on plasma structures in oxygen radio frequency discharges. *J. Appl. Phys*. **1996**, *26*(6), 1685.

SIES, H. Biochemie des Oxidativen Stress. *Angew. Chem.* **1986**, *98*, 1061.

SINGLETON, V.L.; ORTHOFER, R.; LAMUELA-RAVENTOS, R.M. Analysis of total phenols and other oxidation substrates and antioxidants by means of Folin-Ciocalteu reagent. *Methods Enzymol*. **1999**, *299*, 152.

SINGLETON, V.L.; ROSSI, J.A. Colorimetry of total ohenolics with phosphomolybdic-phosphotungstic acid reagents. *Am. J. Enol. Vitic*. **1965**, *16*, 144.

SIVACI, A.; SÖKMEN, M. Seasonal changes in antioxidant activity, total phenolic and anthocyanin constituent of the stems of two Morus species (*Morus alba* L. and *Morus nigra* L.). *Plant Growth Regul*. **2004**, *44*, 251.

SKREDE, G.; WROLSTAD, R. E.; DURST, R. W. Changes in anthocyanins and polyphenolics during juice processing of highbush blueberries (*Vaccinium corymbosum* L.). *J. Food Sci*. **2000**, *65*, 357.

SMALL-WARREN, N.E.; CHIU, L.-Y.C. Lifetime of the metastable $^3P_2$ and $^3P_0$ states of rare-gas atoms. *Phys. Rev. A* **1975**, *11*, 1777.

SMITH, G.J.; MARKHAM, K.R. Tuatomerism of flavonol glucosides: relevance to plant UV protection and flower colour. *J. Photochem. Photobiol. A* **1998**, *118*, 99.

SOCRATES G. Infrared and Raman Characteristics Group Frequencies – Tables and Charts; 3rd edn.; John Wiley & Sons: West Sussex, **2001**.

SONG, H.P.; KIM, B.; CHOE, J.H.; JUNG, S.; MOON, S.Y.; CHOE, W.; JO, C. Evaluation of atmospheric pressure plasma to improve the safety of sliced cheese and ham inoculated by 3-strain cocktail *Listeria monocytogenes*. *Food Microbiol.* **2009**, *26*, 432.

SQUADRITO, L. ; PRYOR, W.A. Oxidative chemistry of nitrit oxide: The roles of superoxide, peroxynitrite and carbon dioxide. *Free Radical Biol. Chem.* **1998**, *25*, 392.

STARK, R.E. & TIAN, S.The cutin biopolymer matrix; In: Biology of the Plant Cuticle; Riederer, M., Müller, C., Eds.; Blackwell Publishing: Oxford, **2006**.

STEFANOVIC, I.; BIBINOV, N. K.; DERYUGIN, A. A.; VINOGRADOV, I. P.; NAPARTOVICH, A. P.; WIESEMANN, K. Kinetics of ozone and nitric oxides in dielectric barrier discharges in O_2/NO_x and $N_2/O_2/NO_x$ mixtures. *Plasma Sources Sci. Technol.* **2001**, *10*(3), 406.

STEINMETZ, K.A.; POTTER, J.D. Vegetables, fruit and cancer. 1. Epidemiology. *Cancer Cases Control* **1991** 5, *325*.

STOFFELS, E.; ARANDA-GONZALVO, Y.; WHITMORE, T.D.; SEYMORE, D.L.; REES, J.A. A plasma needle generates nitric oxide. *Plasma Sources Sci. Technol*. **2006**, *15*(3), 501.

STOFFELS, E.; ARANDA-GONZALVO, Y.; WHITMORE, T.D.; SEYMORE, D.L.; REES, J.A. Mass spectrometric detection of short-living radicals produced by a plasma needle. *Plasma Sources Sci. Technol*. **2007**, *16*(3), 549.

STOFFELS, E.; SAKIYAMA, Y.; GRAVES, D.B. Cold Atmospheric Plasma: Charged Species and Their Interactions With Cells and Tissues. *IEEE Trans. Plasma Sci.* **2008**, *36*(4), 1441.

SUDO, E.; TERANISHI, M.; HIDEMA, J.; TANIUCHI, T. Visualization of Flavonol Distribution in the Abaxial Epidermis of Onion Scales via Detection of Ist Autofluorescence in the Absence of Chemical *Processes. Biosci. Biotechnol. Biochem*. **2009**, *73*(9), 2107.

SULLIVAN, J.H.; TERAMURA, A.H. Field study of the interaction between solar ultraviolet-B irradiation and drought on photosynthesis and growth in soybean. *Plant Physiol*. **1990**, *92*, 141.

SUN, D.; STYLOS, G. K. Fabric Surface Properties affected by low temperature plasma treatment. *J. Mater. Process. Technol.* **2006**, *173*, 172.

TAKAHAMA, U.; HIROTA, S. Deglucosidation of Quercetin Glucosides to the Aglycone and Formation of Antifugal Agents by Peroxidase-Dependent Oxidation of Quercetin on Browning of Onion Scales. *Plant Cell Physiol.* **2000**, *41*(9), 1021.

THIPYAPONG, P.; STOUT, M.J.; ATTAJARUSIT, J. Functional Analysis of Polyphenol Oxidases by Antisense/Sense Technology. *Molecules* **2007**, *12*, 1569.

TOMÁS-BARBERÁN, F.A.; GIL, M.I.; CASTANER, M.; ARTES, F.; SALTVEIT, M.E. Effect of Selected Browning Inhibitors on Phenolic Metabolism in Stem Tissue of Harvested Lettuce. *J. Agric. Food Chem*. **1997**, *45*(3), 583.

TOREL, J.; CILLARD, J.; CILLARD, P. Antioxidant activity of flavonoids and reactivity with peroxy radical. *Phytochemistry* **1986**, *25*, 383.

TORREGIANI, A.; TRINCHERO, A.; TAMBA, M.; TADDEI, P. Raman and pulse radiolysis studies of the antioxidant properties of quercetin: Cu(II) chelation and oxidizing radical scavenging. *J. Raman Spectrosc*. **2005**, *36*, 380.

TOURNAIRE, C.; CROUX, S.; MAURETTE, M.T. Antioxidant activity of flavonoids: efficiency of singlet oxygen ($^1\Delta_g$) quenching. *J. Photochem. Photobiol. B - Biol* **1993**;*19*,205.

TOURNAIRE, C.; HOCQUAUX, M.; BECK, I.; OLIVEROS, E.; MAURETTE, M. Activité anti-oxidante de flavonoïdes Réactivité avec le superoxyde de potassium en phase hétérogène. *Tetrahedron* **1994**, *50*, 9303.

TOURNAS, V.H. Spoilage of Vegetable Crops by Bacteria and Fungi and Related Health Hazards. *Crit. Rev. Microbiol.* **2005**, *31*, 33.

TSAO, R.; YANG, R. Optimization of a new mobile phase to know the complex and real polyphenolic composition: Towards a total phenolic index using high-performance liquid chromatography. *J. Chromatogr. A* **2003**, *1018*, 29.

TUDELA, J.A.; CANTOS, E.; ESPÍN, J.C.; TOMÁS-BARBERÁN, F.A.; GIL, M.I. Induction of antioxidant flavonol biosynthesis in fresh-cut potatoes. Effect of domestic cooking. *J. Agric. Food Chem*. **2002**, *50*, 5925.

USDHHS AND USDA (US DEPARTMENT OF HEALTH AND HUMAN SERVICES AND US DEPARTMENT OF AGRICULTURE, USA) (**2005**). Dietary Guidelines for Americans, 6th Edition; U.S. Government Printing Office: Washington, DC.

UTAKA, M.; TAKEDA, A. Copper(II)-catalyzed oxidation of quercetin and 3-hydroxyflavone. *J. Chem. Soc. Chem. Commun.* **1985**, 1824.

VALLEJO, F.; TOMAS-BARBERAN, F. A.; GARCIA-VIGUERA, C. Phenolic compound contents in edible parts of broccoli inflorescences after domestic cooking. *J. Sci. Food Agric.* **2003**, *83*(14), 1511.

VAN ACKER, S. A.; DE GROOT, M. J.;VAN DEN BERG, D.; TROMP, M. N.; DONNÉ OP-DEN KELDER, G.; VAN DER VIJGH, W.J.; BAST, A. A quantum chemical explanation of the antioxidant activity of flavonoids. *Chem. Res. Toxicol.* **1996**, *9*, 1305.

VAN ACKER, S. A.; TROMP, M. N.; HAENEN, G. R.; VAN DER VIJGH, W. F.; BAST, A. Flavonoids as scavengers of nitric oxide radical. *Biochem. Biophys. Res. Commun.* **1995**, *214*, 755.

VEIT, M.; BILGER, W.; MÜHLBAUER, T.; BRUMMET, W.; WINTER, K. Diurnal changes in flavonoids. *J. Plant Physiol*. **1996**, *148*, 478.

VIALLE, M.; TOUZEAU, M.; GOUSSET, G.; FERREIRAT, C.M. Kinetics of $O(^1S)$ and $O(^1D)$ metastable atoms in a DC oxygen glow discharge. *J. Phys. D: Appl. Phys*. **1991**, *24*, 301.

VIETZKE, E.; TANABE, T.; PHILIPP, V.; ERDWEG, M.; FLASKAMP, K. The Reaction of Energetic O_2^+, Thermal O_2, and Thermal Ar/O_2^+ on Graphite and the Use of Graphite for Oxygen Collector Probes. *J. Nucl. Mater*. **1987**, *145-147*, 425.

VLEUGELS, M.; SHAMA, G.; DENG, X.T.; GREENACRE, E.;BROCKLEHURST, T.; KONG, M.G. Atmospheric Plasma Inactivation of Biofilm-Forming Bacteria for Food Safety Control. *IEEE Trans. Plasma Sci*. **2005**, *33*, 824.

VOGT, T.; GULZ, P.G. Accumulation of flavonoids during leaf development in Citrus-Laurifolius. *Phytochem*. **1994**, *36*, 591.

VOGT, T.; POLLAK, P.; TARLYN, N.; TAYLOR, L.P. Pollination- or wound-induced kaempferol accumulation in petunia stigmas enhances seed production. *Plant Cell* **1994**, *6*, 11.

VOLIN, J.C.; DENES, F.S.; YOUNG, R.A.; PARK, S.M. Modification of Seed germination Performance through Cold Plasma Technology. *Crop Sci*. **2000**, *40*, 1706.

VON KEUDELL, A. Einführung in die Plasmaphysik, 2008. Vorlesungsskript SoSe **2006**, Ruhr-Universität Bochum.

VON KEUDELL, A.; JACOB, W. Elementary processes in plasma–surface interaction: H-atom and ion-induced chemisorption of methyl on hydrocarbon film surfaces. *Prog. Surf. Sci*. **2004**, *76*, 21.

WALKER, J.R.; FERRAR, P.H. Diphenol oxidases, enzyme-catalysed browning and plant disease resistance. *Biotechnol. Genet. Eng. Rev*. **1998**, *15*, 457.

WALTER, W.; SCHALLER, U.; LANGHOFF, H. Fluorescence and absorption in e beam excited neon. *J. Chem. Phys*. **1985**, *83*, 1667.

WALLSTROM, P.; WIRFALT, E.; JANZON, L.; MATTISSON, I.; ELMSTAHL, S.; JOHANSSON, U.; BERGLUND, G. Fruit and vegetable cosumption in relation to risk factors for cancer: a report from the Malmo Diet and Cancer Study. *Public Health Nutr*. **2000**, *3*, 263.

WEIDNER, S.; KÜHN, G.; DECKER, R.; ROESSNER, D.; FRIEDRICH, J. Influence of Plasma Treatment on the Molar Mass of Poly(ethylene terephthalate) Investigated by Different Chromatographic and Spectroscopic Methods. *J. Polymer Sci., Part A: Polymer Chem*., **1998**, *36*, 1639.

WERKER, E.; MARBACH, J.; MAYER, A.M. Relation between the anatomy of the testa, water permeability and the presence of phenolics in the genus *Pisum*. *Ann. Bot.* **1979**, *43*, 765.

WIESER, J.; SALVERMOSER, M.; SHAH, L.H.; ULRICH, A.; MURNICK, D.E.; DAHL, H. Lyman-alpha emission via resonant energy transfer. *J. Phys. B* **1998**, *31*, 4589.

WILSON, D. J.; WILLIAMS, R. L.; POND, R. C. Plasma modification of PTFE surfaces. Part I: Surfaces immediately following plasma treatment. *Surf. Interface Anal*. **2001**, *31*, 385.

WILSON, M.J.; GREENBERG, B.M. Protection of the D1 photosystem II reaction center protein from degradation in ultraviolet radiation following adaption of *Brassica napus* L. to growth in ultraviolet radiation. *Photochem. Photobiol*. **1993**, *57*, 556.

WINKEL-SHIRLEY, B. Flavonoid Biosynthesis. A Colorful Model for Genetics, Biochemistry, Cell Biology, and Biotechnology. *Plant Physiol*. **2001**, *126*(2), 485.

WROBEL, A.M.; LAMONTAGNE, B.; WERTHEIMER, M.R. Large- area microwave and radiofrequency plasma etching of polymers. *Plasma Chem. Plasma Process*. **1988**, *8*, 315.

XU, B.; CHANG, S.K.C. Total Phenolic, Phenolic Acid, Anthocyanin, Flavan-3-ol, and Flavonol Profiles and Antioxidant Properties of Pinto and Black Beans (*Phaseolus vulgaris* L.) as Affected by Thermal Processing. *J. Agric. Food Chem*. **2009**, *57*(11), 4754.

YORUK, R.; MARSHALL, M.R. Physicochemical properties and function of plant polyphenol oxidase: a review. *J. Food Biochem*. **2003**, *27*, 361.

YOUNG, T. An Essay on the Cohesion of Fluids. *Phil. Trans. R. Soc. Lond*. **1805**, *95*, 65.

ZHANG, X.; LI, M.; ZHOU, R.; FENG, K.; YANG, S. Electron plasma wave propagation in external-electrode fluorescent lamps. *Appl. Phys. Lett*. **2008**, *92*, 021502.

ZHOU, J.; WANG, L.F.; WANG, J.Y.; TANG, N. Synthesis, characterization, antioxidative and antitumor activities of solid quercetin rare earth(III) complexes. *J. Inorg. Biochem*. **2001**, *83*, 41.

ZHOU, K.; YU, L. Total phenolic contents and antioxidative properties of commonly consumed vegetables grown in Colorado. *LWT - Food Sci. Technol*. **2006**, *39*, 1155.

ZIETZ, M.; WECKMÜLLER, A.; SCHMIDT, S.; ROHN, S.; SCHREINER, M.; KRUMBEIN, A.; KROH, L.W. Genotypic and Climatic Influence on the Antioxidant Activity of Flavonoids in Kale (*Brassica oleracea* var. *sabellica*). *J. Agric. Food Chem.*, **2010**, *58*(4), 2123.

ZOU, J.J.; LIU, C.J.; ELIASSON, B. Modification of starch by glow-discharge plasma. *Carbohydr.Polym.* **2004**, *55*, 23.

Appendix

A1 List of Figures

A2 List of Schemes

A3 List of Tables

A4 List of Abbreviations

AC	Alternating current
ABTS	2,2'-azino-bis(3-ethylbenzthiazoline-6-sulphonic acid)
ACN	Acetonitrile
AFM	Atomic force microscopy
AIBN	Azodiisobutyronitrile
APP	Atmospheric pressure plasma
APPJ	Atmospheric pressure plasma jet
ATR	Attenuated total reflexion
aqu.	Aqueous
at.	Atomic
atm	Atmosphere [pressure unit]
B3LYP	(BECKE, three-parameter, LEE-YANG-PARR) exchange-correlation functional
BE	Binding energy
BSA	Bovine Serum Albumin
CA	Contact angle
CAN	Diammonium cerium (IV) nitrate
CCD	Charge-coupled device
CHS	Chalcone synthase
CoA	Coenzyme A
CW	Continuous wave
DAD	Diode array detector
DART	Direct Analysis in Real Time
DC	Direct current
DFT	Density functional theory
dm	Dry matter
DMSO	Dimethyl sufoxide
DNA	Desoxyribonucleic acid
DPPH	1,1-Diphenyl-2-picrylhydrazyl
ECR	Electron cyclotron resonance
EDX	Energy dispersive X-ray spectroscopy
EEDF	Electron energy distribution function
ESI	Electrospray ionisation
ET	Energy transfer
F3H	Flavanone 3- β-hydroxylase
F3'H	Flavonoid 3'-hydroxylase
FC	FOLIN-CIOCALTEU
FTIR	FOURIER transform infra red
FWHM	Full-width-half-maximum
GAE	Gallic Acid Equivalent
GC	Gas chromatography
GmbH	*Gesellschaft mit beschränkter Haftung* (engl.: company with limited liability)
HAT	Hydrogen atom abstraction
HB	Hydrogen bonding
HPLC	High performance liquid chromatography
HR	High-resolution
i.d.	Inner diameter
IMS	Ion mobility spectrometry

IP	Ionization potential
ISC	Intersystem Crossing
LC	Liquid chromatography
LDL	Low-density lipoprotein
LPP	Low-pressure plasma
LTE	Local-thermodynamical equilibrium
M	Metal
Me	Methyl group
MeOH	Methanol
MHz	MegaHertz
MS	Mass spectrometry
MW	Microwave
NHE	Normal hydrogen electrode
NMR	Nuclear magnetic resonance
NTP	Non-thermal plasma
OES	Optical emission spectroscopy
p.a.	*pro analysis*
PAL	Phenylalanine ammonia-lyase
PCET	Proton coupled electron transfer
pH	P*otentia hydrogenii* (negative logarithm of molar concentration of dissolved H_3O^+ ions)
ppb	Parts per billion
ppm	Parts per million
PPO	Polyphenol oxidase
ppt_v	Parts per trillion by volume
PTFE	Polytetrafluoroethylene
PTR-MS	Proton Transfer Reaction-Mass Spectrometry
QDG	Quercetin-diglycoside (Quercetin-3,4'-di-β-D-glucoside)
QMG	Quercetin-monoglycoside (Quercetin-4'-β-D-glucoside)
RF	Radio-frequency
R_f	Retention factor
RFGD	Radio-frequency glow discharge
RNS	Reactive nitrogen species
ROS	Reactive oxygen species
RP	Reversed phase
rpm	Rounds per minute
R_t	Retention time
RT-PCR	Real-time polymerase chain reaction
S_n state	n*th* Singlet state
sccm	Standard cubic meter per minute
SD	Standard deviation
SEM	Scanning electron microscopy
SET	Single electron transfer
slm	Standard liter per minute
SPE	Solid phase extraction
TEAC	Trolox Equivalent Antioxidant Capacity
T_n state	n*th* Triplet state
TP	Thermal plasma
TPC	Total Phenolic Content
UV	Ultraviolet
vis	Visible

VOC	Volatile organic compounds
VUV	Vacuum ultraviolet
v/v	volume/volume
XPS	X-ray photoelectron spectroscopy

A5 Fundamental Physical Constants and Conversion Factors

Quantity	Symbol	Value
Elementary charge	q_e	1.6022×10^{-19} C
Electron rest mass	m_e	9.1095×10^{-31} kg
Proton rest mass	m_p	1.6726×10^{-27} kg
Proton-electron mass ratio	m_p/m_e	1836.2
Speed of light in vacuum	c_0	2.9979×10^{8} m/s
Vacuum permittivity	ε_0	8.8542×10^{-12} F/m
Bohr radius	$a_0 = 4\pi\varepsilon_0 \hbar^2/m_e q_e^2$	5.2918×10^{-11} m
Atomic cross section	$\sigma = \pi a_0^2$	8.7974×10^{-21} m^2
Avogadro constant	N_A	6.0220×10^{23}
Boltzmann constant	k_B	1.3807×10^{-23} J/K
Faraday constant	$F = N_A q_e$	96 485.3399 C/mol
Planck constant	h	6.6262×10^{-34} Js
$h/2\pi$	$\hbar$	1.0546×10^{-34} Js
Rydberg constant	$R_\infty = \alpha^2 m_e c_0/2h$	10 973 731.568 m^{-1}
Molar gas constant	$R = k_B N_A$	8.3144 J/(mol K)
Non-SI units accepted for use with the SI		
Electron volt	eV	1.6021×10^{-19} J = 11 605 K
(Unified) atomic mass unit	$u = m_u = {}^1/_{12}\, m(^{12}\mathrm{C})$	1.6606×10^{-27} kg
Non-SI units of some selected observables		
Pressure: $p^0 = 1.0133 \times 10^5$ Pa = 1013.3 mbar = 1 atm = 760 Torr		
Flow rate: Q = 1 slm = 1000 sccm = 18.124 mbar m³s^{-1}		

Eidesstattliche Erklärung

Hiermit erkläre ich an Eides statt, daß ich die vorliegende Arbeit selbständig verfaßt und keine anderen als die angegebenen Hilfsmittel und Quellen verwendet habe. Diese Arbeit wurde bisher keiner anderen Einrichtung zur Begutachtung vorgelegt.

Franziska Grzegorzewski